Università degli Studi di Roma "La Sapienza"
Facoltà di Scienze Matematiche Fisiche e Naturali
Dipartimento di Scienze della Terra

Dottorato di Ricerca in Scienze della Terra
XXIV ciclo

INTEGRATED TECHNIQUES FOR SLOPE EROSION MODELLING AND BADLAND MONITORING IN KEY SITES OF CENTRAL ITALY

Dottoranda: *Dott.ssa Francesca Vergari*
Matricola 694227

francesca.vergari@uniroma1.it

Docenti guida: *Prof. Maurizio Del Monte*
Dott.ssa Marta Della Seta

Coordinatore del dottorato: Prof.ssa Laura Corda*

Docenti Esaminatori:

- Prof.ssa Francesca Bozzano*
- Prof. Carlo Baroni**
- Prof. Riccardo Salvini***

**Dip.to di Scienze della Terra, Università degli Studi di Roma ''La Sapienza''*
***Dip.to di Scienze della Terra, Università di Pisa*
****Centro di Geotecnologie, Università di Siena*

A.A. 2010/2011

INDEX

ANNEXES

RINGRAZIAMENTI

A conclusione del dottorato, vorrei ringraziare numerose persone, che, in diversi modi, mi hanno accompagnata in questo percorso.
Certamente un particolare ringraziamento va al Prof. Del Monte e a Marta, che, più di tutti, conoscono tutte le sfaccettature del mio lavoro e le difficoltà che ho incontrato. Il professore mi ha seguita pazientemente fin dagli anni della tesi di laurea, dandomi sempre fiducia e guidandomi con la sua esperienza, contagiandomi con la sua passione per il rilevamento sul campo, ed insegnandomi a interpretare le cose da diversi punti di vista. Ringrazio Marta, che ha sempre condiviso con me le tutte le difficoltà incontrate, aiutandomi a risolverle, e, come una valvola di sfogo, mi ha sempre ascoltata e spronata a pretendere di più da me stessa!
Un ringraziamento va a tutti i professori del gruppo di Geografia Fisica e Geomorfologia, che mi hanno sempre incoraggiata e accolta con sorrisi e disponibilità. Mi hanno dato l'occasione di partecipare a gruppi di ricerca nazionali, la cui collaborazione mi ha indiscutibilmente arricchito scientificamente.
Desidero ringraziare anche i tecnici di laboratorio, e in particolare Gianfranco, che mi hanno seguita nel corso delle fasi analitiche, con pazienza e competenza. E Cristina, che, nell'ultima fase di stesura, con occhio critico mi ha dato molti consigli per migliorare la tesi.
Un grande grazie va a tutti gli amici e colleghi del Laboratorio di Geografia Fisica….Alessio, col quale ho condiviso tutti gli anni di laboratorio, fin dagli anni della tesi di laurea, sempre prezioso riferimento tecnico e morale, Sabrina, spesso compagna di "luculliani" banchetti a mensa (!), Claudia, arrivata come un vulcano in Laboratorio, e Alessia, con la quale ho trovato subito complicità e, per molti versi, affinità di carattere. Tra gli amici di università non posso non citare Veronica, con la quale sono cresciuta durante gli anni dell'università, inspiegabilmente non ringraziata nella frettolosa confusione della tesi di laurea, e che sicuramente non ho mai ringraziato abbastanza per la profonda amicizia.
Il grazie più grande va senza dubbio alla mia famiglia. A mia sorella, instancabile riferimento e insostituibile dispensatrice di consigli, grazie alle somiglianze di percorso e di carattere che ci contraddistinguono. Alla nuova arrivata, Agata, il cui pensiero mi garantisce un sorriso in ogni momento. A Emanuele, col quale ho scelto di condividere tutti gli ostacoli e i momenti felici della vita, e che, inevitabilmente, si è subito tutte le mie ansie la sera di ritorno a casa, ma che instancabile mi è sempre vicino e mi riporta coi piedi per terra! Ai miei genitori. Non esistono abbastanza parole per ringraziarli dell'affetto e del continuo sostegno. Senza mai pensarci hanno sempre incoraggiato le mie inclinazioni, anche quando, raramente, non condividevano pienamente le mie scelte. A loro più di tutti devo e dedico questo traguardo.

ABSTRACT

The growing interest in studying badland dynamics reflects the need to increase knowledge of geomorphologic processes and dynamics in subhumid badland areas, particularly because of their importance in generating extremes of water and sediment production. Field studies of soil erosion are expensive, time-consuming and data needs to be collected over many years. Though providing detailed understanding of the erosion processes, field studies have limitations because of the complexity of interactions and the difficulty of generalising from the results.

Cost-efficient methods of estimating erosion over whole catchments are required as ways of predicting erosion after disturbance or following various erosion management strategies. Thus, the indirect estimation and the prevision of erosion rates is still one of the main research topics of the scientific community in the field of geomorphology and is far from solved.

This Ph.D. research project is aimed at defining an integrated methodology of denudation intensity estimation and prevision, for areas greatly affected by badlands, and it is based on both quantitative geomorphic analysis and multivariate statistical investigations, in order to deepen the relationships between the main denudation effects and the potential causal factors favoring geomorphologic instability in badlands areas. The research have allowed to propose a statically based method for water erosion hazard assessment, conceived as a spatially distributed prevision of *calanchi* badlands, and associated erosion rate, occurrence. Direct measures of erosion intensity in badlands were used to validate the water erosion estimates and previsions.

As the research project is focused mainly on methodological objectives, well-known study areas of Tyrrhenian side of central Italy, included within the Tevere and Ombrone River Basins, have been selected, in order to compare the results gradually achieved with the earlier available data.

Erosion rate estimations were performed refining some empirical equations ("*Tu* Denudation index"), that estimate the suspended sediment yield (SSY) as a function of morphometric parameters related to drainage network and relief (Ciccacci et al., 1981, 1986). *Tu* denudation index was confirmed to be a good estimator of the suspended sediment yield (SSY) for catchments characterized by the prevalence of sedimentary and weakly coherent outcropping lithologies. The improvement of the regression relations contributed to better estimate sedimentary output for catchment widely affected by badland areas. In these basins, in fact, SSY is strongly correlated to the areal ratio affected by badlands to the total catchment area. Thus, using the not-projected drainage density parameter (D_{3d}), instead of the traditional drainage density parameter (D), even if not improving the SSY estimation for large basins, was considered to better reflect the conditions predisposing erosions than D for smaller catchments, where large *calanchi* badlands and related high slope gradients are present. The dominant role of drainage density in estimating erosion rate for badland areas was confirmed by the attempt of zoning the estimated erosion rates using the Tu Grid Analysis. This attempt proved to be very efficient in estimating the erosion rate due to runoff within badland areas, as confirmed by the comparison between the estimated and the measured erosion rates. This result seems to increase the prospective of using Tu grid analysis when prolonged denudation monitoring is not possible. Moreover, even where punctual erosion rates are measured by pin monitoring, the estimated erosion rate map represents a validated continuous representation of water erosion rate for larger areas.

Geomorphological susceptibility evaluation was performed applying a multivariate statistical method based on conditional analysis (Bayesian interpretation of probability) integrated by a proposal of a new method for most influential causal factors selection. The procedure provided satisfactory results for the unbiased prediction of landslide and water erosion susceptibility for the Upper Orcia Valley. The method is conceptually simple but, at the same time, effective in evaluating the conditional probability of hazardous events given a certain combination of causal factors: the proposed factor selection procedure has proved to be a useful tool for the unbiased detection of the factors really discriminant for instability landforms in the study area, and can be very helpful when analyzing new areas. Moreover the use of vector datasets allow to create vector easy-to-read susceptibility maps, in which

the fragmentation generally characterizing raster outputs is avoided. These characteristics make this susceptibility method easy to be understood and each resulting map easy to be read, thus suitable for policy makers in planning land management strategies.

The association of the estimated erosion rate for *calanchi* badland areas to the surveyed landforms allowed to use the susceptibility method to evaluate the water erosion hazard, since the temporal information about the erosion processes was related to the spatial data. This procedure is proposed when direct erosion rate measures are not available.

Different techniques of direct monitoring of erosion rates and processes have been performed, with the aim of identifying the main geomorphic processes acting in the study areas and quantifying their intensity. In particular, direct measurements (erosion pin monitoring, geomorphologic survey, DGPS survey and digital photogrammetric analysis) were used to validate the results obtained after indirect erosion rate estimations and susceptibility and hazard assessment models application. Even though, interesting remarks have been concluded on the applicability of various methods of erosion monitoring.

The size of the study area, the time available, and the quality of the data required are perhaps the most critical issues to be considered when looking for the most appropriate technique. As well-known, the traditional erosion pin method generally allows to carry out very accurate punctual measures, whose error is measurable in few millimeters. So, it can be used to quantify very detailed temporal variations (monthly or after-event ground level changes). On the other hand, DGPS survey can be proper when a single hillslope of less than few hectares is being monitored, as the time and effort required would be acceptable. For larger areas or wider time interval, high resolution photogrammetric analysis could be more appropriate. However, all these methods are affected by many error sources, that limit their use to very specific time and spatial ranges.

Finally, some new contributions to the knowledge of the physical factors influencing the initiation and the development of different water erosion landforms in the studied badland areas have been achieved.

Comparison of pluviometric data and measured ground level variations for Bargiano site (Tevere River Basin) has highlighted that clay removal by water erosion is generally due to intense rainfall event preceded by quite long dry periods, while accumulation (due to gully banks collapsing) is favoured by intense rainfall after a certain number of rainy days (frequent in spring). Moreover, in inter-rill position, where almost the lonely water erosion acts, intense events are significantly more effective than long events.

Considering the distribution of *calanchi* and *biancane* landforms of Upper Orcia Valley (Ombrone River Basin) among the different classes of the main topographic and physiographic factors, it is a matter of fact that *calanchi* badlands develop on steeper slopes and where higher values of amplitude of relief occur, due to the morphoevolutionary processes. Moreover, observations on present embryonic *biancane* of Lucciolabella site confirm the leading role played by reticular systems of joints in the dissection of original, gently-dipping surfaces. Actually, a resolute difference on dispersivity level of the *biancana* parent material samples of La Piaggia subcatchment was not found with respect to *calanchi* badlands samples of the same subcatchment.

On the other hand, a significant influence of clay properties was observed on the different erosion rates measured during decadal monitoring investigations by means of erosion pins in the study areas. *Calanchi* badlands show lower erosion rates due to surface runoff. The major facility of *biancane* clays to be entrained at very low stream powers is reflected in their major dispersivity, while, in badlands, the morphoevolution and sediment removal is predominantly caused by widespread mudsliding from the rill and gully heads, as also confirmed by the mean positive variations of ground level recorded at some *calanchi* monitoring stations. This observation can be also related to the higher sand content in *calanchi* badlands, which may favour the infiltration processes to the detriment of runoff.

Finally, as already observed by several authors, the agricultural exploitation of these lands lead to a decrease of exchangeable cations concentration (and, thus, clay dispersivity), even if the permanent inhibition of chemical dispersion due to increase of soil stability hypothesized by Phillips (1998) cannot be completely agreed. Decadal monitoring and observation in the study areas and in other sites of central Italy have outlined that badlands initiation is even enhanced by agricultural manipulation: grazing and farming are among the

most important triggers for accelerated water erosion, and tillage erosion has been recognized as an increasing factor of water erosion.

The performed investigations have allowed to carry out some new remarks about both the applied and proposed methodologies and the studied areas and related processes. In particular, results from this research have contributed to improve some methods useful to deepen the knowledge of processes and denudation intensity acting in badland areas of Mediterranean drainage basins.

KEYWORDS: erosion modelling, denudation monitoring, geomorphological hazard, badlands, Central Italy

RIASSUNTO

Tecniche integrate di modellazione della denudazione dei versanti e monitoraggio dell'erosione accelerata in siti chiave dell'Italia centrale

La presente tesi di dottorato è finalizzata alla proposta di un modello integrato di stima e previsione degli effetti dei processi di erosione su versanti e in bacini idrografici caratterizzati da vaste aree soggette a rapida denudazione. Tale obiettivo è stato perseguito organizzando la ricerca nelle seguenti fasi: a) l'applicazione di diversi metodi di valutazione dell'intensità dell'erosione a diversa scala spazio-temporale, b) il miglioramento di alcuni aspetti delle procedure utilizzate, c) la messa a punto di un metodo di valutazione della pericolosità geomorfologica, supportato da una procedura obiettiva di selezione dei fattori predisponenti i dissesti considerati.

La quantificazione delle ingenti quantità di materiale asportato dai processi erosivi risulta fondamentale ai fini della corretta gestione del territorio e della valutazione del rischio geomorfologico. La ricerca presentata si inserisce, quindi, in un più ampio contesto scientifico pregresso ed attuale comprendente studi sull'erosione dei versanti, in cui la stima indiretta dell'erosione rimane un tema di indagine aperto, a causa delle rilevanti risorse richieste dalle misure dirette, in termini di costi e di tempo, che, inoltre, generano risultati di difficile generalizzazione.

Le aree di studio sono state scelte all'interno di due importanti bacini idrografici dell'Italia centrale (Tevere e Ombrone), caratterizzati dalla presenza di ampie zone soggette ad erosione accelerata (definite in letteratura "*hot-spots* erosivi"). Queste zone sono contraddistinte da affioramenti di importanti depositi marini plio-pleistocenici altamente erodibili, e sollevati durante il Quaternario a seguito dell'attività vulcanica degli apparati di Radicofani e del Monte Amiata. Le risultanti elevate pendenze che caratterizzano questi affioramenti, insieme al forte contrasto stagionale umido-secco tipico dell'ambiente

mediterraneo, costituiscono quindi i fattori ideali per il manifestarsi di processi di denudazione accelerata, causando la diffusa presenza forme di erosione, come *calanchi*, *biancane*, *rill, gully e pipes,* e diverse tipologie di frana, tipiche delle aree a *badlands*.

L'attività di ricerca, avendo finalità di carattere prevalentemente metodologico, ha previsto l'applicazione, in parallelo, di diversi tipi di indagine: da una parte sono stati portati avanti alcuni tentativi di quantificare gli effetti dei processi erosivi in aree a *badlands* mediante rilevamenti di campagna (a diversa scala di dettaglio) e altre analisi sperimentali (in particolare volte ad analizzare i principali potenziali fattori predisponenti il dissesto in queste aree). Dall'altra sono stati applicati e messi a punto dei modelli finalizzati a stimare indirettamente i tassi di erosione (sia a livello di bacino idrografico che a livello di aree unitarie), sulla base di parametri geomorfici quantitativi, e a fare previsioni spaziali (analisi di suscettibilità) sui processi di denudazione dei versanti, pervenendo a proporre un modello integrato per la valutazione della pericolosità geomorfologica.

In particolare, la **stima dei tassi di erosione** per l'Alta Val d'Orcia (Toscana meridionale) è stata ottenuta applicando e affinando alcune relazioni che permettono di stimare il trasporto torbido fluviale (indice di erosione *Tu*) alla scala di bacino idrografico, come funzione di alcuni parametri geomorfici quantitativi, dipendenti dalle principali caratteristiche morfologiche, morfodinamiche, strutturali e climatiche del territorio (Ciccacci et al., 1981, 1986). Lo studio condotto ha confermato l'ottima capacità dell'indice considerato di stimare il trasporto torbido fluviale, per bacini idrografici caratterizzati dalla prevalenza di affioramenti di litotipi sedimentari scarsamente coerenti. Inoltre, l'introduzione nel modello di nuove variabili indipendenti, quali, ad esempio, la "densità di drenaggio non proiettata" (D_{3d}), ha dato risultati incoraggianti per una migliore stima dell'erosione per bacini caratterizzati dalla diffusa presenza di aree a *badlands*, per le quali il trasporto torbido fluviale è altamente correlato con la porzione del bacino idrografico affetta da forme di erosione accelerata dovute al dilavamento. Per questi piccoli bacini, a causa delle elevate pendenze, il reale sviluppo della rete idrografica è, infatti, sottostimato dal tradizionale parametro densità di drenaggio (D), il cui valore si ricava da misure planimetriche e non tiene conto perciò delle variazioni altimetriche. Il ruolo dominante della densità di drenaggio nella stima dell'erosione è stato confermato, infine, nel tentativo di

effettuare una zonazione dei tassi di abbassamento della superficie topografica stimati, per aree unitarie, mediante l'indice *Tu*. La tecnica proposta, denominata "*Tu grid analysis*", ha dato risultati confrontabili con quelli ottenuti a seguito del monitoraggio sul campo dell'erosione, configurandosi come un'efficace metodo di stima dei tassi di denudazione, quando misure dirette e prolungate nel tempo non sono possibili. Inoltre, anche quando sono disponibili dati misurati puntuali di variazioni altimetriche del terreno, la carta dei tassi stimati ottenuta mediante la *Tu grid analysis* propone una rappresentazione continua e validata delle intensità della denudazione per aree più ampie.

Per valutare la **suscettibilità geomorfologica** delle aree esaminate è stato applicato un metodo statistico, l'analisi condizionale, che si basa sul confronto della distribuzione delle aree attualmente sottoposte a dissesto (aree in frana, aree a *calanchi*, aree inondate) con quella dei valori dei possibili fattori predisponenti. L'indice di suscettibilità è calcolato considerando i concetti della probabilità condizionata (interpretazione bayesiana della probabilità). L'analisi condizionale è un metodo largamente usato in letteratura per valutare la suscettibilità per frana; nella ricerca descritta è stato integrato da una procedura di selezione dei fattori predisponenti che permette di scegliere in maniera più oggettiva i fattori discriminanti le aree con o senza dissesto. Tale procedura si basa sulla sovrapposizione di ciascuna delle carte tematiche dei fattori predisponenti con la carta dei dissesti rilevati, allo scopo di valutare la distribuzione di questi ultimi nelle diverse classi dei fattori. Essa è valutata attraverso alcuni parametri (la curva di Lorenz e l'indice di Gini), che permettono di evidenziare se la distribuzione dei dissesti è più o meno concentrata in poche classi del fattore studiato. I fattori sono scelti per la valutazione della suscettibilità se il valore dell'indice di Gini indica una distribuzione non omogenea degli effetti dei processi di instabilità geomorfologica nelle classi dei fattori. Sono scartati, infine, alcuni fattori quando la distribuzione dei loro valori è altamente correlata con la distribuzione delle classi di un altro fattore selezionato. Il metodo proposto ha dato risultati soddisfacenti nell'analisi di suscettibilità per frana e per erosione accelerata dovuta al dilavamento dell'Alta Val d'Orcia, risultati validati mediante un metodo statisticamente basato, noto in letteratura. L'uso di dati vettoriali ha permesso, inoltre, di ottenere carte di previsione facilmente interpretabili,

prospettando un possibile utilizzo della metodologia proposta nelle politiche di gestione del territorio.

L'integrazione del metodo di valutazione della suscettibilità geomorfologica con la *Tu grid analysis* ha, infine, permesso di mettere a punto una procedura di **analisi della pericolosità per erosione accelerata** dovuta al dilavamento, in cui la previsione spaziale è effettuata mediante l'analisi di suscettibilità, mentre la previsione dell'intensità dell'erosione è affidata all'applicazione dell'indice di erosione Tu.

Parallelamente ai metodi di stima indiretta e previsione dell'erosione, sono state applicate diverse tecniche di **monitoraggio degli effetti dei processi di erosione**, con lo scopo di identificare i principali agenti morfogenetici responsabili del modellamento delle aree di studio, e quantificarne l'intensità. In particolare, le misure dirette e indirette dell'erosione (rilevamento geomorfologico, analisi foto-interpretativa, monitoraggio della superficie topografica mediante caposaldi, rilevamento sui versanti mediante GPS differenziale e analisi fotogrammetrica digitale) sono state effettuate principalmente per validare i risultati ottenuti a seguito delle stime indirette dell'erosione e delle analisi di suscettibilità e pericolosità geomorfologica. Oltre a ciò, tali indagini hanno contribuito alla comprensione dell'applicabilità delle diverse tecniche di quantificazione dell'erosione alle diverse scale spaziali e temporali, permettendo di fare alcune osservazioni sul grado di incertezza connesso con l'applicazione di ciascuna tecnica. L'estensione dell'area in studio, la disponibilità di tempo e di altre risorse e la risoluzione dei dati necessaria per l'analisi, sono stati certamente gli aspetti più critici da considerare nella scelta del metodo più appropriato. Misure di grande precisione e dettaglio nel tempo e nello spazio (con errore dell'ordine del millimetro) sono state fornite dal monitoraggio mediante caposaldi, ottenendo dati puntuali generalizzabili alle aree adiacenti in simili condizioni topografiche e di uso del suolo. Per aree di studio e intervalli temporali più ampi, quindi, sono stati applicati il rilievo mediante D-GPS (a scala di versante) e l'analisi fotogrammetrica (a scala di piccolo bacino idrografico), tenendo presente però l'incremento dell'ordine di grandezza dell'errore connesso con i risultati ottenuti.

Infine, ulteriori considerazioni sono scaturite dall'analisi dei **fattori predisponenti l'erosione accelerata** nelle aree a *badlands*.

Il regime pluviometrico ha un'influenza preponderante nell'evoluzione delle aree a badlands, come osservato a seguito del confronto effettuato tra i risultati del monitoraggio e l'andamento delle precipitazioni in un'area del bacino del F. Tevere (località Bargiano): l'erosione dovuta al dilavamento prevale quando eventi piovosi seguono periodi secchi, mentre eventi gravitativi (che generalmente provocano il collasso delle sponde dei gully più incisi) prevalgono a seguito di piogge su substrato già saturo (piogge primaverili). Inoltre, in posizione di inter-rill, in cui prevale l'azione delle acque dilavanti, eventi pluviometrici brevi e intensi sono i più efficaci.

Le caratteristiche fisico-chimiche del substrato non bastano a spiegare le differenze morfologiche delle aree a *badlands* riscontrate nelle aree esaminate (presenza di *calanchi* o *biancane* o forme intermedie), ma risultano piuttosto essere in relazione causale con i diversi tassi di erosione misurati. Le aree a *calanchi* mostrano tassi di erosione dovuti all'azione delle acque dilavanti meno accentuati rispetto alle aree a *biancane*, dove invece la maggiore dispersività del substrato argilloso comporta la maggiore facilità ad essere asportato che lo caratterizza, anche a basse energie delle acque correnti superficiali, come risultato dalle analisi geochimiche della frazione pelitica dei campioni prelevati in alcune aree a *biancane* in alta Val d'Orcia. D'altro canto, nelle aree a *calanchi* prevale l'asportazione di materiale dovuta a movimenti gravitativi, in particolare colamenti, confermata dalle frequenti variazioni positive della superficie topografica nei morfotipi monitorati; tale comportamento può esser messo in relazione con il maggiore contenuto in sabbia del substrato dei *calanchi*, che può favorire l'infiltrazione delle acque meteoriche rispetto allo scorrimento superficiale, provocando il veloce arretramento delle testate dei *calanchi*.

I fattori topografici e geologici (pendenza, energia del rilievo, densità e direzione delle fratture, etc.) sembrano invece essere le principali cause che guidano l'evoluzione del rilievo verso forme di erosione a *calanchi* o a *biancane*: è stato più volte riconosciuto in letteratura che i *calanchi* tendono a svilupparsi laddove i versanti sono più acclivi e prevalgono elevati valori di energia del rilievo, come conseguenza di processi morfoevolutivi; lo studio di aree caratterizzate dalla presenza di *biancane* in stadio giovanile (Riserva Naturale Lucciolabella,

Alta Val d'Orcia) ha invece confermato il ruolo dominante della presenza di un sistema reticolare di fratture su superfici debolmente acclivi per la formazione delle *biancane*.

Infine, lo sfruttamento agricolo del territorio è risultato un fattore di accelerazione della denudazione, a causa del rimaneggiamento del terreno provocato dall'aratura. L'eventuale abbandono delle attività agricole, inoltre, può comportare un'intensificazione dei processi erosivi, poiché interventi di manutenzione del territorio adeguati sono raramente effettuati.

In conclusione, le indagini svolte, oltre a approfondire la conoscenza dei processi morfogenetici e dei fattori predisponenti l'erosione agenti nelle aree a *badlands* del settore dell'Italia centrale studiato, hanno permesso di contribuire al miglioramento di alcuni metodi di misura, stima e previsione dell'erosione del suolo e dei dissesti geomorfologici. Tali metodi risultano utili ad approfondire la complessa dinamica dei processi di denudazione dei versanti e la loro intensità e sono particolarmente adatti per bacini idrografici di ambiente mediterraneo caratterizzati dalla larga diffusione di aree in erosione accelerata. In particolare, il modello integrato proposto per la valutazione della pericolosità geomorfologica, essendo finalizzato a realizzare una zonazione delle aree a diversa probabilità del manifestarsi nel tempo e nello spazio degli eventi di dissesto di una certa intensità con tecniche statistiche semplici, e insieme efficaci, si rivela molto utile ai fini della corretta gestione e pianificazione del territorio.

PAROLE CHIAVE: modellazione dell'erosione, monitoraggio, pericolosità geomorfologica, *badlands*, Italia centrale.

INTRODUCTION

Clayey terrains outcropping in many parts of Italy are frequently affected by accelerated erosion processes, producing landforms known as *calanchi* and *biancane* and generally considered as ‘‘badlands’’ by non-Italian authors. The term badland was originally proposed in the “Encyclopaedia of Geomorphology” to describe “*an extremely dissected landscape difficult to cross on horse-back and agriculturally useless”* (Fairbridge, 1968), and this classical definition was particularly referred to the typical landscape of South Dakota in the United States. *Calanchi* badlands are composed of an extremely dissected, rapidly developing landscape, characterized by rill and gully landforms and a very dense dendritic drainage network (Alexander, 1980). *Biancane* badlands appear as clay domes dissected by rills up to about 20 m high (Torri et al., 1994; Torri and Bryan, 1997; Calzolari and Ungaro, 1998). The term “*biancana*” (from “bianco” Italian for “white”) probably comes from the presence of thenardite (Na_2SO_4) crystals on their surface, due to precipitation from capillary waters. The badlands formation and dynamics are mainly the result of the action of the particularly aggressive climatic factors (such as the strong climatic constrasts of the Mediterranean rainfall regime) on weak substrata (clay, silt and sand of the Plio–Pleistocene marine cycles) (Moretti and Rodolfi, 2000). The morphogenetic activity is not only limited to channel erosion, but it is also due to piping and repeated superficial slides (Bryan and Yair, 1982), so that it should be better to consider the *calanco* as the result of a ‘‘combined erosion’’ process (Zachar, 1982). Also, areas where the natural equilibrium has been disrupted by wrongly applied land use techniques can be transformed into badlands with *‘‘…processes and resulting landforms resembling those in naturally-developed badlands*’’ (Torri et al., 2000). The term currently refers to areas of unconsolidated sediment or poorly consolidated bedrock with little or no vegetation, which are useless for agriculture because of their intensely dissected landscape (Gallart et al., 2002).

Badlands are frequently considered to be landscapes that are characteristics of dryland areas. Semi-arid badlands are frequent throughout the Mediterranean, the better-known examples being located in various parts of Spain and southern Italy (Alexander, 1982; López-Bermudez and Romero-Díaz, 1989; Calvo- Cases and Harvey, 1996; Solé-Benet et al., 1997;

Piccarreta et al., 2006; Desir and Marín, 2007). Nevertheless, they also occurred in wetter areas, as in central Italy, where high topographic gradients, bedrock weakness and high-intensity rainstorms coexist, as underlined in different studies (Alexander, 1980; Farabolini et al., 1992; Moretti and Rodolfi, 2000; Lupia Palmieri et al., 2001; Del Monte et al., 2002; Ciccacci et al., 2003, 2008, 2009; Del Monte, 2003; Buccolini et al., 2007; Della Seta et al., 2007; 2009) that led to define the *calanchi* and *biancane* badlands as erosion "hot spots" (Della Seta et al., 2007; 2009).

Badlands geomorphology has been studying for the last 30 years, and there exists a considerable literature on the subject. The growing interest in studying badland dynamics reflects the need to increase knowledge of geomorphologic processes and dynamics in subhumid badland areas, particularly because of their importance in generating extremes of water and sediment production (Gallart et al., 2002; García-Ruiz and López Bermúdez, 2009).

In this context, soil erosion measurement, estimation and prevision still represent a challenge for scientists (Lupia Palmieri, 1983). As summarized by Nadal Romero and Regüés (2010), the literature reviewed could be classified into three groups according to the main purpose of the research: (1) soil erosion and hydrological processes; (2) regolith dynamics and morphological processes; and (3) vegetation dynamics in subhumid badlands. The first group, focusing on the study of soil erosion and hydrological processes, is the best represented, through the measurement, interpretation and modelling of hydrological and erosion processes and sediment production (at hillslope or small-basin scale). The second group addresses the study of morphological and regolith dynamics and properties, normally in small plots; and the third is focused on vegetation dynamics and seed dynamics (normally from slope to small-basin scale).

Field studies of soil erosion are expensive, time-consuming and data needs to be collected over many years. Though providing detailed understanding of the erosion processes, field studies have limitations because of the complexity of interactions and the difficulty of generalising from the results. Field measurements made under natural rainfall conditions are scarce because of the high cost of equipment, the hard fieldwork involved, and the prolonged study periods required to obtain representative data. Experimental catchments (few tens to hundreds of hectares) have been considered, in general, as the most practicable approach to study runoff generation, soil erosion and sediment transport

(Walling, 1991). The catchments are usually chosen to be homogeneous and lithologically and hydrologically representative of the study area. The catchments allow to study the hydrological response during individual rainstorms and over long periods of time, the areas of active erosion, the connectivity between sediment sources and channels, and the role of different processes such as weathering and regolith dynamics (Nadal- Romero et al., 2007; 2008a; 2008b).

Cost-efficient methods of estimating erosion over whole catchments are required as ways of predicting erosion after disturbance or following various erosion management strategies. Thus, the indirect estimation and the prevision of erosion rates is still one of the main research topics of the scientific community in the field of geomorphology and is far from solved.

This Ph.D. research project is aimed at defining an integrated methodology of denudation intensity estimation and prevision, for areas greatly affected by badlands, and it is based on both quantitative geomorphic analysis and multivariate statistical investigations, in order to deepen the relationships between the main denudation effects and the potential causal factors favoring geomorphologic instability in badlands areas.

Erosion rate estimations were performed refining some empirical equations ("*Tu* Denudation index"), that estimate the suspended sediment yield (*Tu*) as a function of morphometric parameters related to drainage network and relief (Ciccacci et al., 1981, 1986), as an exponential increase of *Tu* with the areal ratio of badlands to the whole catchment was proved to exist (Della Seta et al., 2009). In this research, *Tu* denudation index improvement was performed by means of some best fits and a spatially distributed application. Geomorphological susceptibility evaluation was performed applying a multivariate statistical method based on conditional analysis (Bayesian interpretation of probability) integrated by a proposal of a new method for most influential causal factors selection. The integration of denudation intensity estimation (*Tu* denudation index) and the spatial prevision of areas prone to the development of instability landforms allowed the proposal of a method finalized at the evaluation of the water erosion hazard (a spatially distributed prevision of *calanchi* badlands, and associated erosion rate, occurrence).

In this frame, different techniques of direct monitoring of erosion rates and processes have been preformed, with the aim of identifying the main geomorphic processes acting in the study areas and quantifying their intensity. In particular, direct measurements were used to validate the results obtained after indirect erosion rate estimations and susceptibility and hazard assessment models application.

As this research project is focused mainly on methodological objectives, well-known study areas have been selected, in order to compare the results gradually achieved with the earlier available data. In fact, I have applied different erosion evaluation methods in some areas of the Tyrrhenian sector of central Italy in, particularly within the Tevere and Ombrone river basins (Fig. 0.1), where long lasting geomorphologic investigations had been performed during other research projects conducted over the last three decades within the Earth Sciences Department of Università degli Studi di Roma "La Sapienza" (Ciccacci et al., 1981, 1986, 2003, 2008, 2009; Del Monte et al., 2002; Del Monte, 2003; Della Seta et al., 2007; 2009).

This work has been organized as a series of independent studies, reported in single chapters, each of them showing its own material and methods, results and discussion sections. In each study, an introduction upon the most widely diffused analogue methodological approaches available in literature is given. Some of the presented investigations has already been published or submitted for publication in international journals and presented during International scientific Conferences. The chapters have been, in turn, grouped into two principal parts: the former (Part I) presents the results of field monitoring at different spatial scales and laboratory analysis, the latter (Part II) the results of denudation modelling studies. In this frame, investigations from the Part I, together with previous studies, represent an essential scientific knowledge of geomorphological processes acting in the studied badlands areas, and, thus, a basis to propose and validate the indirect methods described in Part II.

Chapter 1 presents the main geological, climatic and geomorphological characteristics of the study areas, which have been selected in Upper Orcia Valley (southern Tuscany,

within the Ombrone River Basin) and in an abandoned cropland in Bargiano site (located in Umbria, within the Tevere River Basin), and which represent small sub-catchments or hillslopes widely affected by badlands developed on uplifted Plio-Pleistocene marine clays. Geomorphological features of Upper Orcia Valley were gathered from field survey and aerial photos interpretation, conducted over different spatial scales, and was useful in identifying the major acting morphogenetic agents.

Thus, in Part I, the results of direct erosion monitoring with pins (§ 2) are presented, and, in § 3 they are compared with rainfall trend and a reconstruction of the geomorphic evolution following cropland abandonment (by means of D-GPS survey and geostatistical analysis) for a sample hillslope of Tevere River Basin (Bargiano site), in order to highlight the effects of rainfall variations and land use changes on denudation rapidity (Vergari et al., submitted a). From single landform and hillslope scale, the investigations are moved to a small (about 4 km^2) subcatchement scale (§ 4), where the performance of digital photogrammetric analysis in evaluating large time span erosion rates was analysed during a research collaboration with Università del Molise (Aucelli et al., 2010).

In § 5 an attempt to identify the most important factors conditioning the different erosion landforms, and related erosion rates, was performed, taking into account the possible cause/effect role of grain size, mineralogical and geochemical composition of badland parent material of some Upper Orcia valley sediment samples (Vergari et al., submitted b).

Erosion modeling is dealt with in Part II, where erosion intensity is estimated refining *Tu* denudation index equations (§ 6), and attempting a zonation of estimated erosion rates, by means of a grid analysis. The estimates are here validated considering the results of direct monitoring. Susceptibility analysis is performed through the analysis of geostatistical spatial relationships between the physical determining factors and the effects of the denudation processes (the erosion landforms). To this aim, conditional analysis is applied to evaluate landslide susceptibility of Upper Orcia Valley in § 7, preceded by a new procedure for selecting the most influential causal factors (Vergari et al., 2011). Finally, § 8 presents a proposal for water erosion hazard assessment methodology, applicable in areas widely affected by badlands, in which erosion rates of badland areas is estimated through *Tu*

denudation index, while spatial probability of *calanchi* badland occurrence is computed by means of the susceptibility assessment method described in § 7.

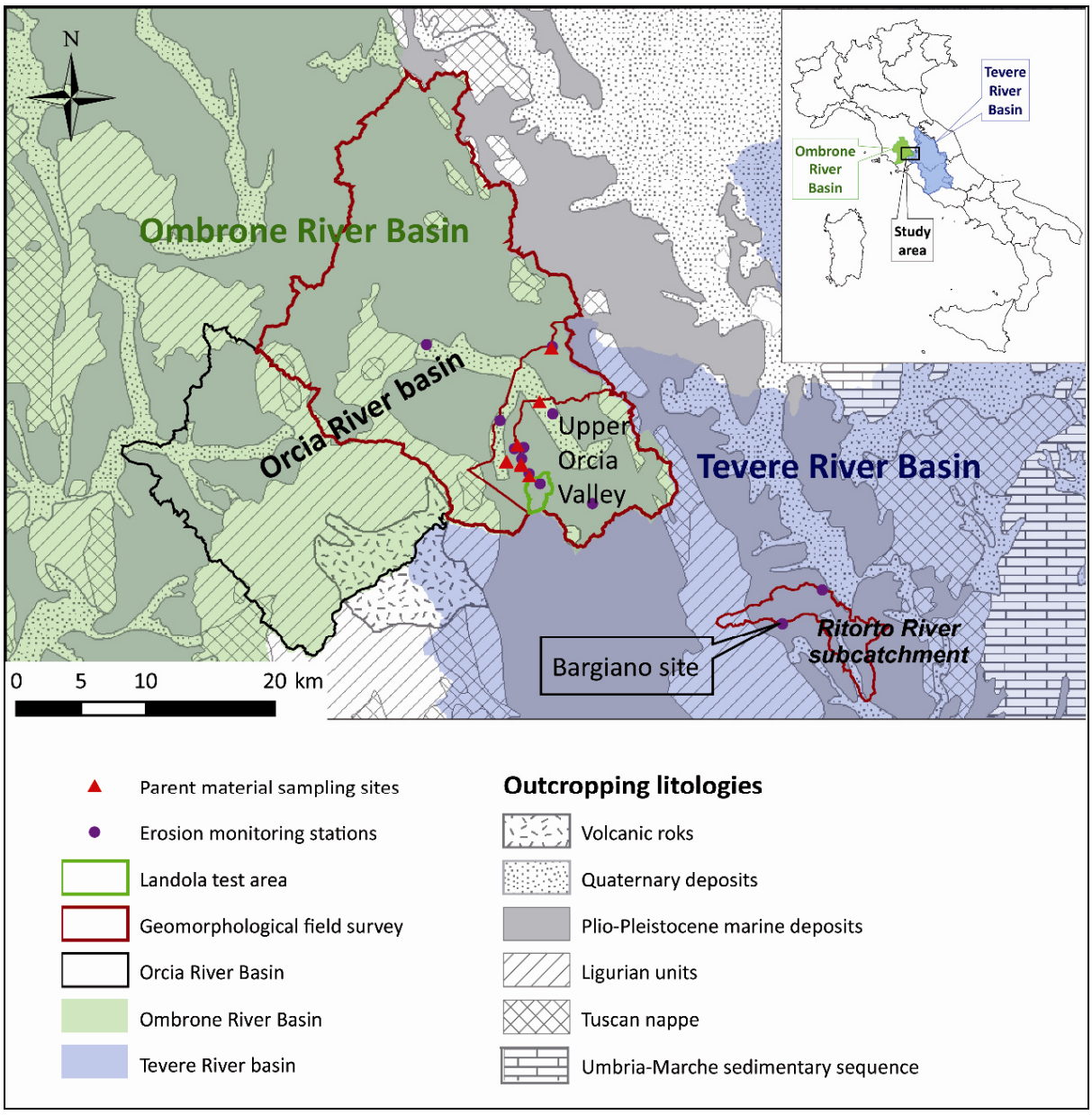

Fig. 0.1 – Location of the study area and monitoring and sampling sites.

1 STUDY AREAS AND GEOMORPHOLOGICAL SURVEY

The erosion evaluation methods have been applied in some key areas affected by badlands located in central Italy, in particular within the drainage basins of Tevere River and Ombrone River basins, where a series of geomorphological studies have been conducted over the past two decades, aimed at the quantitative direct and indirect evaluation of denudation processes (Ciccacci et al.,1981,1983, 1986, 1992, 2003, 2008, 2009; Marini, 1995; Del Monte et al., 2002; Del Monte, 2003; Del Della Seta et al., 2007, 2009).

The choice of well-known study areas was driven by the necessity of refining the used methodologies through the comparison between the obtained results with the available data, in order to focus the aims of the research project on methodological integrations and/or innovation, beside a deepening of the geomorphological processes occurring in the study areas.

In particular, many indirect denudation evaluation methods have been applied in the Upper Orcia Valley (Southern Tuscany), where a relevant dataset of erosion measures was available (Del Monte et al., 2002; Del Monte, 2003; Ciccacci et al., 2003, 2008; Della Seta et al., 2007, 2009). Even so, direct monitoring was carried on in these areas during the three-years research project, at different spatial and temporal scale, as erosion monitoring, different scale geomorphological survey, remote sensing and DGPS survey, with the aim of deepening the comprehension of the entity and velocity of the denudational processes.

During the last years, the field monitoring program, that started about 20 years ago (Marini, 1995; Ciccacci et al., 2003, 2008; Del Monte, 2003; Della seta et al., 2007, 2009) and that was concentrated on the study of natural badlands, has been integrated with the study of a semi-natural site, the Bargiano sample area, located within the Tevere River Basin. In this area, the quantification of the effects of cropland abandonment and rainfall variations on gully development and denudation rates was attempted for a sample hillslope that underwent cropland abandonment (§3).

1.1 Geological setting

The study areas present similar geological features and are located within the Neogene Radicofani and Chiani-Paglia-Tevere graben. These are tectonic depressions, bordered by listric faults, origined during the Miocene extensional tectonic phase (Ambrosetti et al., 1979; Liotta, 1996; Mancini et al., 2003-2004), and filled with thick marine, lacustrine and continental deposits (Martini et al., 2001). The geological evolution of the study area is responsible for widespread outcrops of lithological units very prone to denudation (Fig. 1.1).

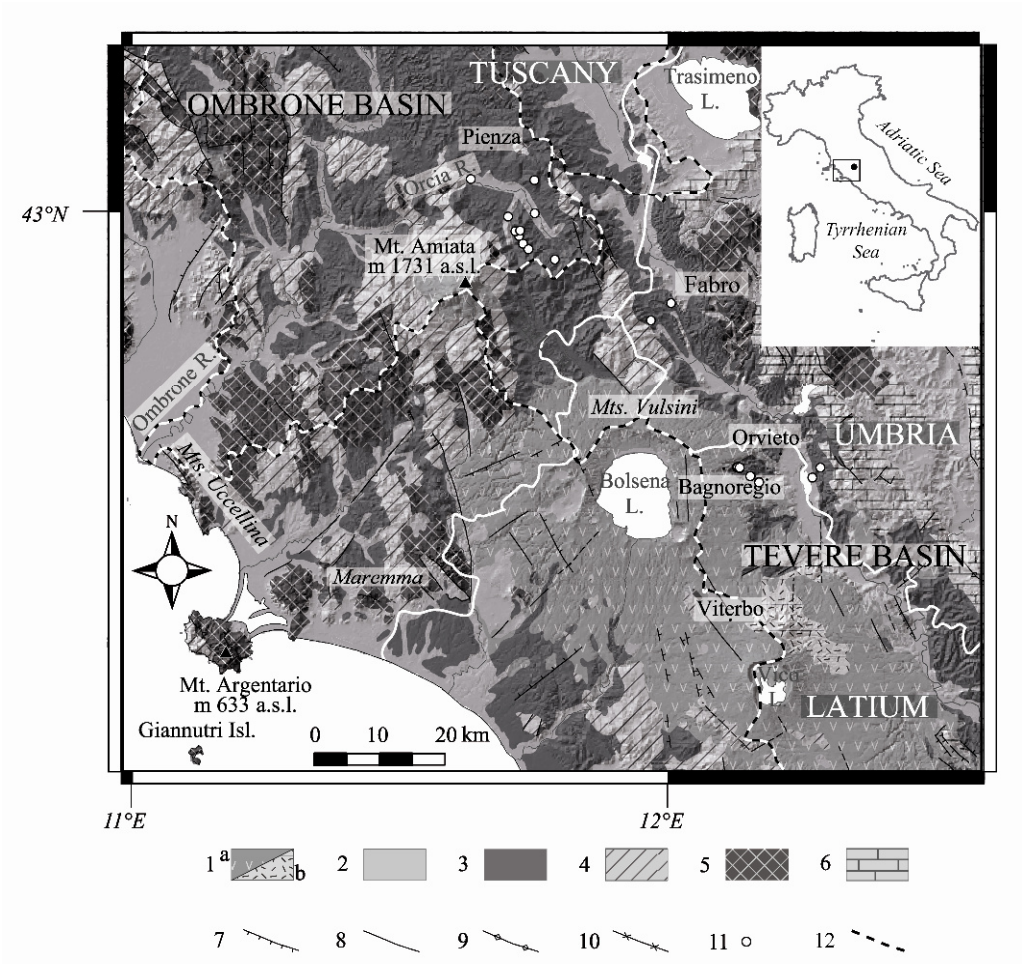

Fig. 1.1: Geological sketch of the study area. 1) (a) Quaternary silica undersaturated to intermediate volcanic rocks; (b) Quaternary (and subordinate Pliocene) acid volcanic rocks; 2) Quaternary undifferentiated continental deposits; 3) Plio-Pleistocene terrigenous marine deposits and Messinian evaporites; 4) sedimentary and metamorphic units of Ligurian and sub-Ligurian nappes (Trias to Lower Cretaceous); 5) sedimentary and metamorphic units of Tuscan nappe (Paleozoic to Miocene); 6) Umbria–Marche sedimentary sequence (Trias to Tortonian); 7) Normal fault; 8) Undetermined fault; 9) Axis of anticline; 10) Axis of syncline; 11) Monitoring sites; 12) Major river basin divides.

The emplacement of the Apennine orogenic wedge (Oligocene to Tortonian) led to the formation of major morphostructures oriented mainly NW-SE and made up of sedimentary sequences (Umbria-Marche sequence, Tuscan Nappe, Ligurian and Subligurian Nappe) overthrust towards the NE. The later collapsing phase started in the Late Miocene, and extensional tectonics, affecting the Tyrrhenian margin of the Italian peninsula, activated several NW-SE-striking normal faults that define a system of horsts and grabens (Baldi et al., 1994; Carmignani et al., 1994) cut by SW-NE transfer faults (Liotta, 1991) (Fig. 1.2). A marine transgression led to the deposition of a Plio-Pleistocene sequence of clay, sands and conglomerates within the major depressions: Radicofani Graben, Val di Chiana Graben and Tevere Graben (Barberi et al., 1994) (Fig. 1.3). Inland, the extensional basins are filled with lacustrine to fluvio-lacustrine continental deposits. During the Quaternary, the Plio-Pleistocene marine deposits were uplifted to several hundreds of meters above the present sea level (Liotta, 1996). This strong uplift was related to pluton emplacement and widespread volcanic activity along the Tyrrhenian side (Acocella and Rossetti, 2002), evidenced by the alignment of many volcanic complexes. Quaternary uplift has been particularly strong along the southern margin of the Radicofani Graben, where locally marine deposits crop out at 900 m a.s.l. (from the Mt. Amiata-Radicofani neck on the western side to Mt. Cetona on the eastern slope of the study area).

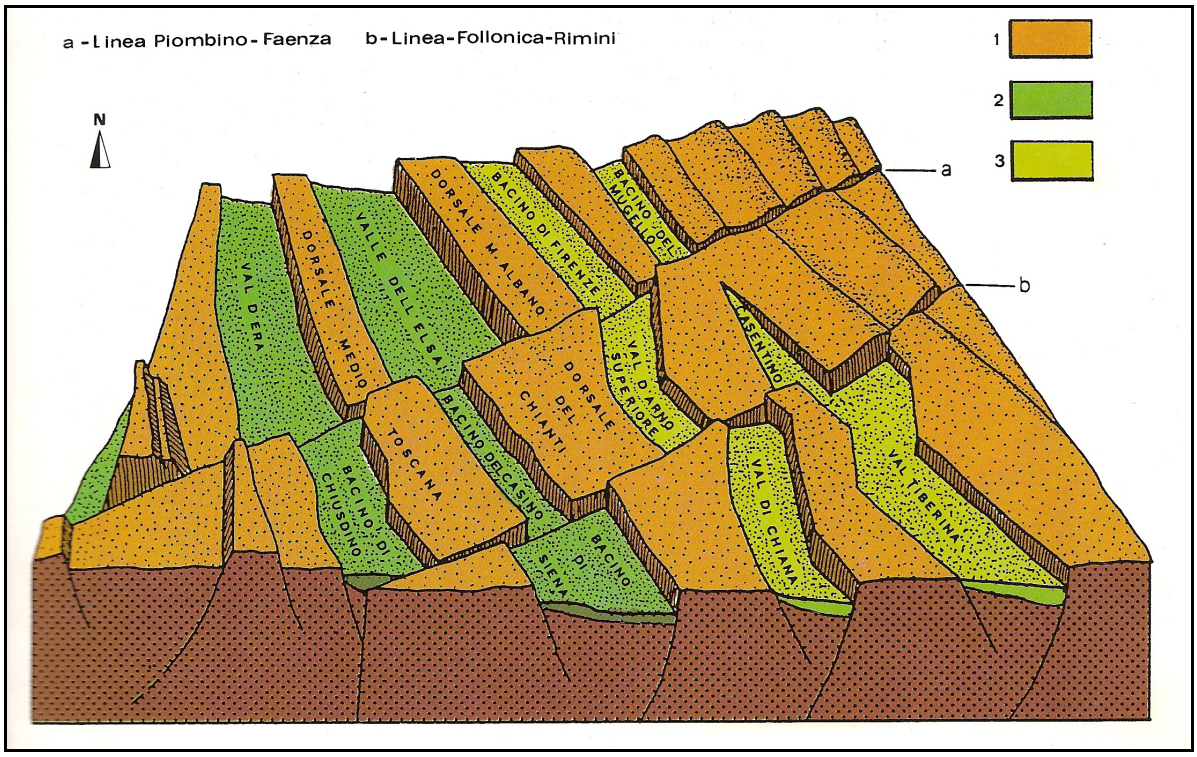

Fig. 1.2: Distribution of pliocene sedimentary basins. Symbols: 1) emerged areas, 2) marine sedimentation, 3) lacustrine sedimentation (Lazzarotto, 1993).

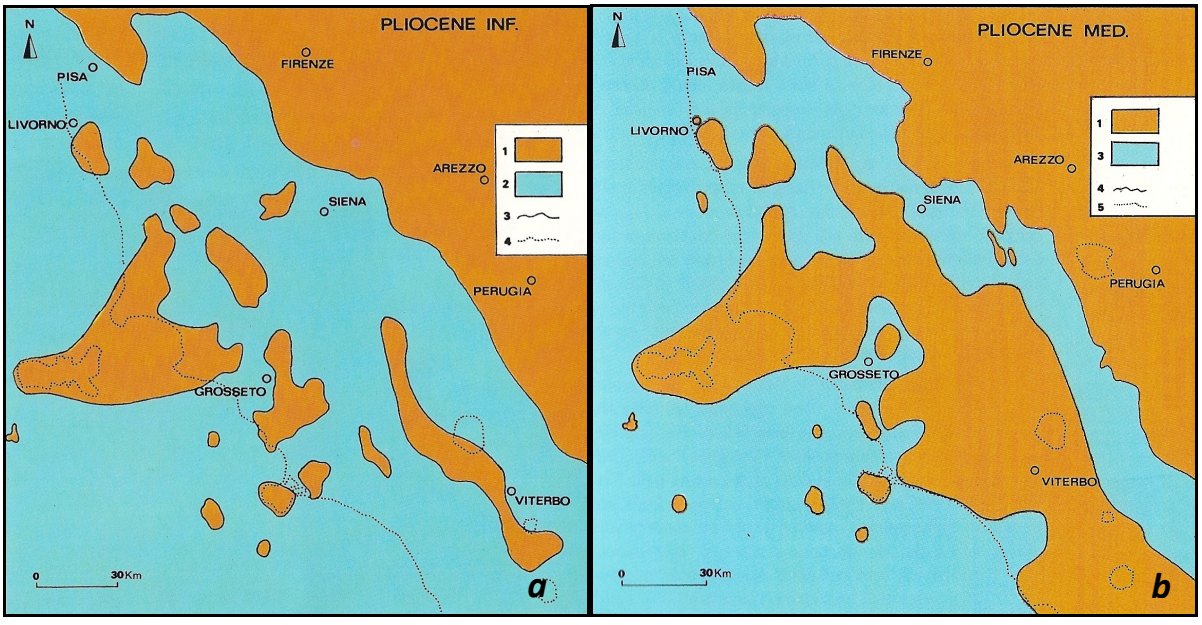

Fig. 1.3: Paleogeography of Tyrrhenian side of central Italy during Early (a) and Mid Pliocene (b). Symbols: 1) emerged areas, 2) submerged areas 3) coastline, 4) present coastline and lake limits (after Ambrosetti et al., 1979).

1.1.1 Upper Orcia valley outcropping lithologies

Upper Orcia Valley is located within the Radicofani Graben. This depression represents the southern prolongation of the Siena sedimentary basin (Fig. 1.3) and is separated from it by the Pienza - S. Quirico d'Orcia ridge. To the East and to the West it is bounded respectively by the Mt. Cetona – Mt. Rufeno and Amiata – Castell'Azzara ridges, while to the South it is linked to the Tevere Graben.

The main sedimentation phase occurred during Pliocene, superimposing the precedent allochthonous tectonic units, and forming the following stratigraphic sequence (from the top to the bottom):

- Continental deposits (Holocene)
- Quaternary volcanic rocks
- Pliocene marine deposits
- Units of Ligurian nappe (Cretaceous-Paleocene)
- Units of Tuscan nappe (Triassic-Jurassic)
- Metamorphic complex (Paleozoinc-Triassic)

METAMORPHIC COMPLEX

It includes Paleozoic and Triassic lithotypes, recognized by means of drillings performed on the eastern side of Mt. Amiata. Starting from the top, slightly metamorphosed sandstone and conglomerate, phyllite and limestone (called "A" Formation) were found, within which a "B" formation formed by phyllite and slightly metamorphosed sandstones with Devonian dolomitic limestone levels was recongnized (Bertini et al., 1991). At the base of "A" Formation, the "C" Formation was found, prevalently characterized by limestone and dolomitic limestone.

TUSCAN NAPPE

Calcareous and dolomitic rocks, outcropping on Mt. Cetona in very thick deposits (Fig. 1.4). The older formations are characterized by stratified Rhaetic limestone with marly beds, dolomite and dolomitic limestone (Calcari a *Rhaetavicula contorta*); overlain by Liassic massive grey limestone, cherty limestone and red ammonitic limestone (Lias), *Posidonia*

marl (Dogger), and chert (Malm). The youngest formation of the Tuscan Series outcropping in the area is the so-called "Scaglia Toscana", characterized by Cretaceous-Oligocenic varicoloured marls and manganese-shales.

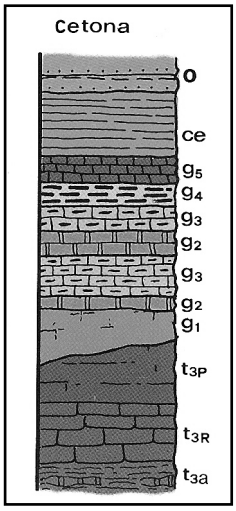

Fig. 1.4: Stratigraphic sequence of Tuscan series on Mt. Cetona. Cretaceous-Oligocene: O) "Formazione del Macigno", ce) Tuscan nappe formation; Siliceous and calcarous formation: g_5) Radiolarite and limestone with *Aptici*, g_4) Marl with *Posidonomya*, g_3) Cherty limestone, g_2) Red ammonitic limestone, g_1) Massive limestone, t_{3p}) Liassic massive grey limestone, t_{3R}) Rhaetic limestone with marly beds, t_{3a}) Burano anhydrite formation and cavernous limestone (Lazzarotto, 1993).

LIGURIAN NAPPE

Two allochthonous formations overlay the Tuscan serie's lithologies. The first one is a thick sequence of claystone, marly claystone, marl and white-greyish cherty limestones thinly-bedded, known as *Palombini* Formation. Ophiolites commonly occur in this Lower Cretaceous sequences.

The *Pietraforte* formation, late Cretaceous-Paleocene in age, overlies the *Palombini* Formation and has a less clay-rich composition. The sequence is formed alternatively of calcarenite, calcilutite, and carbonatic sandstone with silty and clayey interbeds.

NEOGENIC SEDIMENTARY DEPOSITS

A marine transgression led to the deposition of a Plio-Pleistocene sequence of clay, sands and conglomerates within the Radicofani Graben, while, inland, the extensional basins were filled with lacustrine to fluvio-lacustrine continental deposits. This group is prevalently made of marine claystone deposited during the Pliocene marine ingression and that cover most of the sample area and represents the initial marine filling of the Graben. The claystone and sandy claystone (early Pliocene) are several hundred meters thick, and it is easy to find interbeds of graded sands and poorly cemented conglomeratic lenses. More recent Pliocene marine deposits are made of bioclastic limestone with *Amphistegina*.

The claystone outcrops in the central part of the graben, whereas the coarser deposits more commonly outcrop along the eastern and the western boundaries of the watershed.

QUATERNARY VOLCANIC DEPOSITS

These deposits are related to the Quaternary volcanic activity of the Radicofani volcano, situated in the southern-most sector of the Orcia River basin. The age of the volcanic activity is dated to 1,3 ± 0,003 Ma (D'Orazio et a., 1991; Liotta, 1996) by $^{40}Ar/^{39}Ar$ method. Today, the only preserved part of the Radicofani volcano is a neck made of trachybasalts and olivine-latite, with olivine-trachytic scorias (Pappalardo et al., 2001), surrounded by a volcanic debris deposit, up to 2 km^2 wide, that testify the original volcano dimension.

The western sector of the watershed, nearby Piancastagnaio and Abbadia S. Salvatore towns, is characterized by the outcopping of the Mt. Amiata rhyodacite, origined after the effusive activity of this volcano.

QUATERNARY CONTINENTAL DEPOSITS

These deposits are made of volcanic debris, travertine (linked to the S. Casciano dei Bagni thermal springs) and alluvial deposits. Pliocene deposits are ascribable to early huge landslides occurred on dip slopes.

In the Orcia River and its tributaries, the alluvial deposits are very widespread. In fact, streams show an important bed and suspended load; the solid load on the river-bed of streams draining the upper basin is made of cobbles generated by the dismantling of flysch and Pliocene sands and conglomerate, frequently rounded by older erosional cycles.

1.1.2 Bargiano site outcropping lithologies

Bargiano site is included in the Chiani-Tevere graben. The Fabro Formation is the prevalent outcrop and is characterized by a thick clayey deposit, whose bottom is not still known. Higher marine claystone, about 350 m thick, are tilted to ENE and has sandstone with *Flabellipecten* at the top.

Alluvial deposits are very widespread along river valleys due to the high river sediment yield, while effusive rock and pyroclastic deposits are present in the southern sector of the area, products of Pliocene activity of Mt. Vulsini.

1.2 Climatic setting

Two main climatic features characterize the study area: the sea distance and the altitude.

Barazzuoli et al. (1993) described climatic setting of southern Tuscany considering 4 sites representative of 4 different altimetry categories: coastal plain, inland hilly zones and mountain zone. Fig. 1.5 shows the Siena climograph, representative of a hilly zone. Monthly mean values of the De Martonne (1926) index of aridity (I_a) allows to characterize a site defining slow transitions between arid, semiarid, and humid environments or periods:

$I_a = 12p/(t+10)$, where p is mean monthly precipitation in millimeters and t is mean monthly temperature in degree.

According to Barazzuoli et al. (1993), Siena climograph (Fig. 1.5) shows that the winter half-year is cold and humid, while the summer half-year results in the warm and arid zone.

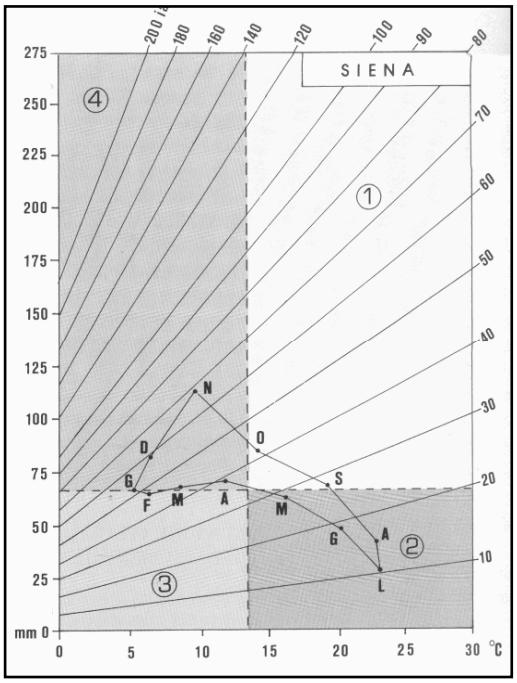

Fig. 1.5: Siena climograph (after Barazzuoli et al., 1993). 1) warm and humid period; 2) warm and arid period; 3) cold and arid period; 4) cold and humid period.

1.2.1 Monitoring sites

Climate data from the 1951-1996 records at several significant stations within the eastern Ombrone River Basin are summarized in Table 1.1. The mean annual rainfall (696 mm) is below the national average (970 mm/a), although its values during the considered time span are discontinuous. Rainfall is heavier in the colder half of the year than in the summer, with a maximum in November and a minimum in July. The most consecutive rainy days are recorded in autumn. The mean annual temperature is around 14°C, and the thermal regime indicates an annual range of about 18°C, with a maximum in July.

As for Bargiano site, mean annual rainfall (1328 mm a-1over 84.5 rainy days) is instead above the national average and seasonal distribution shows the maximum concentration in autumn (418 mm over 18.5 rainy days) with a secondary peak in the spring season (Western Tevere Basin in Tab. 1.1). The minimum rainfall is recorded in July and the mean annual temperature is 14.3 °C, with autumn season slightly warmer than spring (mean seasonal temperature is respectively 20°C and 17°C).

A detailed description of pluviometric data recorded at Orvieto station is described in §3 for Bargiano, where the role of rainfall variations on erosion rates is analyzed.

	Eastern Ombrone Basin (1951-1996)	**Wester Tevere Basin (1920-1996)**
Mean annual rainfall (mm)	696	875
Minimum annual rainfall (mm)	510	446
Maximum annual rainfall (mm)	960	1493
Absolute minimum monthly rainfall (mm)	31 (July)	29 (July)
Absolute maximum monthly rainfall (mm)	93 (November)	122 (November)
Mean annual temperature (°C)	14.4	12.5
Minimum monthly temperature (°C)	5.5 (January)	4.6 (January)
Maximum monthly temperature (°C)	23.3 (July)	22.2 (August)

Tab. 1.1 – Climatic data of the study areas (after Della Seta et al., 2009).

Considering the Upper Orcia valley, mean annual rainfall depth, recorded at La Foce pluviometric station (550 m a.s.l.) for 1951-1999 period, amount to 738 mm, with non-significant diminishing trend (Fig. 1.7). As shown in graph of Fig. 1.6, November is the most rainy month, with 103,7 mm, followed by October, September and December. The most rainy season is thus confirmed to be autumn, while spring and winter present a similar trend and summer shows a mean seasonal rainfall depth of 132 mm (Tab 1.2).

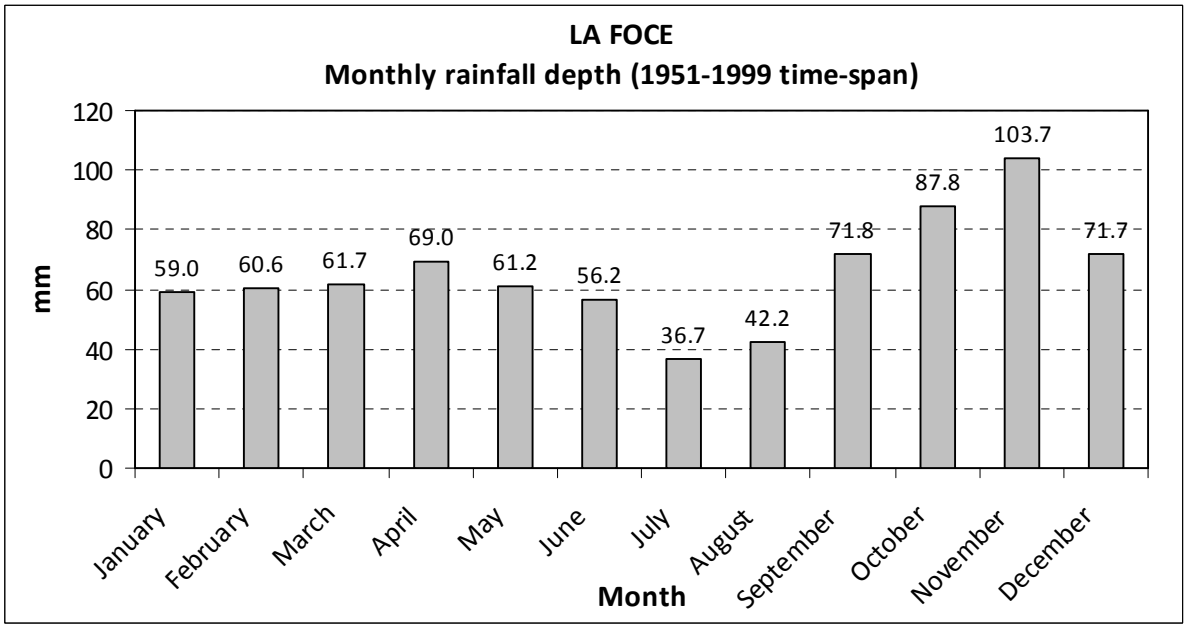

Fig. 1.6 – Mean monthly rainfall depth recorded at La Foce pluviometric station.

	Winter	Spring	Summer	Autumn
mm	191,3	191,9	132,1	263,2

Tab. 1.2 – mean seasonal rainfall depth, La Foce pluviometric station (1951-1999 time-span).

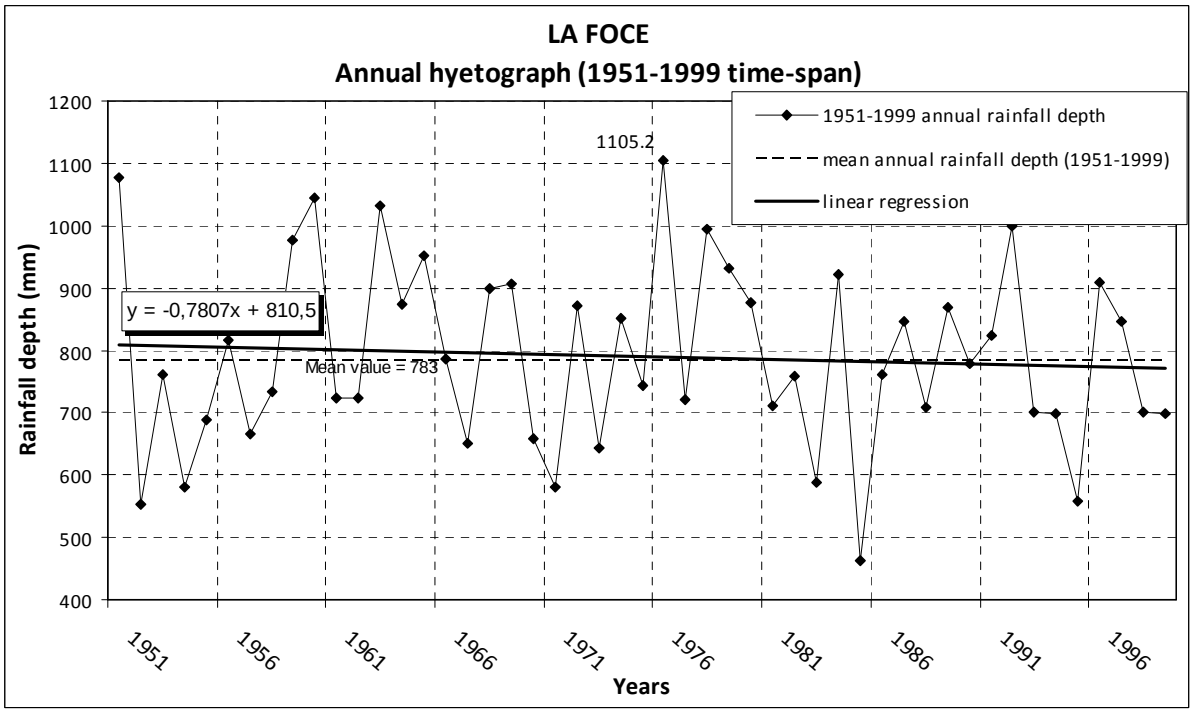

Fig. 1.7 – Annual hyetograph for La Foce pluviometric station.

Analysis of temperatures was performed considering Montepulciano station data (607 km a.s.l.).

For the 1980-1998 period, mean temperature is 14,3 °C, while mean maximum and minimum temperature values amount respectively to 10,1 and 18,6 °C. An increasing trend is recorded for the considered period, which is stronger for the maximum temperatures (about 0,17°C/a, Fig. 1.8).

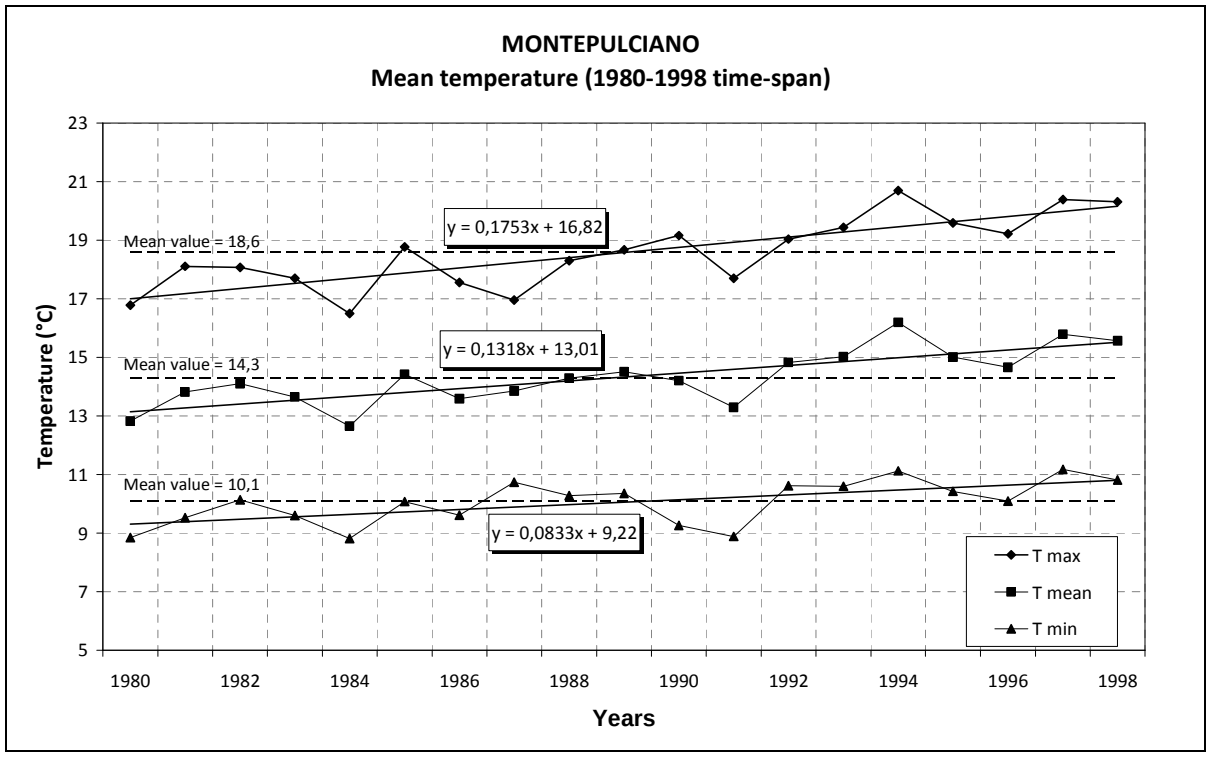

Fig. 1.8 – Annual minimum, mean and maximum temperature values recorded at Montepulciano thermometric station.

Considering the mean monthly and seasonal temperature values (Fig. 1.9), the warmer months result July and August (with maximum values of 30°C), while the colder months are January and February (minimum values of about 2,5°C), pointing out a strong mean annual temperature range.

Autumn is on average warmer than spring.

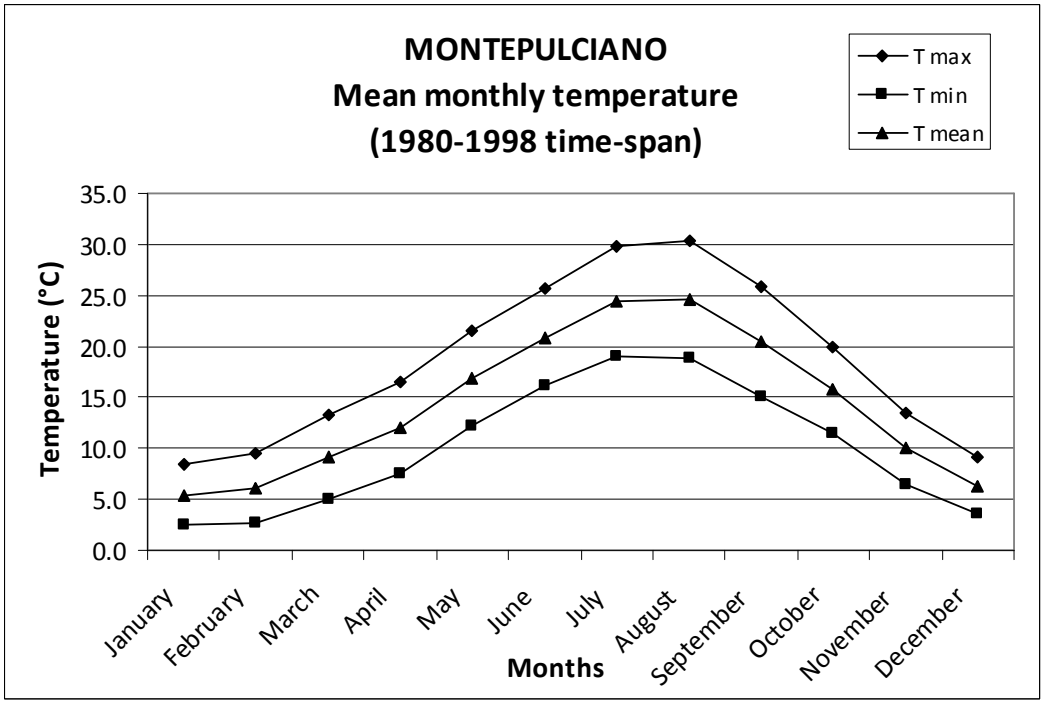

a)

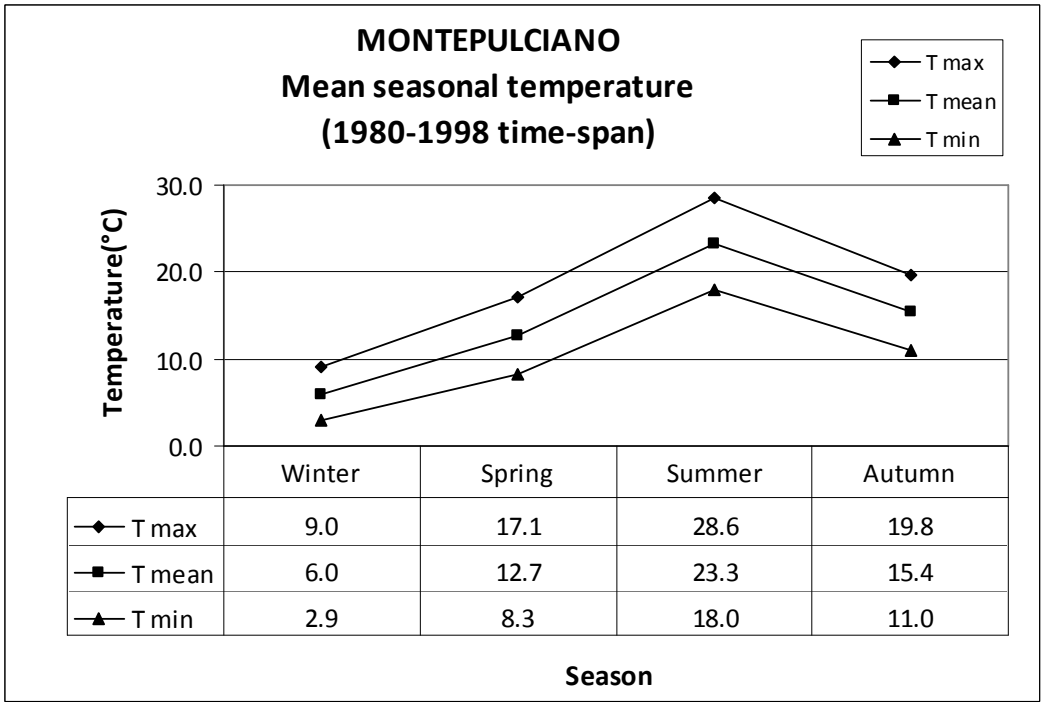

	Winter	Spring	Summer	Autumn
T max	9.0	17.1	28.6	19.8
T mean	6.0	12.7	23.3	15.4
T min	2.9	8.3	18.0	11.0

b)

Fig. 1.9 – Mean monthly (a) and seasonal (b) temperatures, considerino mean, maximum and minimum values recorded at the Montepulciano thermometric station.

In Fig. 1.10 the Bagnouls-Gaussen diagram is shown. The aridity period corresponds to July and August, as well-known for Mediterranean climate. This is confirmed in Barazzuoli et al. (1993), where the authors identfied the Orcia valley climate as a prolongation of the sub-arid climate defined for the coastal strip according to the Thornthwaite Moisture index

(1948). Even though, Orcia basin arid period is less intense and briefer than the aridity period that generally occurs in the Mediterranean coastal zones.

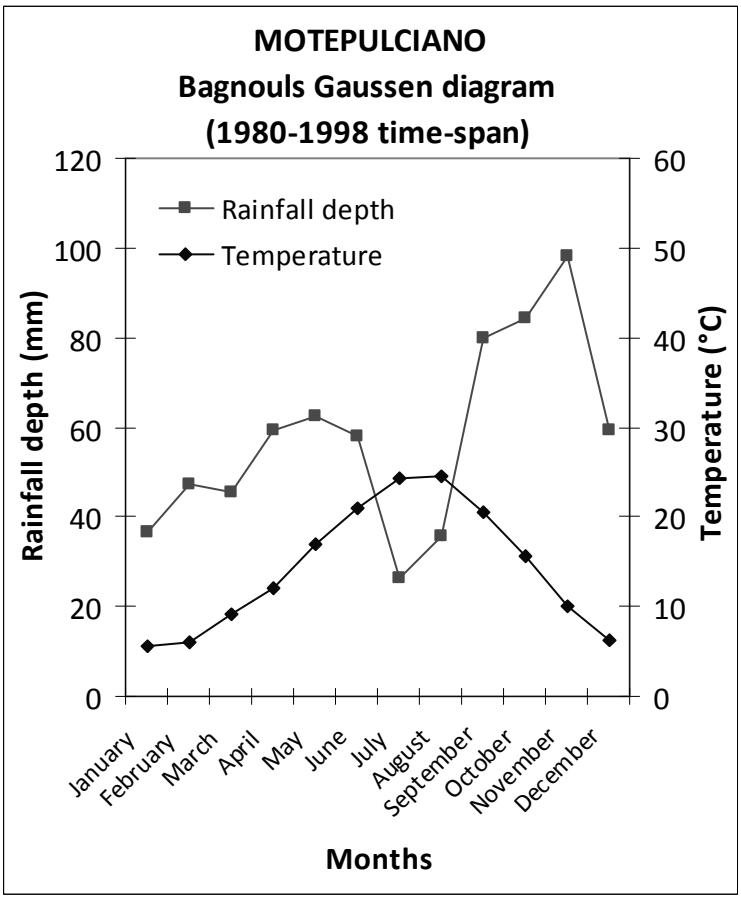

Fig. 1.10 – Bagnouls-Gaussen diagram (pluviometric data from La Foce station and thermometric data from Montepulciano station).

Finally, it has to be underlined that many sectors of the Upper Orcia valley pertain to mountainous zones, as Mt. Cetona, that riches an elevation of more than 1000 m. For this station Barazzuoli et al. (1993), using a temperature/altitude linear regression, computed a mean annual temperature value of 10°C, oscillating between the January mean value of 4°C and the July mean value of 22-23°C. For the same site, mean rainfall depth amounts to 1000-1100 mm/a.

1.3 Geomorphological setting

The following geomorphological description of the study area is performed considering the results of the field surveys carried out during previous studies in Upper Orcia Valley. Even though, during the Ph.D investigations, the mapping of the most intense geomorphological processes effects, due to gravity, runoff and human impact, was performed, by means of field survey and aerial photo interpretation, as well as also updating precedent data, at different spatial scales (Fig. 1.11):

1) for Orcia River basin, (outlet at Monte Amiata gauging station, about 580 km^2), the distribution of main hazardous processes effects was mapped at a scale of 1: 80.000 (*Annex 1*);
2) for Upper Orcia Valley (about 120 km^2, 1:10.000 scale), the map of the effects of the main hazardous processes was updated through field survey, starting from the results achieved during previous studies (results are reported and described in §7 and §8);
3) for a test area (about 30 km^2), corresponding to Miglia subcatchment and Formone-Orcia confluence area, a very detailed geomorphological survey (at a scale of 1:5.000) was carried out, that allowed to produce a geomorphological map at a scale of 1:12.000 (*Annex 2*).

This procedure was carried out in order to better define the processes that act at erosion "hot spots" badland areas and are likely to influence the values of catchment-scale denudation rates (§2). Moreover instability landforms mapped at 1:10.000 scale were used as target features to perform the geomorphological susceptibility and hazard assessment described in § 7 and 8.

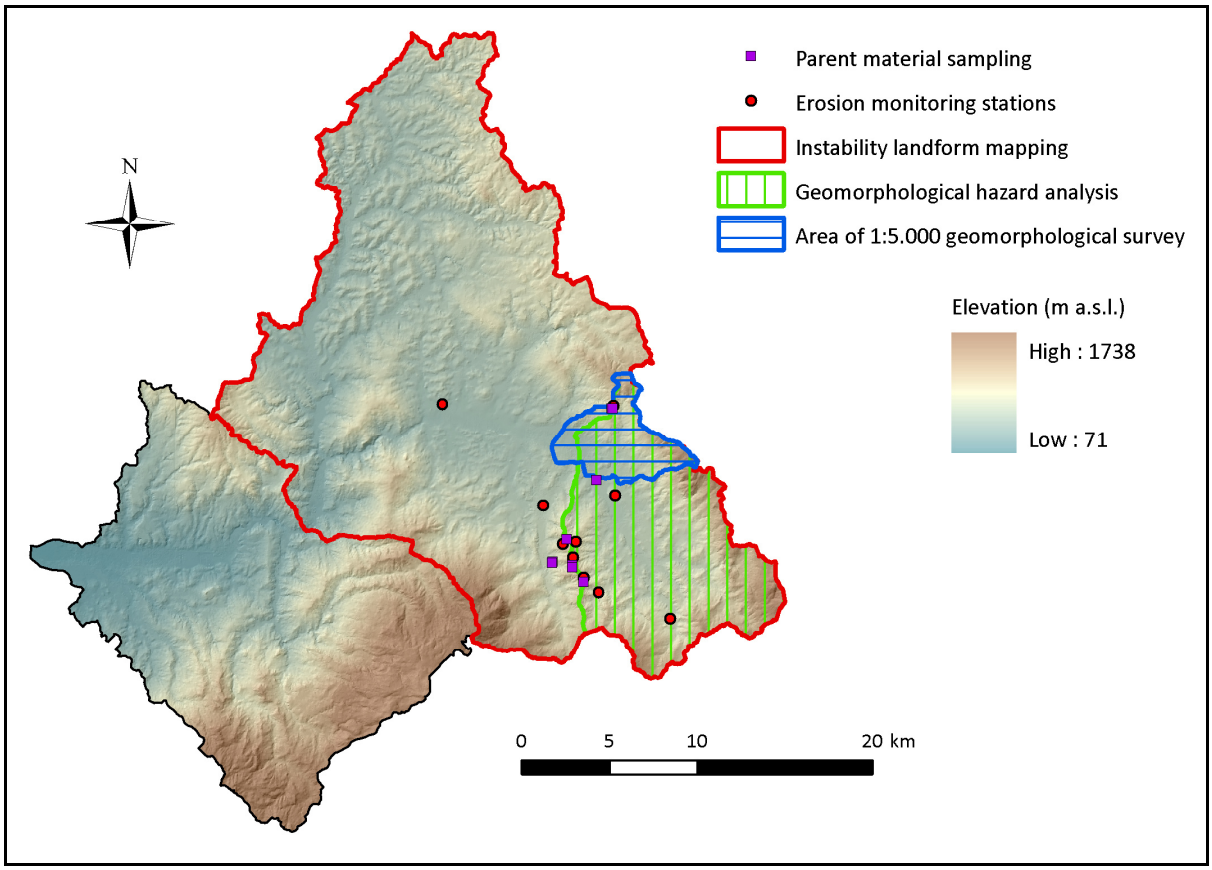

Fig. 1.11 – Location of different cartographic products in Orcia River Basin.

The variety of outcropping lithologies and the tectonic control of Tyrrhenian side of central Italy led to the development of structural landforms. The major landforms are represented by morphostructural ridges bounded by NW-SE-trending fault scarps, dipping towards the graben depressions. Minor morphotectonic elements (E.g., straight channels, saddles, straight ridges) are aligned along (and controlled by) the other structural patterns. However, the study area is characterized by hilly landscapes, with elevations rarely higher than 1000 m a.s.l., due to the widespread outcrops of soft sediments. Near fault scarps and/or where stronger rocks crop out, the landscape is more rugged and the valleys are deeper.

Fluvial erosion, together with slope denudation, contributes significantly to the morphogenesis. Numerous slopes are rapidly evolving, and the rivers show high suspended sediment load. Water erosion is pervasive, due to extensive clayey outcrops as well as to the current climatic conditions and the rapid uplift. Sheet erosion is responsible for the exposure of roots and for colluvium deposition at the slope feet. As the slope increases slightly, rill and

gully erosion prevails, contributing the most to badlands development and soil degradation. Ephemeral gullies (Foster, 1986) are often recognizable in croplands, and they grow rapidly as a consequence of concentrated rainfall. Water erosion on natural slopes leads to typical sharp- and rounded-edged badlands, locally called *calanchi* and *biancane*, respectively (Della Seta et al., 2009, and references therein).

Channelled waters are particularly effective in carving deep valleys and drainage network geometry, together with the shape of catchments, are strongly influenced by the geological structure, such as the NNW-SSE striking graben, which influence the path of the main rivers. Some fracturing patterns influence both the direction of the main valleys and the development of denudation processes. At present, clayey slopes are affected by strong morphogenesis, even leading to suspended sediment yield values among the highest recorded in Italy. Runoff is responsible for widespread "*calanchi*" and "*biancane*" badlands, and gravity causes frequent shallow and deep mass movements, even on gently dipping slopes. Sheet erosion is responsible for exposure of roots and colluvium deposition at the slope foot. As the slope increases slightly, rill and gully erosion prevail, contributing the most to badlands development and soil degradation. A detailed treatise of the different morphoevolution and denudation trends of these landforms will be given in the next subsection, as they are the main objects of this study.

Human impact has significantly affected the landscape of the study areas for a long time. Vegetation cover is sparse, even because of widespread deforestation of the hills reserved to valuable crops and grazing. Wood of tall trees is confined to the hills top or to the steepest slopes, and often it is the result of the conifer reforestation carried out since the '60 to slow down soil erosion. Most of the area is made up of sowable or uncultivated ground.

1.3.1 Monitoring sites

During the last years, the field monitoring program, that started about 20 years ago (Ciccacci et al., 2003, 2008; Del Monte, 2003; Della seta et al., 2007, 2009) and that was concentrated on the study of natural badlands (Fig. 1.12), has been integrated with the

study of a semi-natural site, the Bargiano sample area (Fig. 1.13), located within the Tevere River basin.

Natural badlands areas

The erosion hot spot study areas are characterized by a wide variety of landforms. A smooth hilly landscape marks the northern portion of the area (Southern Tuscany), where typical "*biancane*" landforms are frequent, although often reworked because of crop growing (Fig. 1.12a). They are small clay domes up to about 10 m high, mostly uncovered by vegetation on the southern usually steeper slopes, where rill erosion is particularly strong. The "*biancane*" are typically located near the foot slope as well as at the hill summit and their distribution is always associated to gently dipping slopes (Torri and Bryan, 1997; Della Seta et al., 2009). Towards the South, the presence of horst structures and/or the previously mentioned volcanic structures led to the raising of the Pliocene marine deposits at several hundred meters above sea level. Here the landscape is much rougher and the typical landforms on clayey slopes are represented by "calanchi" badlands (Fig. 1.12b). Here the slopes are generally steeper, often dampening the human activities; thus the morphosculptures are less reworked than those in the "*biancane*" zone. The clay bedrock plays a key role in "*calanchi*" development, along with bedding and caprocks. In particular, "calanchi" are more frequent on scarp slopes and their growth is supported by sandy, gravel, conglomeratic or volcanic caprocks at the summit. When caprocks are completely eroded, the slopes rapidly decrease in steepness and their parallel retreat ceases, according to the evolutionary model proposed by Scheidegger (1961, 1964).

Deep piping is widespread at several calanchi sites, especially in northern Latium where calanchi are more extensive (Fig. 1.12c). According to several authors (Faulkner et al., 2003; Romero-Díaz et al., 2007; Borselli et al., 2006), this process is favoured by land use changes (I.e. cropland abandonment) and by steep hydraulic gradients. In particular, the hydraulic gradient increase at the intersections between sub-horizontal bedding and vertical fractures. Deep pipes probably contribute significantly to denudation and evolve rapidly due to collapsing. Ephemeral gullies develop on cultivated or grazing lands, where they cause a very important path for sediment entrainment (Fig. 1.12d).

On denudational slopes several earth micropyramids are present (with vegetation cover, stones or fossil macrofauna at their summit), while other small landforms are due to piping processes. At the foot slopes, the parallel retreat led to the development of landforms similar to small pediments, as already suggested by some authors (Schumm, 1962; Guasparri, 1978, 1993; Torri et al., 1994).

Moreover, gravitational movements on slopes supply a considerable amount of material to be transported by the major rivers. Apart from some rock falls, slumps and slides occur on steep slopes. However, the influence of gravity is also evident on gentler slopes, where mudflows, soil creep and solifluction are widespread. Due to these prevailing morphogenetic processes, gently undulating slopes characterize the landscape.

Large areas of Upper Orcia Valley have been modified for human activities. Many *biancane* badland and *calanchi* badland were smoothed for agricultural purposes. Deforestation, grazing and farming are among the most important triggers for accelerated water erosion, tillage erosion and gravitational movements on slopes. Moreover, the effects of farming may become stronger if there are land-use changes related to cropland abandonment.

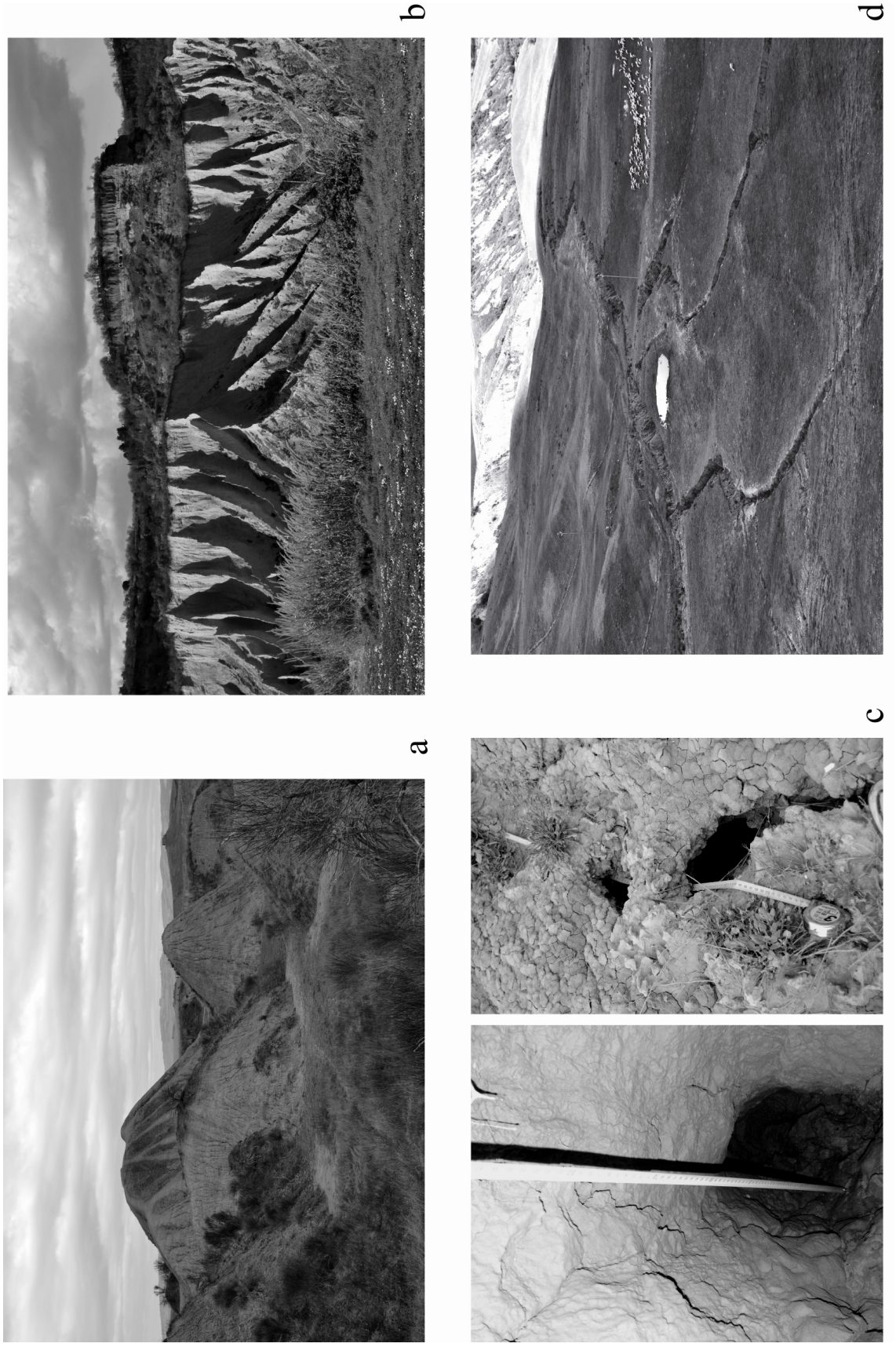

Fig. 1.12 – Some of the most widespread landforms due to accelerated water erosion in the long lasting monitoring areas: a) “biancane” badlands; b) “calanchi”; c) Deep piping at a calanchi badland site and shallow piping at the interface between the weathered pop-corn crust and the undisturbed clay; d) deep gully in a grazing land.

Bargiano site

The sample area of Bargiano is located within the Tevere River Basin (next to the town of Orvieto, Umbria) and consists of a gently dipping slope with an extent of about 4300 m^2. Up to the ’60s it was part of a calanchi badland slope, successively levelled for agricultural purposes (cereal crop). In 1980 the cropland was abandoned, with the consequence of a very rapid development of a close net of meandering rills and gullies, with a parallel geometry that follows the maximum slope direction. The site appears as a miniature catchment (Fig. 1.13a) where it is possible to study the dynamics of surface processes, such as splash erosion, runoff, rill and gully evolution (Fig. 1.13b), and frequent mass movements. More details on the denudational processes affecting the area will be given in § 3, where measured erosion rates are compared with rainfall trend and a reconstruction of the geomorphic evolution following cropland abandonment


a)

b)

Fig. 1.13 – a) Bargiano sample hillslope; b) a detail of the most incised gully.

PART I

FIELD MONITORING AND PHOTOGRAMMETRIC AND PARENT MATERIAL ANALYSES

In the most recent works, the development of indirect models for erosion prediction (Jetten & Favis-Mortlock, 2006) was accompanied by the advance in monitoring techniques (Evans, 1995) and by laboratory experiments (Bryan and Poesen, 1989). In fact, model validation was traditionally performed through direct monitoring performed on parcels or experimental catchments (Richter and Negendank, 1977; Del Monte et al., 2002; Poesen et al., 2003; Della Seta et al., 2007, 2009).

The increasing performance of geoinformatic provides high quality data at different scales when new monitoring techniques are applied such as hyperspectral remote sensing, LiDAR survey, digital photogrammetric analysis, measures of land surface elevation using high resolution GPS and electronic theodolites. Moreover advances on these techniques contribute to increase performance of soil erosion estimation models and can help their validation. Digital Terrain Models (DTM) can be constructed to evaluate elevation variations with different detail and error, depending on the method of data collecting used (Zukowskyj & Teeuw, 2000): for example they can be produced through interpolation of contour data and Differential Global Positioning System (DGPS) point data, and from Digital Photogrammetry techniques, but their applicability for erosion rates estimation has not yet completely deepen and analyzed.

In this part, the applicability of different erosion monitoring techniques is investigated by means of the simultaneous application of several methods in the study areas: besides the continuation of long-lasting erosion monitoring of erosion hotspots of Ombrone River and Tevere River basins (§ 2), an attempt of integration of the use of erosion pins and D-GPS survey has been performed for a sample hillslope located within the Tevere River Basin

(Bargiano site) (§ 3). For this area, where several erosion data were available, the role of rainfall variation on erosion rates has been deepened.

Moreover the results of monitoring with pins have been used to validate an attempt of volumetric estimation of erosion rates performed by some researchers of Molise University. This collaboration was finalized to test the applicability of digital photogrammetric analysis on erosion rates estimation for fairly large time-spans (§ 4).

Finally, textural and geochemical analyses of the parental material have been undertaken to further elucidate their properties on both bare and vegetated surfaces and to discuss them with respect to the development of different badlands processes. Clay dispersivity at different depths in the sample sites was analysed, as a well-known controlling factor of accelerated erosion, providing some interesting clue for understanding badlands processes (§ 5).

2 EROSION MONITORING WITH PINS IN UPPER ORCIA VALLEY

The areas that resulted from field survey to be affected by strong denudation have been monitored, to detect local modifications of the topographic surface with time. In fact, denudation "hot spots" (I.e. badlands) are likely to influence denudation rates at the catchment scale (Della Seta et al., 2009). Thus, understanding and monitoring the processes involved in their development is of crucial importance, especially in regard to distinguishing between on- and off-site effects of water erosion. The goal was achieved by setting up a series of monitoring stations, some of which have been working continuously since 1993 (Marini, 1995; Del Monte et al., 2002; Del Monte, 2003), while others have been active for shorter periods between 1993 and 2011. In particular, both the number of stations and the frequency of a field monitoring program, started about twenty years ago, was increased. The results of the 3-years erosion monitoring are presented here, together with a summary and comparison of the results already achieved during previous studies.

2.1 Material and methods

Field monitoring at the hillslope scale was performed using more than a hundred of monitoring stations in central Italy, where iron pins were placed in significant and poorly accessible zones, in order to avoid tampering. Metallic stakes with section of 1 cm^2 and length of at least 80 cm (Fig. 2.1a) were located at different depths and where piping is absent, in order to cross the weathered horizon in which mud cracks occur, and provided a series of local data indicating the changes occurring on the topographic surface (Marini, 1995). Many microforms, such as earth micro-pyramids, were noticed during field survey, caused by cobbles, wood fragments or gastropods' shells on top of clay rapidly shaped by surface running waters. Thus, earth micro-pyramids have been induced by placing coins on the ground surface, providing further data (Fig. 2.1b).


a)


b)

Fig. 2.1 – a) *Biancana* equipped with erosion pins. b) 2-cm high micro-pyramid induces by a shell.

In Upper Orcia Valley, uphill, downdale and lateral changes in the ground level (Δy) were measured at rill, inter-rill and on-pediment positions, both at *biancane* (hill-summit and foot-slope) and *calanchi* (with caprocks) sites. Moreover, slope retreat (Δx) was measured at pediment pins as well as on caprocks, using horizontal pins. In this study area, erosion pin stations are localized in different sites (Fig. 2.2):

1. about 60 pins, some of them working since 2004, are located in the valley floor of Formone River (a tributary of Upper Orcia River), where a residual *biancane* badlands area survives surrounded by a large remodelled ploughed field;
2. about ten erosion pins have been placed in the Lucciolabella Natural Reserve, where the residuals of the original *biancane* landscape of Upper Orcia valley is protected (Miglia subcathment);
3. about15 pins are located along the Formone-Upper Orcia divide, within *calanchi* and *biancane* badland areas.

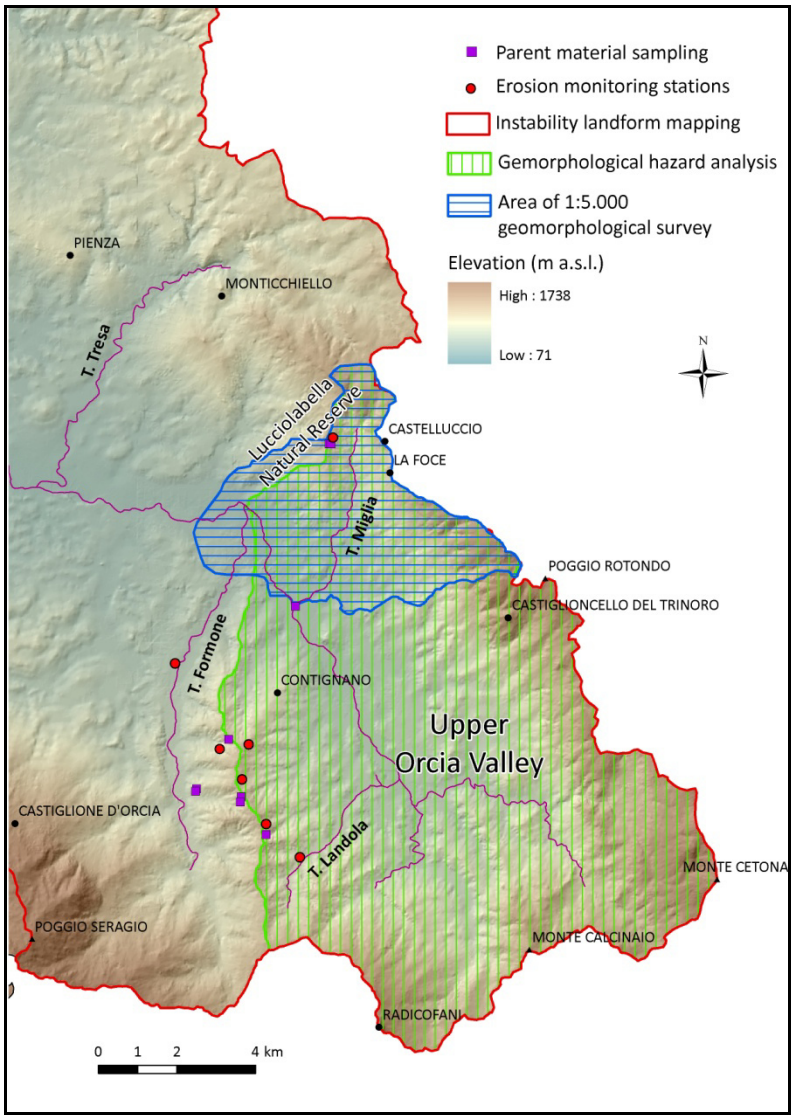

Fig. 2.2 – Location of the erosion monitoring stations in Upper Orcia Valley.

2.2 Results

In the Formone valley floor *biancane* area, pins I_0 and I_1 are located in two *biancana* sides, while pin I_7 is placed on a *biancana* pediment, measuring the *biancana* slope retreat together with the topographic surface modifications.

Pin I_0 was originally inserted near a mud-crack, that was gradually enlarged by erosion, and maybe as an effect of the pin itself. The station experienced a continuous alternation of clay accumulation within the crack and erosion, till the pin was damaged for the crack enlargement. During the 2009 summer it was moved some centimetres away on the same

biancana side (Station I_0 – new in Fig. 2.3). Untill the last measure (June 2011), in the new location a regular negative trend was recorded, whose intensity reaches 4 cm in 20 months, that corresponds to 2.4 cm/a. Until only running waters were acting, also pin I_1 experienced a regular lowering of surface level, measured in a 2.6 cm/a. During 2010 spring, an important mudflow has occurred on the monitored *biancana*, causing at the pin position a temporal cay deposit, as shown in graph of this pin in Fig. 2.3. As for the pediment pin, increases of slope retreat (up to 20 cm from 2004 to 2005), accompanied by a gradual accumulation on the micro-pediment surface, was observed spring 2009. In fact, a first mudflow in spring 2009, and then a second stronger event in spring 2010 occurred on the *biancana* slope (Fig. 2.4), causing a strong advancing of *biancana* slope.

Finally, a *biancana* slope equipped with 46 erosion pins (Fig. 2.5) was monitored, showing a regular negative ground level change, with an average of 2.4 cm/a and a maximum erosion rate of 4.8 cm/a (up to 12 cm in 30 months for pin 44). The most frequent positive oscillations have been recorded during the spring months of 2010 and 2011 (Fig. 2.6 and 2.7).

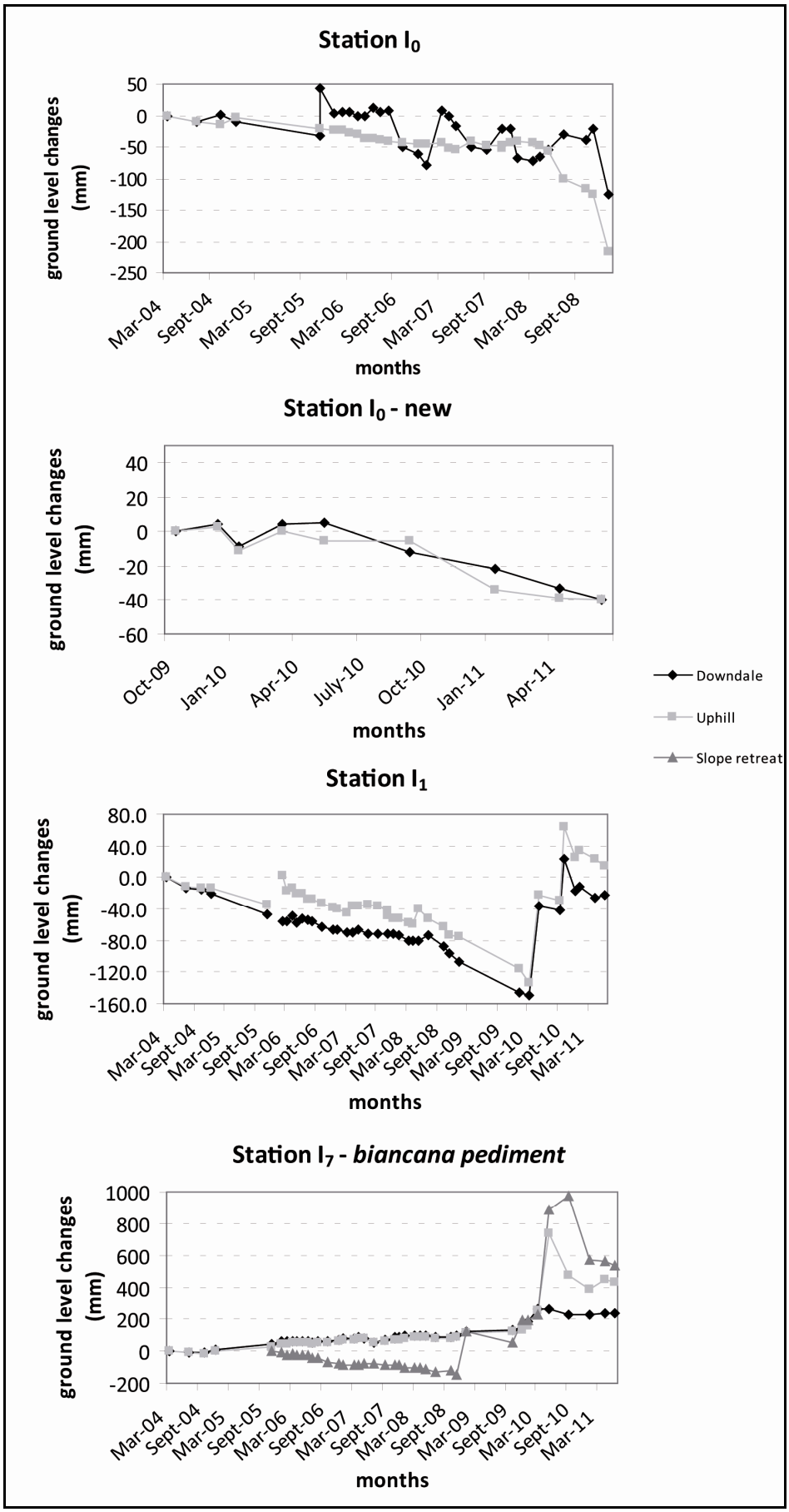

Fig. 2.3 – Erosion pins in a residual *biancane* area of Formone River valley floor.

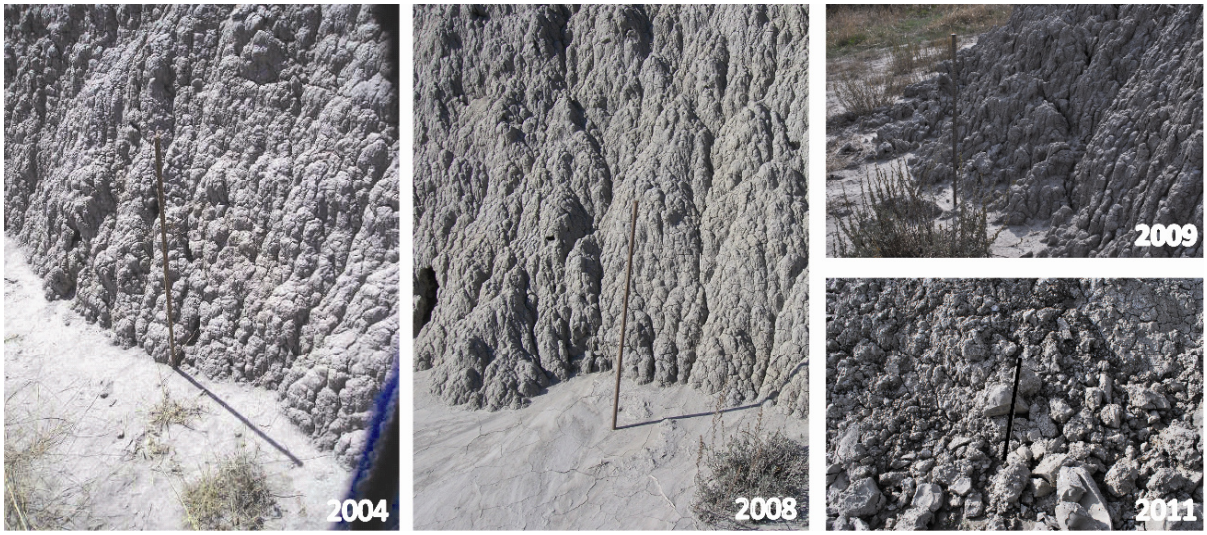

Fig. 2.4 – Slope retreat and mudflow events at I_7 station.

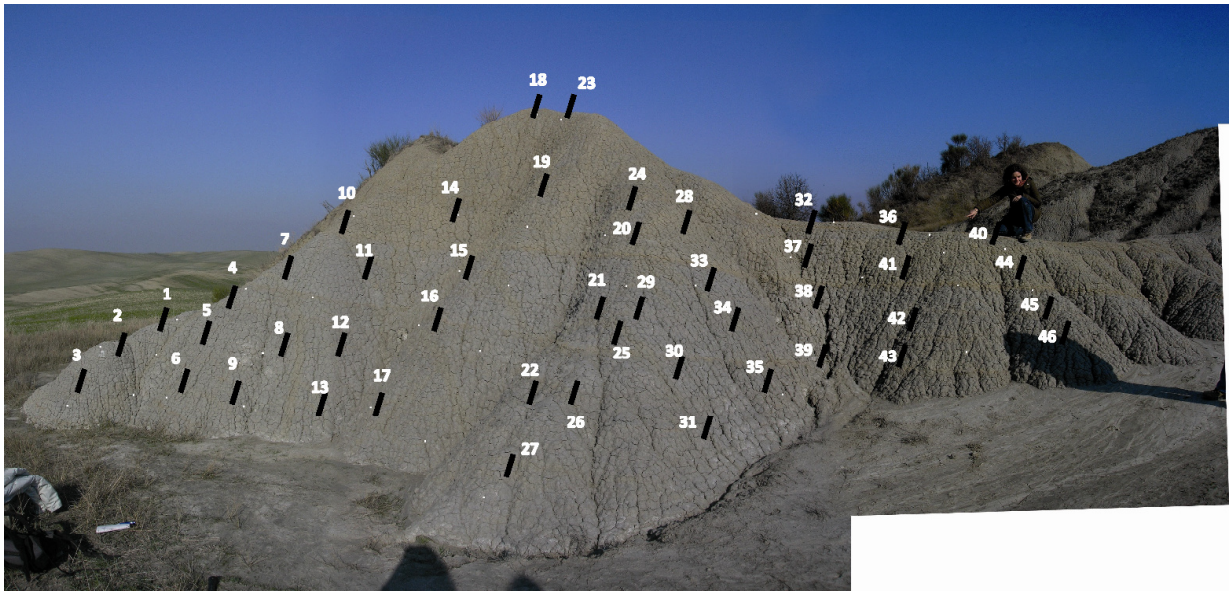

Fig. 2.5 – *Biancana* equipped with 46 erosion pins at Formone valley floor.

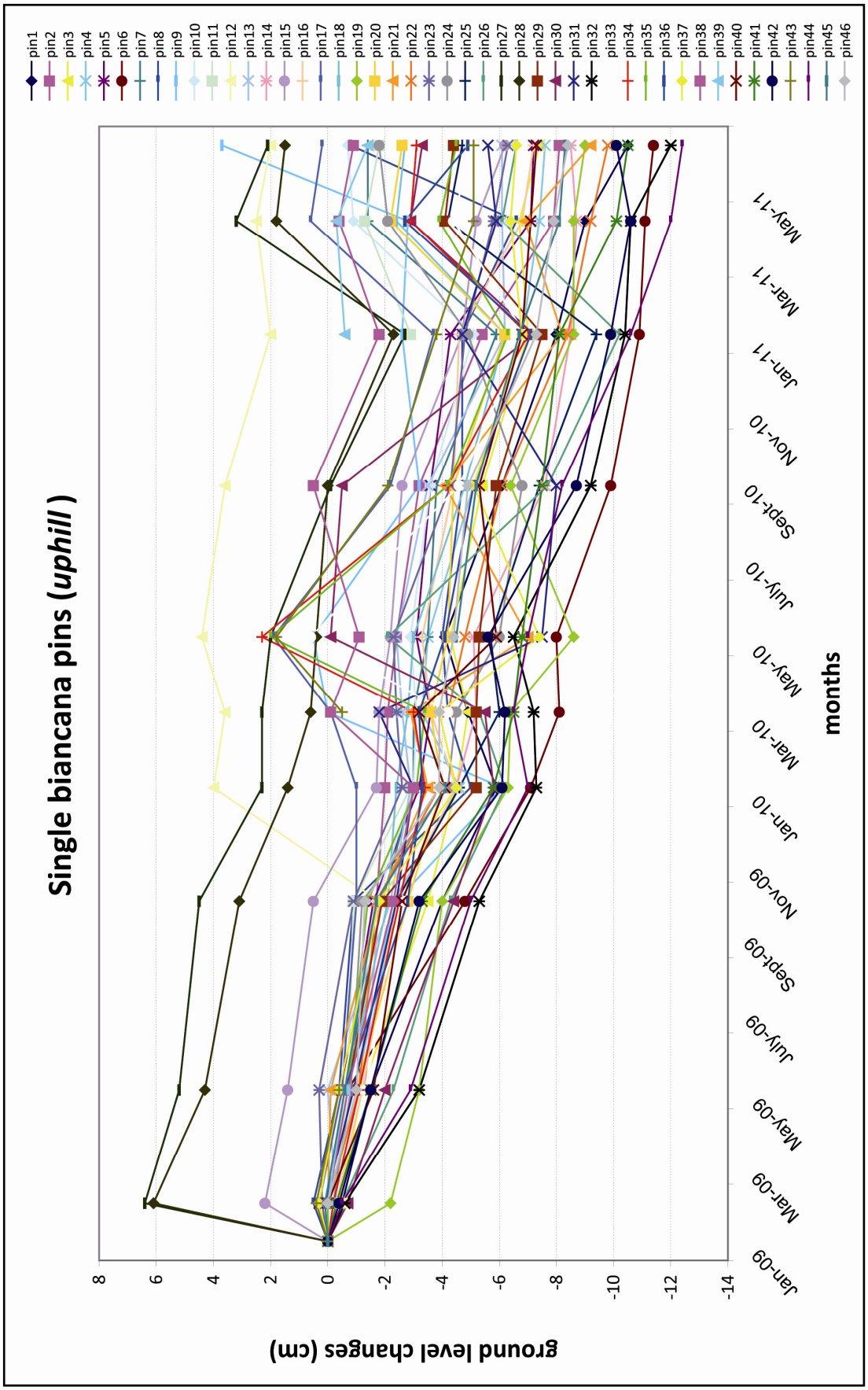

Fig. 2.6 – Uphill topographic level modifications measured by means of 46 pins located on a single *biancana* in Formone valley floor.

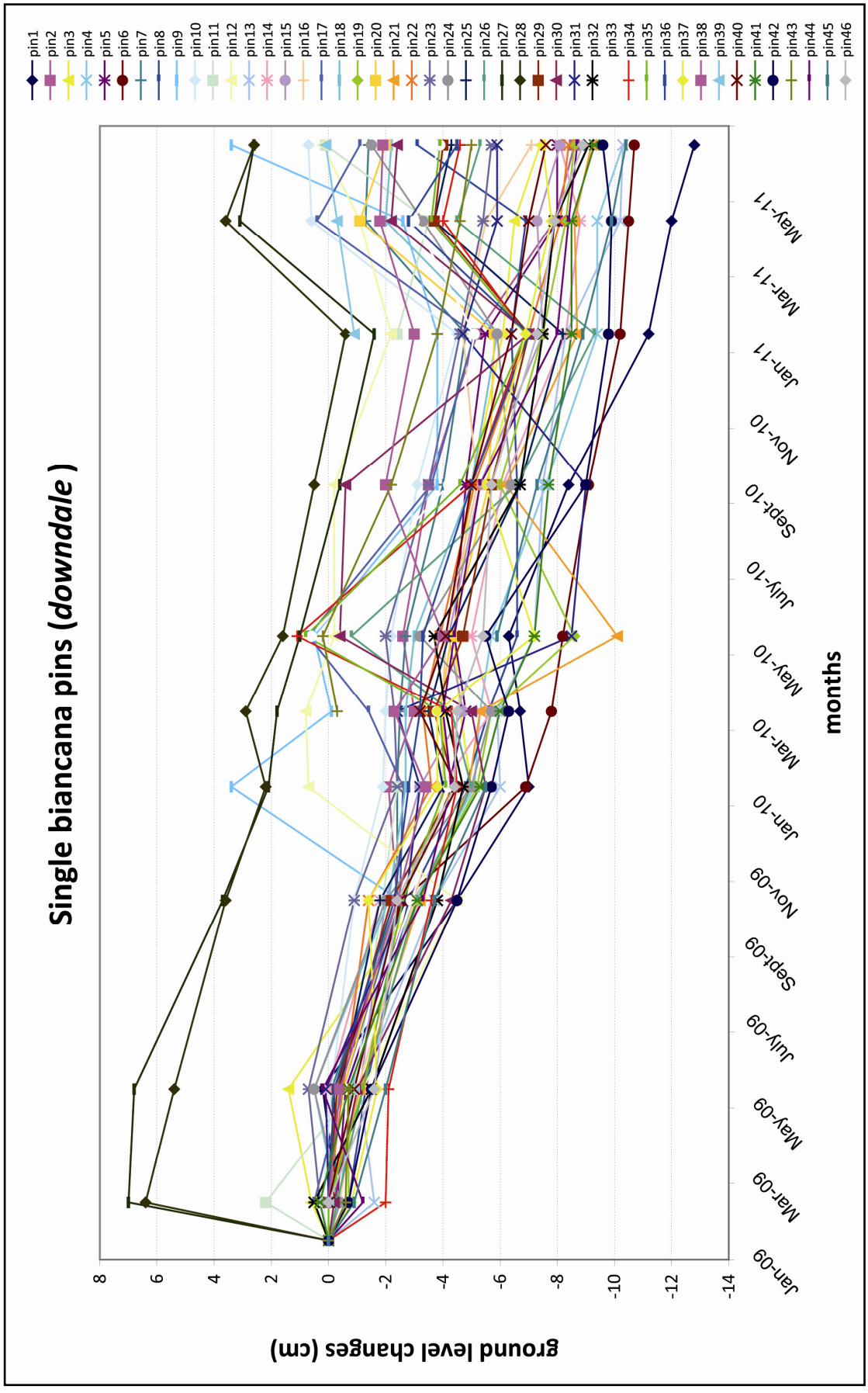

Fig. 2.7 – Downdale topographic level modifications measured by means of 46 pins located on a single *biancana* in Formone valley floor.

In Lucciolabella Natural reserve (Fig. 2.2), erosion pins have been located in a *biancane* badland area in the Lucciolabella hillslope summit (Fig. 2.8a). In this area, L_1 is placed in a *biancana* side, L_2 on a *biancana* pediment, while L_3 and other 3 (L_a, L_b, L_c) stakes are located in an area characterized by the presence of embryonic *biancane* (Fig. 2.8b). A regular strong lowering of topographic surface was observed in this site, where the maximum erosion rate was measured in the surface evolving to *biancane* badlands (Fig. 2.8b): up to 4.5 cm/a (Fig. 2.9 and 2.10). Also the *biancana* pediment of station L_2 experienced accumulation of mudflows occurrence in the *biancana* slope, while the *biancana* slope retreat was regular during all the monitoring period, reaching a rate of 4 cm/a.


a)


b)

Fig. 2.8 – a) Lucciolabella *biancane* badland hillslope. b) Portion of Lucciolabella hillslope characetrized by the presence of embryonic *biancane*.

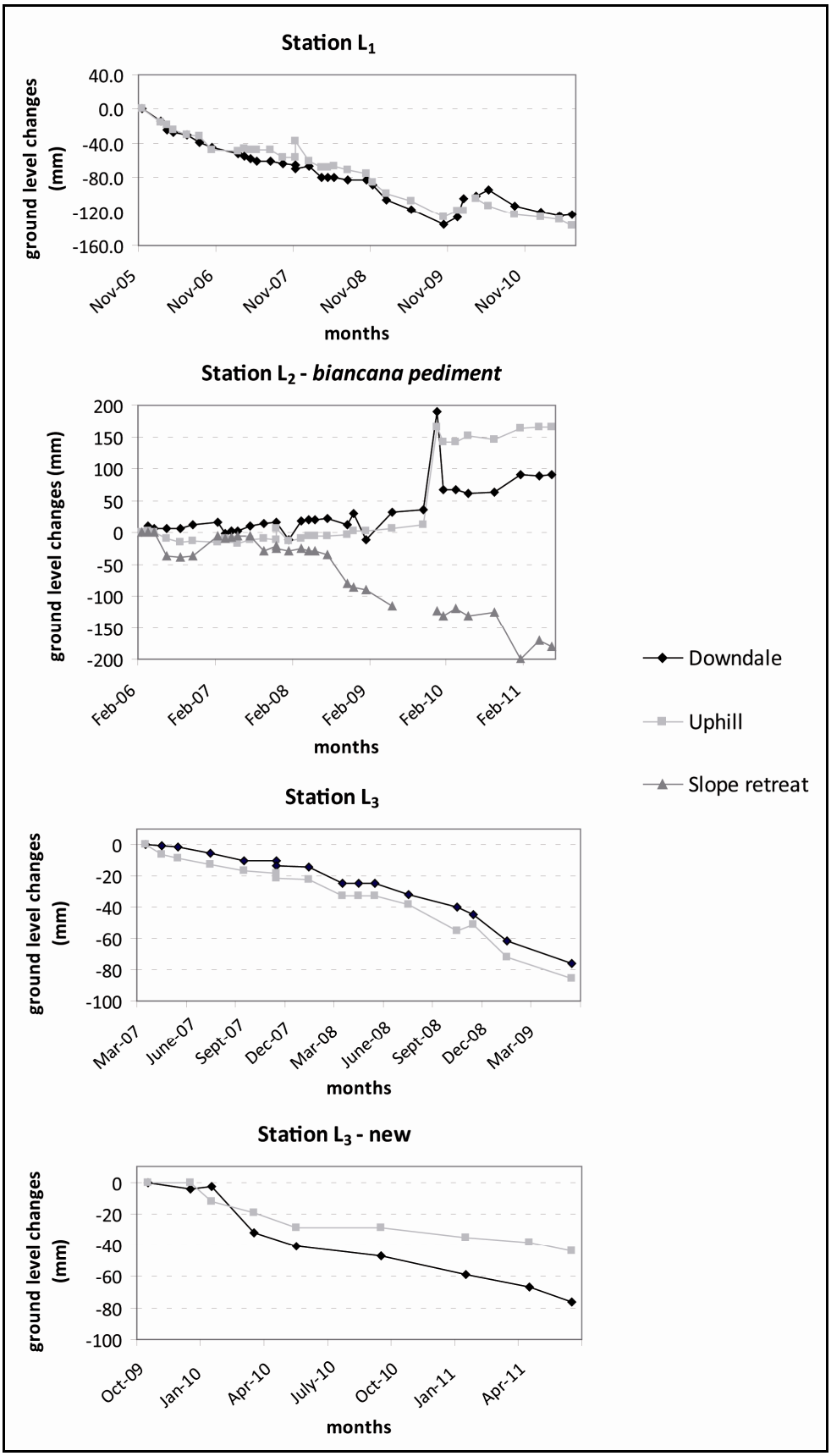

Fig. 2.9 – Erosion pins in a residual *biancane* area of Lucciolabella hillslope.

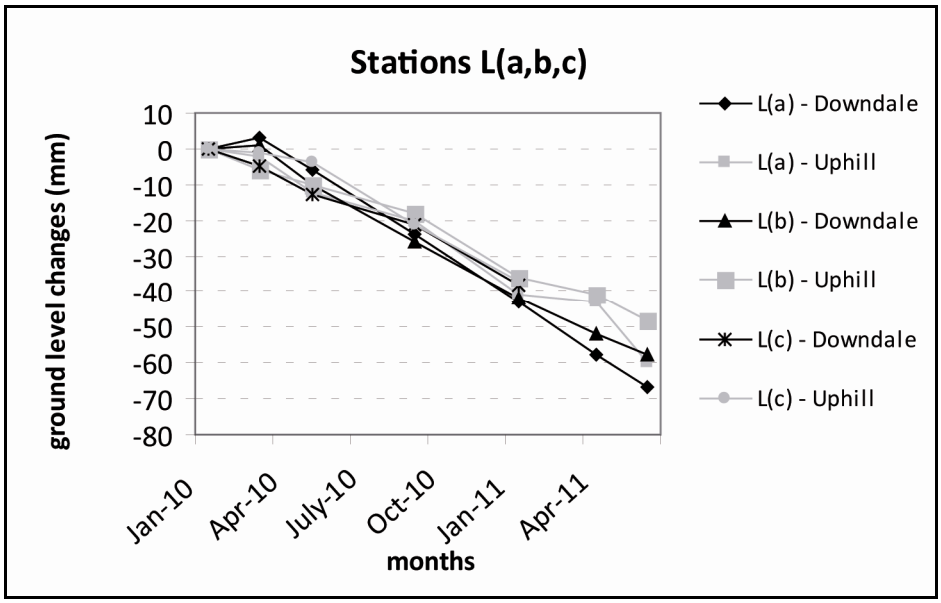

Fig. 2.10 – Ground level changes measured at L_a, L_b and L_c station in Lucciolabella *biancane* hillslope.

Stations of *calanchi* badland area (F and F_0), located along the Formone-Orcia divide, experienced a very rapid denudation, even if lower erosion rates with respect to *biancane* or embryonic *biancane* sites. Unlike other *calanchi* stations in central Italy (Della Seta et al., 2009), in Upper Orcia valley these stations were not affected by temporal accumulations due to earth sliding, since they are place in the *calanchi* with a summit sandy caprock. As underlined by Della Seta et al. (2009) for central Italy *calanchi* stations, *calanchi* slopes capped by resistant rocks generally experience higher denudation rates on the whole. In fact, the presence of caprocks probably favours runoff processes in spite of landsliding.

Station F is running since 1994 and is useful to quantify the most significant erosion rate due to runoff. The regular negative trend shown in Fig. 2.11 for the 1994-2011 time interval corresponds to a net erosion rate of 1,7 cm/a. For F_0 station, an erosion rate of 0,8 cm/a can be computed.

As for the *biancana* site of the Formone Orcia divide (F-L station in Fig. 2.11), up to 2010 a surface lowering rate of 4 cm/a was recorded, but during 2010 a slide accumulation partially buried the pin.

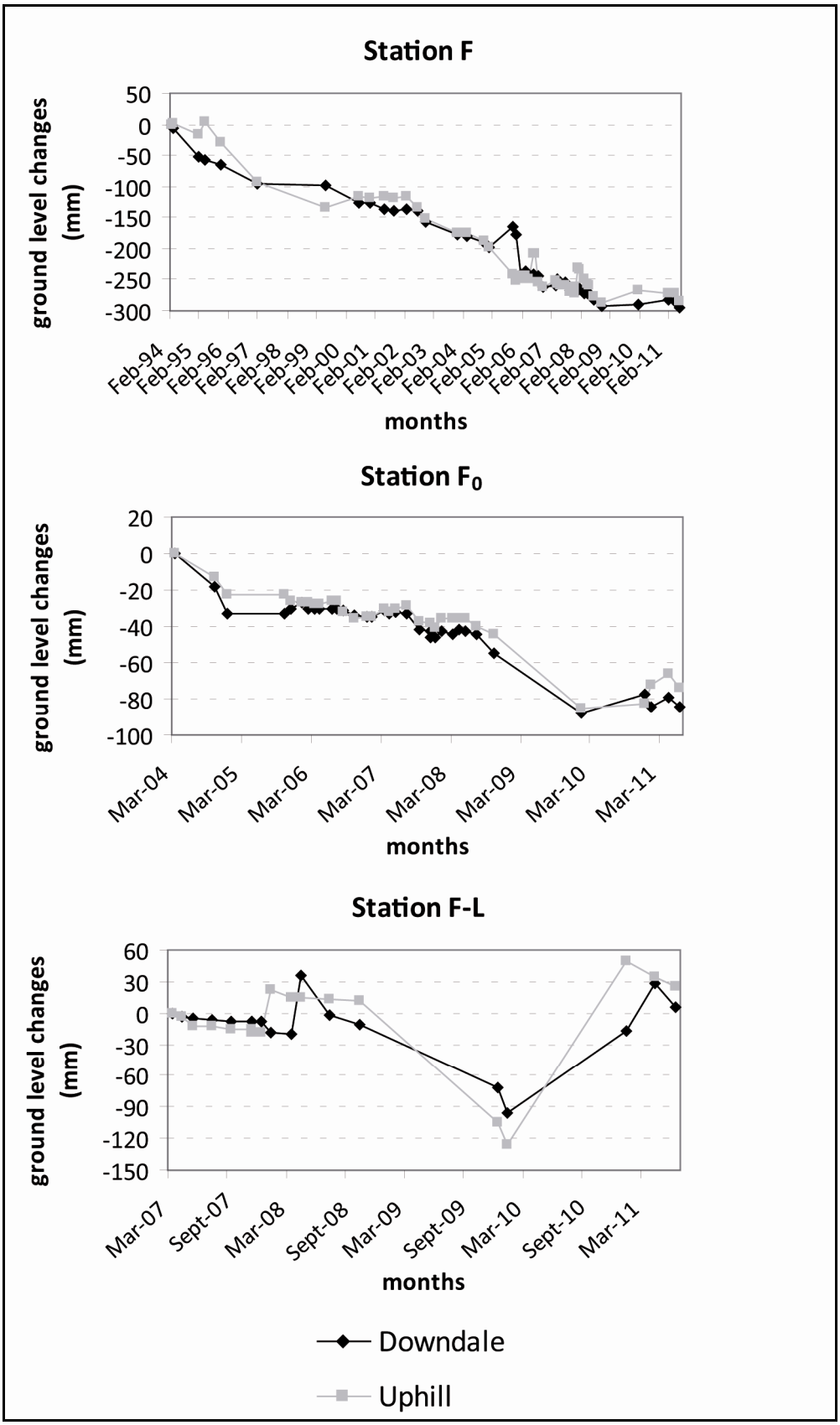

Fig. 2.11 - Ground level changes measured at F, F_0 and F-L stations on the *calanchi* badland hillslope summit along the Orcia-Formone divide.

2.3 Discussion

Biancane stations experienced the stronger surface lowering rate due to water erosion with respect to *calanchi* sites, attaining an average rate of 2.4 – 2.6 cm/a. Moreover, *biancane* in a more juvenile development phase, which correspond to the embryonic *biancane* surface of Lucciolabella Natural Reserve, show the maximum erosion rate, which reach more than 4cm/a. For this surface, a previous and abandoned agricultural exploitation is hypothesized, that could have raisen the surface proneness to water erosion, as a result of ploughing activity. This hypothesis is strengthen by the wide presence of piping in the area, that has been proved to be enhanced by cropland abandonment.

The monitoring results confirm the tendancy of *biancane* pediment of being affected by a slowly accumulation on the topographic surface, being the result of a rapid *biancane* slope retreat (up to 4 cm/a).

Calanchi badlands record a lower erosion rate, between about 1 and 2 cm/a, in Upper Orcia stations, where a more resistant caprock prevents from frequent earth sliding.

Earth slides are proved to be more frequent in spring season, as a result of the spring rainfall over water saturated clayey deposits.

Comparing the results obtained for Upper Orcia Valley with those achieved in other *calanchi* badland sites of Tyrrhenian side of central Italy (Della Seta et al., 2007, 2009; Vergari et al, submitted a), summarized in Fig. 2.9, it has to be underlined that *calanchi* monitoring sites of Upper Orcia Valley do no correspond to a representative sample of *calanchi* badlands. These landforms, in fact, are generally affected by frequent rainfall-triggered landslides (Ciccacci et al., 2003, 2008). For other stations, measurements gave positive or negative net ground changes as a function of pin position with respect to the landslide detachment and accumulation zones. This strong influence was observed in particular on *calanchi* without caprock (Della Seta et al., 2009).

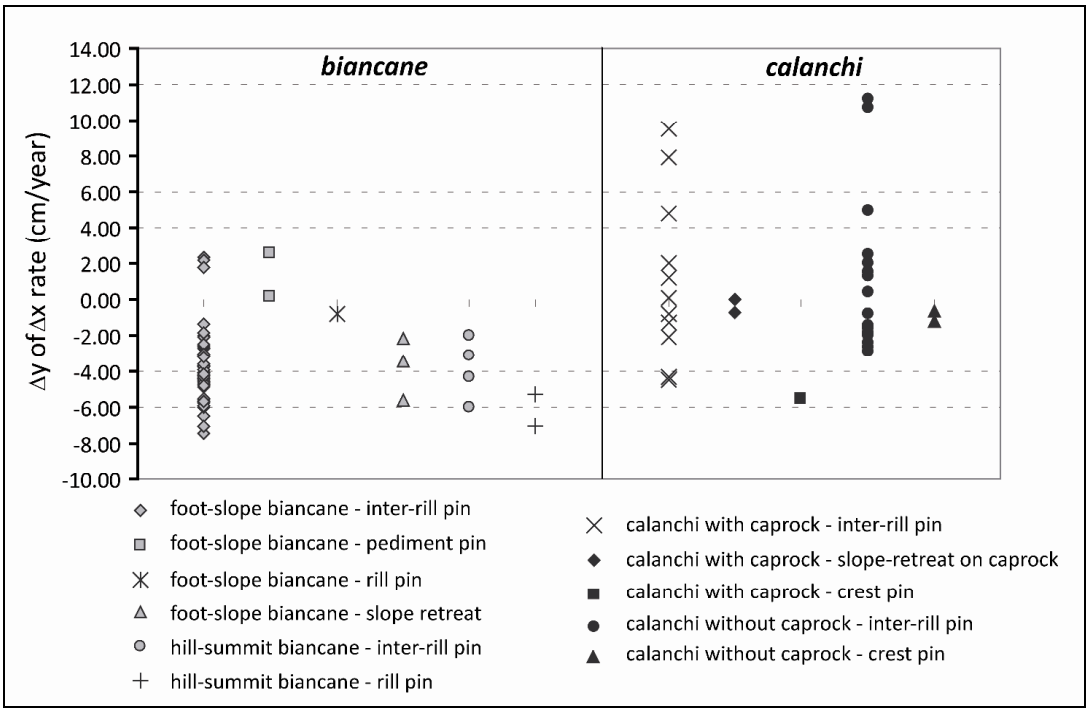

Fig. 2.12 - Summary of the mean erosion rates recorded at all *calanchi* and *biancane* sites during long-lasting geomorphological studies in Tyrrhenian side of central Italy (updated from Della Seta et al., 2009). Both vertical (Δy) and horizontal (Δx) variations of ground level were recorded at different sites and positions on slopes.

3 DIRECT MONITORING ON BARGIANO SAMPLE HILLSLOPE BY MEANS OF D-GPS SURVEY: THE ROLE OF CROPLAND ABANDONMENT AND RAINFALL VARIATIONS

This work (Vergari et al., submitted a) is focused on the quantification of the effects of cropland abandonment and rainfall variations on gully development and denudation rates for a sample hillslope of Central Italy that underwent cropland abandonment, located within the Tevere River Basin. This goal was pursued by the integration of different erosion monitoring and estimation techniques. The application of DGPS surveys let estimating the erosion rate since cultivation was interrupted (30 years ago): in fact a volumetric estimation of the removed material was attempted by performing a geostatistical interpolation of the present and the 1980's surfaces. One of the aim of the current study is, in fact, contributing to the comprehension of the applicability of DGPS surveys to compute erosion rates for fairly large time-spans. Traditional erosion monitoring technique with pins was applied during the two years, in order to validate DGPS survey results and comprehend the dynamics of geomorphic processes affecting the considered denudation hot spot. The measured data have been then compared with rainfall variations recorded at the nearest pluviometric station during the pin monitoring period and during the 30 years time-span considered for the volumetric estimation.

The further comparison of the obtained results with the monitoring data recorded for other monitoring stations of Central Italy, that has never undergone agricultural exploitation during historical times, was performed to deepen the effect of land use changes on erosion rates for these sites.

3.1 Bargiano site

The key monitoring area of Bargiano is located within the Tevere River Basin (next to the town of Orvieto, Umbria) and consists of a gently dipping slope with an extent of about 4300 m^2 (Fig. 3.1).

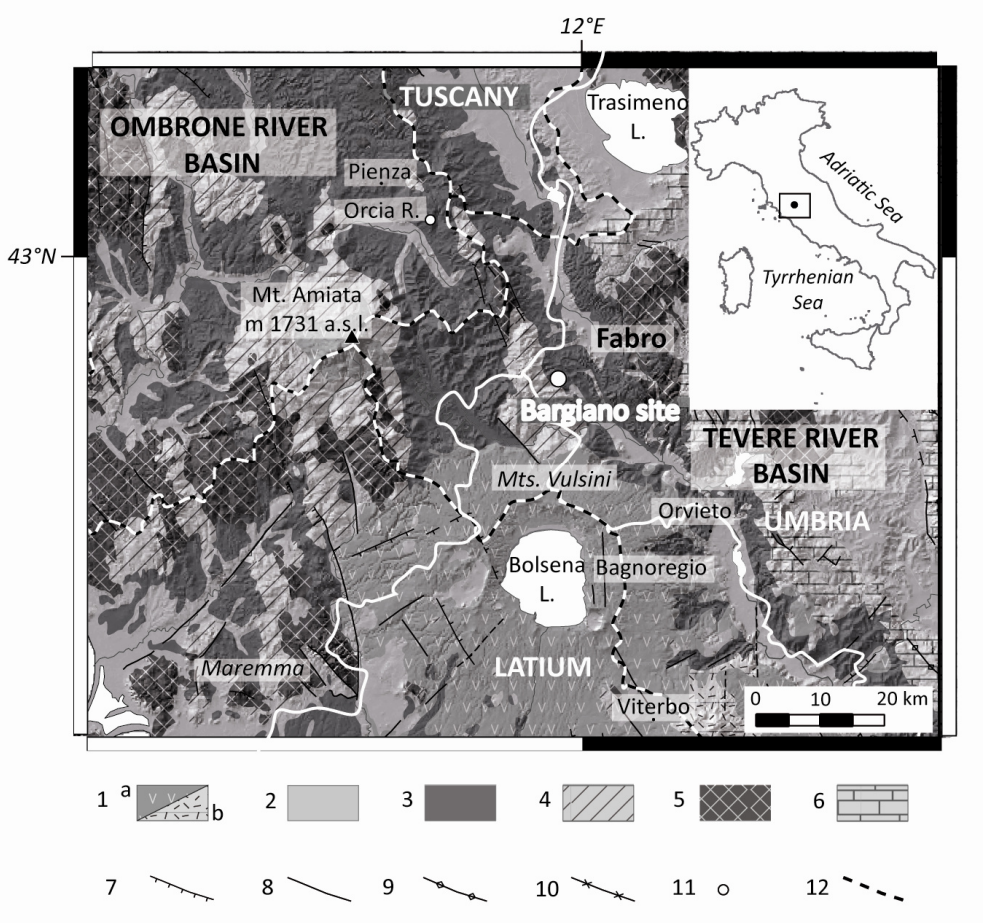

Fig. 3.1 – Location of Bargiano site in a geological sketch of the study area. 1) (a) Quaternary silica undersaturated to intermediate volcanic rocks; (b) Quaternary (and subordinate Pliocene) acid volcanic rocks; 2) Quaternary undifferentiated continental deposits; 3) Plio-Pleistocene terrigenous marine deposits and Messinian evaporites; 4) sedimentary and metamorphic units of Ligurian and sub-Ligurian nappes (Trias to Lower Cretaceous); 5) sedimentary and metamorphic units of Tuscan nappe (Paleozoic to Miocene); 6) Umbria–Marche sedimentary sequence (Trias to Tortonian); 7) Normal fault; 8) Undetermined fault; 9) Axis of anticline; 10) Axis of syncline; 11) Bargiano hillslope; 12) Major river basin divides.

Up to the ’60s it was part of a *calanchi* badland slope, successively levelled for agricultural purposes (cereal crop). In 1980 the cropland was abandoned, as testified by locals, with the consequence of a very rapid development of a close net of meandering rills and gullies, with a parallel geometry that follows the maximum slope direction. The site

appears as a miniature catchment (Fig. 3.2a) where it is possible to study the dynamics of surface processes, such as splash erosion, runoff, rill and gully evolution (Fig. 3.2b). Gravitational movements occur together with water erosion, especially on the steep slopes of the most incised gullies (Fig. 3.2c), determining continuous modifications of the dynamic equilibrium between erosion and deposition. Piping seems to have acted as dominating process since the cropland abandonment. In particular, most of the observed channels show evidence of being collapsed pipes (Fig. 3.2d). As already observed by Faulkner (2007) for other badlands areas, in Bargiano site the material collapsed from gully slopes or piping roofs temporarily protects the sideslopes and gully banks from water erosion, slackening the basal undercutting (Fig. 3.2e). During these short periods of stability, vegetation can colonise the in-channel surface.

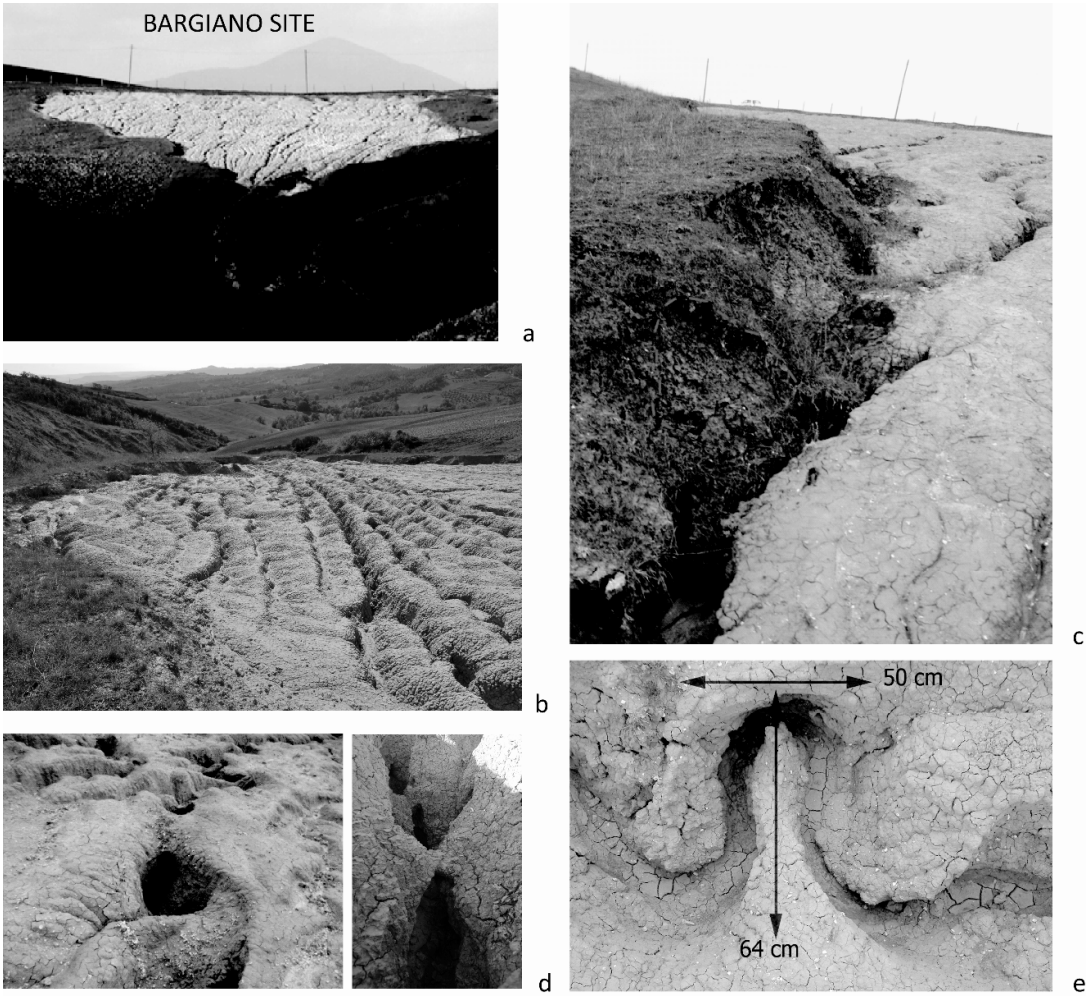

Fig. 3.2 – a) Bargiano hillslope; b) tunneling and gullies originated from collapsing of tunnel roofs; c) failure of most incised gully banks; d) overview of Bargiano's rills and gullies; e) meandering rill, in which lateral erosion of channel is shown.

3.2 Material and methods

At Bargiano site, two methods for direct monitoring of denudation at the hillslope scale have been simultaneously applied :

a) erosion pins, as already done for the long-lasting field monitoring sites:
in Bargiano sample area, 24 iron pins were placed at different depths, in order to cross the weathered horizon, most of them recording uphill, downdale (Δy) and lateral (Δx) ground level changes since January 2008 (Fig. 3.3). They were placed along two rills and along the major gully the rills are flowing into. Each monitoring point consists of two pins, one placed in inter-rill position (pin type: A), the other one within the channel (pin type: B).

b) DGPS survey, to sample the remnants of the 1980 cropland surface and the present (eroded) surface, in order to perform volumetric estimation of the eroded material.

DGPS survey was performed using a Leica GPS 1200 instrument. We sampled 241 points from the remnants of the original 1980 cropland surface, nowadays still vegetated, and 3549 points from the bare eroded surface using the right sampling density for recording the roughness of surfaces (Fig. 3.3). The navigated points were post-processed using the data from GNSS reference station network of Umbria Region and Perugia University (http://labtopo.ing.unipg.it/) in order to ensure a higher vertical accuracy. Through geostatistical interpolation (Ordinary Kriging) performed in GIS environment we obtained the reconstruction of both the original and eroded surfaces. The 1980 surface was reconstructed hypothesizing that it should be a remodelled regular gently slope as others currently levelled for agricultural purposes in the surroundings of the study area. We chose the Ordinary Kriging method, since it is an exact interpolator. Moreover it takes into account both autocorrelation of the considered variable (elevation in this case) and spatial relationships between measured values around unknown point, when assigning weights to measured points (Cressie, 1990 and references therein).

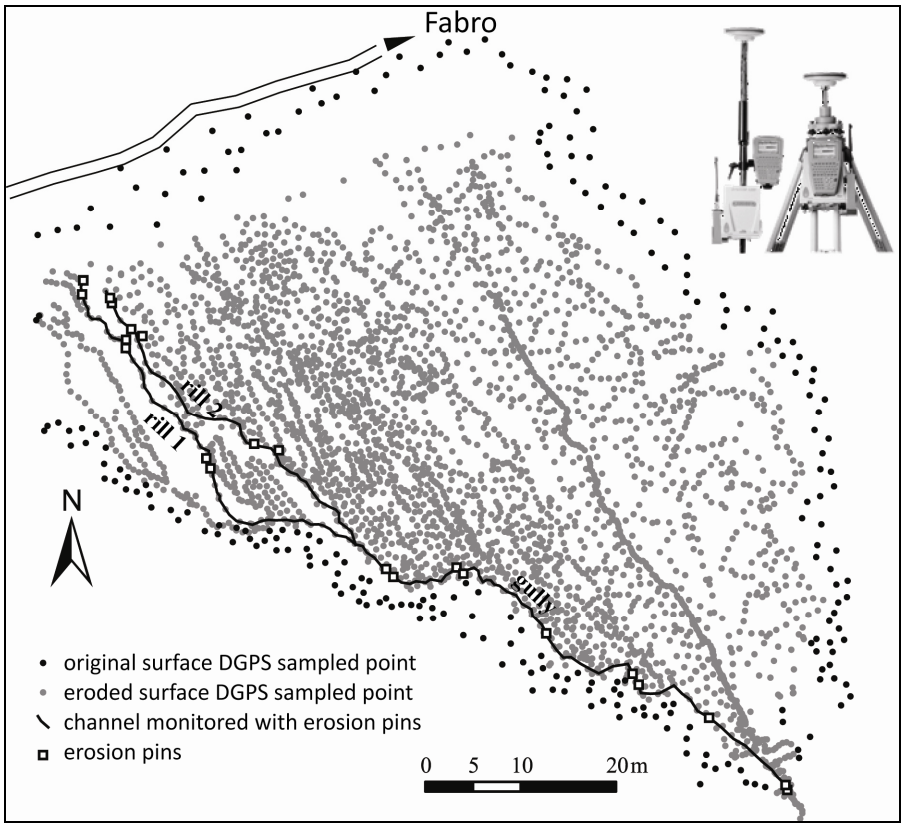

Fig. 3.3 – Location of the channels monitored with erosion pins and DGPS sampled points, that was performed on the remnant of the original cropland surface (1980) and on the eroded surface.

Once the DTMs of the original and eroded surfaces have been obtained, we performed the raster difference. Each pixel in the new output raster records the height difference between the original and eroded surfaces. As the pixel dimension is known (0.3x0.3 m), we derived the volume of eroded material in the considered 30 years time-span.

The measured data have been then compared with rainfall variations recorded at the Orvieto pluviometric station during the monitoring period and during the 30 years time-span considered for the volumetric estimation.

In particular, pluviometric data from 1979 to 2002 relative to the pluviometric station of Orvieto (315 m a.s.l.) were obtained from the National Hydrographic Service. More recent data on pluviometric trends (up to 2009) for the same pluviometric station have been collected thanks to the Umbria Regional Hydrographic Service.

Several authors (Mannaerts and Gabriels, 2000, Boardman et al., 2003, Piccarreta et al., 2006) consider an amount of daily rainfall >10 mm to be an approximate threshold for

runoff initiation in semiarid environments. Della Seta et al. (2007) observed, for several badlands in central Italy, that strong denudation is triggered by rainfall events distributed over a number of consecutive days, though not greatly intense. Particularly, their amount should overcome the threshold of 60 mm per 5 consecutive days to induce centimetric modifications of the topographic surface.

Based on field surveys and long-lasting geomorphological investigations, the authors have concluded that water erosion initiation occurs when daily rainfall exceeds 10 mm.

In order to understand the role of extreme rainfall events in affecting the geomorphological dynamics of the area, the following parameters have been considered for each pin-monitoring time interval:

- Rainy days
- Rainfall depth (mm)
- Rainfall depth (mm) of the worst day
- Rainy days with rainfall depth > 10 mm
- Maximum N. of consecutive dry days
- Maximum N. of consecutive wet days
- N. of dry days prior to events with rainfall depth > 10 mm
- N. of wet days prior to events with rainfall depth > 10 mm
- N. of rainy events longer than 3 days
- Rainfall depth (mm) of the longest rainy event

Annual, seasonal and rainfall data for the 1979-2009 time-span were considered in order to investigate their possible influence on measured and estimated erosion rates.

3.3. Results

a. Ground level changes and rainfall variations during the monitoring period (2008-2009).

During the period of erosion pin monitoring (21 months), a progressive removal of clayey material from the slope by surface running waters was recorded at Bargiano site. In particular, some differences in erosion rates were recorded in rill and interrill position. A

systematic ground surface lowering at the inter-rill erosion pins (type A) was observed, as indicated in Fig. 3.4. This is in agreement with the erosion/accumulation dynamics, giving rise to progressive removal of material where almost the lonely surface running water is acting (inter-rill). During the 2009 spring season, positive changes indicated temporary clayey accumulation just locally, even on the inter-rill surface, as indicated in Fig. 3.4. Erosion pins placed within rills and gullies (type B) typically show positive and negative changes of ground level, as a consequence of the combination of strong incision and accumulation, the latter mainly ascribed to the collapsing of gully banks or piping tunnels. Small falls or overturning of the channel sidewall frequently occurred within the deepest channels, mainly in conjunction with spring rainfall.

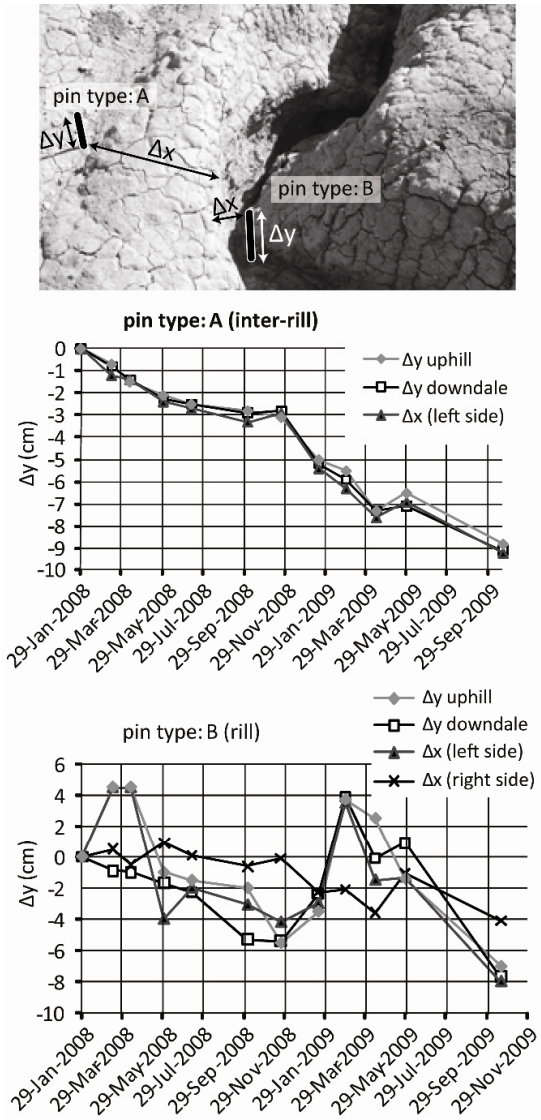

Fig. 3.4 – Examples of rill and inter-rill pins and corresponding denudation graphs covering the monitoring time-span.

Table 3.1 summarizes the mean annual denudation rates of ground level changes for each of the two considered rills and for the gully they flow into. Upper slope area (RILL 1 and RILL 2) clearly underwent the maximum net erosion of 4.26 cm/a (inter-rill) and net erosion was recorded even within rills. On the other hand, within the channel of the monitored gully, located down slope, the maximum net accumulation of 5.06 cm/aΔ was recorded, while the inter-rill areas underwent net erosion, even if slightly lower than in the upper slope inter-rill area. Thus, total mean denudation rates for the area indicate net accumulation within rills of 2.13 cm/a and net erosion on inter-rills of 3.66 cm/a, with a resulting general net erosion rate of 0.52 cm/a.

	MEAN ANNUAL DENUDATION RATE (cm)		
	rill/gully	***inter-rill***	***total***
RILL 1			
3 rill pins	-1.57	-3.87	-2.72
3 inter-rill pins			
RILL 2			
3 rill pins	-1.02	-4.26	-2.64
3 inter-rill pins			
GULLY			
6 rill pins	+5.06	-3.18	+1.63
6 inter-rill pins			
TOTAL	+2.13	-3.66	-0.52

Tab. 3.1 – Mean annual denudation rates obtained from erosion pin record over the first 21 months of monitoring. Negative and positive rates indicate respectively net erosion and net accumulation

Comparing these results with the rainfall trend recorded during the monitoring period, the most critical period was winter 2008, when up to 90 mm in a day and 20 consecutive rainy days were recorded. 2009 spring rainfall over water saturated clayey deposits increased the runoff power and caused the accumulation recorded, as shown in Fig. 3.5a. Table 3.2 summarizes the values of the considered pluviometric parameters and graphs in Fig. 3.5b show the most significant correlation between the measured ground level variations (absolute values) and some of the considered pluviometric parameters for the monitoring time intervals. As the regression coefficients point out, ground level changes recorded in TYPE A pins (inter-rill position) show a fairly strong positive correlation with the rainfall depth for the same period, while for type B pins (rill position) the correlation is not so strong, even if it increases when considering the number of rainy days (Fig. 3.5b) instead of

the rainfall depth. This fact can be explained considering that the considerable ground level changes within rills, due to gravitational movements, do not always occur immediately after an intense rainfall event. As a matter of fact, the further comparison of pluviometric data (Tab. 3.2) and measured ground level variations highlights that clay removal by water erosion is generally due to intense rainfall event preceded by quite long dry periods, while accumulation (due to gully banks collapsing) is favoured by intense rainfall after a certain number of rainy days. Moreover, graphs in Fig. 3.5b indicate that in inter-rill position, where almost the lonely water erosion acts, intense events are significantly more effective than long events.

period	Monitoring time intervals	N. of days	N. of rainy days	Rainfall depth	N. of rainy days with rainfall depth > 10mm	Maximum N. of consecutive dry days	Maximum N. of consecutive wet days	Rainfall depth for the worst rainy event	Mean N. of dry days prior to events with rainfall depth > 10 mm	Maximum N. of dry days prior to events with rainfall depth > 10 mm	Mean N. of wet days prior to events with rainfall depth > 10 mm	Maximum N. of wet days prior to events with rainfall depth > 10 mm	N. of rainy events longer than 3 days	Rainfall depth for the longest rainy event	Rainfall depth of the worst rainy day
1	29/01/08 - 15/03/2008	47	13	84,8	3	21	4	39,3	0	0	1,67	2	2	39,3	23,8
2	16/03/08 - 11/04/2008	27	12	70,6	2	10	7	42,6	3	6	0,5	1	2	42,6	19,4
3	12/04/2008 - 31/05/2008	50	24	117,2	2	5	7	58,3	0	0	3,5	4	3	58,3	40,4
4	01/06/2008 - 12/07/2008	42	15	71,4	1	12	8	46,2	0	0	6	6	2	46,2	23,4
5	13/07/2008 - 04/10/2008	85	14	98,6	5	32	5	59,4	2,6	9	1	3	1	59,4	31,2
6	5/10/2008 - 23/11/2008	50	22	148	8	12	7	75	0,25	1	2	5	3	75	26,8
7	24/11/2008 - 18/01/2009	56	37	419	11	4	9	126	0,36	2	1,81	7	5	144	95,8
8	19/01/2009 - 28/02/2009	41	19	95,2	3	7	8	42,6	1,33	4	3,33	6	3	42,6	16,2
9	29/02/2008 - 14/04/2009	45	15	81,4	5	7	6	49	1,6	7	1,6	4	1	49	15,2
10	15/04/2008 - 29/05/2009	45	15	70,8	2	11	5	20	0,5	1	0,5	1	2	20	27
11	20/05/2009 - 20/10/2009	144	27	356,8	10	28	4	58	0,3	2	0,8	2	5	136,6	69,6

Tab. 3.2 – Pluviometric parameters considered for each monitoring time interval.

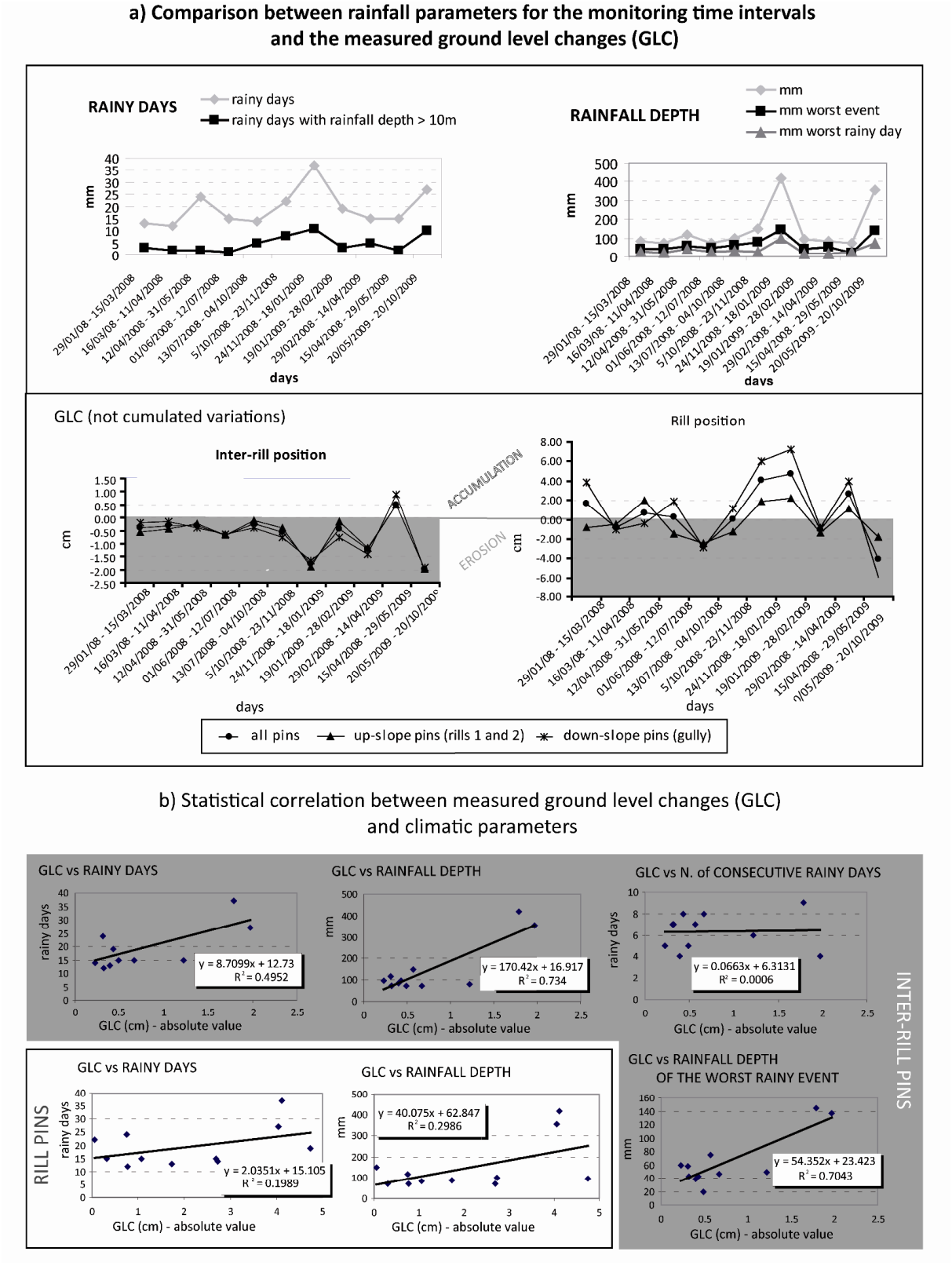

Fig. 3.5 – a) rainy days and rainfall depth recorded at Orvieto pluviometric station for the monitoring time intervals and measured ground level changes (GLC); b) most significant graphs of statistical correlation between the measured ground level variations and some of the considered pluviometric parameters for the monitoring time intervals.

b. Volumetric estimations and pluviometric trend for the 30 years time-span (1980-2009)

Fig 3.6 shows the raster outputs of DGPS sampled points interpolations. The reconstructed 1980 cropland is, as expected, a smoothed, gently shelving surface (Fig. 3.6a). The present day eroded surface is, on the contrary, well represented with its close net of quite parallel rills flowing into deep gullies located down slope (Fig. 3.6b). The raster difference between the DTMs of the original and eroded surfaces shows up to 2.7 meters of surface lowering in 30 years (Fig. 3.6c). The strongest variations appear to have affected the central part of the Bargiano hillslope , leading to the deep incision of the major gully.

The calculated volume of removed material over the 30 years time-span is 3971.39 m^3. Considering the bulk density of clay (about 2 t/m^3) the removed materials amount to 7942,78 t over 30 years. Thus the mean annual denudation rate is about 810.16 t/ha/a. Taking into account the extent of the experimental hillslope, we calculated an erosion rate of about 121.5 cm over 30 years, that corresponds to a mean surface lowering rate of 4,05 cm/a.

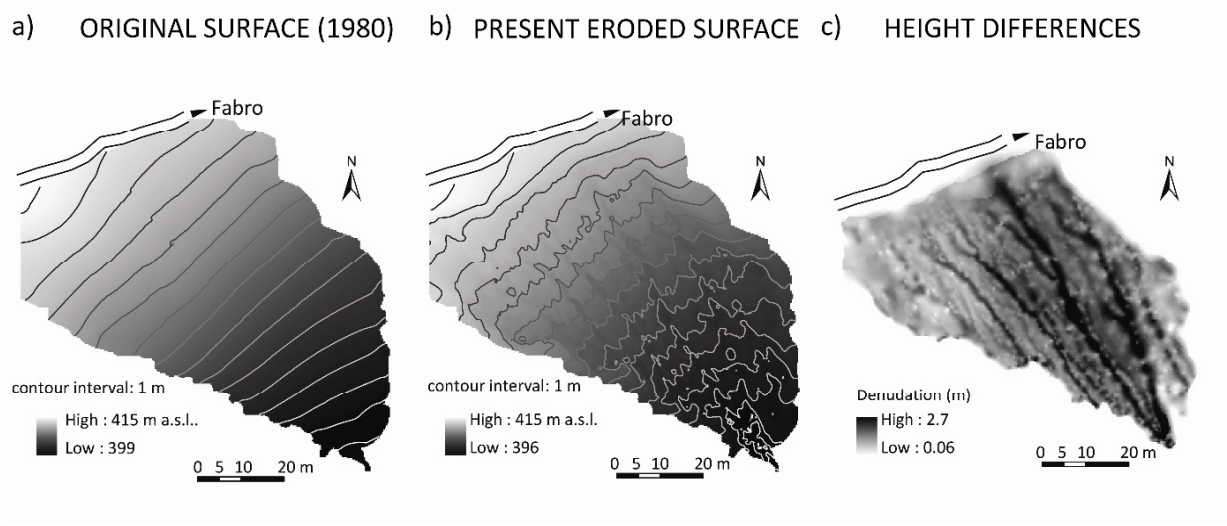

Fig. 3.6 – Original (a) and eroded (b) surfaces of Bargiano site experimental hillslope, from the geostatistical interpolation of DGPS sampled points. Raster difference between these surfaces produced a new raster representing height differences (c).

The analysis of rainfall data over the 30 year considered time-span (Fig. 3.7a) shows a mean annual rainfall depth of about 160 mm, lower than the mean value relative to the

1921-2009 period, but the annual rainfall trend over the last 30 years points out a moderate increase. Seasonal trends indicate a progressive increase of variability, particularly for autumn rainfall depth (Fig. 3.7b). The total annual rainfall depth for 2008 and 2009 (monitoring years) appears higher than the mean value for the 1979-2009 period, so it can't explain the lower erosion rate recorded during the monitoring period. Moreover, the analysis of extreme events for the entire 1981-2009 period doesn't show a decrease of the number or intensity of events several days long (Fig. 3.7c).

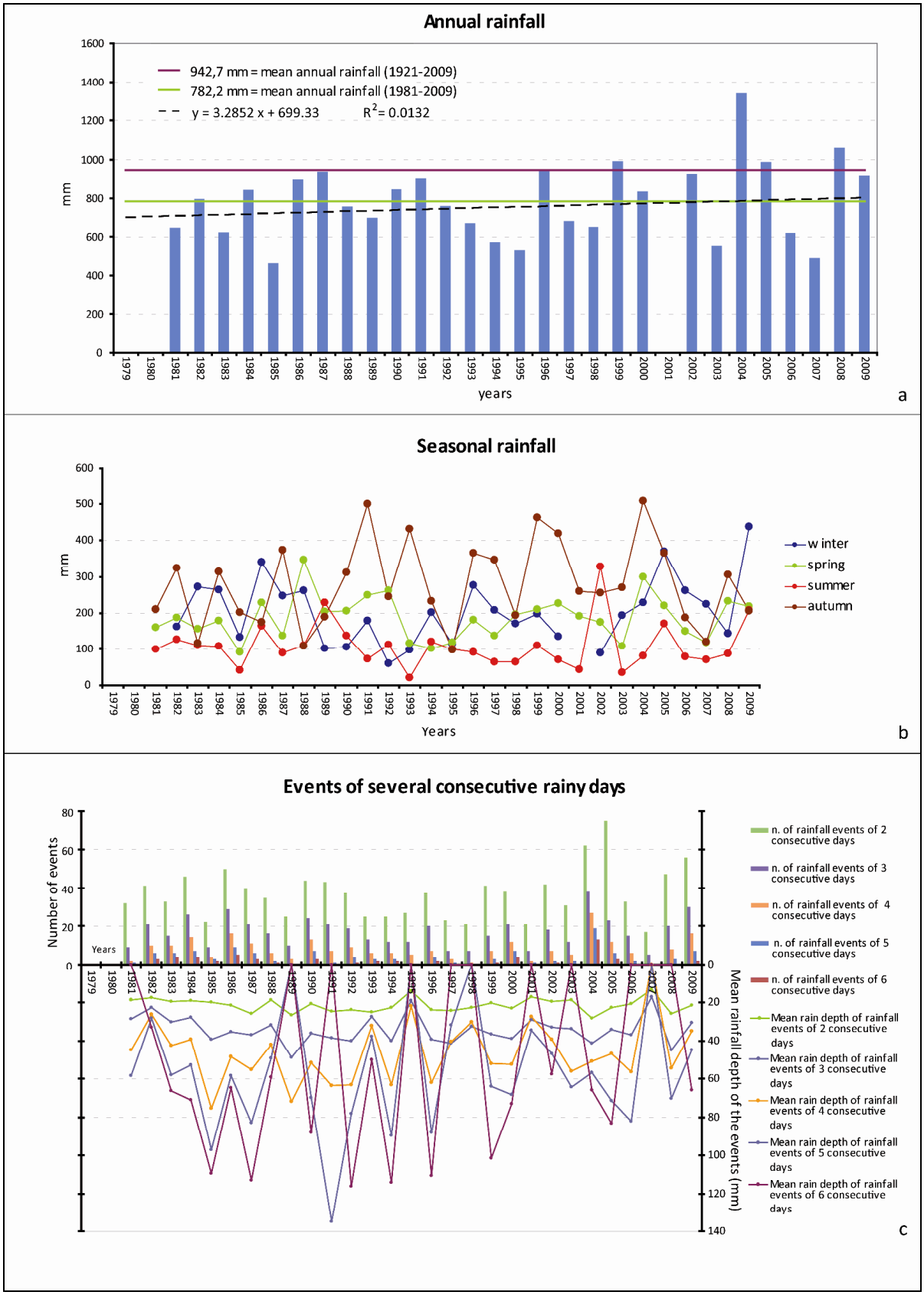

Fig. 3.7 - Rainfall data about annual (a), seasonal (b) and extreme events (c) over the 1979-2009 time-span for the Orvieto pluviometric station (315 m a.s.l.).

3. 4 Discussion

Mean annual erosion rate obtained through volumetric estimation from DGPS survey (81015.91 t/km^2/a) is a very high value that reflects the strongly accelerated erosion on the Bargiano experimental hillslope. The corresponding mean surface lowering rate of 4.05 cm/a is not comparable to the total mean value obtained by erosion pin records (0.52 cm/a). Nevertheless this discepancy may be discussed as follows:

a) erosion pins were places, up to now, just on a limited portion of the hillslope, thus the obtained mean denudation rates could be not representative of the whole site, while DGPS survey was performed on the entire site surface.

b) The gully monitored with pins is located close to the major scarp delimiting the boundary between the original and the eroded surface. This scarp is particularly steep and high, thus experiencing frequent landsliding that on the whole contribute to strong net accumulation (positive variations) within the channel. This fact influences, obviously, the total mean denudation rate, with respect to the ones obtained separately for rill and inter-rill areas. Moreover, the inter-rill area (where net erosion systematically occurs) is, on the whole, more extended than the rill area, even if in the averages we obtained they have the same weight since we placed the same number of rill and inter-rill pins.

c) The initial strong cutting rate of 1980 might have progressively decreased, probably as a consequence of increasing partial accumulation down slope of materials removed from uphill. In fact, a decrease of powerful rainfall events was not recorded. Moreover the reaching of the bedrock below the weathered layer might have braked erosion intensity, that initially was fastened by the presence of ploughed soil, that favoured the development of pipes.

d) Last but not least, the erosion pin monitoring was performed, up to now, over a considerably short time-span. Thus the observations at pins, even if providing detailed

information about the acting processes, cannot be significant for the 30 years period over which the volumetric estimation of eroded material was performed.

Nevertheless, if we consider only the inter-rill pin data, it must be outlined that the net erosion rates recorded over the 2008/2009 monitoring period (3.66 cm/a) are not so far from the mean erosion rates over the last 30 years (4.05 cm/a).

Mean annual erosion rate obtained through volumetric estimation for Bargiano site is consistent with the range of values estimated for many catchments of central Italy, especially those widely affected by denudation hot spots (I.e. badlands; Ciccacci et al., 1992, 2003, 2008; Del Monte et al., 2002; Della Seta et al., 2007, 2009). These erosion rate estimations have been performed using the denudational index (Tu) method (Ciccacci et al., 1981, 1986), that consists of a series of empirical equations that allow the estimation of suspended sediment load (Tu, $t/km^2/a$) based on statistical correlations among quantitative geomorphic parameters and measured suspended sediment load data. The estimated mean annual suspended sediment load for Ritorto River basin, which is the Tevere River tributary the Bargiano gullies flow into, is 5708 $t/km^2/a$ (Della Seta et al., 2009), that, as expected, is a very low value compared to the calculated value of the removed material at the Bargiano site (810.16 t/ha/a): this can be explained considering that the sample hillslope represents a denudation hot spot, where we obviously expect higher denudation rates due to the abandonment of agricultural exploitation and badlands development. Certainly, the cropland abandonment in Bargiano site has caused an increase of erosion rate with respect to the trend assumed for the croplands around: the considered bare eroded surface presently lies up to 2,7 meters below the vegetated soil around.

In addition, monitoring data from other monitoring sites in central Italy, characterized by similar physiographic conditions and accelerated erosion, showed lower or comparable erosion rates even on steeper slopes: Figure 2.9 shows comparable erosion trends for several steeper "*biancane*" and "*calanchi*" badland hillslopes in central Italy, that has never been subjected to agricultural exploitation during the last centuries (or historical times). In fact, direct measurements over periods longer than a decade indicate that mean annual values of denudation range between 1 and 2.5 cm/a for slopes affected by sharp-edged and/or rounded edged badlands. Higher denudation rates (3–4 cm/a) were obtained only for

shorter observation periods; still higher rates were recorded on bedrock for short periods at the gully bottom or in coincidence with mass movements before bench marks were turned up or damaged (Della Seta et al., 2007, 2009).

For Bargiano site an evolutionary scenery can be summarized as follows. When during the '60s the badland slope was leveled for agricultural exploitation, this might have imply an over-reworking of clay material, reducing the bedrock bulk density and changing infiltration properties. Thus, when the cropland was abandoned (1980), piping (or tunneling, as subsurface erosion is defined by Bryan & Harvey, 1985, when it develops in non-homogeneous material) might have been enhanced, exploiting the increased erodibility of the soil. Going on tunnel enlargement, the loss of material might have caused the collapse of tunnel roofs, giving rise to very incised gullies. At the present time, some gullies present roofs in limited stretch, evidencing their origin from tunnel collapsing. The present erosion rate seems to be lower, due to different causes. Lateral erosion of channel slopes is widespread, implying considerable collapse of material that rises gully bottom and temporally protect channel sideslopes. The material accumulation downslope have decreased the local slope, carrying to the gully longitudinal profile towards temporal equilibrium. Last, but not least, locally the unweathered clayey bedrock has been uncovered, resulting in a more resistant lithology than the ploughed abandoned soil. Piping seems now to affect homogeneous clay, giving rise to deep pipes that naturally characterize badlands areas.

A brief final discussion should concern the error and the applicability associated with the considered erosion monitoring methods. The size of the study area, the time available, and the quality of the data required are perhaps the most critical issues to be consedered when looking for the most appropriate technique. As well-known, the traditional erosion pin method generally allows to carry out very accurate punctual measures, whose error is measurable in few millimeters. So, it can be used to quantify very detailed temporal variations (monthly or after-event ground level changes), but certainly the obtained erosion rates cannot be representative of large areas. On the other hand, DGPS survey can be proper when a single hillslope of less than few hectares is being monitored, as the time and effort

required would be acceptable. For larger areas or wider time interval, high resolution photogrammetric analysis could be more appropriate. GPS accuracy is affected by many sources of inaccuracy (Kaplan and Hegarty, 2006), caused by the satellite position geometry (that provokes the so-called DOP or diluition of precision), the multipath effect (caused by the reflection of the satellite signals on close obstacles), the atmospheric effect (the reduction of signal speed during the troposphere and ionosphere crossing) and clock inaccuracy. The application of DGPS aid by-passing many of the sources of error and, in rural areas of moderate to low relief, satellite obscuration is minimized. Measures perfomed at Bargiano area by means of DGPS survey were affected by a mean elevation error of 2,2 cm considering the points sampled along the presently eroded bare surface and 1,7 cm along the remnants of the 1980 surface. This order of magnitude can be assumed as an acceptable error for the purpose of the DGPS survey, since metric variations of ground level were recorded for 30-years time-interval.

To conclude, in the present study the geostatistical interpolation of the 1980 and the present surfaces was another bias susceptible procedure. Cross-validation is a statistical analysis that allows to quantify the error associated with the performed interpolation, since it removes each measured point in turn, predicts a value for that location based on the rest of the data and compares the measured and predicted values (as shown in the graphs of Fig. 3.8 relative to the two interpolated surfaces). For both the surfaces the mean prediction error (difference between predicted and measured values) reported by the validation is around 2 mm.

a) Cross-validation of the 1980 interpolated surface

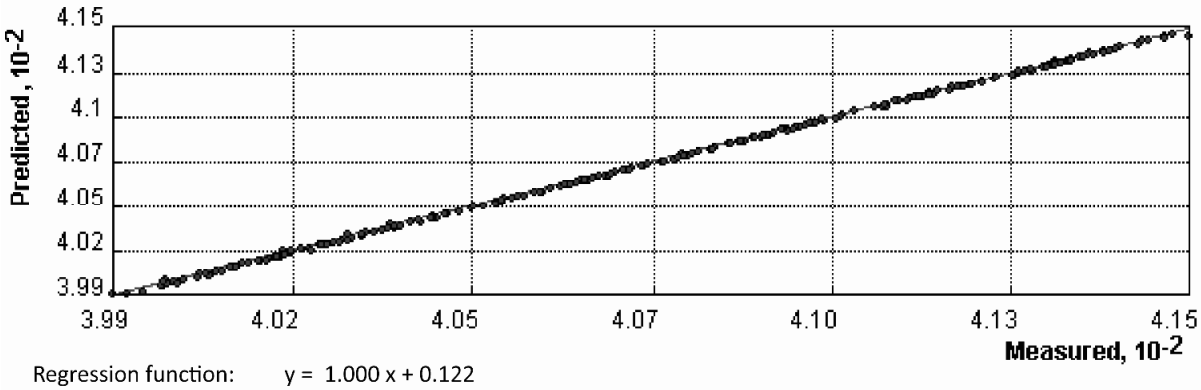

Regression function: y = 1.000 x + 0.122
Mean prediction error: 0.002187
Root mean square 0.06987
Average standard error: 0.8341

b) Cross-validation of the 2009 interpolated surface

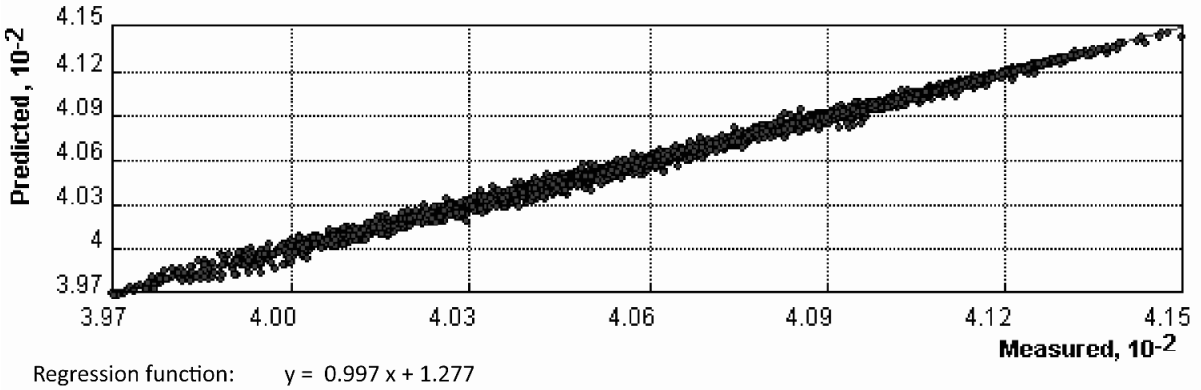

Regression function: y = 0.997 x + 1.277
Mean prediction error: 0.001737
Root mean square 0.2432
Average standard error: 0.4703

Fig. 3.8 - Cross validation relative to the geostatistical interpolation of the 1980 surface (a) and of the 2009 eroded surface (b).

4. COMPARISON BETWEEN FIELD EROSION MONITORING DATA AND PHOTOGRAMMETRIC ANALYSIS: THE CASE OF LANDOLA SUBCATCHMENT

This work is aimed at quantifying at different spatio-temporal spans the erosion rates for a small experimental area located within the Upper Orcia Valley. To evaluate the spatio-temporal development of denudational processes, particularly badland erosion and related rates, direct measurements at erosion "hot spots" and a digital photogrammetric analysis (Biasini and Salvatore, 1993, 1995; Betts and DeRose, 1999; Chiaverini et al. 1999; Martinez-Casasnovas et al., 2003; Ciccacci et al., 2008; Salvini, 2008) at hillslope and catchment scale have been performed in the Landola subcatchment test area (Tuscany). The dual purpose of the analysis was the assessment of the morphodynamics of erosion hotspots of the Upper Orcia Valley in the last 30 years and the cross-checking of the obtained results, in order to test the applicability of the two methods. This chapter summarizes the preliminary results of the research conducted during a collaboration with some researchers of the Department of Sciences and Technologies for the Environment and Territory of Molise University (Aucelli et al., 2010), in the frame of PRIN Project 2007, funded by the Ministry of Instruction, University and Research (MIUR), "*Messa a punto di un modello integrato per la valutazione preventiva dell'erosione idrica del suolo in ambiente mediterraneo*" (National coordinator G. Rodolfi, Research Unit coordinator E. Lupia Palmieri). Even if the digital photogrammetric analysis was largely performed by researchers of Molise University, its results can be very interesting for the purposes of this thesis, in particular in this section (Part I), where the applicability of different techniques for erosion rate quantification is investigated. Within the research cooperation, my contribution was focused mainly on the choice of the study area, the data collection, the D-GPS survey, besides erosion direct measurements on field.

4.1 Landola test area

For process-based assessment of erosion dynamics we focused on a sample sub-catchment, the Landola catchment, which is representative of the geomorphic processes typically acting in the Upper Orcia Valley (Fig. 4.1). This is a catchment of about 4.4 km^2 where the majority of slopes are rapidly evolving for denudation processes and rivers show high suspended sediment loads. In fact, water erosion is pervasive and leads to typical rounded-edged *biancane* and sharp-edged *calanchi* badlands. Gravitational processes contribute as well to slope denudation with landslides (even on gentler slopes), soil creep and solifluction. Badlands correspond to denudation "hot spots" within catchments and field monitoring at these sites suggests that rill, inter-rill and gully erosion contribute the most to the overall denudation at the catchment scale, through extreme episodic events at the hillslope scale, triggered by rainfall events several days long (Della Seta et al. 2007, 2009).

Fig. 4.1 – Location of Landola test area within the Upper Orcia Basin.

4.2 Material and methods

A digital photogrammetric analysis of landforms has been performed on four series of black and white aerial photographs dating to 1976 (the "EIRA" flight, nominal scale of 1:13.000), 1994 (the "Tuscany Region" flight, at a nominal scale of 1:30.000) and 2003 (the "Siena" flight, at a nominal scale of 1:7.500), respectively. The aerial photos have been scanned with a resolution of 1200 dpi (472 dots per centimeter) and saved in TIFF format. The digital photogrammetric restitutions have been made by using a Z-Map digital photogrammetric workstation, considering the 1976, 1994 and 2003 photos. In order to obtain the best image orientation, a differential global position system (DGPS) survey was carried out using a Leica GPS 1200 instrument, and about 70 ground control points (GCP) were located within and around the test area (Fig. 4.2), based on three reference points of the IGM95 geodetic network (Point n. 129610 "Monte Calcinaio", Point n. 129606 "San Piero in Campo" and Point n. 129609 "Bagni San Filippo"). The mean measured post-processing error was included in the 1 – 1,5 cm order of magnitude. Location of the GCPs was previously planned considering their contemporary evidence on the photos of the considered three years. Root Mean Square Errors of aerial triangulation phase were around 1-2 m.

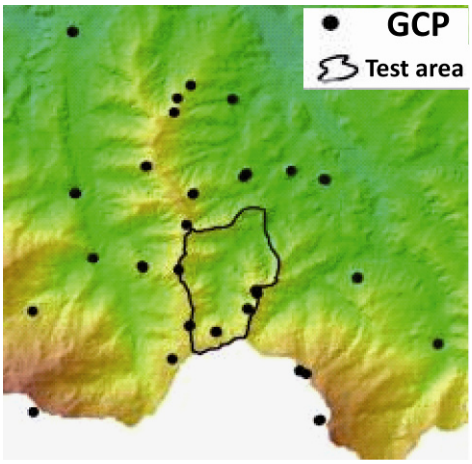

Fig. 4.2 – Ground control points (GCP) distribution within and around the Landola test area (after Aucelli et al., 2010).

Digital Elevation Models (DEMs) have been derived from each set of photos on a stereopair-by-stereopair basis and then mosaicked to produce a DEM for each photo with a cell size of 2m (Fig. 4.3). An Area Based Image Matching algorithm was used to derive the DEMs.

The quantitative evaluation of the sediment loss rate was computed by overlaying the obtained DEMs. This operation produced a new grid with the altitude difference for each cell of the grid. Negative values in the difference grid represent erosion areas, while positive values are filling or accumulation areas (Martınez-Casasnovas, 2003). In addition, photo interpretation, carried out for each set of aerial photos, allowed to map the denudation processes and the main topographic changes from 1976 to 2003. Data analysis was performed within a Geographic Information System.

Direct measurement of erosion rates have been achieved from results from previous studies (Ciccacci et al., 2003, 2008, 2009; Della Seta et al., 2007, 2009), as well as from the updating of the monitoring database for the Upper Orcia Valley (see §2).

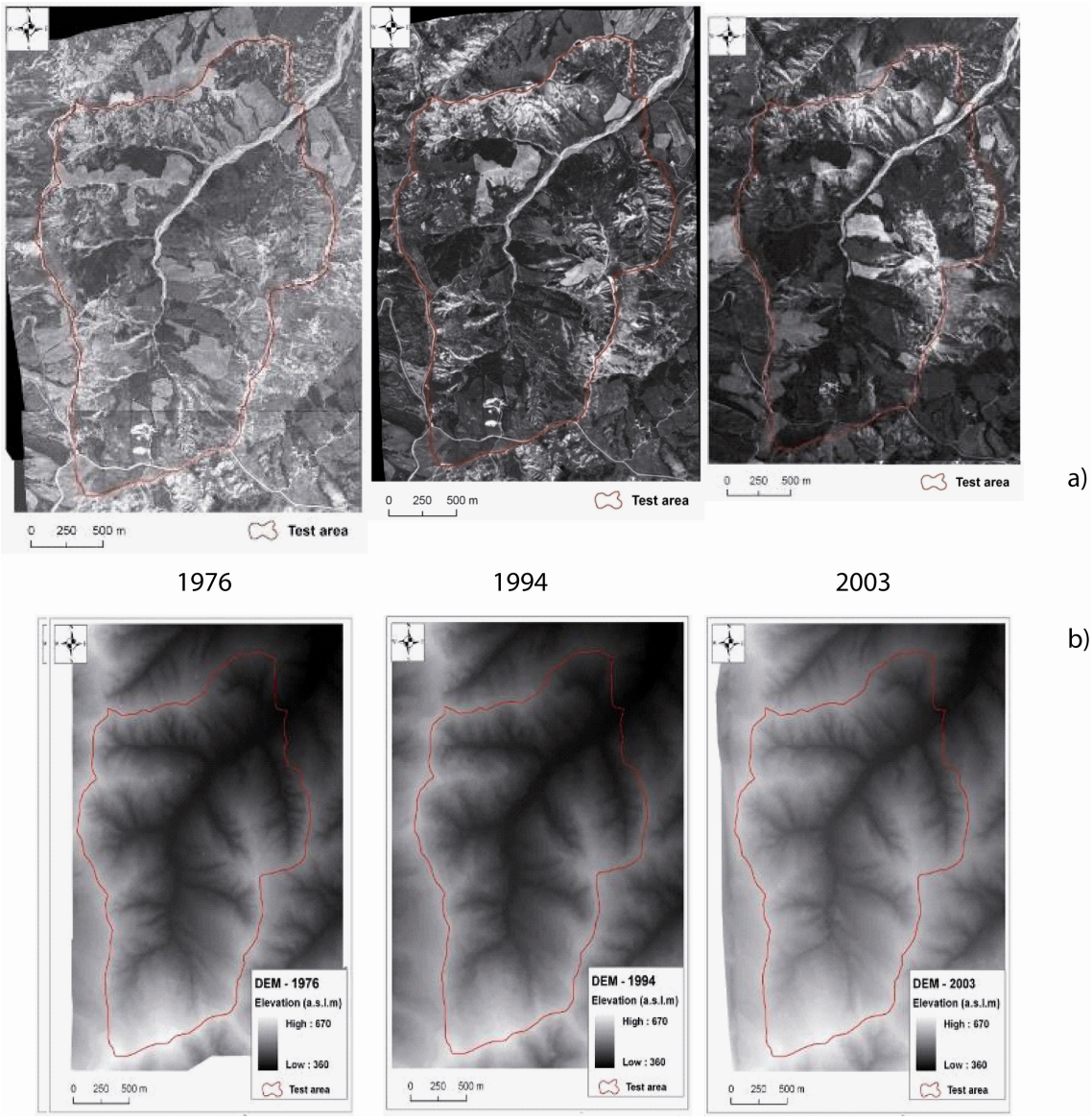

Fig. 4.3 – Used aerial photographs (a) and obtained DEMs (b) during the photogrammetric analysis.

4.3 Results

Photo interpretation showed that the dominant denudational processes within the test area consist of gully erosion, different typologies of landslides and *calanchi* badlands, affected by frequent mudflows (as exemplified in Fig. 4.4).

The digital photogrammetric and multi-temporal analysis allowed to reconstruct the morpho-topographical changes which have occurred during the considered period (1976-2003) within the study area which is often affected by important denudation processes due to gravity and the action of surface running water. The slopes affected by *calanchi*, as expected, show the most severe morphological changes. In particular, a maximum headwater retreat reaching up to 10-15 cm/a is recorded (Fig. 4.5).

Photo interpretation and transversal profiles (Fig. 4.6), extracted from DEMs referring to 1976 and 2003, respectively, show frequent landslides in areas affected by badlands, due to the retreat of the head with an accumulation of sediment at the slope foot.

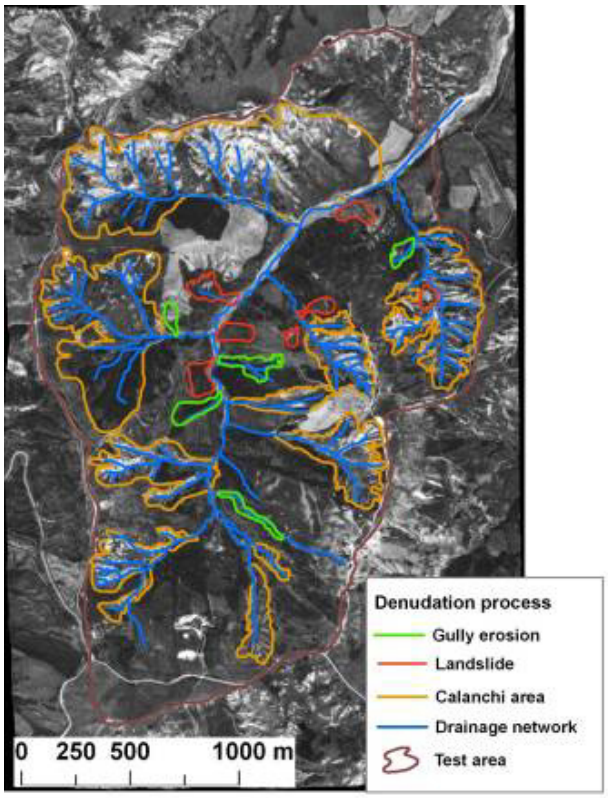

Fig. 4.4 – Main denudation processes in Upper Orcia Valley (from 1994 aerial photo interpretation).

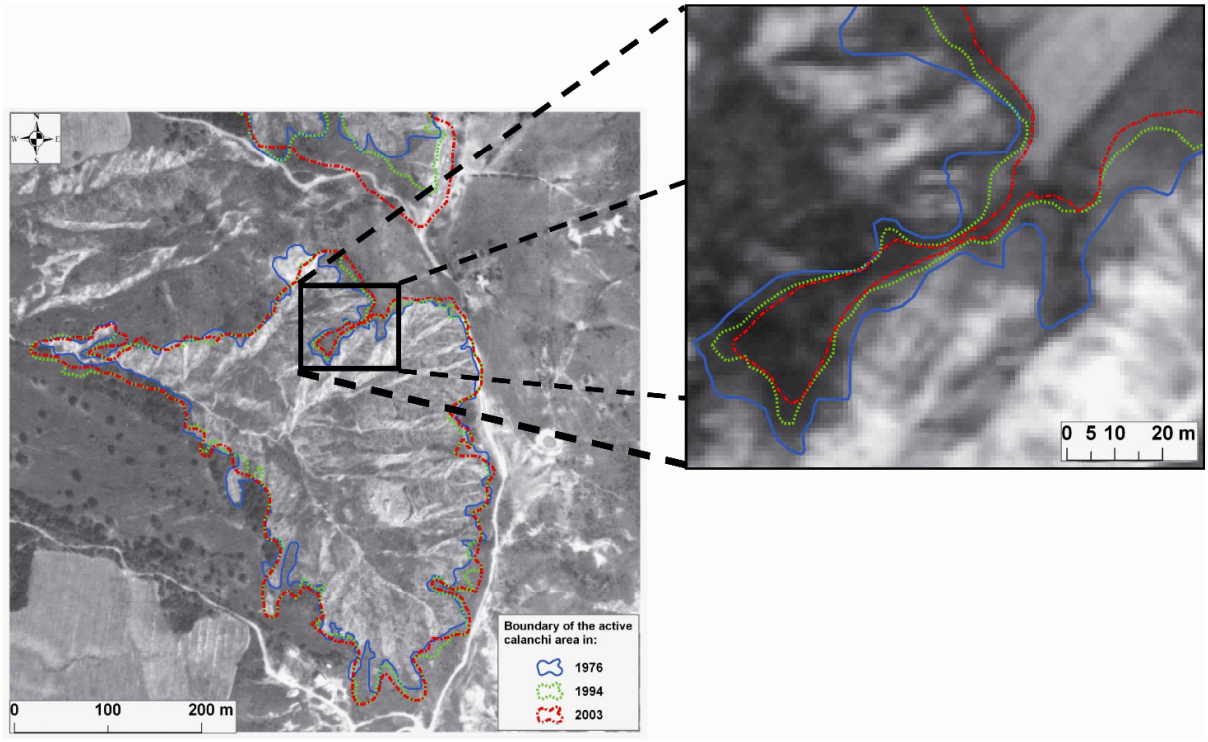

Fig. 4.5 – *Calanchi* slope retreat during the 1976-2003 time span.

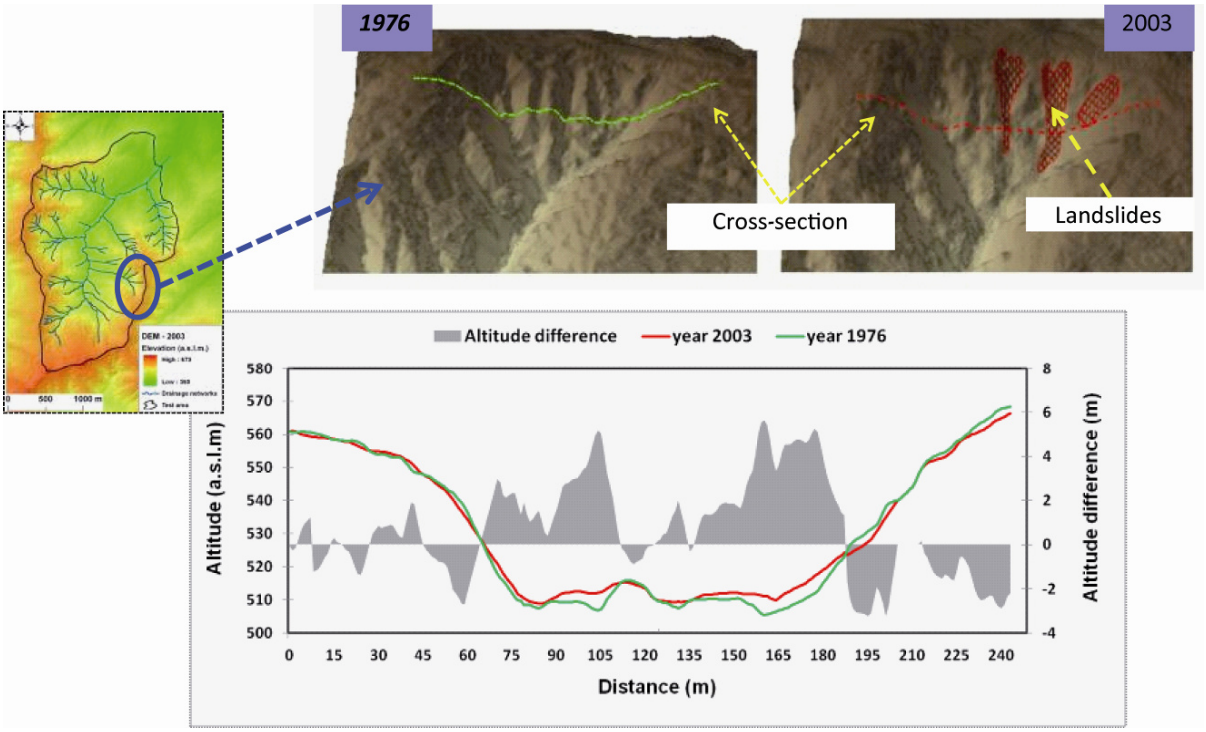

Fig. 4.6 – Transversal profiles of a single *calanco* badland.

The “Difference Maps” obtained by comparing the three DEMs, show the areas affected by erosion or accumulation, respectively (Fig. 4.7a). This kind of analysis, while requiring further investigation, already enables us to make some significant preliminary considerations:

i. the areas mainly affected by erosion are placed within the upper portions of hill-slopes, close to the top of *calanchi* slopes, and along the highest part of the slopes' main ridges;
ii. erosion rates were higher during the period 1976-1994 (in average 2.61 cm/a) than during the period 1994-2003 (1.1 cm/a), most likely because significant changes of the drainage systems and important interventions along slopes allowed to mitigate erosion processes (Fig. 4.7b). The mean erosion rate obtained by digital photogrammetric analysis for the longer period 1976-1994 is rather consistent with that recorded at a *calanchi* monitoring station within the sample catchment for the 1994-1995 (mean erosion rate of 3.6 cm/a, Marini, 1995).

The comparison of the DEMs allowed to assess the topographic changes between periods 1976-1994 and 1994-2003 (Fig. 4.7c), respectively. For the whole test area an average erosion rate of 1.2 cm/a was calculated for the period 1976-2003, with a computed sediment loss of about 230 t/ha/a. Higher rates result for the 1976-1994 period, for which *calanchi* badlands areas show an average denudation rate of 6.6 cm/a. Computed erosion rates for *calanchi* sites are in agreement with those obtained by Ciccacci et al. (2008, 2009) and Della Seta et al.(2009), monitored by using photogrammetric analysis and erosion pins, as well as with those resulted during this Ph.D monitoring activity (Fig. 2.9), for the sample catchments in Tuscany region.

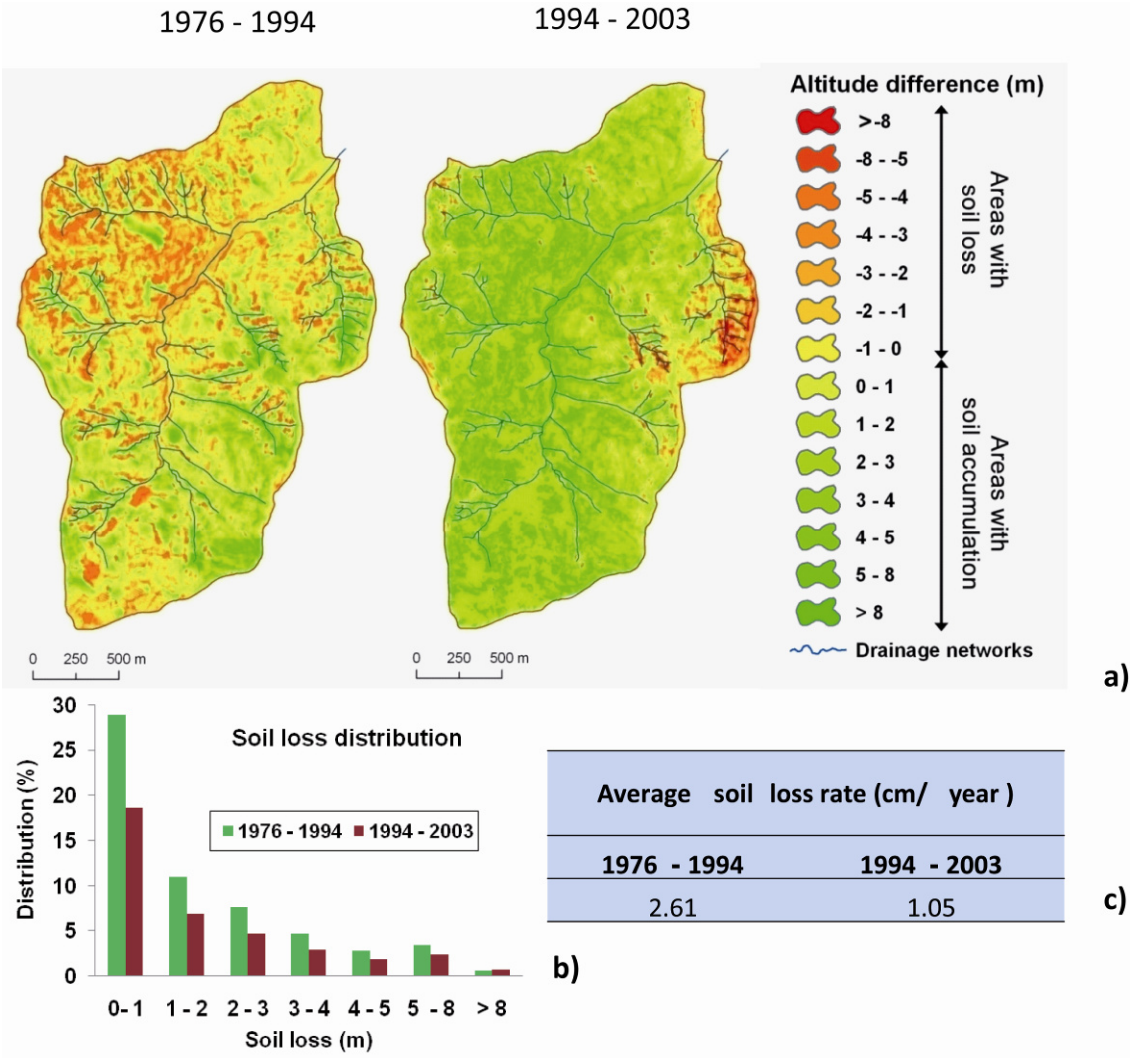

Fig. 4.7 – a) Height Difference maps, obtained after the comparison of 1976, 1994 and 2003 DEMs; b) Soil loss distribution over the 1976-1994 and 1994-2003 time spans; c) average soil loss rates for the two time spans.

4.4 Discussion

The application of digital photogrammetric methodologies has revealed to represent a powerful and low cost tool to evaluate the rate and spatial-temporal development of denudation processes, as confirmed by the comparison with point monitoring in the field. These methods can be very useful for sustainable land management, planning of erosion control measures and calibration of regional prediction models in Italy, as well as in other Mediterranean environments. The proposed method can be considered very useful to better locate denudation landforms and associated processes and to assess related erosion rates.

Moreover, multitemporal photogrammetric analysis allows to reconstruct historical landscape changes and morphological evolution when direct measurements are not possible or not available, as resulted for the period preceding the field monitoring phase in the Landola test area.

Photogrammetric analysis methodology is nevertheless affected by many error sources, starting from the limitations caused by the aerial image resolution and quality, together with those caused by the data interpolation in DEM constructing phase. Moreover, the obtained DEMs should be cleaned by the vegetation cover differences in height between the considered time span, in order to compute a more accurate erosion rate.

The reliability of the achieved results is still under investigation at Department of Sciences and Technologies for the Environment and Territory of Molise University, with particular reference to the evaluation of estimation errors of altitude differences, and, thus, of the computed erosion rates. Even though, this first comparison of the computed erosion rates with those measured during erosion decadal monitoring shows an overall convergence of the results. Finally, the applicability of 1954 photographs ("GAI" flight, taken at nominal scale 1:33.000, missing of calibration certificate) for denudation rates computation is being tested, considering the encouraging results achieved in previous studies (Salvini, 2008). Deeper knowledge of the strong modification of the Crete Senesi landscape, occurred with the advent of intense farming techniques (Guasparri, 1993), and the resulting effects on the territory morphodynamics during the last 60 years could emerge, with particular attention to the protection and conservation of residuals of the *biancane* and *calanchi* badland areas.

5 PARENT MATERIAL GRAIN SIZE AND GEOCHEMICAL COMPOSITION AS POTENTIAL EROSION FACTORS

Extensive literature on badlands has pointed out how, together with geological and climatic factors as well as human impact, more local conditions, such as parent material properties, play a relevant role in explaining the measured erosion intensities, as well as the development of different slope landforms in these sites.

Different authors have investigated pedological, mineralogical, grain size and geochemical properties of clay-rich terrains outcropping in badland sites of Italy, Southern Spain and Morocco (Vittorini, 1977; Alexander, 1982; Imeson et al., 1982; Pinna and Vittorini, 1989; Torri et al., 1994; Torri and Bryan, 1997; Phillips, 1998; Faulkner et al., 2000, 2003; 2004; Robinson and Phillips, 2001; Battaglia et al., 2002, 2011; Piccarreta et al., 2006; Romero-Dìaz et al., 2007), identifying them as crucial factors for badland evolution.

Summarizing, the main scopes of these investigations were to emphasize the role of sediment size and clay mineralogy and geochemistry in: 1) explaining the trigger and development of different types of badland landforms (such as *calanchi* badlands, *biancane* badlands, intermediate landforms and piping); 2) understanding the effects of human activities (in particular agriculture) on parent material properties; 3) finding diagnostic “site signatures”.

The clay capacity of cation exchange is responsible for soil behaviour during erosion by water: in particular, the presence of more than a few percentage of monovalent cations (particularly sodium) relative to divalent and trivalent cations in pore water will tend to make the sediment dispersive in water (Rolfe et al., 1960; Mitchell, 1976). In fact, sediment containing deflocculated clay can be entrained at very low stream powers (Sherard et al., 1976; Torri et al., 1994). Swelling behaviour of smectite seals the surface, favouring the rill erosion. Moreover, Imeson et al. (1982) indicated that, together with smectite (montmorillonite), illite and other clay minerals will also swell in sodium rich environment. In this conditions, the sediment size distribution, and in particular the clay percentage, become

very important (Robinson and Phillips, 2001). On the other hand, when crack, macropores or fractures are available, dispersion can encourage the process of subsurface erosion.

Considering possible differences in material characteristics that discriminate landform types, *biancane* badland sediment show a higher clay fraction than *calanchi* badland, where sand content is significantly greater (Alexander, 1982; Pinna & Vittorini, 1989; Battaglia et al., 2002). Both *calanchi* and *biancane* can develop in intermediate grain size, such as silty clays and clayey silts, as well as intermediate landforms, as "*calanchi mammellonari*" or "*bialanchi*" described by Castelvecchi and Vittorini (1970), Vittorini (1977), Alexander (1980) and Piccarreta et al. (2006). On the contrary, mineralogical differences between *calanchi* and *biancane* are not completely joined within literature: whereas Battaglia et al. (2002) did not find particular trend in clay mineralogy of Tuscany samples to be correlated with the different landforms, Alexander (1980) and Vittorini (1977) suggested a higher smectite content in *biancane* clays than in *calanchi* parent material. The more dispersive character of *biancane* clays is finally pointed out in different studies, as pore water composition of *biancane* generally shows higher sodium concentrations relative to divalent cations than in *calanchi* pore waters (Vittorini, 1977; Alexander, 1982; Battaglia et al., 2002), even if Piccarreta et al. (2006) did not find this differentiation for the southern Italy sites. Sherard et al. (1976) underlined that clay dispersivity is responsible for the development of subsurface large pipes and tunnels, as in materials with a high percentage of swelling clays the presence of crack and fissures on the surface can sometimes appear to offset the reduction in infiltration rates, as a consequence of the spontaneous dispersion of the colloids that cover the fissures walls, when rainfall penetrates them (Faulkner, 1990). The linkage of piping formation and *biancane* landform to high clay dispersivity led Alexander to an interesting hypothesis on *biancana* landforms initiation (1982): he supposed that *biancane* origin could be due to the enlargement of pipes and the following terrain collapse, leaving *biancana* cones as residuals. Even if *biancana* origin has afterwards been related also to other factors, such as tectonic lineations (Torri and Bryan, 1997; Della Seta et al., 2009), the widespread micropiping on *biancane* areas is undeniable.

Higher sodium content, as well as coarser sediment, are generally found in upper surface sediment, with clay content and related dispersivity level increasing downward. Since both Ca^{2+} and H^{+} can exchange with Na^{+} during infiltration, stabilisation can occur

either by buffering by Ca^{++}, mobilising the Na^{+} to relocate down profile, or as a consequence of the organic acids released by a vegetation cover. However, these two exchanges will have conflicting effects on pH (one raising pH, the other lowering it.). Faulkner et al., (2000) observed for some Almeria badland sites (SE Spain), that the higher pH values indicate the success of Ca^{++} in exchange with Na^{+}, especially in the upper horizons of soil, suggesting a greater potential for chemical stabilization of one of the investigated sites. On the other hand the presence of microalgal crust and other vegetation that produced organic acids in surface material could lead to lower pH value for the same sodium adsorption ratio (SAR) in another site. However, this stabilisation model may be complicated by the possible relocation of clay minerals down-profile in time. Lopez-Bermudez and Romero-Díaz (1989) found for Almerıa soils generally, that when smectite is present, its abundance increases with depth, replacing illite. Once dispersed, reactive double-layer clays are relocated, then swelling and clogging the lower layers of the soil profile. In clay-rich materials, this causes a decrease in permeability with depth (Sherard and Decker, 1976; Shainberg, 1992), predisposing the site for hydraulic conductivity (HC) reduction, and affecting subsequent infiltration, overland flow, surface wash and rilling. From the evolutionary point of view, piping processes should prevail in a young badland site, until the HC decreases and consequently piping becomes micropiping within the shallow sub-crust layer (Torri et al., 1994; Romero-Diaz et al., 2007). During this progressive stabilization, the surface material changes from dispersive to potentially dispersive and loses its proneness to piping.

The role of vegetation in stabilizing the clayey sediments is thus due to the lowering in dispersivity levels in the upper soil horizon. The effect of land reclamation for arable cultivation has been investigated by different authors, especially for the Crete Senesi landscape of Southern Tuscany badlands sites, where this process is really widespread and ascribable to the land reforms of the 1950s and, during the last decade, to the European Common Agricultural Policy (CAP). Phillips (1998) pointed out that the reduction in the exchangeable sodium percentage (ESP) following reclamation is the critical factor in increasing soil stability, even if the organic content remains low. This is probably because of the rapid leaching of salts from the profile after the reshaping process that has exposed the soil to the erosive weather elements. This rapid decline in the ESP below the 15% threshold leads to an increase in soil stability in the period immediately following reclamation.

Although this increase is slight, it is enough to inhibit chemical dispersion and, therefore, the activity of the badland forming processes. As such, the badlands are no longer actively evolving and therefore the inherent landscape of the Crete Senesi is disappearing permanently. Marignani et al. (2008) have observed that vegetation facilitates water infiltration and leaching of sodium: this stabilizes the topmost centimeters of soil, but at the same time allows more water to reach the pipe system. Also Romero-Díaz et al. (2007) underlined that in a abandoned lands of SE Spain, very high exchangeable sodium percentage (ESP) values were found more easily with depth than surface, this difference appearing to explain tunnel initiation at subsurface levels. In the same study they did not find a difference in sodium content along the vertical profile in a site hypothesized as never been cultivated. This hypothesis was witnessed by the observation that potassium levels have remained almost constant with depth.

Faulkner et al. (2000) have proposed three “site signatures” in order to explain the morphological variety found in badland areas, summarizing the described influences that textural, geochemical and mineralogical properties of parental material exert on erosion processes. These signatures are 1) the relationship between electrical conductivity and sodium adsorption ratio (SAR), originally proposed by Rengasamy et al. (1984); 2) the relation between particle size and SAR, diagnostic in the development of a non-dispersive superficial layer; 3) pH/SAR ratio, to indicate the buffering role of calcium and vegetation in stabilization processes.

The aim of this work has been the characterization of the mineralogical, geochemical and size composition of parental materials to further elucidate their properties on both bare and vegetated surfaces and to discuss them with respect to the development of different badlands processes.

These new data allowed to deepen and better define the variability of mean erosion rates measured at different erosion landforms, as well as to discuss the results with respect to the initiation and development of different badlands forming processes in the study area.

5.1 Collection of samples

Since the objective of the research was to point out possible differences in the parent material characteristics for different badlands types, as well as for vegetated and bare soils, the sampling phase has been focused on some significant sites of Upper Orcia Valley, characterized by different land use categories and different erosion landforms (Fig. 5.1 Tab. 5.1):

1) a hillslope characterized by embryonic *biancane* badlands, located within the Lucciolabella Natural Reserve site (Fig. 5.2a), where the residuals of the antic *biancane* landscape of Upper Orcia valley is protected (Miglia subcathment);
2) a subcathcment partly characterized by badlands erosion, partly exploited for agricultural purposes (La Piaggia subcatchment of T. Formone, Fig. 5.2b).
3) On *calanchi* badlands sites, characterized by intense denudation rates due to water erosion together with landsliding (different sites of Upper Orcia valley, Fig. 5.2c).
4) on the valley bottom of the Orcia River, in a sunflower field.

In order to underline possible differences at different depths for *biancane* badlands and vegetated sites, samples were extracted at increasing depths on the basis of different degree of weathering for the groups 1 and 2. *Biancane* sites are in fact characterized by a relevant shallow horizon of weathered soil, where, moreover, thenardite (Na2SO4) crystals are often found. On the other hand, agricultural activity can enhance the differences between the topsoil and the subsoil properties. In *calanchi* badlands sites, where the weathered layer is very thin or absent due to rapid denudation, and thus the unweathered clay results exposed, samples were collected at a unique depth, as shown in Tab.5.1.

SAMPLE	POSITION (C. S. UTM WGS84 32T) LONG	LAT	ELEVATION (m s.l.m.)	SITE	LANDFORM	DEPTH (cm)
L1 L1-A L1-B	724795	4768132	559	Lucciolabella Natural Reserve	Vegetated surface	0-10 0-30 30-50
L2-A L2-F-A L2-F-B L2-F-C	724799	4768132	556	Lucciolabella Natural Reserve	Embryionic biancane - Inter-rill Embryionic biancane - Oxidized horizon	0-10 0-10 10-30 30-50
L3-A L3-B	724801	4768126	554	Lucciolabella Natural Reserve	Embryionic biancane - rill	0-30 30-50
L4-A L4-B	724808	4768129	556-557	Lucciolabella Natural Reserve	Embryionic biancane – Vegetated biancana summit Embryionic biancane - Biancana base	0-10 0-10
L5-A L5-B L5-C	724801	4768127	555	Lucciolabella Natural Reserve	Embryionic biancane Inter -rill	0-10 10-40 40-55
L6-A L6-B L6C	724841	4768128	549	Lucciolabella Natural Reserve	Vegetated surface	0-10 10-30 30-60
LP1-A LP1-B	721418	4759354	558	La Piaggia	Biancana badland (middle flank)	0-10 10-45
LP2-A LP2-B	721389	4759290	556	La Piaggia	Cultivated fluvial terrace	0-10 10-45
PP	723187	4758189	560	Podere Paiccia	*Calanco* badland	10-20
PR	722235	4760611	538	Poggio Reggiano	*Calanco* badland	10-20
M1	0723934	4763996	324	confluence Miglia-Orcia sunflowers field	Vegetated Alluvial plain	0-30
M7	722552	4759151	575	La Piaggia	*Calanco* badland	0-30
M9	722534	4759015	555	La Piaggia	*Calanco* badland	0-30

Tab. 5.1 – Samples collected within the Upper Orcia catchment.

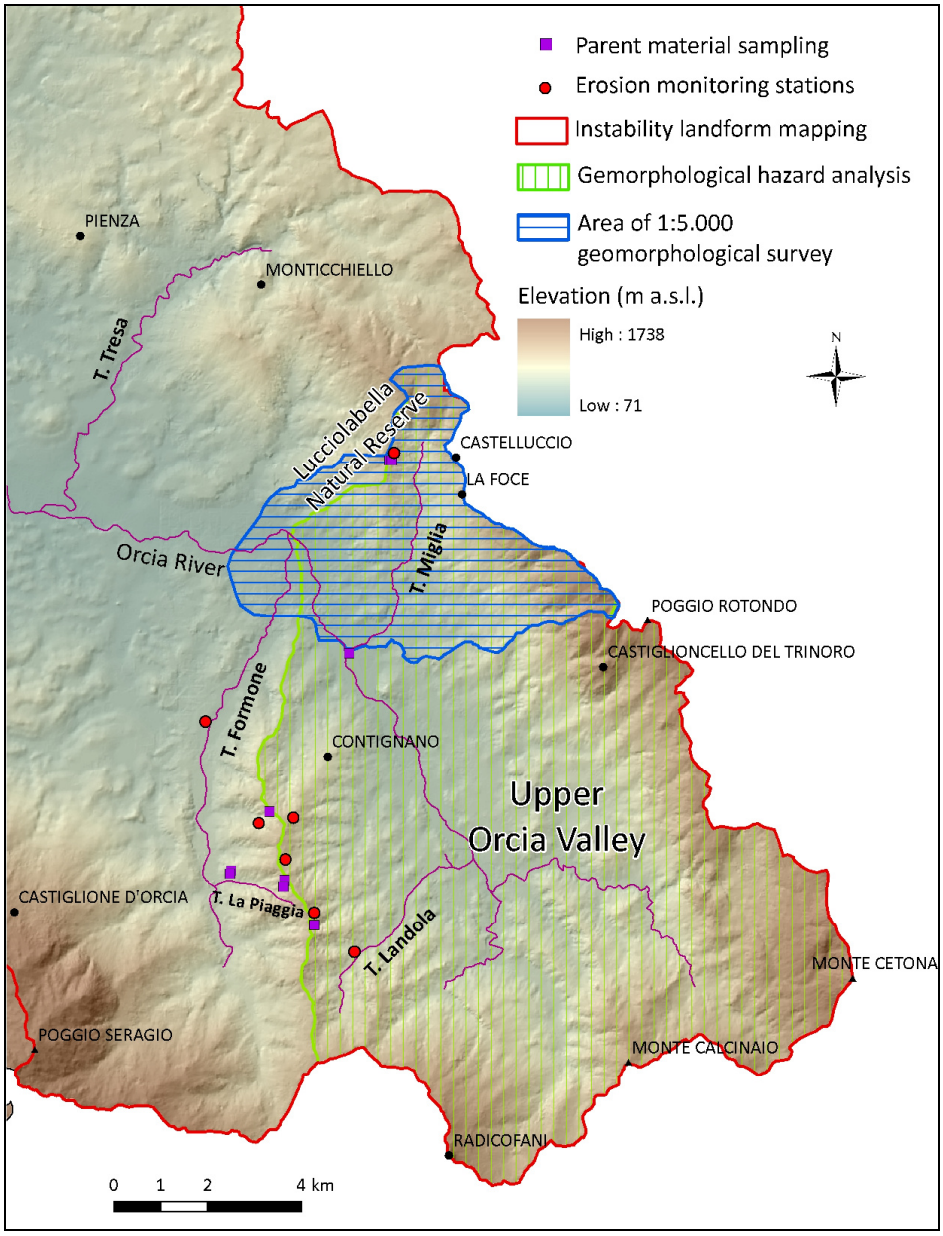

Fig. 5.1 – Location map of parent material sampling sites.

Fig. 5.2 – Sample sites. a) embryonic *biancane* of Lucciolabella site; b) cropland in La Piaggia sucbcatchment; c) Podere Paiccia *calanchi* badlands, affected by mass movements.

5.2 Analytical procedures

For grain size analyses, each sample was handled with hydrogen peroxid to discard the organic matter that, if present, may cause deflocculation of the finest grained component during the analytical procedure. Samples were successively washed with distilled water to remove salts and two granulometric fractions for each sample were separated using a 63 µm sieve. The two distinct fractions were successively dried and weighted and the grain size distribution was analyzed using a set of ASTM sieves (for the coarser fraction: grain size > 63 µm) and a laser granulometer (for the finer fraction: grain size < 63 µm). The qualitative mineralogical composition of bulk samples and the clay fractions was analysed using an X-ray diffractometer. The present clayey and non-clayey minerals were identified on the <4 µm fraction, picked by means of fractioned sedimentation in accordance with Stokes' law, using a sedimentation cylinder (Bellotti & Valeri, 1975).

Pore water soluble ions concentration was determined on a saturation extract prepared mixing the sediment with distilled water in the 1:10 ratio, then shaken with a magnet in a Tehtnica ROTAMIX 560 MMH agitator for 24 hours, to favor the solubilization of cations and anions. The saturation extract was filtered with a 45 µm filter and analyzed for the major cations (Ca^{2+}, Mg^{2+}, Na^{+}, K^{+}, Li^{+}, Sr^{2+}, NH_4^{+}) and anions (Cl^{-}, SO_4^{2-},Br^{-}, F^{-}, NO_2^{-}, NO_3^{-}, PO_4^{3-}, HCO_3^{-}) by a Methrom IC 761 Cromatograph.

For each sample we determined the total dissolved solids concentration (TDS, here used also to estimate the electrical conductivity) and the cation exchange capacity (CEC) of sediments, which is an indication of both the nature of material and its behavior during water erosion (Alexander, 1982). In fact, clay fraction is the principal source of exchangeable cations (Kelley, 1964).

$$CEC = \Sigma(\text{exchangeable } Ca^{2+,} Mg^{2+}, K^{+}, Na^{+}) \quad (1)$$

As increasing the percentage of exchangeable sodium among the exchangeable cations the sediment will be more dispersive in water (Rolfe at al., 1960; Mitchell, 1976), thus we calculated both the sodium percentage (PS) and the sodium adsorption ratio (SAR) using the following equations:

$$PS = [Na^{+}/(Na^{+}+K^{+}+Ca^{2+}+Mg^{2+})] *100 \quad (2)$$

$$SAR = Na^{+}/[(Ca^{2+}+Mg^{2+})/2]^{1/2}) \quad (3)$$

5.3 Results

As shown in Fig. 5.3 and Tab. 5.2, most of the samples fall in mud grain class, where the proportions of clay and silt are approximately the same. A considerable sand content is observed in samples PR (49%), LP2B (42%), LP2A (28%), PP (21%), M7 (12%), M9 (8%), LP1A (6%). These samples were picked in *calanchi* badlands sites (PP, PR, M7, M9), in cultivated lands (LP2A, LP2B and M1) and one in a *biancane* site (LP1A). All the samples collected in Lucciolabella *biancane* site fall in the mud grain class, with a general increase of the silt fraction, with respect to clay, in the samples picked in vegetated areas: L1A, L1B, L6A collected in the vegetated surface surrounding the area evolving into *biancane* landform; L4A, taken in the vegetated summit of a small *biancana*; and L2FB, taken within an oxidized joint in the *biancana* badlands area. As for sample depth, the content in clay seems to slightly increase proportionally, even if not strongly.

Sample	Sand	Silt	Clay	M_z (Φ)	σ_1 (Φ)	D_{50}(mm)
L1	1,25	65,82	32,93	7,21	1,63	0,007
L2A	0,02	48,44	51,54	7,89	1,37	0,004
L2FB	0,43	55,56	44,01	7,67	1,46	0,005
L4A	0,29	64,3	35,41	7,38	1,53	0,006
L4B	0,11	55,39	44,5	7,66	1,47	0,005
L6C	0	50,02	49,98	7,83	1,4	0,004
LP1A	5,98	46,73	47,29	7,75	1,63	0,004
M 9	7,78	49,61	42,61	7,54	1,87	0,005
L1A	0,28	55,02	44,7	7,63	1,52	0,005
L1B	0,37	56,05	43,58	7,58	1,55	0,005
L2FA	0	52,31	47,69	7,79	1,39	0,004
L3A	0	50,78	49,22	7,8	1,42	0,004
L3B	0,12	51,95	47,93	7,75	1,46	0,004
L5A	0,06	55,27	44,67	7,67	1,47	0,005
L5B	0	50,55	49,45	7,8	1,43	0,004
L5C	0,04	52,28	47,68	7,75	1,45	0,004
L6A	0,31	52,44	47,25	7,74	1,46	0,004
L6B	0,03	50,19	49,78	7,83	1,41	0,004
LP1B	0	50,24	49,76	7,86	1,35	0,004
LP2A	28,38	44,3	27,32	5,59	3,65	0,012
LP2B	41,93	35,74	22,33	5,08	3,38	0,023
M1	33,09	46,48	20,43	5,67	2,44	0,022
M 7	12,26	54,25	33,49	6,92	2,19	0,007
PP	21,16	39,6	39,24	6,61	2,65	0,006
PR	48,76	29,11	22,13	4,84	3,06	0,051

Tab. 5.2 – Grain size composition of samples and main descriptive statistics (expressed in Φ units).

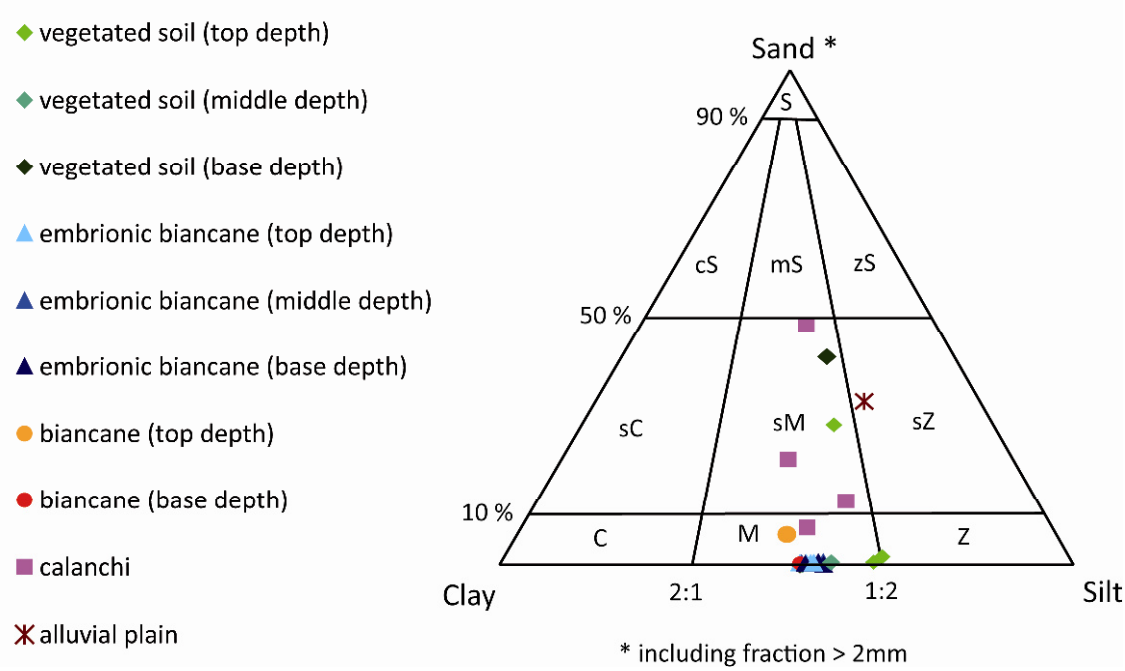

Fig. 5.3 – Grain size composition of samples plotted in the Folk (1954) ternary diagram. S = sand; cS = clayey sand; mS = muddy sand; zS = silty sand; sC = sandy clay; sM = sandy mud; sZ = sandy silt; C = clay; M = mud; Z = silt.

Clayey mineralogy appear quite uniform: the main non-clay minerals are quartz, calcite and feldspars, while the clayey components are chlorite, kaolinite, poorly crystallized illite and mixed layer minerals, the last giving an expandable character to clays.

Pore water composition and related calculated parameters controlling clay dispersivity (TDS, PS, SAR) are shown in Tab. 5.3, together with pH and EC values. These ions represent the products of the reaction between some mineral phases and interstitial water.

The monovalent cations are represented mainly by sodium and potassium, the second one in smaller concentrations. Calcium is always dissolved in the liquid extract, while magnesium is absent in some surface samples. As for the anions, the sulphate is the most abundant and generally increases with the soil depth, while the other secondary dominating anions are chloride and nitrate. pH values are between 8.24 and 9.75 and *calanchi* parent materials, as well as vegetated soil sediments, show lower pH values with respect to *biancane*.

As shown in Table 5.3, samples from the Lucciolabella vegetated sites (L1, L1-A, L1-B, L6A, L6B e L6C) show a progressive increase of TDS and SAR with depth. The maximum PS

value was measured in the intermediate depth (sample L1-A, at 10-30 cm depth interval). This evidence suggests that, according to what observed by Torri (personal communication) in the same study area, in this site the soil stabilization at depth < 10 cm was due to the presence of vegetation that favors the H^+ mobility ascribed to roots activity and consequent lowering of Na^+ abundance.

The samples collected on embryonic *biancane* show PS values over 80% and SAR values quite high, thus suggesting the predominance of dispersive processes. All the samples from *calanchi* sites show salt content considerably lower than the one in *biancane* parent materials. In particular we observed low dispersivity evidenced by low SAR and PS values.

In order to confirm the above results, we compared the different parameters that control clay dispersivity, taking into account, among others, the site signatures proposed by Faulkner et al. (2000).The relationship between EC and SAR, plotted versus the Regasamy et al. (1984) domains show that the samples collected in vegetated or cultivated sites and on *calanchi* slopes are potentially dispersive, while the ones taken in *biancane*, or in the Lucciolabella slope evolving into *biancane* landforms, fall in the dispersive domain (Fig. 5.4). A slight logaritmic positive correlation between SAR and EC was observed (n=24, R^2=0.43).

Sherard et al. (1976) correlated SAR, PS and TDS values with clay dispersivity and this correlation was attempted in plot of Fig. 5.5. According to these authors, clays of zone A have a high tendency to spontaneous dispersivity, while the clays of zone C are ordinary erosion-resistant clays. Sediments of zone C may be dispersive or non dispersive, showing an intermediate behaviour. All the clay samples collected in embryonic *biancane* sites are clustered in zone A, showing an important proneness to produce colloidal dispersion when saturated with rainwater, while *calanchi* parent material falling in zone C were interpreted as more resistant to erosion. These results are in agreement with those previously obtained by Vittorini (1977), Alexander (1982) and Battaglia et al. (2002).

The relationships between SAR, pH and grain size, proposed by Faulkner et al. (2000) as site signature indicators, were explored for the Upper Orcia Valley samples (Fig. 5.6).

Considering the SAR/pH relation (Fig. 5.6a), a sort of positive relation is observed, making likely the hypothesis that SAR values reduction can be linked to cation exchange with hydrogen under vegetation cover, in particular for vegetated soil samples, whose upper

portion show lower pH and SAR values. This is confirmed by the pH/Ca^{2+} relation that do not show a typical trend (Fig. 5.7). Considering the low variability of mean sediment size, the SAR/grain size site signature was replaced by SAR/clay % of the samples, as already suggested by Piccarreta et al. (2006). A strong relation is not shown, even if SAR values increase with the sample clay % (Fig. 5.6b).

Sample	Ubication	Soil depth (cm)	Na^+	K^+	Ca^{2+}	Mg^{2+}	SO_4^{2-}	Cl^-	No_3^-	HCO_3^-	TDS	PS	SAR	pH
L1	vegetated soil (top depth)	0-10	0,24	0,35	1,76	0,29	0,03	0,01	0,00	2,67	5,79	9,23	0,24	8,35
L1A	vegetated soil (middle depth)	0-30	2,00	0,52	0,51	0,69	2,17	0,19	0,20	1,10	7,43	53,81	2,58	8,89
L1B	vegetated soil (base depth)	30-50	10,08	1,11	9,03	3,02	4,51	0,07	0,01	18,60	46,50	43,39	4,11	8,69
L2-A	embryonic biancane	0-10	8,70	0,53	0,10	0,01	6,25	0,36	0,82	2,00	18,80	93,12	37,42	9,38
L2-F-A	embryonic biancane	0-10	6,72	0,62	1,01	0,00	1,87	0,04	1,38	4,03	16,72	80,43	9,44	9,05
L2-F-B	embryonic biancane	10-30	3,80	0,41	0,14	0,20	2,08	0,41	0,52	1,44	9,11	83,51	9,20	9,03
L2-F-C	embryonic biancane	30-50	3,43	0,34	0,16	0,21	2,34	0,52	1,15	0,04	8,29	82,78	7,89	9,32
L3-A	embryonic biancane	0-30	13,04	0,78	1,30	3,54	3,12	0,02	11,14	3,00	36,68	69,87	8,38	8,90
L3-B	embryonic biancane	30-50	9,74	1,01	3,63	1,15	0,00	0,57	1,49	13,37	31,06	62,72	6,30	9,06
L4-A	embryonic biancane (vegetated biancana summit)	0-10	0,20	0,22	1,07	0,01	0,17	0,07	0,39	0,10	3,02	13,60	0,28	8,43
L4-B	embryonic biancane	0-10	3,54	0,59	0,41	0,41	2,90	0,15	0,04	1,84	9,92	71,48	5,53	9,75
L5-A	embryonic biancane	0-10	8,77	1,07	3,76	2,03	1,99	0,48	1,01	12,12	31,27	56,12	5,16	9,44
L5-B	embryonic biancane	10-40	7,50	0,84	0,29	0,35	6,04	0,66	0,57	1,64	17,98	83,53	13,23	9,10
L5-C	embryonic biancane	40-55	6,86	0,59	0,10	0,49	4,63	0,51	0,43	2,31	16,09	85,30	12,59	9,20
L6 -A	vegetated soil	0-10	0,18	0,17	1,58	0,00	0,07	0,08	0,15	1,62	3,99	9,24	0,20	8,51
L6 - B	vegetated soil	10-30	0,56	0,19	0,79	1,71	0,13	0,15	0,10	2,75	6,53	17,17	0,50	8,67
L6 - C	vegetated soil	30-60	0,83	0,16	4,37	1,78	0,94	0,08	0,07	5,98	14,28	11,63	0,47	8,50
LP1-A	biancane	0-10	12,39	0,44	1,74	1,84	10,41	1,29	0,94	3,00	32,07	75,49	9,26	8,79
LP1-B	biancane	10-45	7,64	0,22	14,40	2,64	6,23	1,02	1,03	16,51	49,78	30,68	2,62	8,24
LP2 -A	cultivated soil	0-10	1,24	0,17	1,75	5,10	5,07	0,14	0,11	2,91	16,51	15,06	0,67	8,61
LP2 - B	cultivated soil	10-45	0,46	0,18	0,92	0,39	0,34	0,14	0,30	1,11	3,95	23,60	0,57	8,76
PP	calanchi	10-20	3,59	0,70	2,01	11,23	8,31	0,10	0,05	9,02	35,03	20,48	1,39	8,40
PR	calanchi	10-15	1,03	0,52	11,16	3,95	2,21	0,10	0,15	14,15	33,31	6,19	0,37	8,39
M 1	alluvial plain	0-30	0,11	0,15	1,25	0,04	0,09	0,06	0,95	0,36	3,09	7,04	0,14	8,47
M 7	calanchi	0-30	0,41	0,18	1,01	0,67	0,35	0,14	0,27	1,48	4,59	18,08	0,45	8,36
M 9	calanchi	0-30	0,33	0,12	1,15	0,27	0,10	0,14	0,49	1,11	3,72	17,53	0,39	8,57

Tab. 5.3 – Pore water composition of collected samples (in meq/L) and related parameters controlling clay dispersivity.

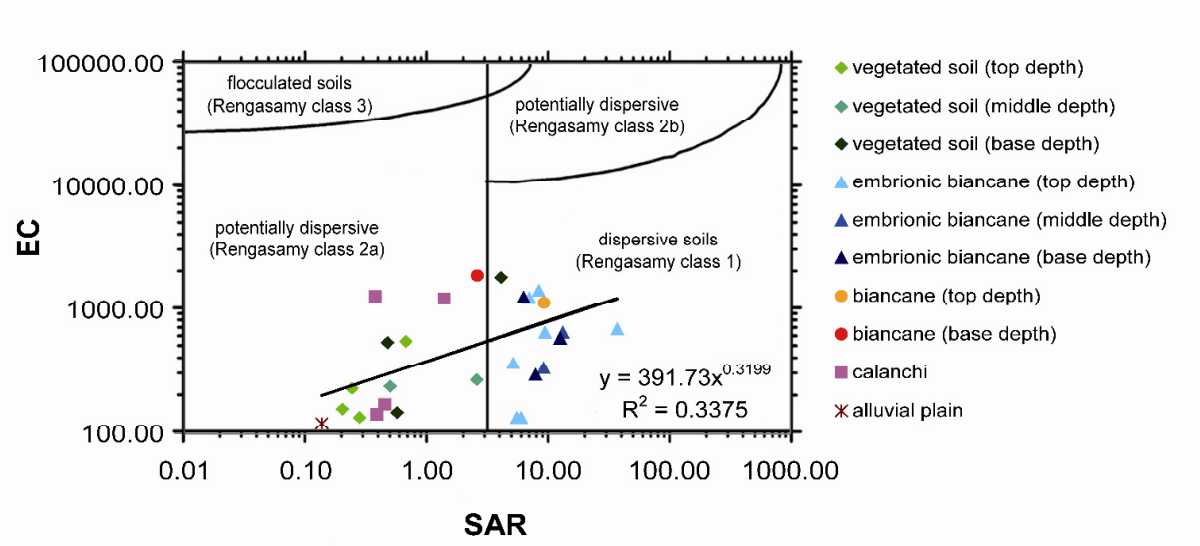

Fig. 5.4 – Electrical conductivity values (µS/sec) in relation to SAR values, in the Rengasamy domains of dispersivity (Rengasamy et al., 1984).

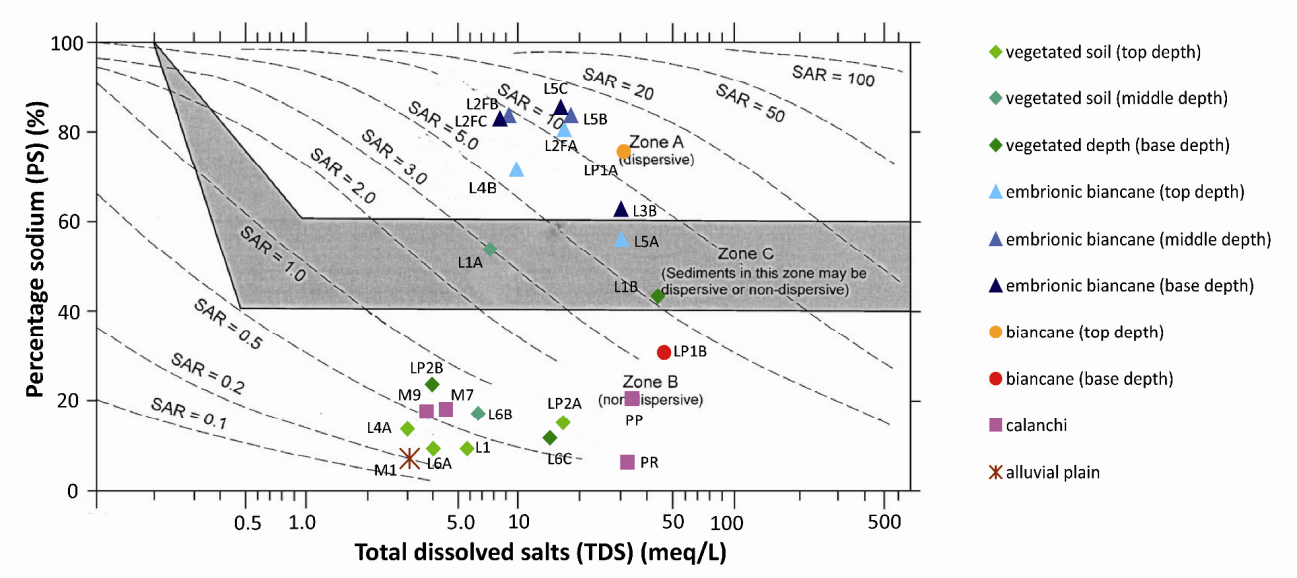

Fig. 5.5 – Relation between sediment dispersivity and pore water composition (expressed through the PS, TDS and SAR parameters), as established by Sherard et al. (1976).

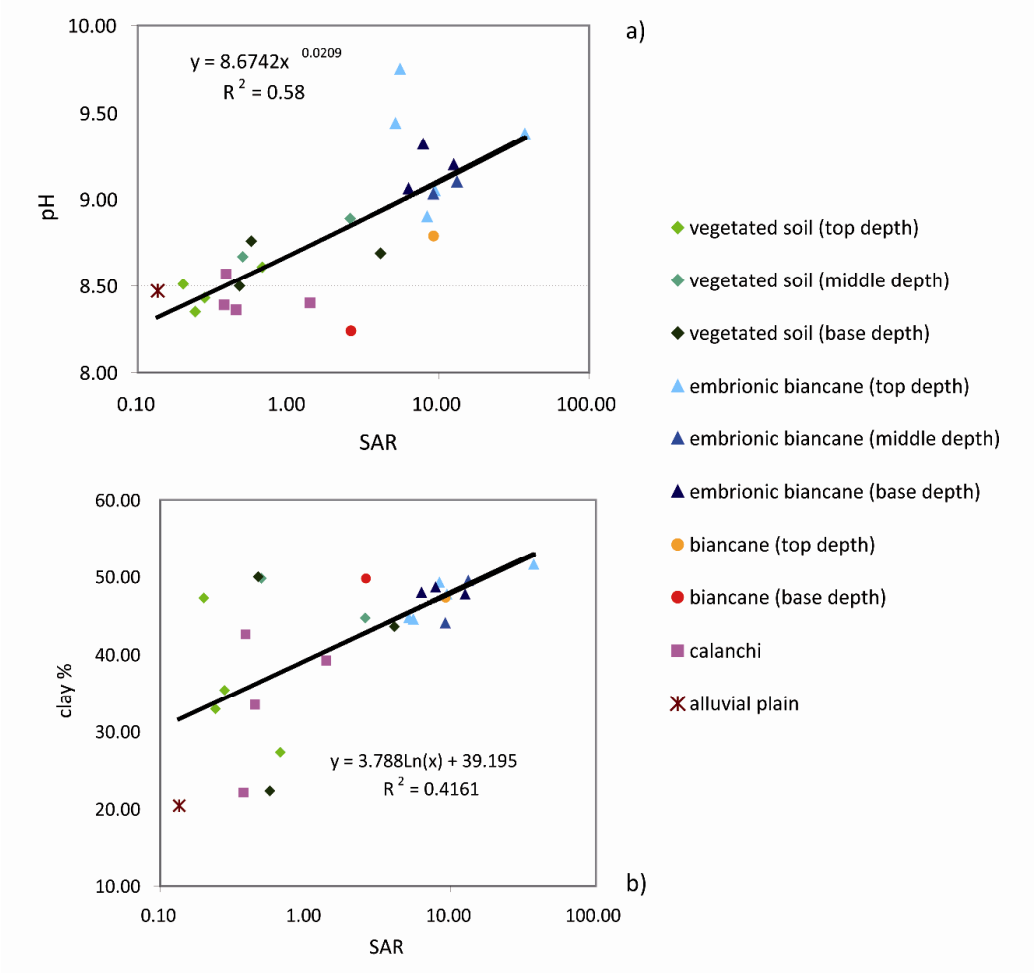

Fig. 5.6 – pH/SAR and grain size/SAR site signatures for the Upper Orcia Valley samples.

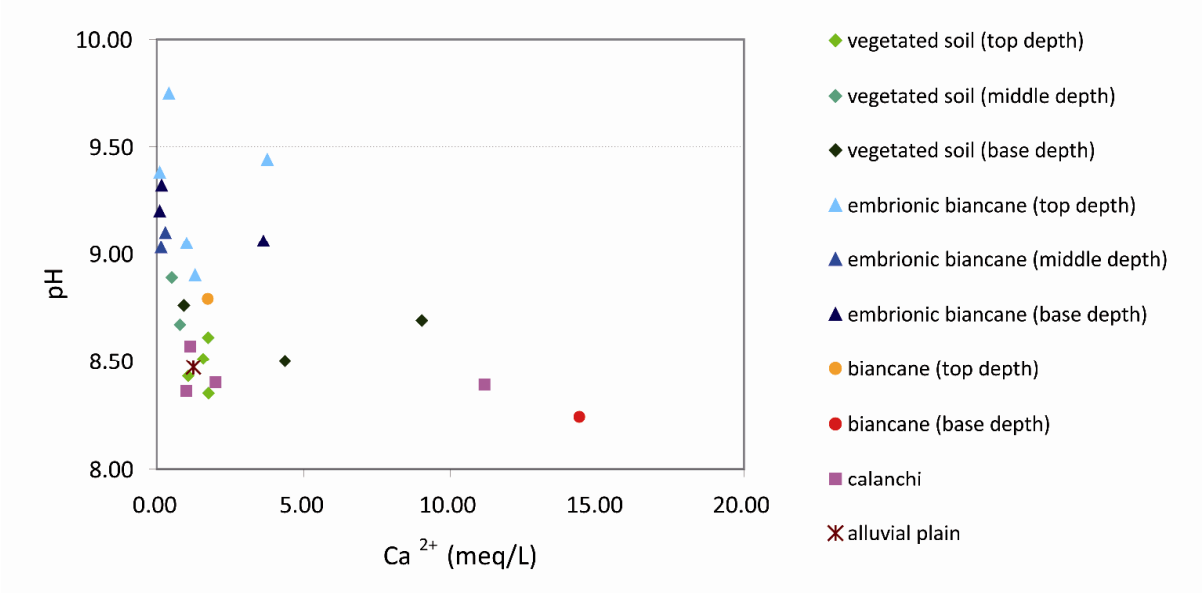

Fig. 5.7 – Relationship between pH and Ca^{2+} concentration (meq/L).

5.4 Discussion

Results from parent material analyses on the sampled badlands areas in Upper Orcia Valley showed some interesting results on the different factors influencing the diverse badlands landform types in the study area. Even if none of the samples show SAR values higher than the threshold for deflocculation (SAR = 15, Piccarreta et al., 2006), considering the dispersive power of the analysed clays, a higher Na^+ content relative to other cations has been observed in the well-developed and embryonic *biancana* parent materials with respect to *calanchi* samples. This evidence confirms the stronger tendency of *biancane* clays to spontaneous colloidal dispersion with respect to *calanchi* clays, as already observed by Vittorini (1977), Alexander (1982) and Battaglia et al. (2002). Moreover, *biancane* parent materials are characterized by a slightly finer grain size. These results, along with the observed prevalence of piping on *biancane* sites than on *calanchi* badlands for the Upper Orcia catchment area, is in agreement with the hypothesis that clay dispersivity is directly linked to subsurface erosion. Nevertheless, the long-lasting investigation of the *badlands* denudation hot spots of Upper Orcia Valley lead us to consider that grain size, chemical and mineralogical properties of the parent materials cannot explain alone the initiation and development of the different badland landforms. Some more arguments should be discussed in order to unravel the cause/effect relationships among factors and geomorphic processes. In fact, considering the distribution of *calanchi* and *biancane* landforms of the study area among the different classes of the main topographic and physiographic factors (Fig. 5.8), it is a matter of fact that *calanchi* badlands develop on steeper slopes and where higher values of amplitude of relief occur, due to the morphoevolutionary processes. Moreover, observations on present embryonic *biancane* of Lucciolabella site confirm the leading role played by reticular systems of joints in the dissection of original, gently-dipping surfaces (Colica and Guasparri, 1990; Torri and Bryan, 1997; Farifteh and Soeters, 2006; Della Seta et al., 2009). As for the *calanchi* evolution, their slopes probably evolve by substantial parallel retreat as long as caprock is present (Scheidegger, 1961, 1964), until caprock remnants finally disappear. Actually a resolute difference on dispersivity level of the *biancana* samples of La Piaggia subcatchment was not found with respect to *calanchi* badlands samples of the same subcatchment.

On the other hand, a significant influence of clay properties was observed on the different erosion rates measured during decadal monitoring investigations by means of erosion pins in the study area. As summarized in Fig. 2.9, *calanchi* badlands show lower erosion rates due to surface runoff. The major facility of *biancane* clays to be entrained at very low stream powers is reflected in their major dispersivity, while, in badlands, the morphoevolution and sediment removal is predominantly caused by widespread mudsliding from the rill and gully heads, as also observed within the Volterra basin (central Tuscany) by Battaglia et al. (2011) and confirmed by the mean positive variations of ground level for some *calanchi* monitoring stations (Fig. 2.9). This observation can be also related to the higher sand content in *calanchi* badlands, which may favour the infiltration processes to the detriment of runoff.

The increase of clay dispersivity downward along the soil profiles seems to be linked to the stabilization due to vegetation cover, since a marked difference in dispersivity level occurred only in the samples collected in the vegetated or cultivated sites and since the SAR values were proved to be positively correlated to the pH values. As already observed by several authors, the agricultural exploitation of these lands lead to a decrease of exchangeable cations concentration, even if the permanent inhibition of chemical dispersion due to increase of soil stability hypothesized by Phillips (1998) cannot be completely agreed. The authors overview after decadal monitoring and observation in the study area and in other sites of central Italy (Della Seta et al., 2007, 2009) is that badlands initiation is even enhanced by agricultural manipulation: grazing and farming are among the most important triggers for accelerated water erosion, and tillage erosion has been recognized as an increasing factor of water erosion (we have recorded up to 24 g/l turbidity values in cropland gully water during heavy rainfall events in November 2005). This is in agreement with the observations made by Torri et al. (2002), concerning the possibility that human reshaping of badlands slopes for agricultural purposes increases the proneness to water concentration in soils, thus favouring the development of ephemeral gullies. Similar observations were also underlined for other Mediterranean semiarid environments, such as many sites in Spain (López-Bermudez and Romero-Díaz, 1989; Calvo-Cases and Harvey, 1996; Calzolari et al., 1997; Borselli et al., 2006; Torri et al., 1999; Desir and Marín, 2007; Faulkner et al., 2008; Nadal-Romero and Regüés, 2010). Ephemeral gullies (Foster, 1986) are often

recognizable in croplands, and grow rapidly as a consequence of concentrated rainfall. Moreover, the effects of farming may become stronger if land use changes determine cropland abandonment (Faulkner et al.,2003; Romero-Díaz et al., 2007; Lesschen et al., 2008): when converting cultivated lands in abandoned lands, in presence of semiarid conditions, vegetation recovery is limited by water and seed dispersal (Pugnaire et al., 2006), especially because re-vegetation with indigenous species is rarely performed. Investigations on other sites of central Italy (Vergari et al., submitted) together with several studies in different Mediterranean sites (Faulkner et al.,2003; Borselli et al., 2006; Romero-Díaz et al., 2007; Lesschen et al., 2008), proved that cropland abandonment provokes an intensification of erosion rate with respect to the erosion rates measured on non-exploited lands in similar topographic conditions.

Summarizing, the following main conclusions have been highlighted:

a) parent material of *biancane* samples are characterized by a finer grain size and a more dispersive clay fraction than *calanchi* samples, according to previous literature;

b) results from this work, together with those from previous studies, confirm that topographical and geological features of Upper Orcia Valley denudation-hot spots have a more significant influence than physico-chemical properties of parent material in explaining the initiation and development of different badland landforms (*calanchi* and *biancane*);

c) clay properties have been proved to be directly related to different erosion intensity measured at *calanchi* and *biancane* sites;

d) vegetation cover seems to stabilize upper layers of soil profile, even if not permanently: agricultural manipulation and cropland abandonment increase the proneness to gully formation and related accelerated erosion.

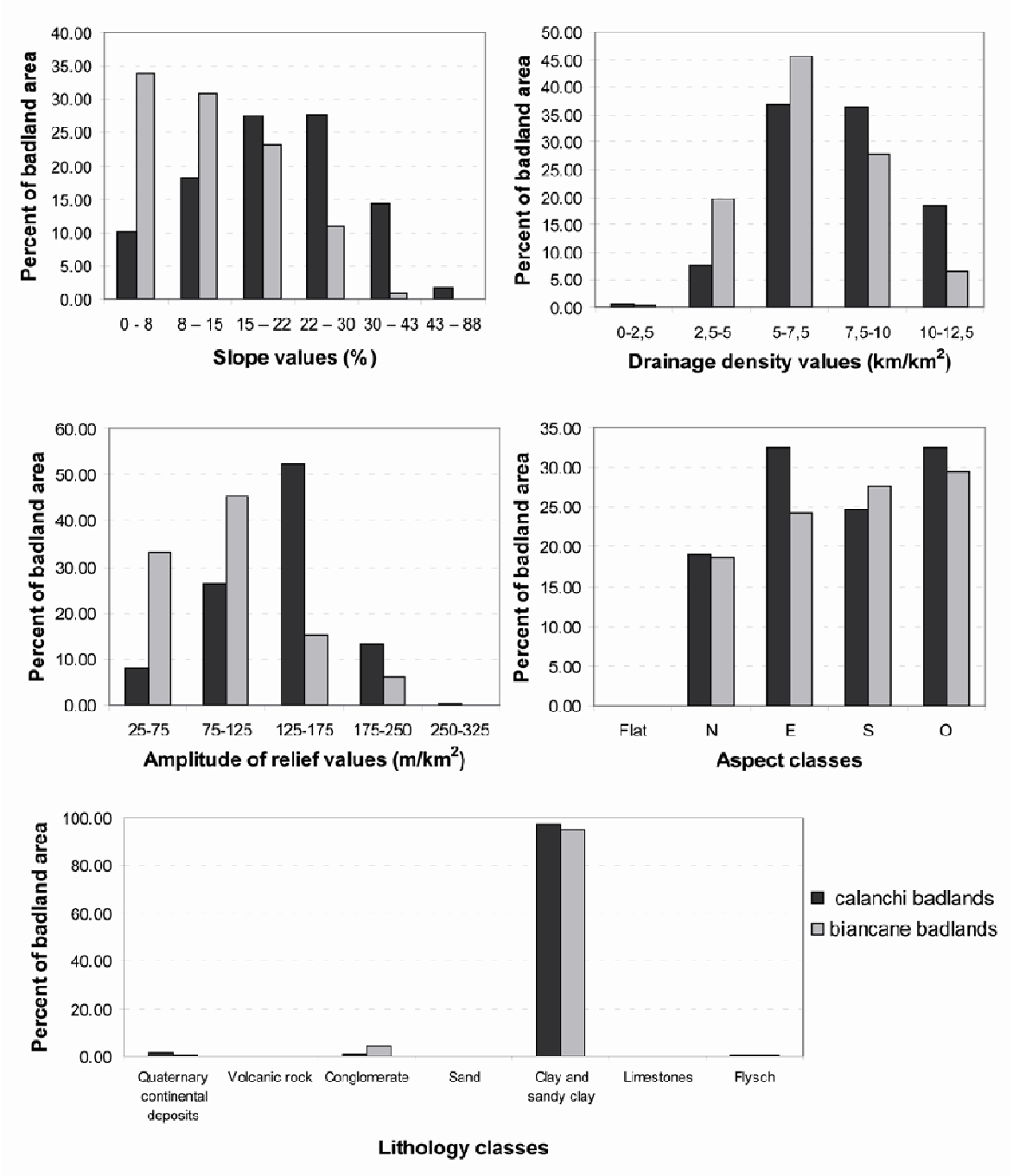

Fig. 5.8 – Distribution of Upper Orcia Valley *calanchi* and *biancane* badlands areas in the classes of the main conditioning factors.

PART II

DENUDATION MODELING AND WATER EROSION HAZARD ASSESSMENT

Several methods have been implemented to model soil loss, and can be synthetically classified into two categories: empirical and physically-based. The empirical methods estimate soil erosion by exploring statistical relationships between a set of influencing parameters and erosion effects, which have been optimized from empirical observations in sample areas (test basins or plots). These methods have been applied quite extensively, despite the fact that they have been implemented in regions characterized by specific physical conditions The physically-based methods mathematically describe the proceses of detachment, transportation and deposition of the eroded soil. These methods can easily be exported to different environments, but they require a large and extremely detailed set of parameters, which are often not available on a basin scale.

Recently developed conceptual models have provided outputs in a spatially distributed manner, as a consequence of the widespread use of Geographic Information Systems (GIS). In fact, it is possible to approach the study of soil erosion by observing the geostatistical relationships between the physical determining factors and the effects of the process: the erosion landforms (Conoscenti et al., 2008a).

This section is focused on the integration of denudation intensity estimation method (*Tu* denudation index) and the spatial prevision of areas prone to the development of instability landforms, aimed at the proposal of a method finalized at the evaluation of the water erosion hazard (a spatially distributed prevision of *calanchi* badlands, and associated erosion rate, occurrence).

Erosion intensity is estimated refining *Tu* denudation index equations (§ 6), and attempting a zonation of estimated erosion rates, by means of a grid analysis. The estimates are here validated considering the results of direct monitoring. Susceptibility analysis is performed through the analysis of geostatistical spatial relationships between the physical determining factors and the effects of the denudation processes (the erosion landforms). To

this aim, conditional analysis is applied to evaluate landslide susceptibility of Upper Orcia Valley in § 7, preceded by a new procedure for selecting the most influential causal factors (Vergari et al., 2011). Finally, § 8 presents a proposal for water erosion hazard assessment methodology, applicable in areas widely affected by badlands, in which erosion rates of badland areas is estimated through *Tu* denudation index, while spatial probability of *calanchi* badlands occurrence is computed by means of the susceptibility assessment method described in § 7.

6 SOIL EROSION ESTIMATION MODEL

Field studies of soil erosion are expensive, time-consuming and data needs to be collected over many years. Though providing detailed understanding of the erosion processes, field studies have limitations due to the complexity of interactions and the difficulty of generalising from the results. Cost-efficient methods of estimating erosion over whole catchments are required as ways of predicting erosion after disturbance or following various erosion management strategies. Thus, the indirect estimation of erosion rates is still one of the main research topics of the scientific community in the field of geomorphology and is far from solved.

This study presents the preliminary results of the application of an erosion evaluation technique aimed at the proposition of a spatially distributed model for estimation of present water erosion rates in badland areas.

The mean annual erosion rate zonation has been carried out by means of a grid analysis of the denudation index (*Tu*), originally proposed in 1981 by Ciccacci et al. and based on the statistical correlations among quantitative geomorphic parameters and suspended sediment yield data measured for some Italian catchment basins. The comparison of estimated erosion and the erosion landforms, mapped after field survey, has allowed to associate an estimated typical erosion rate to each water erosion landform type (*calanchi* badlands and *biancane* badlands), that was then validated by means of field erosion monitoring data.

6.1 Modelling approaches to the estimation of soil erosion

The number of available erosion estimation methods differ in their applicability (spatial and temporal scales), for how they represent geomorphological processes and the type of results that provide. With the increased computing powers of the last 20 to 30 years, there

has been a rapid increase in the exploration of catchment erosion and sediment transport through the use of computer models. The range of model application is extremely diverse in terms of their modelling expertise, the questions they are exploring and the level of detail and scales at which these questions need to be addressed. Some models are event based, attempting to predict soil erosion after storm events, while others predict average annual soil loss. As for the spatial resolution, the models are generally applied to predict soil erosion for plot, hillslope or catchment scales.

Many research work have tried to summarize the available soil erosion estimation methods, starting from Gregory and Walling (1973), that classified them from the "*Physical*" ones, where the studied processes were reproduced in laboratory, to the "*Digital*" ones, prevailing from the widespread use of computers, that aided the elaboration of large datasets (Tab. 6.1). These "digital" models have been then classified in two macro-categories: *empirical* and *physically based models* (Morgan, 2005), the former founded on the statistical relationships between a set of influencing parameters and erosion effects monitoring datasets, the latter based on the mathematical equations explaining the physical laws involved in the studied processes. Zhang et al. (1996) proposed to identify a third category, called "*Process models*", to include the methods describing the processes of sediment generation, transport and deposition (such as models proposed by Rose, 1993; Haan et al., 1994; Foster and Meyer, 1972; Foster, 1982; Rose et al., 1983a,b; Lane et al., 1995). The same category was called "*Conceptual models*" in several other reviews (Lane et al., 1988; Wheater et al., 1993; Merrit et al., 2003), emphasizing the assumption of representing the catchment as a series of internal storages. Recently developed conceptual models have provided outputs in a spatially distributed manner, as a consequence of the widespread use of Geographic Information Systems (GIS). A fourth category of erosion modeling approaches was thus indentified by Li Zhang et al. (1996) as the "*spatially distributed models*", based on modeling soil erosion data from Digital Elevation Models (DEMs).

TYPE	DESCRIPTION		
Physical	Scaled-down hardware models usually built in the laboratory; need to assume dynamic similitude between model and real world		
Analogue	Use of mechanical or electrical systems analogous to system under investigation, e.g. floe of electricity used to simulate flow of water		
Digital	Based on use of digital computers to process vast quantities of data		
	Physically based	Based on mathematical equations to describe the processes involved in the model, taking into account the laws of conservation of mass and energy	
	Stochastic	Based on generating synthetic sequences of data from the statistical characteristics of existing sample data; useful to generate input sequences to physically based and empirical models where data are only available for short periods of observation	
	Empirical	Based on identifying statistically significant relationships between assumed important variables where a reasonable database exists. 3 types of analysis are recognized:	
		Black-box	Only main inputs and outputs are studied
		Grey-box	Some detail of how the system works is known
		White-box	All details of how the system operates is known

Tab. 6.1 – Classification of erosion estimation methods after Gregory and Walling (1973).

Physics-based models are founded on the solution of fundamental physical equations describing streamflow and sediment and associated nutrient generation in a catchment. Standard equations used in such models are the equations of conservation of mass and momentum for flow and the equation of conservation of mass for sediment (e.g. Bennett, 1974). The major limits of physically based models are the large data requirements, the limited knowledge of complex processes and interactions between these processes at catchment scale (de Vente et al., 2006).

Empirical models are based primarily on field observations and try to characterize response from these data. The computational and data requirements for such models are usually less than for the other types, often being capable of being supported by coarse measurements. Many empirical models are based on the analysis of catchment data using stochastic techniques. Such models generally assume stationarity (underlying conditions remain unchanged for the duration of the study period): this assumption limits the potential for such models to be applied for predicting the effects of catchment changes. Moreover,

they are not event-responsive, ignoring the processes of rainfall-runoff in the catchment. De Vente et al. (2006) have divided empirical models in a) regression relations (or lumped models), that relate sediment yield to basin properties; b) semi-quantitative models, that explore process knowledge and identify significant sources of sediment, such as the Factorial Scoring Model (FSM, Verstraeten et al., 2003; de Vente et al., 2005) and the Pacific Southwest Interagency Committee Model (PSIAC, PSIAC, 1968); c) the distributed models, such as the RUSLE (Renard et al., 1997) and SDR (Young et al., 1995; Ferro et al., 1998; Jain and Kothyari, 2000; Kinnel, 2000; Van Rompaey et al., 2001, 2005; Brath et al., 2002; Ferro et al., 2003;) models. One of the limits of empirical models is that they generally do not consider sediment production from gully and bank erosion and from mass movements and their use outside the regions for which they were developed is often problematic.

The Universal Soil Loss Equation (USLE) is the most widely used empirical overland flow or sheet-rill erosion equation (Wischmeier and Smith, 1978). The USLE is essentially an empirical formulation. All factors are based on observation and dimensionless and express each factor's effect on erosion. The equation was developed as a tool to control erosion and maintain soil productivity in developing catchment management plans. The equation is given by:

A = RKLSCP

where:

A is the soil loss averaged over the slope length;

R is the combined erosivity of rainfall and runoff;

K is the soil erodibility;

L is the slope length; S is the slope angle;

C is the vegetation cover;

and P is management practices.

The limits of this approach are that: a) since it was developed to estimate long-term mean annual soil loss, it cannot be used to predict erosion from an individual storm, b) merely multiplying together 6 factor values, the interdependence among them is not considered, c) it is based on a wide input database, but limited to USA east of Rocky Mountains (for limitations of USLE see: Foster 1982; Millington, 1986; Nearing et al., 1994). The more recent version of the USLE is called the Revised USLE (RUSLE) (Renard, et al.,

1991). The RUSLE has modified the techniques in determining R, K, C and P factors and is expected to provide more accurate results for soil erosion. Finally, another version of the USLE which is widely used to estimate sediment yield is the Modified USLE (MUSLE) (Williams and Berndt, 1977). The MUSLE is intended to estimate sediment yield for a single event.

In Tab. 6.2 a number of available and well-known models are summarized, grouped in the physically-based and empirical models categories, considering the spatially distributed models as a way to provide model outputs.

TYPE	MODEL	SCALE	REFERENCE
Physically based models	WEPP	Hillslope/catchment	Nearing et al. (1989); Laflen et al. (1991)
	GUEST	Plot	Yu et al. (1997); Rose et al. (1997)
	EUROSEM,	Small catchment	Morgan et al. (1998)
	LISEM	Small catchment	Takken et al. (1999); De Roo and Jetten (1999)
	ANSWERS	Small catchment	Beasley et al. (1980)
	TOPOG	Hillslope	CSIRO Land and Water, TOPOG Homepage; Gutteridge Haskins and Davey (1991)
Empirical models	USLE	Hillslope	Wischmeier and Smith (1978)
	SEDNET	Catchment	Prosser et al. (2001)
	TU INDEX	Catchment	Ciccacci et al. (1981, 1986)
	FSM	Catchment	Verstraeten et al. (2003); de Vente et al. (2005)
	SDR	Catchment	Young et al., 1989; Ferro et al., 1998, 2003; Jain and Kothyari, 2000; Kinnel, 2000; Van Rompaey et al., 2001, 2005; Brath et al., 2002
	PSIAC	Catchment	PSIAC, PSIAC, 1968
	Morgan, Morgan and Fienny method (SEMMED)	Catchment	Morgan et al., 1984; Morgan, 2001

Tab. 6.2 – Some available and well-known models to the estimation of erosion of soil erosion.

6.1.1 Estimation of catchment-scale sediment yield

In 1981 Goudie stated that “probably one of the most important environmental problems associated with soil erosion by water is the high level of suspended sediment in river channels”. Sediment deposition within riverbeds or reservoirs causes problems for navigation, water supply or energy production. Furthermore, sediment loads disturb aquatic environments, especially if many pollutants, e.g. phosphates or heavy metals, are adsorbed to sediment particles. Prediction of annual sediment delivery values to river channels is therefore a major challenge, as it can give an order of magnitude of the intensity of erosion processes acting within catchments, but this is also a problem for the measurement of sediment delivery (Verstraeten and Poesen, 2002).

Several empirical models specifically predict sediment delivery. These models generally combine an upstream erosion model with a sediment delivery ratio (SDR; e.g. Prosser et al. 2001; Van Rompaey et al. 2001). The SDR concept is considered as a classical method linking sediment delivery to erosion within the basin, defined as the ratio of sediment delivered at the catchment outlet (or area specific sediment yield, SSY, t km^{-2} $year^{-1}$) to gross erosion (t $km^{-2}year^{-1}$; Maner 1958; Walling 1983). Indeed, only a fraction of eroded soil moves through the catchment system and contributes to the sediment yield. The remaining part is deposited on hillslopes and/or in river plains and channels.

As summarized by Lupia Palmieri (1983), over the past years, many attempts to identify the best relationship between the fluvial sediment yield and some of the main factors influencing erosion in the catchment areas have been carried on. Several authors have stressed the influence of climatic conditions: Langbein and Schumm (1958), based on data from 265 river basins in the U.S.A., have highlighted that there would be a maximum of suspended sediment transport for values of average annual rainfall ranging between 250mm and 350mm, that is in conditions of semi-arid climates; for lower and higher rainfall values, there is a sharp decrease of the turbulent transport, due, respectively, to a not significant runoff and to the increased vegetation cover, which protects soil from erosion (biostasis conditions). Fournier, in 1960, proposed a "precipitation factor" and an "orographic factor," finding a rather significant equation to assess the extent of erosion on a global scale, a scale

where climatic differences may be one of the main discriminating elements. But at the single catchment level, or when comparing adjacent areas, climatic conditions may be similar, and, therefore, not suitable in explaining the differences on a local scale. In this regard, Douglas (1968) has highlighted the relationship between suspended sediment yield and the average annual rainfall, the average annual runoff, the rainfall coefficient of Fournier and the relief ratio of some basins of Queensland (Australia). Cooke and Doornkamp, in 1974, have considered, together with the Fournier coefficient, the bifurcation ratio and drainage density. These relations are valid locally, of course, losing significance if extended to areas with different characteristics. For the Italian river basins, Gazzolo and Bassi (1961) proposed to consider also the geological factors, the degree of forest cover and soil conditions, dividing the land into "very erodible", "semi-erodible" and "slightly erodible." The evaluation of these parameters, however, includes a certain degree of subjectivity.

Ciccacci et al. (1981, 1986) suggested models for indirectly estimating denudation rates, based on statistical correlations among quantitative geomorphic parameters and suspended sediment yield data. The “denudation index” (Tu) showed noticeable spatial variability of estimated denudation, with the highest Tu values indicating erosion “hot spots”, represented by small sub-catchments affected by badlands developed on uplifted Plio-Pleistocene marine clays in Italy. Considering reservoir sedimentation data of 44 Italian catchments, de Vente et al. (2006) explored the potential of FSM and PSIAC models to predict sediment yield, and indicated the most important sediment sources. They concluded that models results confirmed the hypothesis that processes other than upland erosion are probably responsible for sediment yield in the Italian catchments. A promising future development of the models is by the use of detailed spatially distributed data to determine the scores, decrease model subjectivity and provide spatially distributed output.

Verstraeten and Poesen (2001) tried to deepen the relation between measured sediment yield and several catchment parameters for a number small cultivated catchments (10–10 000 ha) in central Belgium, concluding that even if summarizing the catchment properties in single parameters values in regression models is important, the use of spatially distributed erosion and sediment delivery models is necessary.

In the past, in the absence of reliable spatially distributed process-based models for the prediction of sediment transport at the drainage basin scale, area-specific sediment yield

(SSY) has been often assumed to decrease with increasing drainage basin area (A), (e.g., Dendy and Bolton, 1976; Milliman and Meade, 1983; Milliman and Syvitski, 1992; Summerfield and Hulton, 1994; Einsele and Hinderer, 1997; Radoane and Radoane, 2005; Renwick et al., 2005). This thesis was reinforced by the assumption that increasing the catchment area, the sediment deposition possibilities increase, due to the decrease of mean slope gradients. Over the last two decades, various studies have revealed cases where a very poor relation, a positive relation or a combination of a positive and negative relation between A and SSY was found (e.g., Church and Slaymaker, 1989; Gögüs and Yener, 1997; Lane et al., 1997; Krishnaswamy et al., 2001; Schiefer et al., 2001; Dedkov, 2004; García Ruiz et al., 2004; de Araújo and Knight, 2005; de Vente and Poesen, 2005; Haregeweyn et al., 2005; Jiongxin and Yunxia, 2005; de Vente et al., 2006; Restrepo et al., 2006; Della Seta et al., 2009), since, beside basin area, sediment yield is closely related to other basin characteristics such as topography, climate, lithology, land use and vegetation cover. De Vente et al. (2007) provided an overview of the different relations between A and SSY reported in literature and in observed trend. Summarizing their conclusions, the presence of a positive relation between A and SSY was linked to the presence of a welldeveloped vegetation cover, limited human disturbance, and a dominance of channel erosion over hillslope erosion processes (i.e., sheet, rill and ephemeral gully erosion), where recruitment of sediment along a channel and channel degradation is observed, possibly in combination with substantial delivery of sediments to the main rivers by massive landsliding. In contrast, an inverse relation between A and SSY was found characteristic for intensely cultivated basins, with an important contribution of hillslope erosion processes to sediment yield, where deposition of sediments during transport and channel aggradation occurs. Various authors have emphasized the scale dependency of sediment yield and have provided examples of a complex non-linear relation between A and SSY (eg, Lane et al., 1997; Osterkamp and Toy, 1997; de Vente and Poesen, 2005; Jiongxin and Yunxia, 2005; Fang et al., 2006; Slaymaker, 2006). They stated that at small scales, where splash and sheet erosion are the dominant erosion processes, SSY is relatively low. With increasing A more erosion processes become active (ie, rill erosion, gully erosion, channel erosion, landslides) leading to a rise in SSY with increasing A. This rise in SSY continues until a threshold in A is reached beyond which SSY starts to decrease with increasing A due to decreasing slope gradients,

resulting in reduced erosion rates and significant sediment storage on foot-slopes, in dry channels, floodplains and other sinks.

Delmas et al. (2009) proposed a method to estimate a sediment yield index at a large spatial resolution for European river basins, considering the major processes forcing sediment redistribution within drainage areas. Four indicators representing processes respectively considered as sources (mass movement and hillslope erosion), sinks (deposits), and transfers of sediments (drainage density) were defined using distributed data, and an index which adds the two sources and transfers, and subsequently subtracts the sink term was proposed.

6.1.2 The Denudation index (Tu)

The specificness of the equations proposed by Ciccacci et al. (1981, 1986) lies in considering the contribution of quantitative geomorphic analysis as a suitable tool for an objective characterization of the river basins, in order to evaluate the intensity of erosive processes. The proposed mathematical relationships are indeed the result of a series of multiple regressions, statistically significant, which relate the values of some geomorphic and climatic parameters for a number of Italian basin with the suspended sediment yield measured in gauging stations located at the outlets of the same catchments. Even if the total amount of stream load should be known, bed load and dissolved load are rarely measured and with different techniques; consequently, indirect evaluation of erosion entity is generally based on suspended sediment data. Denudation index estimates the average annual suspended sediment yield (Tu) operated by rivers, which, for basins, in humid climates and characterized prevalently by terrigenous substrates, also represents 90% of the total sediment entrainment by rivers. In these conditions, stream load can partially and approximately express the amount of the erosional processes acting within drainage basins, expressing the specific degradation and allowing the comparison among basins different in size.

According to the authors, the indipendent parameters represent a comprehensive and concise expression of the main factors controlling erosion processes, and the selected basins

are an Italian sample, that, though limited, is sufficiently representative of the physiographic conditions found in various regions of the country. The selected Italian river catchments (Fig. 6.1) are listed in Tab. 6.3, and parameters used in the study are:

- p^2 / P (Fournier, 1960), where p is the rainfall depth of the wettest month and P the total annual rainfall depth (in mm);

- P x σ (Ciccacci et al., 1977), where P is the total annual rainfall depth (in mm) and σ the standard deviation from the mean monthly rainfall;

- Θ, the slope gradient of river channels, defined as the ratio between the difference in height of the extreme points of the river segment and the linear length of each river segment (average value for each considered catchment);

- D, drainage density, obtained by drawing all the possible surface drainage ways detectable on topographic maps (scale 1:25,000) and aerial photos;

- Ga, hierarchical anomaly density, and Δa, hierarchical anomaly index (Avena et al., 1967; Avena and Lupia Palmieri, 1969), taking into account the frequency of anomalous confluences of the various river segments and their distribution in various orders, important in indicating instability phenomena.

For the Italian drainage basins, the only extensively available data about stream load refer to the suspended sediment yield measured by the network of gauging stations controlled, until about ten years ago, by the Hydrographic Office of the Ministry of Works.

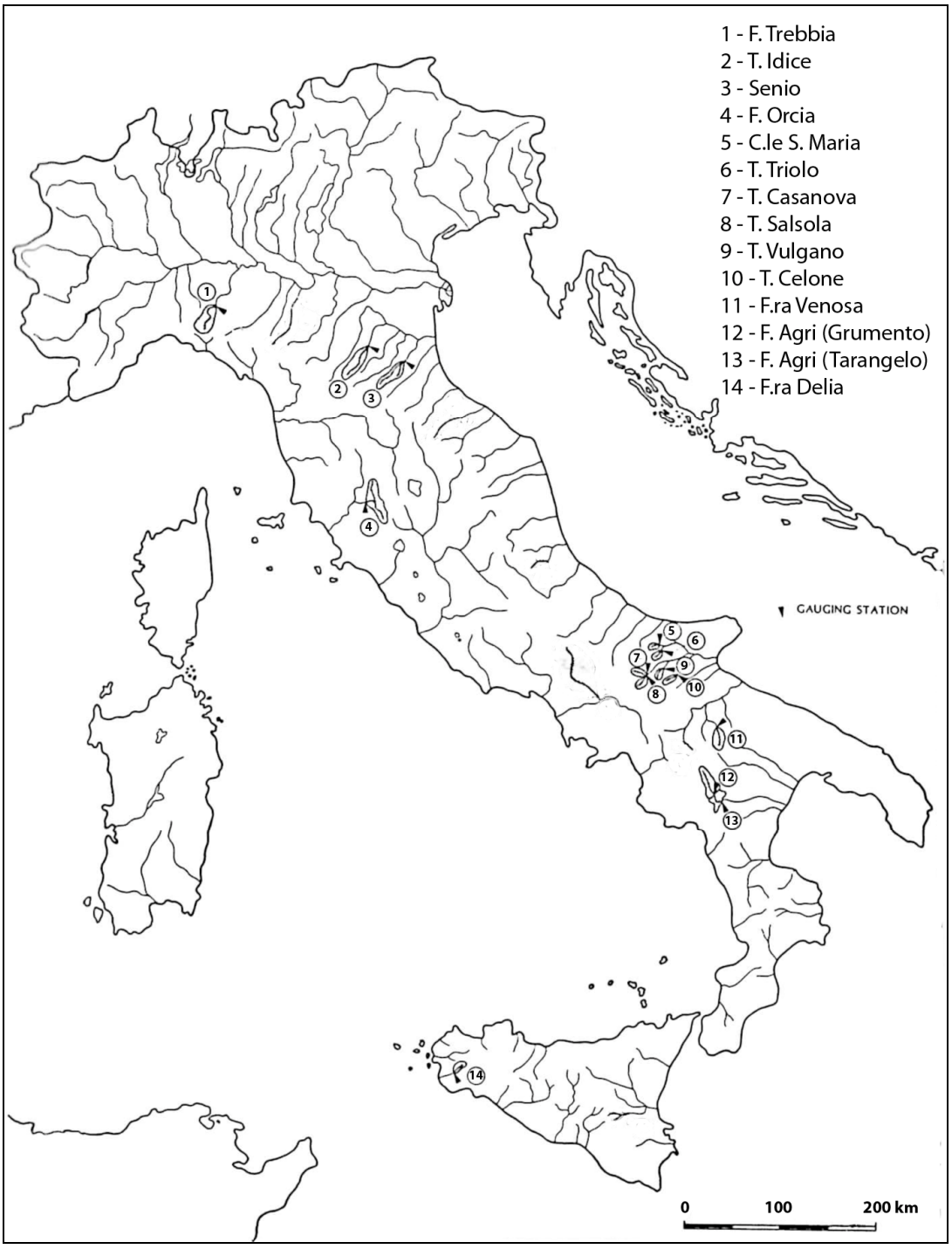

Fig. 6.1 – Location map of the 14 drainage basins considered in the Ciccacci et al. study (1981).

Catchment	Tu (tonn/km^2/year)	D	θ	Δa	ga	p^2/P	p x σ
F. Trebbia (Valsigiara)	1523	4,9	22	1,59	19,35	81,52	224080
T. Idice (Castenaso)	2397	5,61	17,1	0,86	30,27	33,01	48984
T. Senio (Castelbolognese)	857	4,17	21,1	1,32	15,1	39,54	56951,32
F. Orcia (Monte Amiata)	1430	4,8	11,9	1,34	17,6	35,21	38804,92
C.le S. Maria (P.te Lucera-Torremaggiore)	170	2,21	5,01	1,14	3	35,25	26048,02
T. Triolo (P.te Lucera-Torremaggiore)	285	2,6	7,08	0,91	2,8	31,1	27727,34
T. Casanova (P.te Lucera-Motta)	179	2,7	8,07	0,36	1,4	28,82	26805,61
T. Salsola (Casanova)	228	2,6	9,7	1,15	4,6	28,25	27998,67
T. Vulgano (P.te Troia-Lucera)	247	2,44	9,25	0,94	3	26,81	28958,21
T. Celone (S. Vincenzo)	255	2,8	10,5	0,76	3,1	23,91	27914,13
F.ra di Venosa (P.te S. Angelo)	225	2,76	6	1,08	2,9	23,82	21675,17
F. Agri (Grumento)	231	2,42	15,5	1,1	4,3	51,3	73736,71
F. Agri (Tarangelo)	340	3,06	14,8	1,4	10,8	48,85	75857,91
F.ra Delia (Pozzillo)	152	2,59	5,64	0,57	2,05	38,48	38235,16

Tab 6.3 – Values of measured Tu and independant variables for the 14 italian drainage basins cosidered in the 1981 study by Ciccacci et al.

Ciccacci et al. (1981) underlined the weak statistical relation between Tu and parameters related to climate and relief. They instead highlighted the high values of the determination coefficients (R^2) of regressions showing the relation between Tu and parameters related to drainage network, in particular D. Several works, in fact, proved some of the considered indirect parameters to be suitable for expressing the characters of the drainage network (such as extension and hierarchization degree) that strongly affect denudation intensity (Strahler, 1957; Dramis and Gentili, 1977; Ciccacci et al., 1981; Tokunaga, 1984, 2000; Ciccacci et al., 1986, 1988; Marini, 1995; Del Monte et al., 2002).

In particular, R^2 values are very significant for the following regressions:

$\log Tu = 0{,}35312\ D + 1{,}43225 \qquad R^2 = 0{,}96221 \qquad (\text{with } D < 6) \qquad (1)$

$\log Tu = 2{,}93936 \log D + 1{,}13430 \qquad R^2 = 0{,}94987 \qquad (\text{with } D > 6) \qquad (2)$

The equation (2), even if showing a lower R^2, was assessed as better for basins characterized by very high D values, for which the Tu estimation with equation (1) resulted in values overcoming the maximum Tu values for Italian catchments (Passerini, 1934; Cotecchia, 1960, 1961, 1963, 1968; Morandini, 1962).

Moreover, the authors demonstrated that R^2 increase considering the following multiple regressions:

$\log Tu = 0{,}29561\, D + 0{,}0074\, ga + 1{,}56102 \qquad R^2 = 0{,}96435 \qquad (\text{with } D < 6) \qquad (3)$

$\log Tu = 1{,}82818 \log D + 0{,}01796\, ga + 1{,}53034 \qquad R^2 = 0{,}96490 \qquad (\text{with } D > 6) \qquad (4)$

$\log Tu = 0{,}33479\, D + 0{,}15733\, \Delta a + 1{,}32888 \qquad R^2 = 0{,}97688 \qquad (\text{with } D < 6) \qquad (5)$

$\log Tu = 2{,}79687 \log D + 0{,}13985\, \Delta a + 1{,}05954 \qquad R^2 = 0{,}96128 \qquad (\text{with } D > 6) \qquad (6)$

In 1986, Ciccacci et al. tried to improve the obtained equations by increasing the number of drainage basins representing the Italian sample of physiographic conditions. The new regressions confirmed D as the best predictor of Tu, since it synthetically expresses many of the factors controlling erosion entity: a) it is strongly depending on climatic conditions; b) it is tied to the type and density of vegetation cover; c) it can be partially modified in response of human activity; d) it is a function of rock permeability and fracturing degree, synthesizing the erodibility level of the sedimentary substrate outcropping in the studied areas.

6.2 Update of the Tu index method

The attempts of improving the denudation index methodology was driven by the following considerations:

1) parameter D, drainage density, refers to the density of river network and ephemeral streams, whose density is linked to the seasonal distribution of rainfall. It has been calculated in the previous studies, considering the drainage pathways derived from available maps (1:25.000), thus considering a representation of the projected area. This parameter, so computed, underestimates the real lengths of the drainage pathways in those areas where the steepness is high, and it is assumed that this limit can lead to underestimate the intensity of river load in these sites;

2) as a result of the quantitative geomorphic investigations, the geomorphological survey and the erosion monitoring in the study areas of central Italy, also according to several studies conducted by different authors in the same areas and other areas greatly affected by badlands and instability due to water erosion (e.g. Ciccacci et al., 2003, 2006), it is considered extremely important to give greater weight to the influence that runoff, diffuse and concentrated, has in the evaluation of erosion intensity. In fact, the calculated drainage density at scale 1:25.000 does not reach a level of detail that can account for the small channels, that, in badland areas, form a dense network.

To fulfil these limitations, two new independent variable have been added in the multivariate statistical analysis:

1) a new parameter, called 3D- drainage network (D_{3d}) was therefore calculated, representing a drainage density that is not projected. In fact, despite the traditional values of the D values also reflect the different slope gradients along the waterways, which in turn affect the river yield, it was considered interesting to use a parameter that allows to evaluate the effective development of surface drainage in a basin by reducing the intrinsic error due to the deformation that occurs as a result of the representation of the earth's surface on a two-dimensional plane (Marazzotti, 2005-2006). This parameter is obtained by knowing the actual linear length of the river courses (L_{eff}) and the basin area (A):

$D_{3d} = \Sigma L_{eff} / A$,

where L_{eff} can be easily computed applying the Pythagorean theorem, as indicated below:

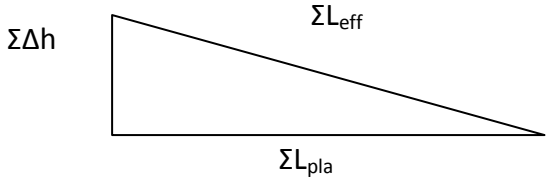

ΣL_{eff} = cumulative length of real river channels,

ΣL_{pla} = cumulative lentgh of projected river channels (D parameter in Ciccacci et al. 1981, 1986),

$\Sigma \Delta h$ = mean slope gradient of river channels (θ parameter in Ciccacci et al. 1981, 1986)

Computed D_{3d} values, shown in Tab. 6.4, together to D values, reflect mean θ values along drainge network.

2) in order to give more weight to the portion of the denudation due to runoff, the Ad parameter was introduced in the study of indirect assessment of the erosion entity, representing the areal ratio affected by badlands (A_b) to the total catchment area (A):

$A_d = A_b / A$

For some of the considered basins, the Ad values were already available in previous work (Ciccacci et al., 1995); the missing Ad values have been elaborated by mapping badland areas from aerial photo interpretation (Tab. 6.4).

Bacino	Area bacino (km^2)	D_{3d} (km/km^2)	A_d
F. Trebbia	226	5,017179	0,276265
T. Idice	397	5,69143	0,2489
T. Senio*	269	4,261815	0,09
F. Orcia	580	4,833867	0,45661
C.le S. Maria*	59,8	2,212772	0,02
T. Triolo*	53,8	2,606508	0,02
T. Casanova*	52,3	2,708778	0,01
T. Salsola*	43,1	2,612203	0,04
T. Vulgano*	94	2,450416	0,04
T. Celone*	85,8	2,815393	0,04
F.ra di Venosa	261	2,764964	0,025318
F. Agri (Grumento)	278	2,448898	0,043243
F. Agri (Tarangelo)	507	3,093332	0,06218
F.ra Delia	138,8	2,594116	0,018214

Tab.6.4 – D_{3d} and Ad values of the 14 drainage basins considered by Ciccacci et al. (1981) to estimate denudation index "*Tu*" (* indicate basins for which Ad values were available in Ciccacci et al., 1995).

In Tab. 6.5 correlation matrix between the considered parameters and Tu values is shown. The matrix shows the correlation coefficients, which express the degree of linear relationship for each pair of variables, and the P values, which show the value of the test which assumes that the correlation coefficient is zero (null hypothesis). The p value for rejecting the null hypothesis must be lower than 0.05. P-value is lower than 0.05 for all pairs of variables whose correlation coefficient is high (greater than 0.5).

Comparing the different variables with simple or logarithmic values of Tu, shows that the correlation is high for D, LogD, ga, D_{3d}, $logD_{3d}$, A_d. As already stressed in the 1981 study, little significance have shown the relationship between Tu, or its logarithm, and climate parameters.

In the present study, we tried to understand what improvements can make the two new parameters to the estimation of the extent of denudation.

	Tu	log Tu	D	log D	θ	Δa	ga	p^2/P	p x σ	D_{3d}	log D_{3d}
log Tu	0,961 0										
D	**0,97** 0	**0,981** 0									
log D	**0,944** 0	**0,975** 0	0,995 0								
θ	0,642 0,013	0,753 0,002	0,712 0,004	0,729 0,003							
Δa	0,32 0,265	0,492 0,074	0,388 0,171	0,405 0,151	0,581 0,029						
ga	**0,972** 0	**0,963** 0	0,965 0	0,948 0	0,739 0,003	0,438 0,118					
p^2/P	0,34 0,234	0,411 0,144	0,388 0,17	0,393 0,165	0,676 0,008	0,596 0,024	0,399 0,157				
p x σ	0,429 0,126	0,501 0,068	0,482 0,081	0,49 0,075	0,716 0,004	0,581 0,029	0,46 0,098	0,955 0			
D_{3d}	**0,969** 0	**0,982** 0	1 0	0,996 0	0,723 0,003	0,395 0,162	0,966 0	0,4 0,156	0,494 0,073		
log D_{3d}	**0,942** 0	**0,975** 0	0,995 0	1 0	0,74 0,002	0,412 0,144	0,949 0	0,403 0,153	0,5 0,069	0,995 0	
Ad	**0,821** 0,001	**0,860** 0	0,851 0	0,844 0	0,492 0,091	0,473 0,093	0,783 0,002	0,362 0,232	0,409 0,175	0,846 0	0,840 0

Tab. 6.5 – Correlation matrix for Tu and independent variables data. In bold type the maximum Tu and log Tu correlation values.

Substituting D with D_{3d} parameter the following two equations have been found (Fig. 6.2):

$\log Tu = 0{,}3438\ D_{3d} + 1{,}4517$ $\quad R^2 = 0{,}9637$ (7)

$\log Tu = 2{,}8906 \log D_{3d} + 1{,}1481$ $\quad R^2 = 0{,}9512$ (8)

R^2 coefficients slightly increase with respect to the the analogous relations between Tu and D (Eq. 1 and 2).

Also the Tu / A_d regression show a strong power relation between the two variables (Fig. 6.3).

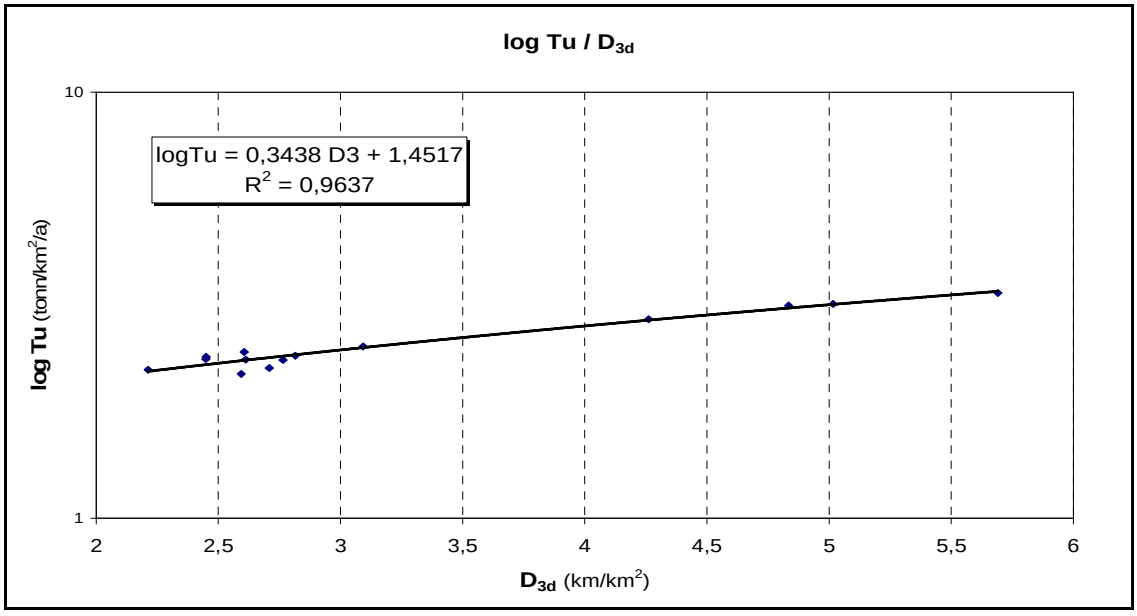

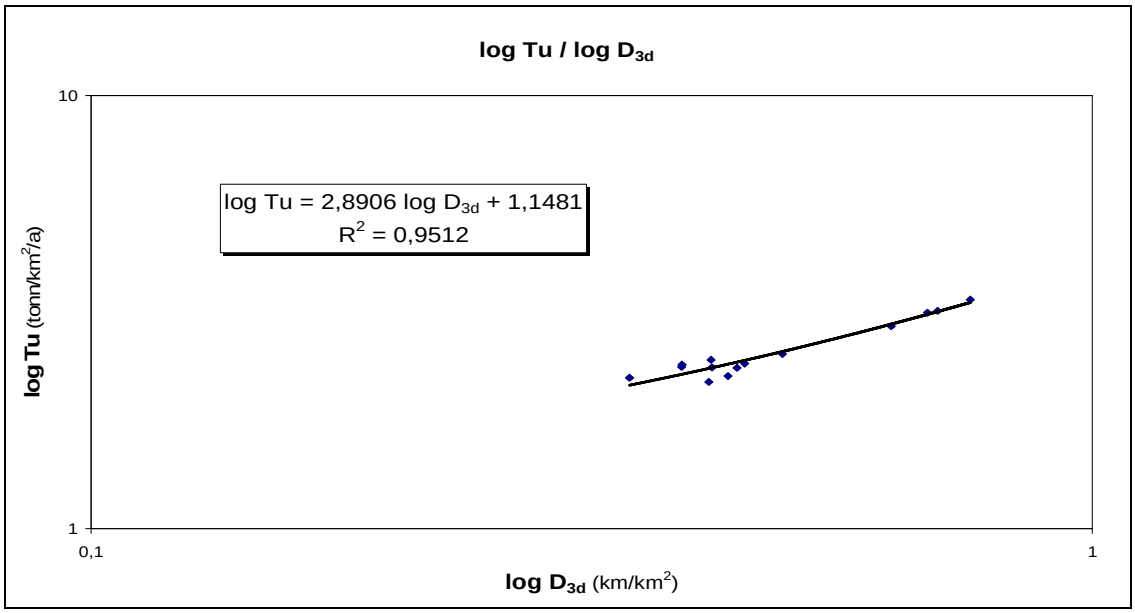

Fig. 6.2 – Tu / D_{3d} regressions.

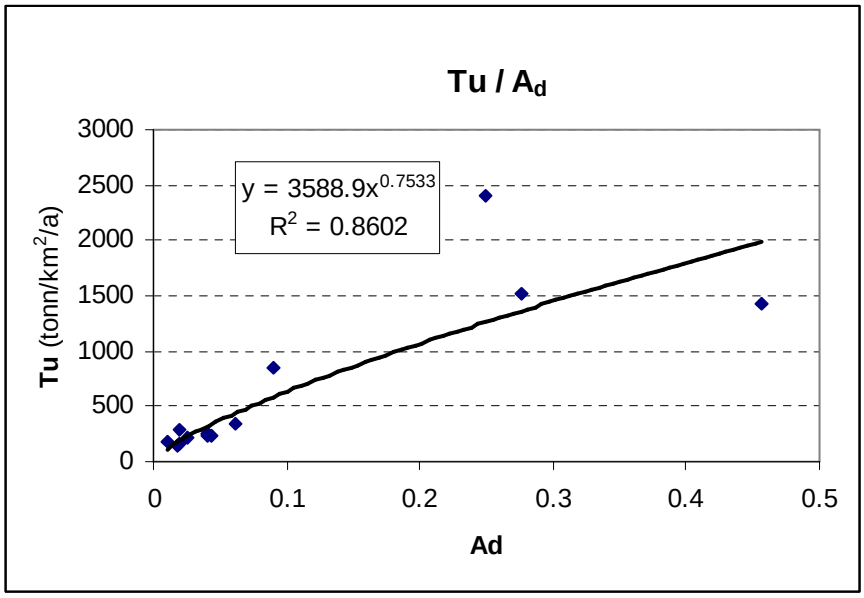

Fig. 6.3 – Tu / A_d regression.

Moreover determination coefficients even improve when attempting a quadratic or cubic best fit of Tu with D_{3d} (Fig. 6.4):

$\log Tu = 1{,}491 + 0{,}3211\ D_{3d} + 0{,}00293\ (D_{3d})^2$ $R^2 = 0{,}964$ (9)

$\log Tu = 2{,}974 - 0{,}910\ D_{3d} + 0{,}3266\ (D_{3d})^2 - 0{,}02712\ (D_{3d})^3$ $R^2 = 0{,}968$ (10)

$Tu = 1421 - 994{,}8\ D_{3d} + 204{,}3\ (D_{3d})^2$ $R^2 = 0{,}996$ (11)

The quadratic regression Tu-D_{3d} (eq. 11) shows the best significance, but a too high constant value, which corresponds to the Tu value when D = 0. Since when drainage is absent also the river yield is absent, we tried to add the data (0,0). The new regression analysis gave the following results (Fig. 6.5):

$Tu = 3{,}02 + 152{,}8\ D - 91{,}44\ D^2 + 25{,}10\ D^3$ $R^2 = 0{,}997$ (12)

$Tu = 2{,}51 + 168{,}4\ D_{3d} - 97{,}30\ (D_{3d})^2 + 24{,}95\ (D_{3d})^3$ $R^2 = 0{,}996$ (13)

Regression significance is very high for both the equations and constant values are now very low, better representing the real situation when D = 0.

Considering a multiple regression that relate Tu with D (or D_{3d}) and A_d, the following equations have been obtained:

$\log Tu = 1{,}50 + 0{,}325\ D + 0{,}276\ Ad$ $R^2 = 0{,}965$ (14)

$$\log Tu = 1{,}52 + 0{,}313\ D_{3d} + 0{,}308\ Ad \qquad R^2 = 0{,}967 \qquad (15)$$

$$\log Tu = 1{,}26 + 2{,}61 \log D + 0{,}388\ Ad \qquad R^2 = 0{,}955 \qquad (16)$$

$$\log Tu = 1{,}28 + 2{,}55 \log D_{3d} + 0{,}411\ Ad \qquad R^2 = 0{,}957 \qquad (17)$$

where including the (0,0) data is not necessary.

The inclusion of the parameter A_d, in addition to the density of drainage, to explain *Tu* could seem not very significant considering that this new parameter has a rather high correlation coefficient (> 0.8) when compared with the D or D_{3d} (see correlation matrix in Tab. 6.5). Even though, we considered that this is only true for areas characterized by not very high drainage density values. In fact, when the drainage network thickens of very small channels due to the runoff, the level of detail to which we compute the density of drainage (usually on maps at the scale 1:25.000) turns out to be not high enough to capture the real density of drainage network, leading to an underestimation. And in these cases the equations known in the literature underestimate the intensity of erosion, especially in river basins of small to medium size.

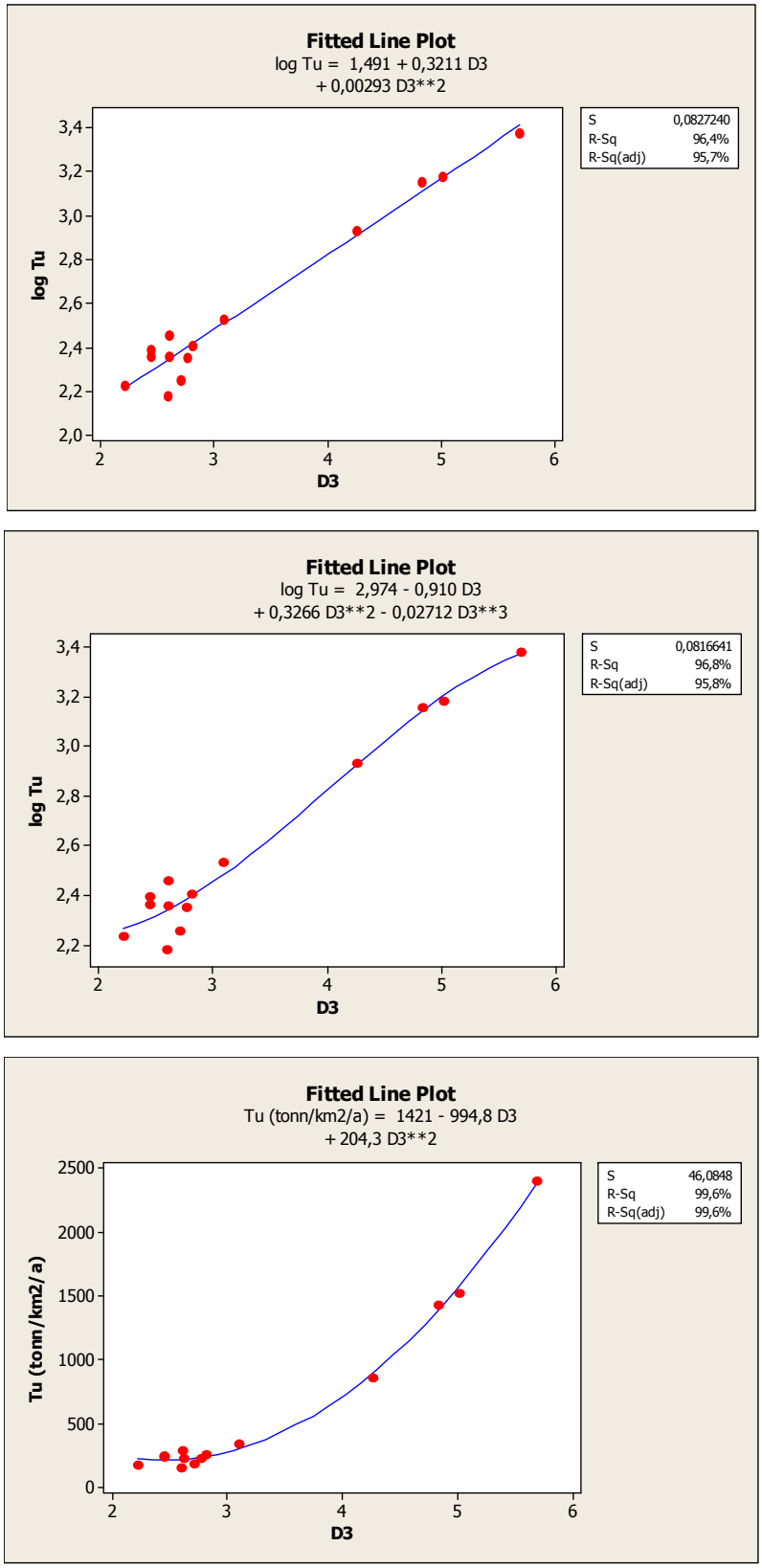

Fig. 6.4 – Quadratic and cubic regressions of Tu e D_{3d} (in the graphs indicated as D3).

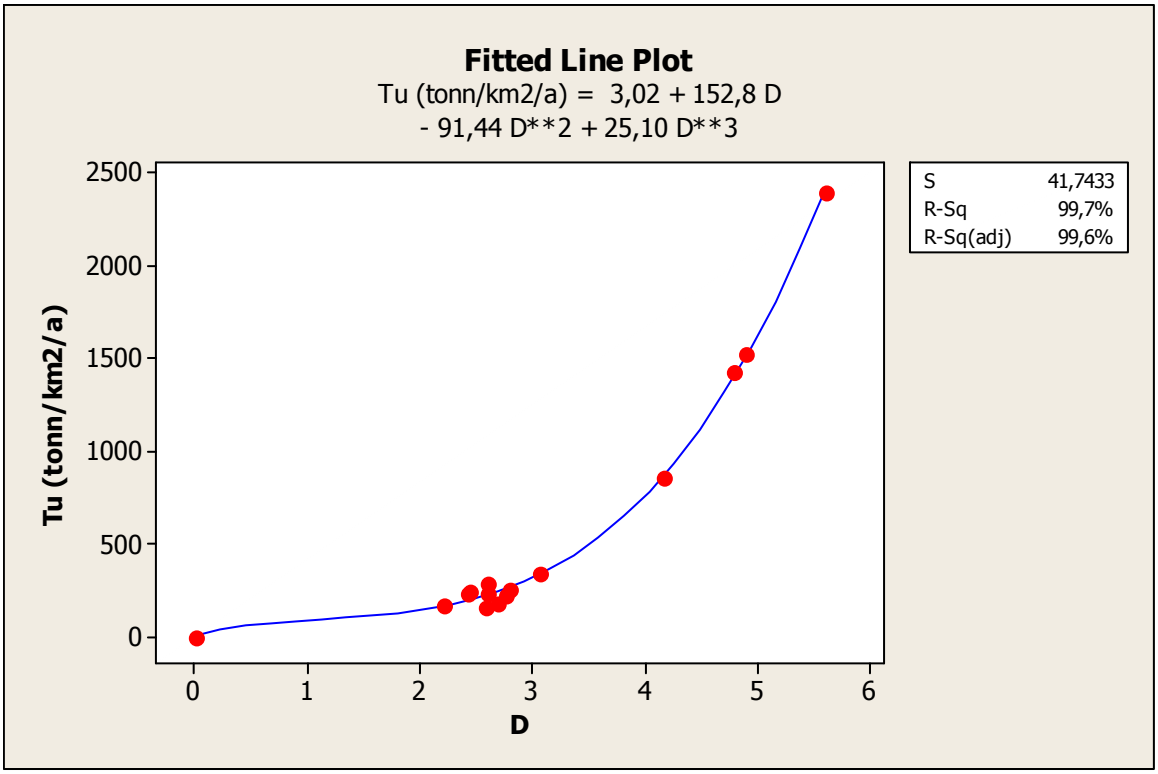

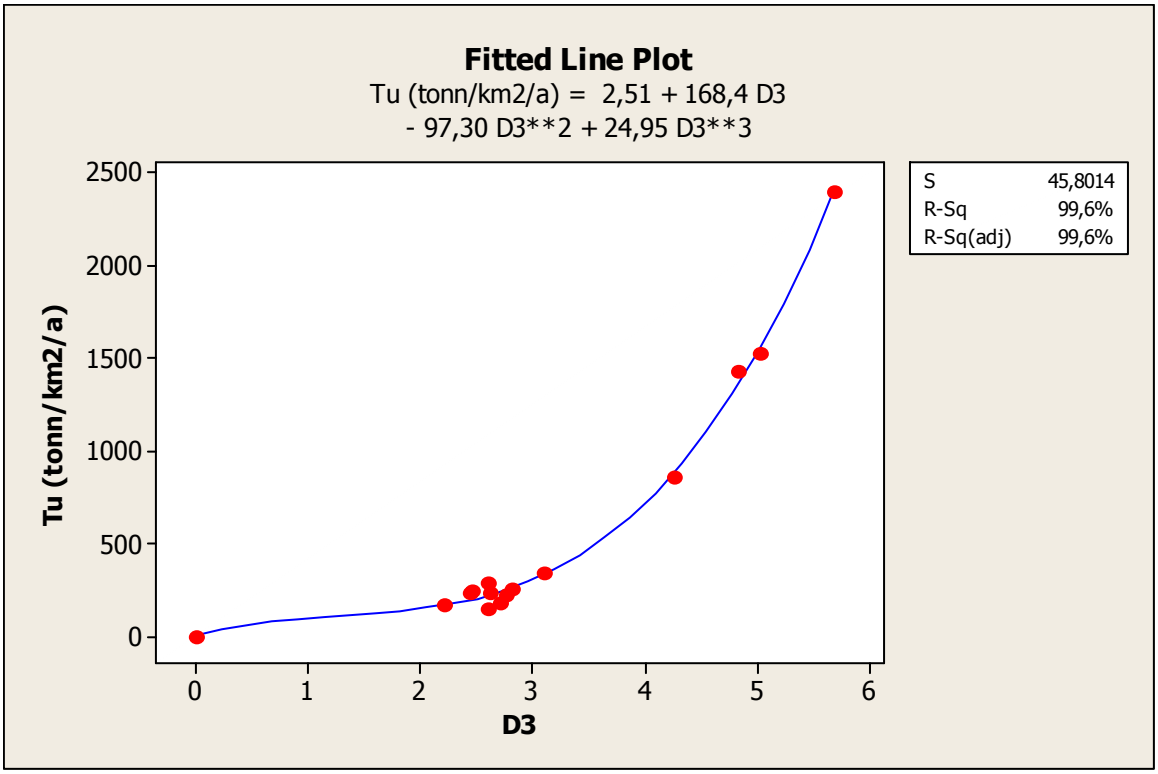

Fig. 6.5 – Relations between Tu and D (above) and between Tu and D_{3d} (bottom, the last indicated as D3), considering the (0,0) data.

Concluding, the attempt aimed at updating the Ciccacci et al. (1981) equations, has brought to the following remarks.

a) Considering that Tu variability explained by equations 14, 15, 16 e 17, is only slighlty lower than that explained by relations proposed in 1981 (equations 3, 4, 5, 6), we can consider that Ad is well related to erosion entity.

b) Even if D_{3d} does not improve the Tu estimation done with D, we consider that this is true for the large sized basin sample, in which θ is generally low, resulting in a small difference between D and D_{3d} values. For smaller basins, with higher θ, D_{3d} should better reflect the conditions predisposing erosions than D.

c) Equations 12 e 13 (Fig. 6.5) give the best estimation of Tu.

d) The sample size, however, is considered not sufficient to suggest the introduction of improvements to the regressions of 1981. Moreover, as can be seen from the analysis of regressions residuals for both the new and the 1981 relationships, the assumptions underlying the regressions (the residuals are independent, homoskedastic and normally distributed, Di Ciaccio et al., 1996) are not always verified, and then we can not take for granted the reliability of the estimation models, although the coefficients of significance are very high. In Fig 6.6 the exemplifying error analysis of equation 15 is shown, which investigates the distribution of differences between estimated and observed Tu values. The four graphs are used to study the goodness of the estimation model. Their interpretation shows an asymmetry in the distribution of residuals (in the graph "histogram of the residuals"), the presence of outliers (in the graph "residuals versus fitted values", the points far away from their average value, or zero), variance of residuals is a function of the estimated values (in the graph "residuals versus fitted values" it is evident that the residual variance decreases with increasing values of estimated values, indicating that the data are better estimated for high Tu values). Other equations show instead (from the analysis of the chart "Normal probability plots of the residuals") a non-random distribution. It can be concluded that although the assumptions made to represent a challenging road in the indirect assessment of the erosion entity, it would be desirable to perform a more detailed statistical analysis of data, as well as a spatial-temporal availability of more observations.

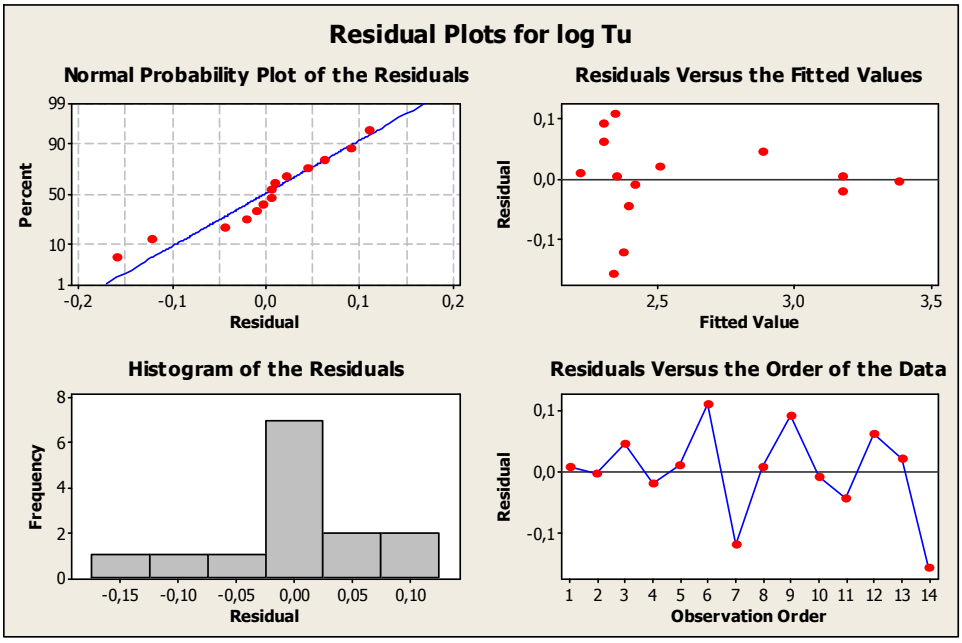

Fig. 6.6 – Residual analysis of regression in equation 15.

6.3 Spatially distributed erosion rate estimation: *Tu* grid analysis

Applications of *Tu* denudation index have produced satisfying results in in estimating the erosion entity in areas diffusely affected by badland erosion (Lupia Palmieri et al., 1995, 2001; Ciccacci et al., 2003; Agnesi et al., 2007; Della et al., 2007, 2009; Di Lisio et al., 2007). In fact, in the previous studies, it was underlined that where fluvial deepening prevails, Tu values were as much lower as more than one order of magnitude compared to values calculated for catchments strongly affected by "*calanchi*" badlands and by mass movements. This is in agreement with the statement that gully erosion is one of the dominant sediment sources in the Mediterranean region (Poesen and Hooke, 1997). Moreover, from the computed subcatchment Tu values (tonn/km^2/a), considering the average bulk density of clay, the most widespread outcropping lithology, an average erosion rate for the subcatchments was computed (cm/a). In order to verify these indirect results, the spatial variations of these modeled denudation rates were compared with field measurements: extreme values of the mean annual suspended sediment yield (Tu), obtained for the small catchments greatly affected by badlands are consistent with results obtained by direct monitoring of denudation with erosion pins (Della Seta et al., 2007).

Given these encouraging results, an attempt has been made to perform a more detailed zonation of the modeled denudation rates, in order to better zoning the negative ground level changes of badland sites within the catchment area (cm/a), starting from the sediment output data (tonn/km^2/a). The equations considering the only D parameter were used (Eq. 1 and 2), considering its powerful erosion estimation capacity.

The fist attempt was performed for an Upper Orcia River subcatchment, the Miglia subcatchment, 15 km^2 large, where *biancane* badlands are greatly widespread. The Miglia subcatchment area was divided using a grid of 1 km^2 cells. For each cell the drainage density (D) was calculated from drainage network digitized from 1:10.000 topographic maps (Carta Tecnica Regionale, CTR, Regione Toscana), considering that the D values computed from 1:25.000 topographic maps drainage network underestimate the erosion rate for badland areas (Fig. 6.7a).The equation 1 and 2 were applied to compute the Tu value corresponding to each cell (Fig. 6.7b): in this step, the Tu value in tonn/km^2/a estimated to each cell corresponds to the estimated sediment output of a fictitious basin having the D equal to that calculated for the cell. The Tu value was converted into the average negative ground level change of the cell (cm/a), assuming a mean bulk density of outcropping clays equal to 2 tonn/m^3. These estimated erosion rates were assigned to the cells' centroids (Fig. 6.7c), in order to get a point cloud to be used to geostatistically interpolate the obtained values, carrying out the estimated erosion rate map of Miglia catchment.

The 1km^2 grid was then shifted 0,7km to SE (half the cell diagonal length) in order to double the number of points to use in the geostatistcal interpolation in ArcGIS environment. The selected interpolation method was the spline interpolation method, that estimates values using a mathematical function that minimizes overall surface curvature, resulting in a smooth surface that passes exactly through the input points.

In Fig. 6.8, the estimated erosion map of Miglia subcatchment is shown. The highest erosion rates are estimated for the east-facing slope, where the Lucciolabella natural reserve was established in 1996 to protect the typical *biancane* badland landscape of Crete Senesi. Here, the estimated rates were compared with the rates measured by erosion pins, in order to verify the reliability of the results. For the area the measured denudation rates reach more than 3 cm / year, underlining the good estimation performed.

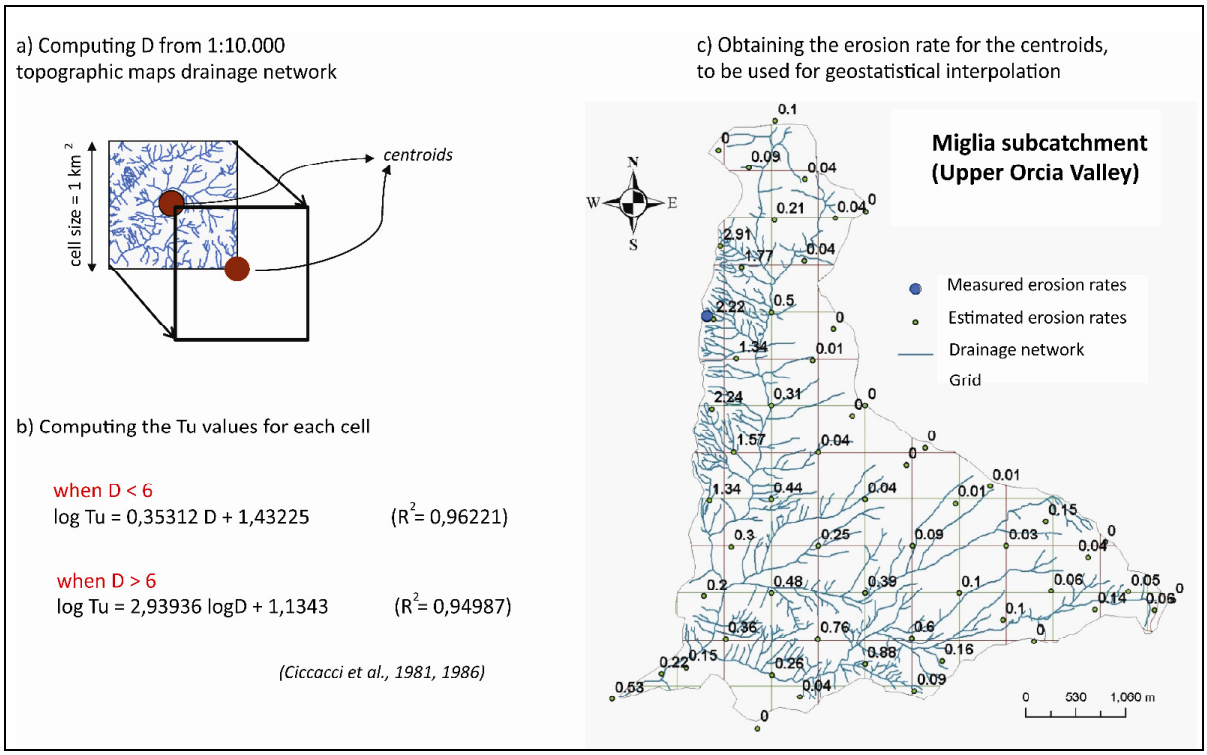

Fig. 6.7 – Tu Grid analysis procedure.

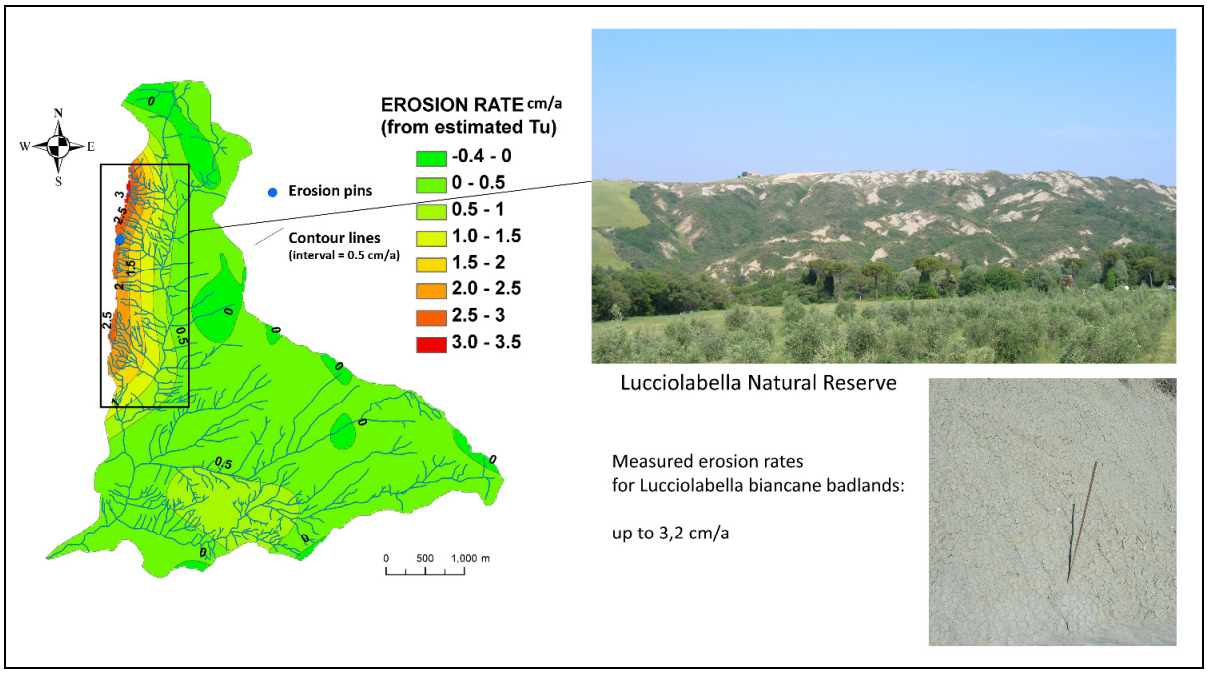

Fig. 6.8 – Estimated erosion rate map of Miglia subcatchment.

6.3.1 Upper Orcia Valley erosion rate map

Starting from the drainage network of the Upper Orcia Valley (about 120 km^2, Fig. 6.9a), digitized from 1:10.000 topographic maps (CTR, Tuscany Region), the present erosion rate map (Fig. 6.9b) was carried out, through the Tu grid analysis and using the equations 1 and 2. The map was then validated by comparing the estimated erosion rates with those measured in the last 20 years. The graph in Fig. 2.9 summarize the average ground level changes measured in the last two decades using erosion pins located in different erosion landforms. The average measured erosion rate, only due to runoff, in badlands areas was calculated in 1.5 - 2.5 cm/a, while for *biancane* areas the rate is even higher, despite here average slope gradients are lower (refer to § 2). The overlapping of the estimated erosion rate map and the areas affected by *calanchi* and *biancane* badlands (Fig. 6.10) shows that both landforms fall in areas with very high erosion, with *biancane* more developed on areas with the highest values (up to 3 cm/a). Some areas, for which very high erosion rates have been estimated, correspond to nowadays remodelled *biancane* badlands areas, so that, in fig. 6.10, they result not affected by present badland erosion, even if high erosion rates are supposed to persist.

Finally, it must be stressed that the erosion rates estimated using the Tu index does not include the contribution of gravitational movements to the total sediment load produced from badland areas, that are far more common on *calanchi* badlands than on *biancane* and involve a considerable removal of material, besides temporary accumulations.

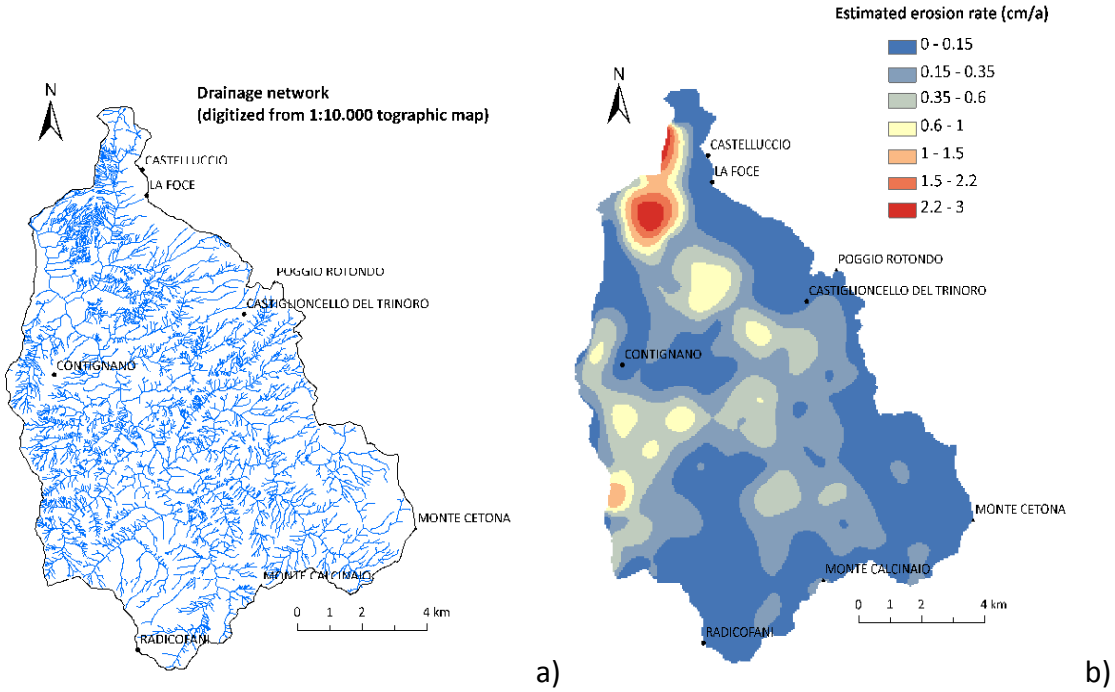

Fig. 6.9 – Drainage network (a) and estimated erosion rate map (b) of Upper Orcia Valley.

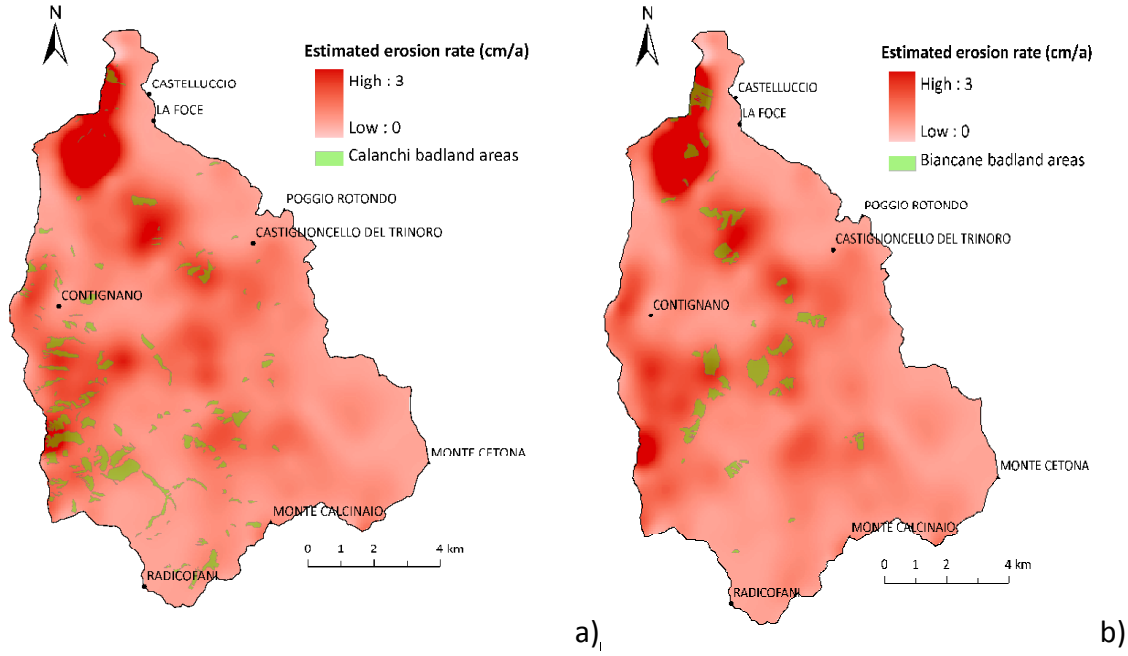

Fig. 6.10 – *Calanchi* badlands (a) and residual *biancane* badlands (b) areas overlaid in the estimated erosion rate map of Upper Orcia Valley.

7 PROPOSAL OF A GEOMORPHOLOGICAL SUSCEPTIBILITY ASSESSMENT METHOD

In this section, a statistically based susceptibility evaluation method is described, partly inherited from previous studies, partly originally proposed (Vergari et al., 2011). In this chapter, the method is applied to evaluate Upper Orcia landslide susceptibility, while, in the following section, will be described as a fundamental base to assess water erosion hazard.

7.1 Introduction

Since the 1970s, many authors have proposed GIS-supported methods to evaluate geomorphological hazard, that is, the probability that a geomorphological event of given intensity will occur in a given area and in a given time span (Brabb, 1984; Panizza, 1987).

Despite geomorphological hazard may be predictable for some processes, such as floods (E.g. Della Seta et al., 2005), landslide hazard prediction may be difficult because it is often impossible to evaluate the spatial and temporal distribution of past events for large areas, due to gaps in the historical record and in the geographic information, especially when studying gravitational movements. Thus, several methods developed and implemented in this field of research have focused on evaluating geomorphological *susceptibility*, and GIS technology makes easier the application of quantitative techniques in hazard assessment and mapping.

Landslides are the most studied processes when analyzing geomorphological susceptibility, as periodically summarized by several authors (Crozier, 1984; Carrara et al., 1995; Soeters and van Westen, 1996; Guzzetti et al., 1999), but the same methods can be generalized also to other geomorphological instability processes. These methods are generally based on the more or less clear statement that mass movements are more likely to occur in the presence of the same conditions that led to past and present instability (Varnes, 1984; Carrara et al., 1991, 1995; Marini, 1995). For this reason, most of the landslide

susceptibility evaluation methods are generally focused on the study of the factors influencing slope instability (causal factors).

Landslide susceptibility methods can be divided into three classes (Carrara et al., 1992): heuristic, deterministic and statistical methods. In heuristic (or index) methods the causal factors are weighted subjectively (Hollingsworth and Kovacs, 1981; Bosi et al., 1985; Neeley and Rice, 1990; Montgomery et al., 1991; van Westen et al., 1999). Deterministic models are based on the physical laws driving landslides (Okimura and Kawatani, 1987; Hammond et al., 1992; Montgomery and Dietrich, 1994; Terlien et al., 1995; Pack et al., 1999; Iverson, 2000) and are generally more suitable for small areas or for slope-specific stability studies. The statistical approach, instead, is founded on the multivariate relationships between causal factors and past and present landslide occurrence. The multivariate relationships are often identified through conditional analysis (Bonham-Carter et al., 1989; Carrara et al., 1995), discriminant analysis (Agterberg, 1974; Carrara, 1983; Carrara et al., 1995, 2003; Baeza and Corominas, 2001), linear or logistic regression (Atkinson and Massari, 1998; Guzzetti et al., 1999, and references therein; Gorsevski et al., 2000; Dai and Lee, 2003; Ohlmacher and Davis, 2003; Ayalew & Yamagishi, 2005) and artificial neural networks (Aleotti et al., 1996; Lee et al., 2001; Wang and Sassa, 2006; Falaschi et al., 2009; Pradhan and Lee, 2010).

Statistical models have been developed to overcome the uncertainty due to subjective evaluation and are generally suitable for susceptibility assessment at catchment scale (as the present study case). In the statistical approach, particularly when applying conditional analysis, the causal factors are generally selected by the operator (Zêzere et al., 2004; Clerici et al., 2006; Conoscenti et al., 2008b).

Here is presented a method for geomorphological susceptibility evaluation, based on statistical conditional analysis, often applied to assess landslide susceptibility. Traditional conditional analysis is integrated with an unbiased bivariate statistical procedure for selecting causal factors. The crucial point of the method is the dual purpose of achieving the minimum complexity in the methodological sequence, based on perceptive statistical procedures, and the clearest possible vector susceptibility output maps to allow their use even for non-expert users and to guide decision makers in land management. It can be applied for evaluating geomorphological susceptibility due to different processes, such as landslides, floods and water erosion.

The susceptibility evaluation method is here described for the landslide application, as it descends from the landslide studies only just described. Even though, it has been conceived to be applied for both landslide and water erosion susceptibility evaluation, as exemplified in the application described in § 8. Even if not yet tested by means of a study case application, this method should be also applicable to flood hazard evaluation, integrated by the correct related precautions.

7.2 Methodological background

The proposed landslide susceptibility assessment procedure (Fig. 7.1) is part of a well-established group of statistical models. It is based on a method originally proposed in previous studies (Marini, 1995; Del Monte et al., 2002; Della Seta et al., 2005) and consisting of a multivariate analysis, where the conditional independence among causal factors had been assumed. In this procedure, the conditional dependence among factors is assumed and the susceptibility analysis is preceded by a new statistical procedure to select the most important causal factors for each type of landslide.

Separate analyses should be performed for different instability landform types as suggested also by Soeters and van Westen (1996), Guzzetti et al. (1999), Remondo et al. (2003). In fact the most influential factors and their weights may vary considerably for different process types as well as, for the same type, in different areas.

The proposed procedure for factor selection is a bivariate statistical analysis aimed at understanding the distribution of the occurred instability events within the different classes of possible controlling factors. The selection of the causal factor, in fact, is based on the concept that the more the past events are concentrated in few classes of a factor, the more this factor will be important in discriminating the areas more or less prone to the future occurrence of that hazardous process.

In this method, the study area is divided into sub-areas characterized by a unique combination of classes of pre-selected causal factors (Marini, 1995; Del Monte et al., 2002). These map units conceptually correspond to the Unique Condition Units proposed by Carrara et al. (1995) and Chung et al. (1995), but formally differ from them because in this methodology they come from vector datasets so that we called them vUCUs (vector Unique Condition Units). Moreover, the vUCUs are different for each instability landform type susceptibility analysis, as a consequence of the application of the factor selection procedure. Vector datasets are used in order to obtain vector susceptibility outputs, which are expected to be less fragmented than the raster ones, and consequently more easy to be interpreted by users.

The conditional analysis is a multivariate statistical approach based on Bayesian theory, which considers the causal factors as conditionally dependent causes for instability events (Bonham-Carter et al., 1989; Carrara et al., 1995). This statistical procedure is generally applied to calculate the *susceptibility index* for each map unit, where the simple attribution of an *a priori* landslide probability determination is conditioned, and thus updated, considering information on the combination of selected factors that caused past events.

A well-structured susceptibility evaluation procedure should consider the terrain conditions preceding the instability events, since the failure occurrence could cause strong topographic modifications of these areas (Chung and Fabbri 1999, 2008; Fernandez et al. 2003; Ayalew and Yamagishi 2005; Nefeslioglu et al. 2008; Clerici et al., 2010). When assessing landslide hazard, for example, our procedure provides for the application of the susceptibility analysis using, for landslide inventory, the depletion zones and the outer buffer areas from the depletion zones, the latter to be dimensioned as a function of the input data resolution. In fact, the outer buffer area from depletion zones preserves pre-landslide conditions (Süzen and Doyuran, 2004), and it can be also affected by retrogressive activity of the landside process (Cruden and Varnes, 1996): it is, thus, very useful when input data about the terrain conditions preceding the instability events are not available.

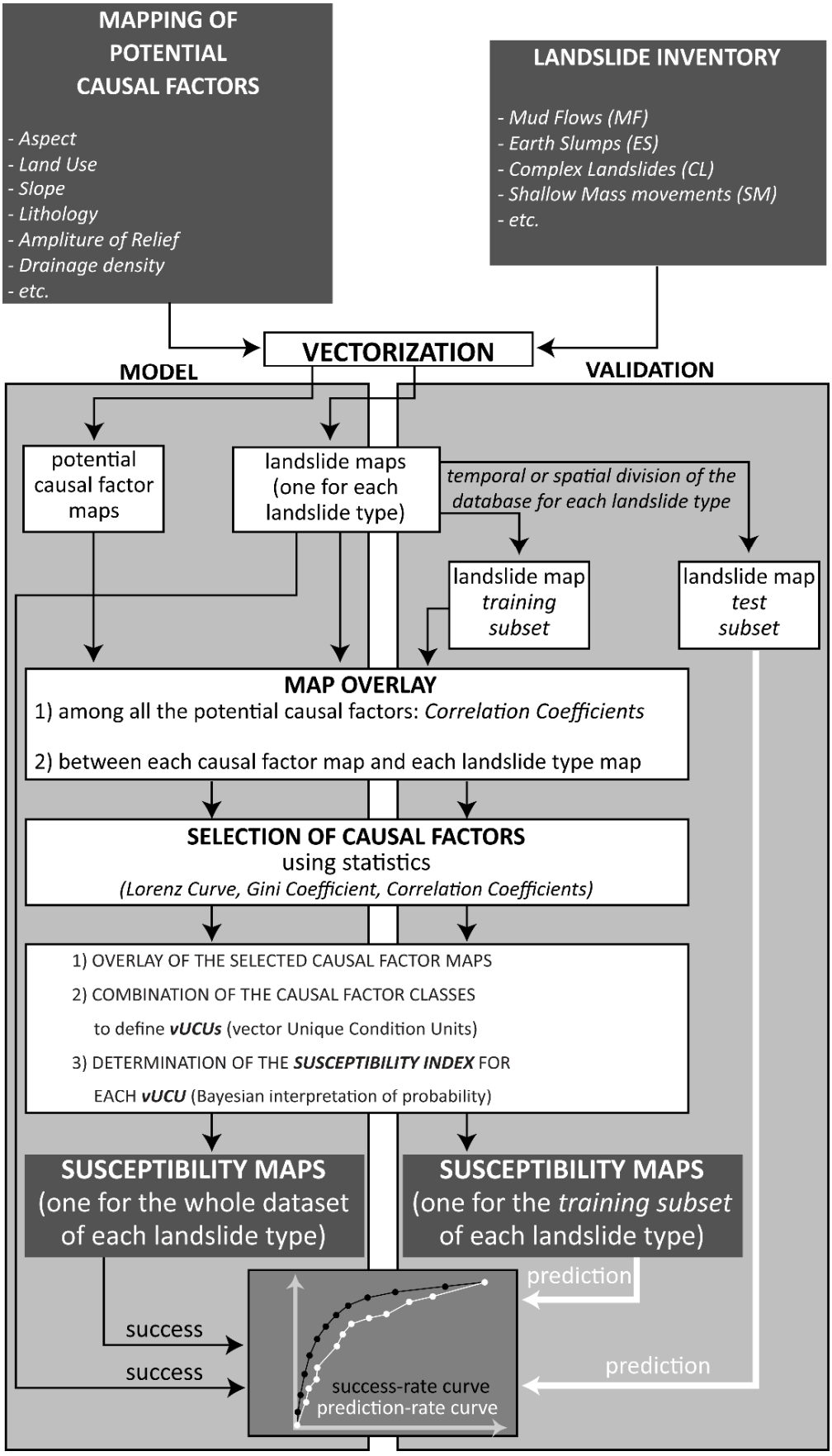

Fig. 7.1 – Landslide susceptibility assessment procedure (Vergari et al, 2011).

Considering the importance of verifying the reliability of the spatial prediction model (Guzzetti et al., 2006), the validation of the model is the last step of the proposed procedure. Several validation methods have been proposed by different authors, with the aim of immediately testing the model, overcoming the difficulty of waiting for future instability event occurrence and comparing their distribution with the assessed classes of susceptibility. In this study, the validation procedure proposed by Chung and Fabbri (2003) was applied, in which a temporal subdivision of instability landforms is recommended: a *training subset* of data is exploited to produce a new prediction map (*training susceptibility map*), while the other subset (*test subset*) simulates the unknown *target pattern*, as better explained in the following paragraphs.

7.3 Factor selection procedure

The implementation of geomorphological susceptibility prediction models involves a series of tricky problems to be solved when identifying and mapping a suitable set of potential causal factors.

a) Identification and mapping of a suitable set of instability factors, bearing a causal relationship with instability landforms, needs an *a priori* knowledge of the main causes of slope instability processes (Guzzetti et al., 1999).

b) Once some potential causal factors have been correctly identified, a further constraint for a successful geomorphological susceptibility evaluation lies in their suitability for the study case: in fact, each causal factor can be more or less discriminant in explaining the distribution of the same landform type in different study areas.

c) The identified controlling factors must be then classified in a suitable number of classes to best represent the variability of the factor values. In fact, too many classes lead to excessively small and diverse vUCUs and, thus, to low statistical significance of the landslide distribution in each vUCU, while too few classes can hide the effective variability of data. To perform an unbiased classification, the correct method should be chosen depending on the data frequency distribution (Jenks and Caspall, 1971).

d) Once the factor values have been correctly classified, it is necessary to select the correct number of factors, because, again, the greater the diversity of vUCUs, the lower the extent of the spatial units and, the lower, the significance of the statistical analyses (Clerici et al., 2006, 2010). However, filtering techniques to cancel out or merge small and insignificant areas can introduce bias or errors in the procedure (Guzzetti et al., 1999). When using UCUs, the maximum number of causal factors to use in the landslide susceptibility assessment should depend on the extent and on the physiographic variability of the study area, as well as on the input data resolution.

Applications of simple statistical methods, such as conditional analysis, are rarely preceded by an unbiased causal factor selection procedure (He & Beighley, 2008). Some factor selection procedures, such as those proposed by Chung et al. (2002), Remondo et al. (2003) Clerici et al. (2010), provide for selecting the most significant factors after having computed all the possible susceptility maps from all the possible combinations of the potential causal factors and having tested the results by means of a validation method.

To select the most influencing factors likely responsible for future events in a given study area, we propose to use some statistical parameters before the application of the conditional analysis (Fig. 7.2), as a conceptually simple and effective method. This method is aimed at solving the above points b), c) and d), considering that the point a) is common to all the approaches aimed at evaluating geomorphological susceptibility and is strongly depending on the operator knowledge of geomorphological processes.

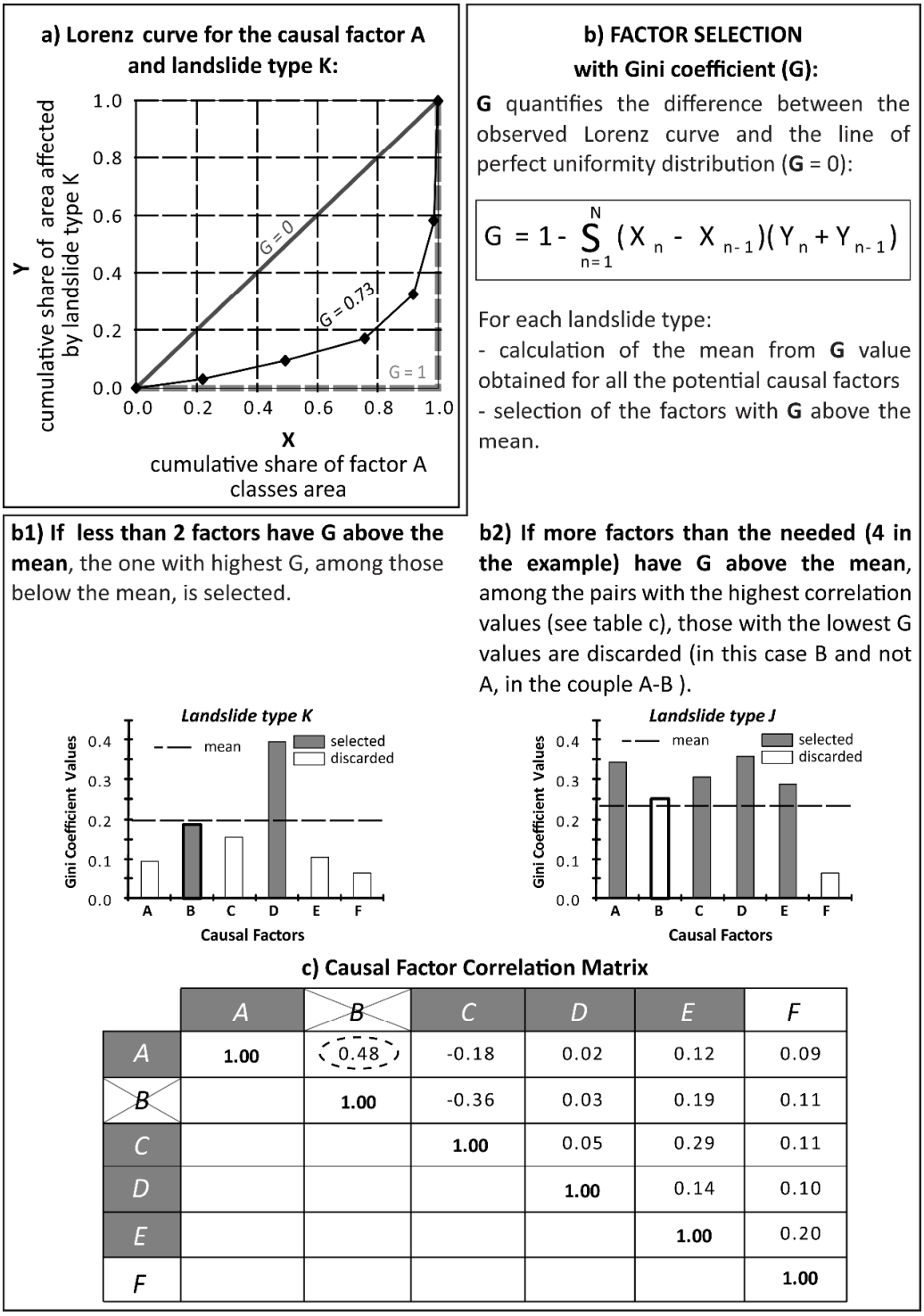

	A	B	C	D	E	F
A	**1.00**	0.48	-0.18	0.02	0.12	0.09
B		**1.00**	-0.36	0.03	0.19	0.11
C			**1.00**	0.05	0.29	0.11
D				**1.00**	0.14	0.10
E					**1.00**	0.20
F						**1.00**

Fig. 7.2 - Factor selection procedure: a) Example of Lorenz curve representing the distribution of landslide within the different classes of a potential causal factor K; the 1:1 solid line represents the homogeneous distribution of landslides with respect to factor classes, while the dotted line represents the perfect inequality distribution. b) Factor selection based on Gini coefficient value (G) with respect to the mean of the G values of all the considered factors. b1) Factor selection if only one factor has G value above the mean. b2) Factor selection if more factors than the needed number have G value above the mean. The degree of correlation between these factors (c) has to be considered, in order to discard, from the statistically correlated ones, those with lowest G values (Vergari et al., 2011).

In particular, our factor selection consists of measures of inequality distributions (Gini, 1914), computation of Lorenz curves (Lorenz, 1905) and use of some indices of correlation between variables. Gini's index of inequality and Lorenz curves were conceived, in the field of economics, to measure social inequality and to represent income distribution over a population. In this study, we applied them to understand the distribution of occurred hazardous events within the different classes of influencing factors. The Lorenz curves were constructed after the intersection of each causal factor map with each instability landform type map. Each point on the Lorenz curve (Fig. 7.2a) represents the cumulative area affected by a given hazardous event type versus the cumulative portion of the study area characterized by a certain class of a given potential causal factor. The line of perfect inequality (dotted line in Fig. 7.2a) represents the situation in which all the landforms of each type are clustered in a single factor class, whereas their homogeneous distribution in all the factor classes is represented by the line of perfect equality (the 1:1 solid line in Fig. 7.2a).

The Gini coefficient (*G*) is graphically represented by the area between the line of perfect equality and the computed Lorenz curve, and it is expressed as the portion of the area between the line of perfect equality and the line of perfect inequality (Gini, 1914). This area can be approximated with trapezoids, and can be calculated using the following formula:

$$G = 1 - \sum_{n=1}^{N} (X_n - X_{n-1})(Y_n + Y_{n-1})$$

where:

n = factor class

N = total number of factor classes

X_n = cumulative portion of the study area characterized by the factor class k, with $X_0 = 0$, $X_N = 1$

Y_n = cumulative portion of instability landform area falling in the factor class k, with $Y_0 = 0$, $Y_N = 1$

For each instability landform type analysis, a factor is selected if the corresponding *G* value is higher than the average of the coefficient values of all of the considered factors, as shown in Fig. 7.2b. The mean value is a simple measurement of the central tendency of the data and accounts for the specific range of *G* values for each landform type. In this way, independently of the absolute *G* values, factors with *G* higher than the mean value will be

more discriminant than the others for the same instability process type occurrence in the study area. If only one factor has a *G* value higher than the mean, then the factor with the second highest *G* value must be selected as well (case b1 in Fig. 7.2). If more factors than the needed number have a *G* value above the mean, we propose a method of exclusion based on the correlation between these factors, in order to avoid that the vUCUs provide redundant information about the hazardous event distribution (Clerici et al., 2010). Thus a unique correlation matrix for all the possible pairs of potential factors is computed, using *Pearson correlation* when comparing two numerical variables (such as slope and drainage density), the *Cramer Index* when comparing two nominal variables (such as lithology and land use), and the η^2 index when comparing a numerical variable to a nominal variable (such as lithology and amplitude of relief) (Pearson, 1896; Cramer, 1999). So, when too many causal factors have *G* values above the mean, from the pairs with the relatively highest correlation value, the factor with lowest *G* value must be discarded (case b2 in Fig. 7.2).

The susceptibility evaluation for each instability landform type has to be preceded by a careful evaluation of the best factor classification method.

7.4 Susceptibility index determination

Once the causal factors are finally selected for each instability type, the conditional analysis allows obtaining a number of vUCUs from all of the possible selected factor combinations in the study area. The *susceptibility index* for each vUCU (used to draw up the susceptibility maps for each considered instability process type) is successively calculated using the Bayesian interpretation of probability. The importance of applying conditional probability models has been strongly emphasized in the Earth Sciences literature, especially for predicting hazardous events or mapping mineral potential (Bonham-Carter et al., 1989) and was then applied by several authors for landslide susceptibility evaluation (Chung and Fabbri, 1999; Irigaray et al., 1999; Clerici et al., 2006, 2010; Zêzere et al., 2004; Conoscenti et al., 2008b). The Bayes rule allows the probability of future hazardous events to be predicted once the area of each vUCU affected by past events is known. The Bayes rule specifies a

prior probability, which is then updated in light of new relevant data (called "likelihood" in Bayesian theory). In the study case, this means that the simple attribution of an *a priori* determined probability has to be updated considering information on past events. Thus, the *susceptibility index* corresponds to the conditional (or posterior) probability P(*f*|vUCU), which is the probability of the occurrence of a hazardous event type given a certain combination of selected causal factors (vUCU). If we consider as an example a vUCU defined by the spatial combination of the areas pertaining to two classes of two causal factors k_g and j_h (where *k* and *j* represent two causal factors, such as lithology and hillslope aspect, and *g* and *h* represent single classes of the factors), the *susceptibility index* is:

$$P(f \mid k_g \bigcap j_h) = \frac{P(k_g \bigcap j_h \mid f)}{P(k_g \bigcap j_h)} \cdot P(f) \qquad (1)$$

where:

$P(f)$ = *prior probability* of instability landform *f* = ratio of the study area presently characterized by instability landforms);

$\frac{1}{P(k_g \bigcap j_h)}$ = *proportionality factor* = 1/ratio of the study area presently characterized by the concomitant presence of k_g and j_h, in which the denominator indicates the *prior probability* of the simultaneous presence of the two classes of the factors *k* and *j* (for example clayey outcrops, for lithology factor, and north-facing slopes, for aspect factor);

$P(k_g \bigcap j_h \mid f)$ = *conditional probability* (*likelihood* or updated value of probability) of the simultaneous presence of the two classes of the factors *k* and *j,* given the instability landforms *f* = area of intersection between k_g, j_h and area affected by instability landforms *f* / total area presently characterized by instability landforms;

and

$P(f \mid k_g \bigcap j_h)$ = *posterior probability* of instability landforms *f*, which is proportional to the *prior probability* updated with the *likelihood.*

The *susceptibility index* (S_{index}) for each *i*-th vUCU and each instability landform type can be computed more easily because it corresponds to the ratio between the instability landform area affecting $vUCU_i$ (Af_{vUCUi}) and the area of $vUCU_i$ (A_{vUCUi}):

$$S_{index} = \frac{Af_{vUCUi}}{A_{vUCUi}} \quad (2)$$

The S_{index} values for each vUCU indicate the probability of the instability process type occurrence conditioned by the concomitant presence of the selected causal factor categories. S_{index} of a vUCU may be expressed by a percentage, thus theoretically ranges between 0 and 100%, where 100% is the maximum probability of a hazardous event, given by the complete coverage of the vUCU by hazardous events.

7.5 Validation procedure

As validation procedure, the method by Chung and Fabbri (2003) is applied in the last step of the proposed susceptibility evaluation method. In fact, we considered the importance of testing the reliability of the susceptibility evaluation method and validating the different output models. This method provides for a chronological partition of the instability landform database into a *training subset* and a *test subset* (Fig. 7.1), considering the second one as the unknown future target pattern of instability events. The procedure must be applied after the susceptibility maps for each instability process type are generated using all of the landforms surveyed in the study area. The main steps are 1) dividing the past events into two chronological sets, using the air-photo mosaic of a specific year within the inventory time span: the ones that occurred before that year will represent the training subset, while the ones that occurred after that year will be the test subset; 2) applying the susceptibility analysis already applied to the whole landform inventory (procedure to obtain the susceptibility maps), only to the training subset (thus obtaining a training susceptibility map for each considered instability process); and 3) comparing the distribution of the test subset landforms with the training susceptibility map resulting from step 2.

The comparison of past and future events is simulated by pretending to evaluate the susceptibility at the year of the air-photo mosaic, and considering that the instability events of the test subset have not yet developed. As suggested by Chung and Fabbri (2003), when it is not possible a temporal partition of the instability landform dataset, a random spatial subdivision is an acceptable alternative. By intersecting each training susceptibility map and the instability landforms of the test subset, it is possible to construct a prediction-rate curve, while the success-rate curve is elaborated by comparing each susceptibility map, obtained by considering the whole set of each type of instability landforms, with the distribution of all the landforms that have been used to obtain this map.

Since we used vector layers, we constructed the curves by plotting the cumulative area of vUCUs ordered by decreasing S_{index} values (*x*-axis) versus the cumulative area affected by instability processes within each vUCU (*y*-axis).

As it is generally assumed that future hazardous events will occur in the same conditions that provoked the already occurred ones in the same area, the *success-rate curve* measures the model fitness, assuming that the model is correct. On the other hand the *prediction-rate curve* provides a measure of the predictive capability of the model. Ideally, the tangent of a *prediction-rate curve* should be monotonically decreasing, to indicate that the most hazardous classes predict most of the “future” events, and the trend regularly decreases with the gradual reduction of the susceptibility value. However, as described by Chung and Fabbri (2003), empirical *prediction-rate curves* usually do not satisfy this condition. A 1:1 trend of the prediction-rate curve indicates that the prediction map is randomly generated. Thus, the further the prediction-rate curve is from a straight line, the more the susceptibility estimation is significant. Moreover, the steeper the curve is in its first part, the greater the predictive power of the prediction map (Remondo et al., 2003).

7.6 Landslide susceptibility evaluation for the Upper Orcia Valley

The landslide susceptibility method was applied in the Upper Orcia Valley, which is the easternmost portion of the Ombrone River basin. The area is located in the Tuscan Pre-Apennines, close to Siena, north of Radicofani, and it covers about 120 km^2, with an altitude ranging from about 350 to 1148 m a.s.l. (Mt. Cetona). The drainage pattern and catchment shape are structurally controlled by the regional morphostructure of the Radicofani Graben (Baldi et al., 1994; Carmignani et al., 1994), whose major axis is oriented NW-SE. The location of the Orcia River basin southern divide, which corresponds to the boundary between the Tevere River and Ombrone River basins, is controlled by the Monte Cetona horst and the Monte Amiata and Radicofani Quaternary volcanoes.

7.6.1 Landslide inventory map

The landslide inventory map (Fig. 7.3, here shown as a sketch map) has been surveyed at the scale of 1:10,000 through geomorphological field surveys and the interpretation of 1988-1989 aerial photographs ("Volo Italia 1988-'89", performed by Compagnia Generale Ripreseaeree (C.G.R.) S.p.A. at a scale of about 1:70,000), and 1993 aerial photographs of Regione Toscana (performed by C.G.R. S.p.A., scale 1:30,000). This multi-temporal analysis also allowed the temporal division of the landslide database into two subsets, in order to perform the validation procedure.

The Upper Orcia River valley slopes are widely affected by landslides, solifluction and creep. According to the landslide classification of Cruden and Varnes (1996), we considered the most frequent typologies of landslides, which are mud flows (MF), earth slumps (ES) and complex landslides (CL). Moreover, we used the term shallow mass movements (SM) to represent a fourth category, that consists of portions of hillslopes affected by solifluction and very small and frequent mud flows, whose extent is not mappable at the study scale (1:10,000). These landforms were mapped after field survey, and not clearly definable on aerial photos, thus they lack the temporal information. We discarded rock fall landslides and earth slides because they are too few and small to be significant for the statistical analysis of

susceptibility. It is noteworthy that all the detected and mapped landslides are recent and active and thus comparable to the time scales of all of the considered factors.

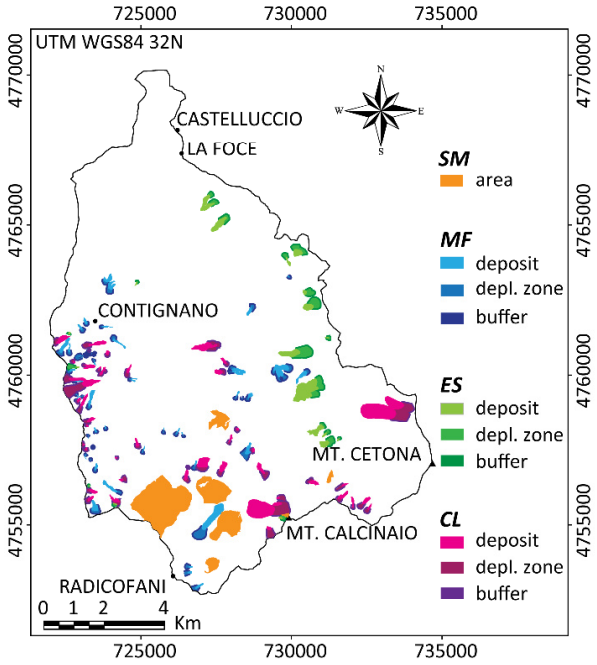

Landslide type	Slope instability landform	Number of events	Total area (m^2)	Training subset area (m^2)	Test subset area (m^2)	Mean single landslide area (m^2)	Standard deviation (m^2)
MF	50 m buffer	57	1137164.12	715153.35	422010.77	23931.19	12661.83
	depletion zone		537932.49	407500.22	130432.26	9437.41	14657.23
ES	50 m buffer	22	633906.25	555189.03	78717.23	28810.36	24956.79
	depletion zone		641726.10	610102.10	31624.00	29169.37	32217.75
CL	50 m buffer	50	1196634.99	593025.79	603609.20	22159.91	13699.06
	depletion zone		1136649.00	851086.06	285562.94	22732.98	35712.48
SM	portion of hillslope affected by SM	7	4314729.99	/		616389.99	695859.19

Fig. 7.3 - Landslide inventory maps. For each landslide type, the deposit, the depletion zone and the 50 m outer buffer area from the depletion zone are shown. Total area and mean extent of each landslide type are listed in the table.

All landslide types were mapped and digitized in a GIS environment, as vector datasets. For the same type of landslide, we run the susceptibility evaluation model twice, using first the depletion zones and then an outer buffer from depletion zones. For the study case, we discarded the possibility of using a buffer size proportional to the landslide extent and considered as significant a fixed buffer of 50 m. In fact, proportional buffers would have caused the smallest ones to be not significant with respect to the resolution of the input

data and the largest ones to include too much spatial variability of the causal factor values. We removed the portion of the buffer areas passing over the divide line and dissolved the buffer polygons when intersecting each other.

We used both depletion and buffer areas for all the landslide types, except for SM. In fact, for SM we considered the whole instable areas because detachment and accumulation zones are not detectable at the spatial and temporal scales of the study. Figure 7.3 shows the 50 m outer buffer areas from the depletion zones, the accumulation zones and the detachment zones for the considered landslide types, as well as the extent of the datasets used for susceptibility and validation analyses.

MF are very frequent in the study area due to the widespread outcrops of clays (Fig. 7.4a). As observed during the monitored time span, these flows can be reactivated several times in one year, especially during the winter half-year, although intensive agricultural activity has recently and frequently leveled these landforms (Della Seta et al., 2009; Ciccacci et al., 2008). Small but frequent MF have been observed on badlands slopes or where the bare clayey bedrock crops out.

ES are frequent in the eastern part of the study area and sometimes show considerable extent (Fig. 7.4b). Although anthropogenic actions have tried to mitigate the effects of landslides, these processes are so strong that, just 24 or 48 hours after a rainstorm, significant modifications of the topographic surface appear on slopes. ES often evolve to earth flows towards the toe, giving rise to CL (Fig. 7.4c).

SM produce typical lobes and irregular surfaces on hillslopes (Fig. 7.4d), even if showing gentle slope, especially those affected by deforestation. The same hillslopes are affected by small and frequent mud flows, often leveled by farmers. These landslides are difficult to be mapped because surface running waters rapidly reshape the surface. In these cases, we mapped the portions of slopes affected, on the whole, by SM.

We decided to apply the susceptibility evaluation procedure separately for each landslide type since in the area the occurrence of different landslide types can produce very different effects on hillslopes: MF (Fig. 7.4a) generally cause long and narrow surface landslide bodies, ES (Fig. 7.4b) are deeper, involving large volumes of material and SM (Fig. 7.4d) are not single gravitational landforms but rather instability events affecting entire

portions of hillslopes. As for CL, they generally provoke an elongation of the deposits at their toe (Fig. 7.4c) and were, thus, considered separately from ES for the susceptibility analysis.

Fig. 7.4 - Examples of the mass movements widespread in the study area: a) mud flow; b) earth slump; c) complex landslide (earth slump evolving into a mud flow); d) shallow mass movements

7.6.2 Potential causal factors

We chose six potential causal factors, as suitable in accounting for the physiographic conditions of the study area, and mapped their spatial distributions, as shown in Fig. 7.5. The values of each variable have been classified, and, for each landslide type, the fraction of the total landslide area within each factor class was evidenced in histograms. For clarity of the outputs, we decided to work with vector data, so each raster layer, derived from a DTM with a resolution of 25 m, was converted to a vector dataset. The DTM was constructed from digitized point elevation and contour lines of the 1994 topographic maps at scale 1:10,000 of

Regione Toscana and from it we derived the terrain analysis parameters slope, aspect and amplitude of relief.

Slope (S)

The slope map (Fig. 7.5a) was derived from the 25 m cell-sized DTM, using the analysis tools in ArcGIS 3D-Analyst. The output raster was aggregated (nearest-neighbor re-sampling technique) to a 50 m cell-sized grid, to avoid the excessive fragmentation of the vUCUs . S values were grouped into six classes using the Jenks (natural breaks) method and the raster dataset was converted to a vector format. Classes from 1 to 4 are all widespread within the study area (16% to 26%), whereas classes 5 and 6 cover, respectively, 6.8% and 1.5 % of the area and are concentrated where the most coherent lithologies crop out.

The distribution of depletion zones in S classes (Fig. 7.5a) seems to be gaussian, with some differences in the mode, depending on the landslide type: MF and SM have their mode in class 3, ES are more concentrated in class 4, and CL are very frequent in both classes 3 and 4. The distribution of the outer buffer areas from depletion zones shows a similar distribution, but with smaller frequency differences among the S classes.

Aspect (A)

The aspect map (Fig. 7.5b) was derived using the terrain analysis tool in GIS environment. The 50 m cell-size raster output was classified into five groups of A (flat, N, S, E, W). The horizontal areas do not have significant extent, while the other classes are all well distributed in the study area. ES show a progressive increase in frequency, going clockwise from the N class to the W class. The frequency of CL also shows a maximum on west-facing slopes, even if they also occurred on northeast-facing slopes. This can be understood considering the structural influence related to the right slope of the Upper Orcia Valley. MF are preferentially concentrated on the north- and east-facing slopes (generally corresponding to dip slopes) and show the lowest frequency on west- and south-facing slope, such as SM. These distributions can be explained considering that the development of MF needs wetter conditions, even if the relationship between landslides and A is also conditioned by other factors.

Amplitude of relief (AR)

The amplitude of relief map (Fig. 7.5c) represents the maximum difference in height per unit area and was derived by raster calculations from the DEM in ArcGIS. We decided to visualize the results using contour lines and to derive from them a polygonal vector dataset, which was classified using the natural breaks method. This parameter provides a measure of fluvial erosive action. It was verified that, other conditions being equal, the spatial distribution of this parameter can provide information about vertical displacements (e.g. local fault activity or regional uplift) (Della Seta et al., 2004).

As shown in Fig. 7.5c, the highest AR values are clustered along the basin's northeastern divide, where the western flank of the Castelluccio-Mt. Cetona horst is bounded by fault scarps.

Although the lowest classes of this factor are widespread in the area, ES are concentrated in class 4. On the other hand, AR factor does not seem particularly significant in MF distribution, which is quite homogeneous in classes 2, 3 and 4. The distribution of CL indicates an intermediate behavior, while SM are more frequent in classes 3 and 4. Concerning the buffer area, ES, MF and CL have a frequency distribution similar to that of the depletion zone, but for the AR factor, the differences among the frequencies in the factor classes are less relevant.

Drainage density (D)

The drainage density map (Fig. 7.5d) was derived by calculating the cumulative length of stream segments of the drainage network digitized from 1:25,000 topographic maps falling within unit areas of 1 km^2. As for the AR map, we decided to visualize the map using contour lines and to derive from them a polygonal vector dataset classified into equal intervals of D (2.5 km/km^2). D is a parameter which indirectly accounts for the erodibility and permeability of outcropping rocks, the degree of tectonization, the vegetation cover, the slope gradient and the mean annual raifall in the drainage basin. More than 50% of the study area is characterized by high or very high D values (between 5 and 12.5 km/km^2), due to the widespread outcrop of clays (73% of the total area). Moreover, the heads of several

catchments are affected by badlands, where runoff is absolutely dominant with respect to infiltration.

Most of the ES fall in class 2 of this factor, highlighting that they are preferentially concentrated where infiltration is considerable. On the other hand, MF and SM are favored by higher values of D (maximum frequency in class 3), while CL do not seem to be much influenced by this factor. Considering the buffer area distribution with respect to D values, the frequency of MF in the highest D classes appears enhanced.

Land use (LU)

The land use map (Fig. 7.5e) was drawn up after the interpretation of 2004 digital orthophotos (Volo Siena 2004, at a scale of about 1:7,500) and field surveys. We used and simplified the Corine Land Cover legend (1st, 2nd and 3rd levels; EEA, 2007), as indicated in Tab. 7.1. For the susceptibility analysis, we excluded the wetlands that are are not as useful for the susceptibility evaluation due to homogeneously flat slopes. The density of landslides within each LU class shows a maximum frequency in the three more frequent classes (arable lands, untilled lands and hardwood natural forests). In particular, ES occur especially on forest-covered slopes, MF on arable lands, and SM and CL on natural grasslands.

LAND USE UNITS	CORINE LAND COVER UNITS
1. ARTIFICIAL SURFACES	1 (artificial surfaces)
2. AGRICULTURAL AREAS	2.1 (arable land) 2.3 (pastures) 2.4 (heterogeneous agricultural areas)
3. PERMANENT CROPS	2.2 (permanent crops)
4. FOREST AND SEMI-NATURAL AREAS	3.1.1 (broad-leaved forests) 3.2.4 (transitional woodland scrub)
5. REAFFORESTATION AREAS	3.1.2 (coniferous forests)
6. SHRUBBY AND/OR HERBACEOUS VEGETATION AREAS	3.2.1 (natural grassland) 3.2.2 (moors and heathlands) 3.3 (open spaces with little or no vegetation)

Tab. 7.1 - Classification of Corine Land Cover units in land use classes.

Lithology (L)

The lithological map (Fig. 7.5f) was drawn up by grouping the outcropping rocks according to their response to denudation processes, as summarized in Tab. 7.2. The geological setting of the area is well known, and the rock units reported in the existing geological map have been grouped into eight lithological units.

Figure 7.5f also shows the frequency of each landslide type in each L class. This distribution is obviously influenced by the extent of outcrops in the study area (clayey deposits cover about 73% of the Upper Orcia river basin, while volcanic rocks only crop out on the Radicofani neck, which is statistically meaningless for the study area). Nevertheless, we included this factor in the susceptility assessment procedure, since the selection method is conceived precisely in order to quantify the capability of the factors to discriminate the spatial distribution of the landslides. Examining the density of the depletion zones in the different L classes, it can be stated that MF and SM preferentially develop on clay and sandy clay, while ES are homogeneously distributed over continental deposits, conglomerate, clay, sandy clay and flysch deposits, but always on steep slopes. CL mostly developed on clay and sandy clay and on dolomitic limestone. Similar frequency of buffer areas and depletion zones was observed over the classes of this causal factor.

LITHOLOGICAL UNITS	**GEOLOGICAL UNITS (from Carta Geologica d'Italia, at the scale of 1:100,000)**
QUATERNARY CONTINENTAL DEPOSIT	*Pebbly, sandy and clayey sandy alluvial deposits* *Slope talus* *Eluvium/colluvium – red shales – black shales*
VOLCANIC ROCK	*Trachybasalt and olivinic andesite*
CONGLOMERATE	*Polygenic puddingstone and sandstone* *Polygenic puddingstone locally containing Cirripeds and Oysters*
SAND	*Sand and clayey sand* *Sand and clayey sand with shells, pudding lenses and peat*
CLAY AND SANDY CLAY	*Clay and sandy clay with pudding lenses and scattered pebbles* *Interbeds of fossiliferous clay and sandy clay*
LIMESTONES	*Organogenic calcarenites*
FLYSCH	*Sandstone and siltstone* *Clay, silty clay, marly clay with calcareous interbeds*
DOLOMITIC LIMESTONE	*Thin layered jasper variously colored and often weathered* *White and gray layered limestone with chert nodules* *Limestone and dolomitic limestone – marls and calcareous marls intercalated to clay layers* *Nodular reddish limestone and marly limestone – dolomitic limestone*

Tab. 2 – Classification of Geological Units in Lithological classes.

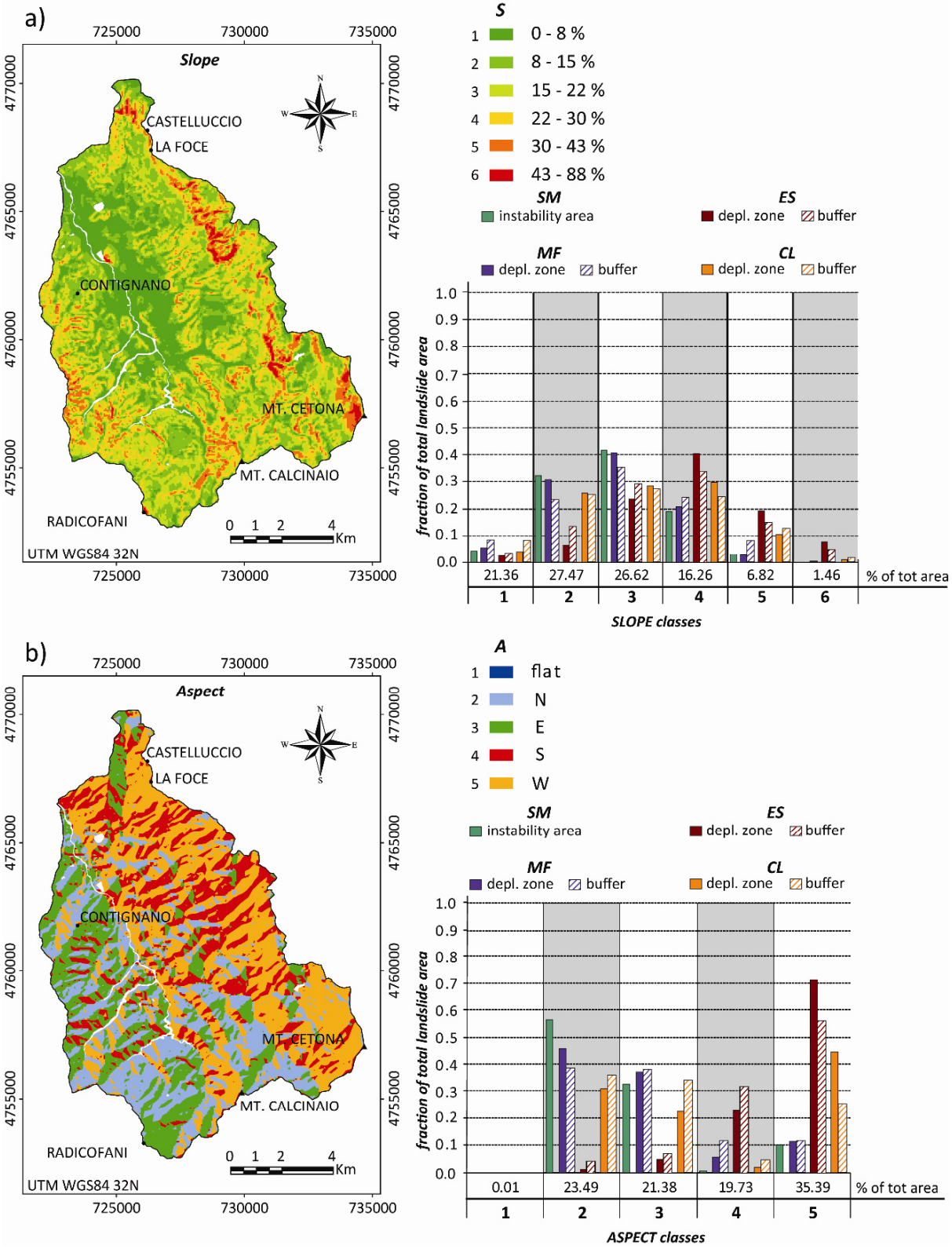
a)
Slope
725000
730000
735000
4770000
4765000
4760000
4755000
CASTELLUCCIO
LA FOCE
CONTIGNANO
MT. CETONA
MT. CALCINAIO
RADICOFANI
0 1 2 4 Km
UTM WGS84 32N
S
1 0 - 8 %
2 8 - 15 %
3 15 - 22 %
4 22 - 30 %
5 30 - 43 %
6 43 - 88 %
SM
instability area
ES
depl. zone
buffer
MF
depl. zone
buffer
CL
depl. zone
buffer
fraction of total landslide area
1.0
0.9
0.8
0.7
0.6
0.5
0.4
0.3
0.2
0.1
0.0
21.36
27.47
26.62
16.26
6.82
1.46
% of tot area
1
2
3
4
5
6
SLOPE classes
b)
Aspect
CASTELLUCCIO
LA FOCE
CONTIGNANO
MT. CETONA
MT. CALCINAIO
RADICOFANI
0 1 2 4 Km
UTM WGS84 32N
A
1 flat
2 N
3 E
4 S
5 W
SM
instability area
ES
depl. zone
buffer
MF
depl. zone
buffer
CL
depl. zone
buffer
fraction of total landslide area
0.01
23.49
21.38
19.73
35.39
% of tot area
1
2
3
4
5
ASPECT classes

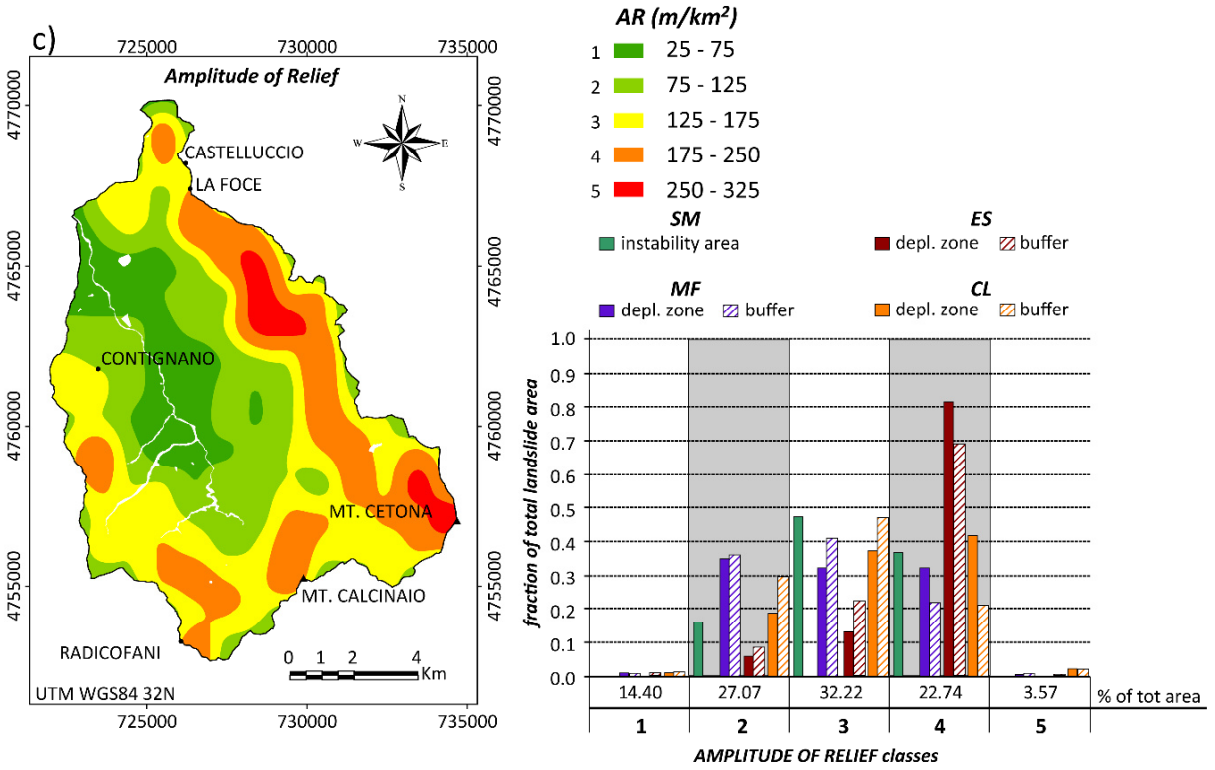
c)
Amplitude of Relief
725000
730000
735000
4770000
4765000
4760000
4755000
CASTELLUCCIO
LA FOCE
CONTIGNANO
MT. CETONA
MT. CALCINAIO
RADICOFANI
0 1 2 4 Km
UTM WGS84 32N
AR (m/km²)
1 25 - 75
2 75 - 125
3 125 - 175
4 175 - 250
5 250 - 325
SM
instability area
ES
depl. zone
buffer
MF
depl. zone
buffer
CL
depl. zone
buffer
fraction of total landslide area
1.0
0.9
0.8
0.7
0.6
0.5
0.4
0.3
0.2
0.1
0.0
14.40
27.07
32.22
22.74
3.57
% of tot area
1
2
3
4
5
AMPLITUDE OF RELIEF classes

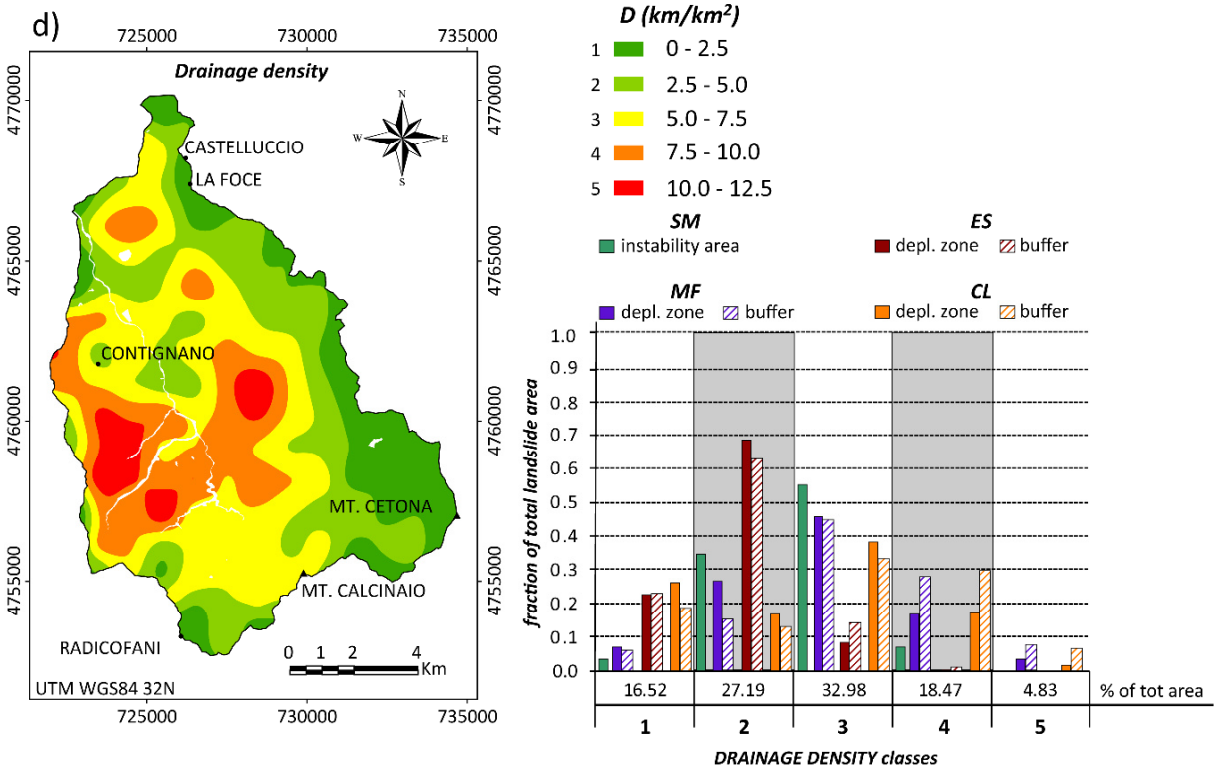
d)
Drainage density
725000
730000
735000
4770000
4765000
4760000
4755000
CASTELLUCCIO
LA FOCE
CONTIGNANO
MT. CETONA
MT. CALCINAIO
RADICOFANI
0 1 2 4 Km
UTM WGS84 32N
D (km/km²)
1 0 - 2.5
2 2.5 - 5.0
3 5.0 - 7.5
4 7.5 - 10.0
5 10.0 - 12.5
SM
instability area
ES
depl. zone
buffer
MF
depl. zone
buffer
CL
depl. zone
buffer
fraction of total landslide area
1.0
0.9
0.8
0.7
0.6
0.5
0.4
0.3
0.2
0.1
0.0
16.52
27.19
32.98
18.47
4.83
% of tot area
1
2
3
4
5
DRAINAGE DENSITY classes

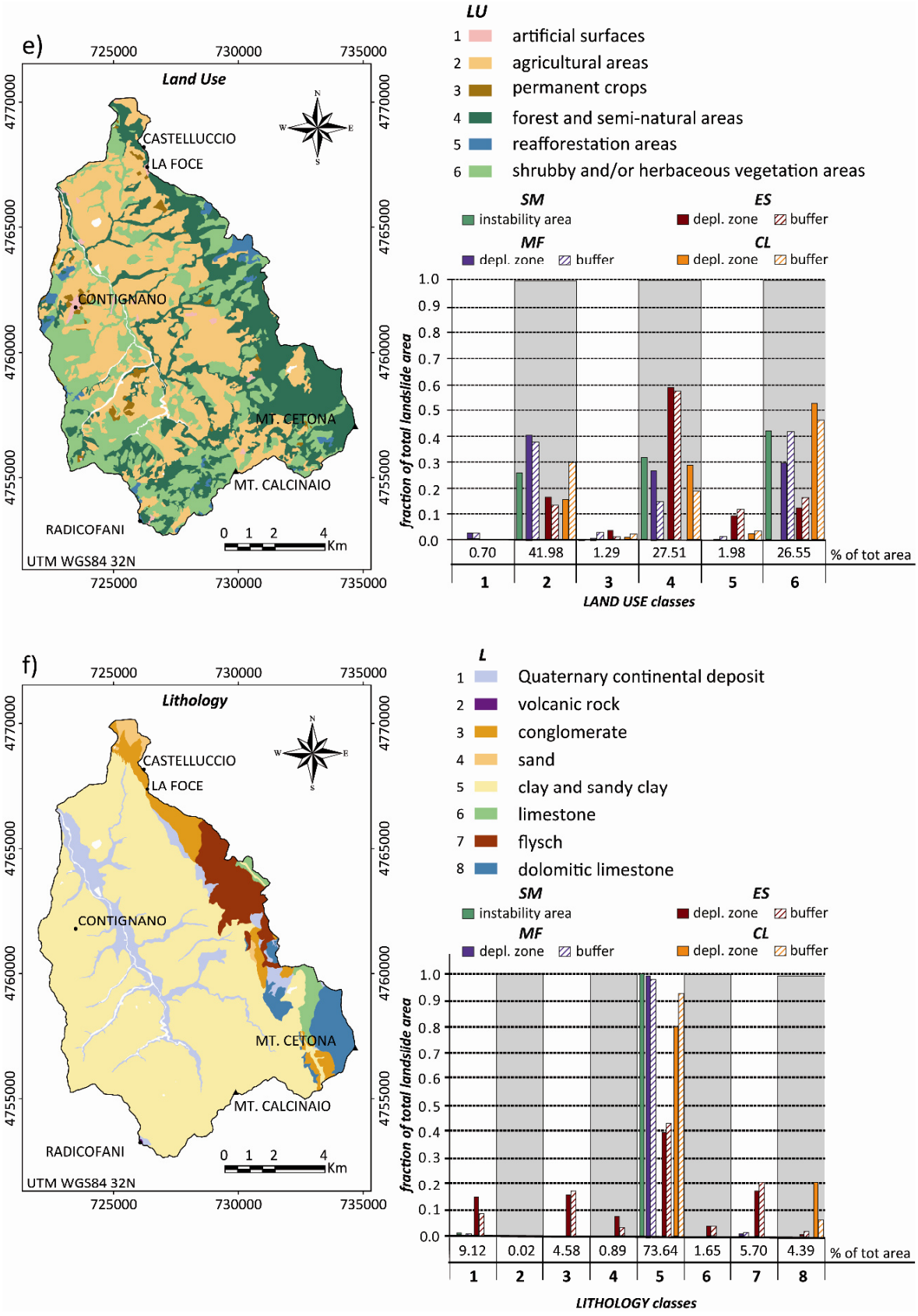

Fig. 7.5 – Thematic maps showing the spatial distribution of potential causal factors for landslides: a) Slope (*S*); b) Aspect (*A*); c) Amplitude of Relief (*AR*); d) Drainage density (*D*); e) Land Use (*LU*); f) Lithology (*L*). The values of each variable were classified and, for each landslide type, the fraction of the total landslide area within each factor class is reported in the histograms (Vergari et al, 2011).

7.6.3 Factor selection

For the study case, we noted that a minimum of 2 and a maximum of 4 slope causal factors had to be selected for the susceptibility analysis. In fact, since the extent of the study area is of about 120 km^2, we calculated that the intersection of more than 4 factors (each one reclassified in no less than 5 categories) resulted in vUCUs with an extent comparable to the factor map resolution and thus not statistically significant (Clerici et al., 2010).

Figure 7.6 shows the Lorenz curves for the considered landslides, while Fig. 7.7 shows the histograms of the obtained G values for each landslide type, the matrix of the degree of association/correlation between the pairs of factors and the tables indicating the factors finally selected for each landslide type. Only a few pairs of factors have relatively higher absolute values of correlation: in particular, S and AR (Pearson correlation of 0.48), AR and D (Pearson correlation of -0.36), and D and L ($\eta 2$ index value of 0.29).

The most influential factor for MF is A (G value of 0.395, Fig. 7.6) using depletion zones, because they are greatly clustered on the north and east-facing slopes, as shown in Fig. 7.5b. Land use was always discarded, since MF are widespread in arable lands, semi-natural areas and shrubby and herbaceous vegetation lands, which are also the three most frequent classes of this factor. Moreover, by using the depletion zones, the S, AR, A, and L factors were selected, while, when using the MF buffer areas, only factors D and A were finally selected, and the other factors related to the topography were discarded. This discrepancy was also observed for other landslide types. In order to discuss this apparent contradiction (same study area, same type of landslide, different influencing factors), we noted that the failure occurrence generally causes strong topographic modifications in correspondence of the depletion zones with respect to the general slope morphology. As a consequence, the topographic parameters become more distinctive for the depletion zones, and generally less effective in estimating the probability of a landslide type event when we consider buffer areas. Moreover, in the same example, L was discarded and D was selected, which makes sense, considering that the variability of D reflects changes in lithological features. So the indirect influence of lithology was included even if L was discarded.

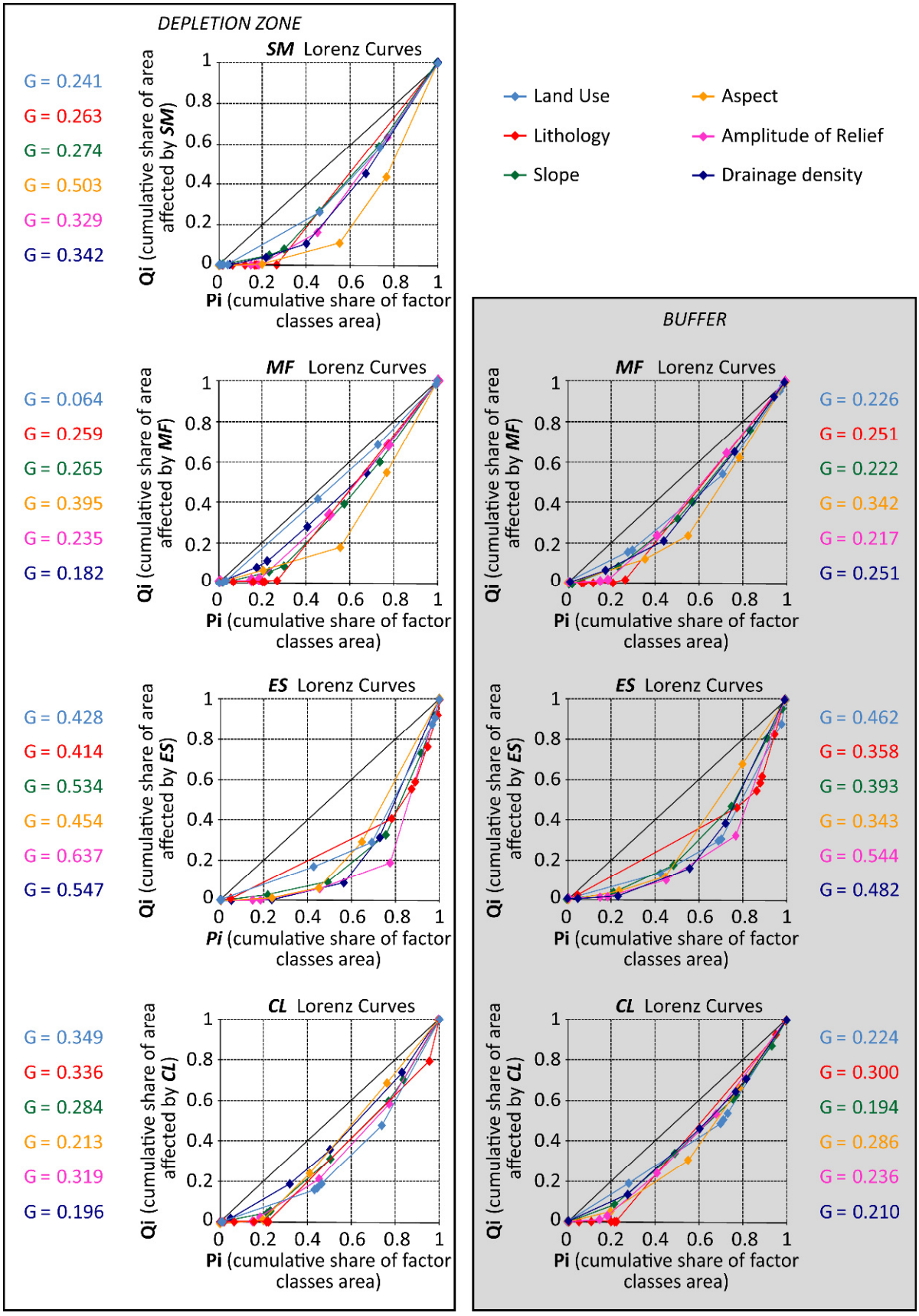

Fig. 7.6 – Lorenz curves for each causal factor and each landslide type. Different curves are computed for depletion zones (or the whole area affected by shallow mass movements) and for the 50 m outer buffer areas (Vergari et al., 2011).

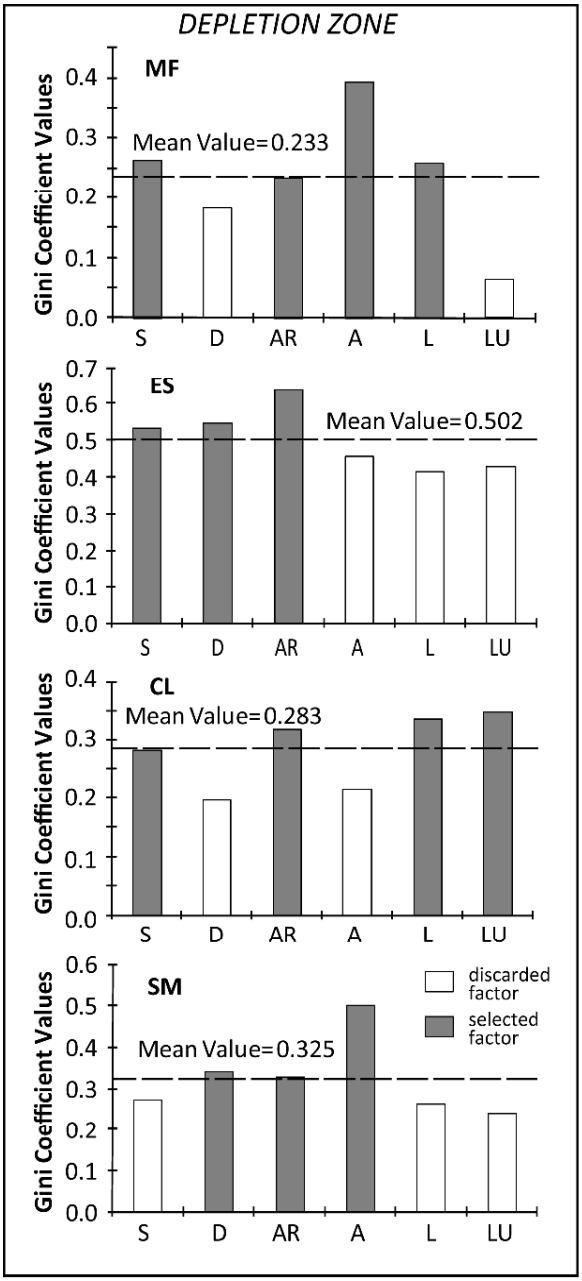

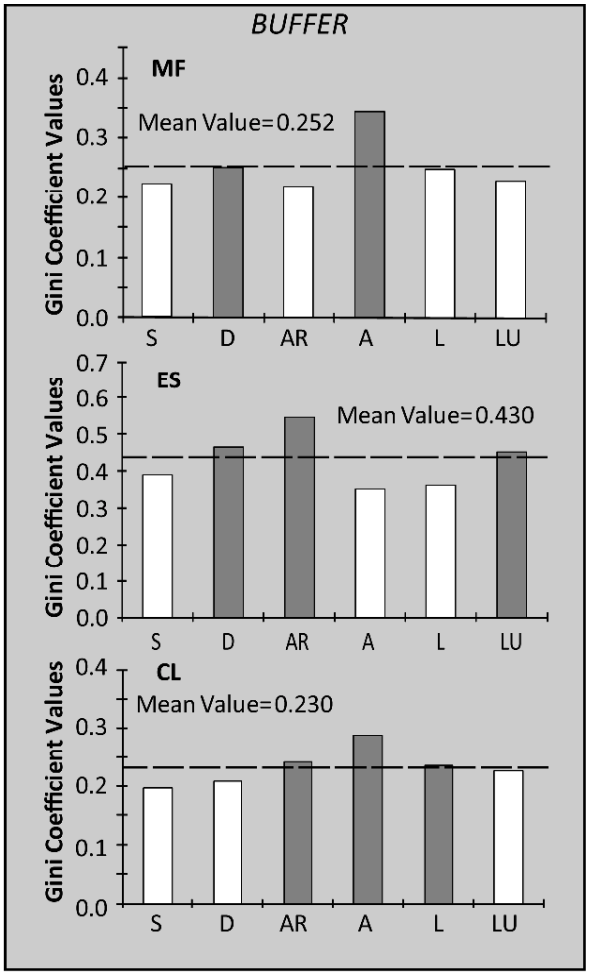

CORRELATION MATRIX

	S	AR	D	A	L	LU
S	1.00	0.48	-0.18	0.02	0.12	0.09
AR		1.00	-0.36	0.03	0.19	0.11
D			1.00	0.05	0.29	0.11
A				1.00	0.14	0.10
L					1.00	0.20
LU						1.00

FINALLY SELECTED FACTORS

CL
DEPLETION ZONE
Slope
Amplitude of Relief
Lithology
Land Use
BUFFER
Amplitude of Relief
Aspect
Lithology

ES
DEPLETION ZONE
Slope
Drainage density
Amplitude of Relief
BUFFER
Drainage density
Amplitude of Relief
Land Use

SM
DEPLETION ZONE
Drainage density
Amplitude of Relief
Aspect

MF
DEPLETION ZONE
Slope
Amplitude of Relief
Aspect
Lithology
BUFFER
Drainage density
Aspect

Fig. 7.7 - Histograms of the Gini coefficient value distribution for each landslide type obtained after the spatial intersection between each causal factor map and each landslide type map. The matrix of association/correlation degree between pairs of factors and the tables indicating the factors finally selected for each landslide type are shown.

In the case of ES, the potential influencing factors generally show higher G values (0.414 to 0.637 using depletion zones and 0.343 to 0.544 for the buffer areas). This suggests that in the study area, ES generally clustered in specific factor classes because, with respect to MF or SM, they are less closely linked to the clayey outcrops. Moreover, they are more concentrated where high values of AR occur. When considering ES buffer areas, the S factor is discarded while LU becomes very important because the outer buffer areas from the depletion zones are clustered within forests (in most cases, on slopes reforested to mitigate the effects of denudation). Together with L, also A was always discarded for this landslide type. This suggests that ES in this area are poorly linked to this terrain parameter: in fact, landslide survey of the area confirm that ES are not strictly associated with north-facing slopes (wet soil conditions), as mud flows do. Instead, they generally occur on coherent litologies, or where weaker lithologies have sandy, gravel, conglomeratic or volcanic caprocks at the hillslope summit which help in preserving high values of AR.

For CL susceptibility assessment, S, AR, L and LU were selected as causal factors when using depletion zones, while AR, A and L were selected when using buffer areas. The recurrent exclusion of D for CL is reasonable, if we consider that this landslide type usually occurs in variable conditions of permeability, lithology and rock fracturing.

The most influential factors for the SM distribution are D, AR and A, similarly to those obtained for MF, except for the S factor, which does not strongly influence the presence of this type of slope instability in the study area. This is consistent with the abundance of small mud flows within the SM type.

In the Upper Orcia Valley case, we did not need to exclude preselected factor using the correlation matrix because no more than 4 factors ever showed G values above the mean (case b2 in Fig. 7.2).

To sum up, using depletion zones for the bivariate analysis generally resulted in higher G values than using buffer areas. Moreover, the analysis performed using the buffer areas always led to the exclusion of the S factor. These facts can depend on the widespread levelling practices for agricultural purposes, which have increased starting from the seventies (thus before the occurrence of the majority of the mapped landslides). These activities tend to rapidly smooth the natural roughness of the hillslope surface, thus causing the S factor to become less variable in space and not so discriminant as a causal factor.

Conversely, landslides occurring on these surfaces generally cause S discontinuities in correspondence of the depletion zones. Moreover, D parameter can increase just after a landslide event, and then progressively decrease with time. On the other hand, L, A and AR values should not significantly change after a landslide event (if not very large).

7.6.4 Susceptibility assessment

From the intersection of the selected factor maps and the different landslide type inventories, seven vUCU maps have been drawn up: four derived from the factors selected using depletion zones, and the other three from the factors selected using buffer areas, excluding the case of SM. The number and mean extent of the vUCUs are summarized in Tab. 7.3. The further overlay of each vUCU map with the corresponding landslide map led to the processing of seven susceptibility maps, two for each landslide type (one using depletion zones, the other using buffer areas, except for SM). These maps are based on the conditional probability of each vUCU to be affected by the occurrence of a landslide type event, as shown in Fig. 7.8.

For each landslide type, the susceptibility index (S_{index}) corresponds to the conditional probability of future landslide event, given the selected number of factors. S_{index} values were classified in a suitable number of categories and we decided to use the same color scale for the seven susceptibility maps, in order to compare the obtained zonation maps and examine the relative distribution of susceptibility index values.

Landslide type	Slope instability landform	Combined factors (defining vUCUs)	Number of vUCUs	Mean extent of the vUCUs (m^2)
CL	*depletion zone*	*S, AR, L, LU*	568	207356.54
	buffer	*AR, A, L*	125	26232227.19
MF	*depletion zone*	*S, AR, A, L*	567	207722.25
	buffer	*D, A*	23	5120805.00
ES	*depletion zone*	*S, D, AR*	126	934750.12
	buffer	*D, AR, LU*	112	1051593.89
SM	*portion of hillslope affected by SM*	*D, AR, A*	93	1266435.65

Tab. 3 - Number and mean extent of the vUCUs of each susceptibility zonation described in the text.

Landslide susceptibility maps

The obtained susceptibility maps (Fig. 7.8) show the spatial probability of future landslide events for each landslide type in the study area. Most of the maps indirectly contain information on the discarded causal factors, since the performed factor selection was efficient in detecting the most discriminant factors. This is the case of the ES susceptibility map obtained using depletion zones that shows the maximum susceptibility in correspondence of outcrops of coherent lithologies on the eastern ridge of Castelluccio-Mt. Cetona ridge, even if factor L was discarded. In fact, the higher S_{index} values have been caused by a combination of D, AR and S values clearly related to the outcrop of the most coherent lithologies. Moreover D, AR and S contained an intrinsic set of additional information that allowed estimating high probability values: for example, D is strictly linked not only to the permeability of rocks but also to the presence of vegetation cover and to the spatial distribution of the mean annual rainfall. As well as for ES, also the MF susceptibility map derived from buffer areas, even if having discarded the L factor, fits well the lithological outcrop distribution: the highest S_{index} values concentrate where clay or clayey sand crop out, and particularly the town of Contignano results quite seriously prone to this type of landslide, as well as to SM. Moreover, among the clayey slopes, the northeast-facing ones are the most susceptible to MF, since they are also dip slopes.

However, the range of S_{index} values is very different for the landslides type maps, since the conditional probability values are sensitive to the number and to the extent of the map

units: in fact, the density of past landslides decreases with the increase of the vUCU area. In the case study, the MF susceptibility maps (Fig. 7.8) are characterized by low S_{index} values (< 10%), which can reflect the low lithological diversity of slopes in the study area with a clear prevalence of clay compared with the other lithologies, so that MF are likely to occur on most of the slopes. But it must be outlined that the MF area ratio within the vUCUs, and consequently the S_{index} values, were underestimated since in the study area MF are frequent and rapidly levelled by the intense agricultural activity, thus many of them were not mapped or, especially the smallest ones (not mappable at the scale 1:10,000), were placed in the SM database. Nonetheless, the maps well evidence the areas relatively most susceptible to future landslides.

The CL susceptibility map obtained using depletion zones shows not very high S_{index} values for most of the area, apart from some small regions with both clayey and quite steep slopes, where the probability reaches the 33-45% S_{index} class, located close to the western divide and in the surroundings of Mt. Calcinaio. Multivariate analysis showed that on these slopes, not only reforestation failed to curb slope instability processes, but the re-planted trees represented an overload that favored landsliding. In fact, even if replanting trees has decreased the mud flows occurrence and runoff intensity, on the other hand they represented an overload on the hillslopes that sometimes favored deeper landslides, as ES and CL. In the case of this type of landslide, the map derived from buffer areas provides less information about the most susceptible areas because the S_{index} values are in a very much narrower range (between 0 and 11%).

The SM susceptibility map confirms that A is the most influential factor for this type of landslide. In particular, SM occur mostly on the wetter north-facing slopes, then preferentially where AR and D show medium to high values. The susceptibility map for this type of slope instability process clearly show the wider extent of the higer S_{index} values, underlining that these shallow mass movements represent a serious threat for the stability of the arable and grazing lands in Upper Orcia Valley.

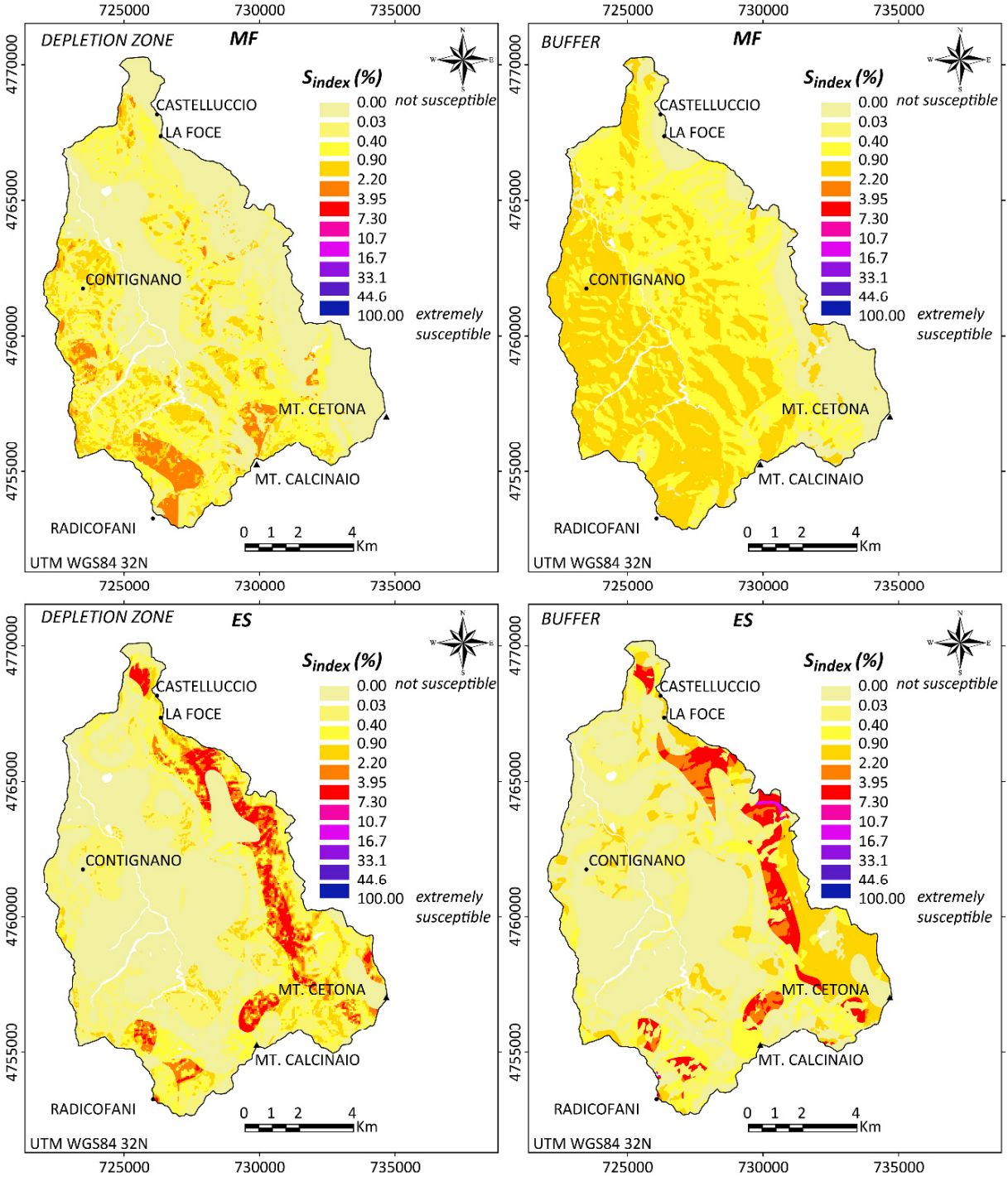
DEPLETION ZONE
MF
BUFFER
ES
S_{index} (%)
0.00 not susceptible
0.03
0.40
0.90
2.20
3.95
7.30
10.7
16.7
33.1
44.6
100.00 extremely susceptible
CASTELLUCCIO
LA FOCE
CONTIGNANO
MT. CETONA
MT. CALCINAIO
RADICOFANI
0 1 2 4 Km
UTM WGS84 32N
725000
730000
735000
4770000
4765000
4760000
4755000

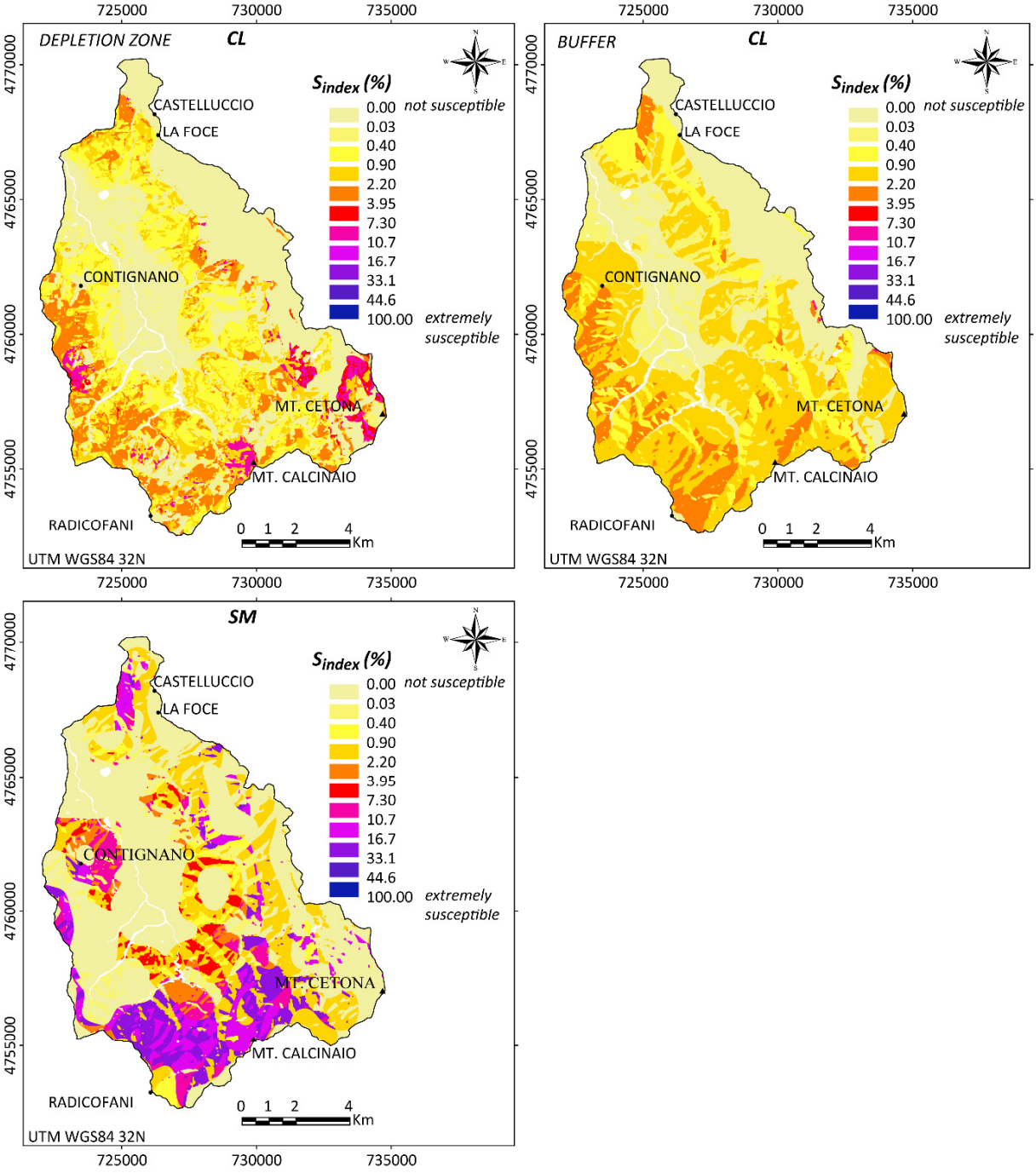

Fig. 7.8 – Susceptibility maps of the Upper Orcia Valley obtained through the conditional analysis for each landslide type. For each landslide type, the susceptibility index (S_{index}) values correspond to the conditional probability of the landslide event, given the selected number of causal factors. S_{index} values are classified in 11 intervals

7.6.5. Validation

Since the landslide inventory was created using two different sets of aerial photos (years 1988-1989 and 1994), a temporal subdivision of the dataset was made (as indicated in the table of Fig. 7.3), with the training subset containing landslides occurred before 1988 and the test subset containing landslides occurred after the same year, thus simulating an analysis performed in 1988. Validation was not performed for the SM because temporal information was not available (they were mapped after field survey). Neither a spatial partition was possible for SM, because this type of landslide includes portions of hillslopes affected by small and frequent mud flows, the latter periodically leveled by farmers and difficult to be mapped. So while the extent of these areas is considerable, their number is not high enough for a spatial partition.

The validation outlined that success-rate curves obtained from the analysis of buffer areas generally show lower initial steepness compared with the curves generated using the depletion zones (Fig. 7.9). This can be explained considering the more specific terrain conditions of the depletion zones, due to the strong modification generally determined by landslide occurrence. Moreover, the buffer areas are not always more representative of the environmental conditions preceding the landslides. In fact, some gravitational movements often occur in areas where other landslides already took place and are thus characterized by post-event terrain conditions. This is, for example, the case of new crowns developed upwards from older landslide scarps.

The best success-rate curve for MF was the one generated using the depletion zones (Fig. 7.9a). Even if the corresponding prediction-rate curve is not monotonically decreasing, its first part is considerably steep, indicating that the most hazardous 6% of the predicted area estimates the distribution of 29% of the MF that occurred within the following 20 years (after 1988). On the other hand, the prediction-rate curve generated using the buffer areas (Fig. 7.9b) indicates that the “future” landslides are well estimated within the classes 0-25% and 60-100%, so that the classes included in these intervals are effective prediction classes.

Both the success-rate curves for ES are very well shaped (their steepness smoothly decreases monotonically; Fig. 7.9c,d), while the corresponding prediction-rate curves are not so satisfying because the curve generated considering depletion zones shows a

discontinuous trend and that generated using buffer areas is not very far from the 1:1 line, indicating a certain degree of randomness in the prediction results. This finding can be explained by considering that the test subset for this type of landslide is not very large, thus producing some randomness in the probability estimation of future events occurring in the areas predicted as hazardous using the training subset. In this case, the best model should be chosen only based on the best success-rate curve, which suggests to select the map prepared using the depletion zones (steeper slope of the success-rate curve in the initial part).

The validation curves for the CL susceptibility evaluation show that the use of the depletion zone area is somewhat better than that of the buffer areas because the initial steepness of the prediction-rate curve is higher (Fig. 7.9e,f).

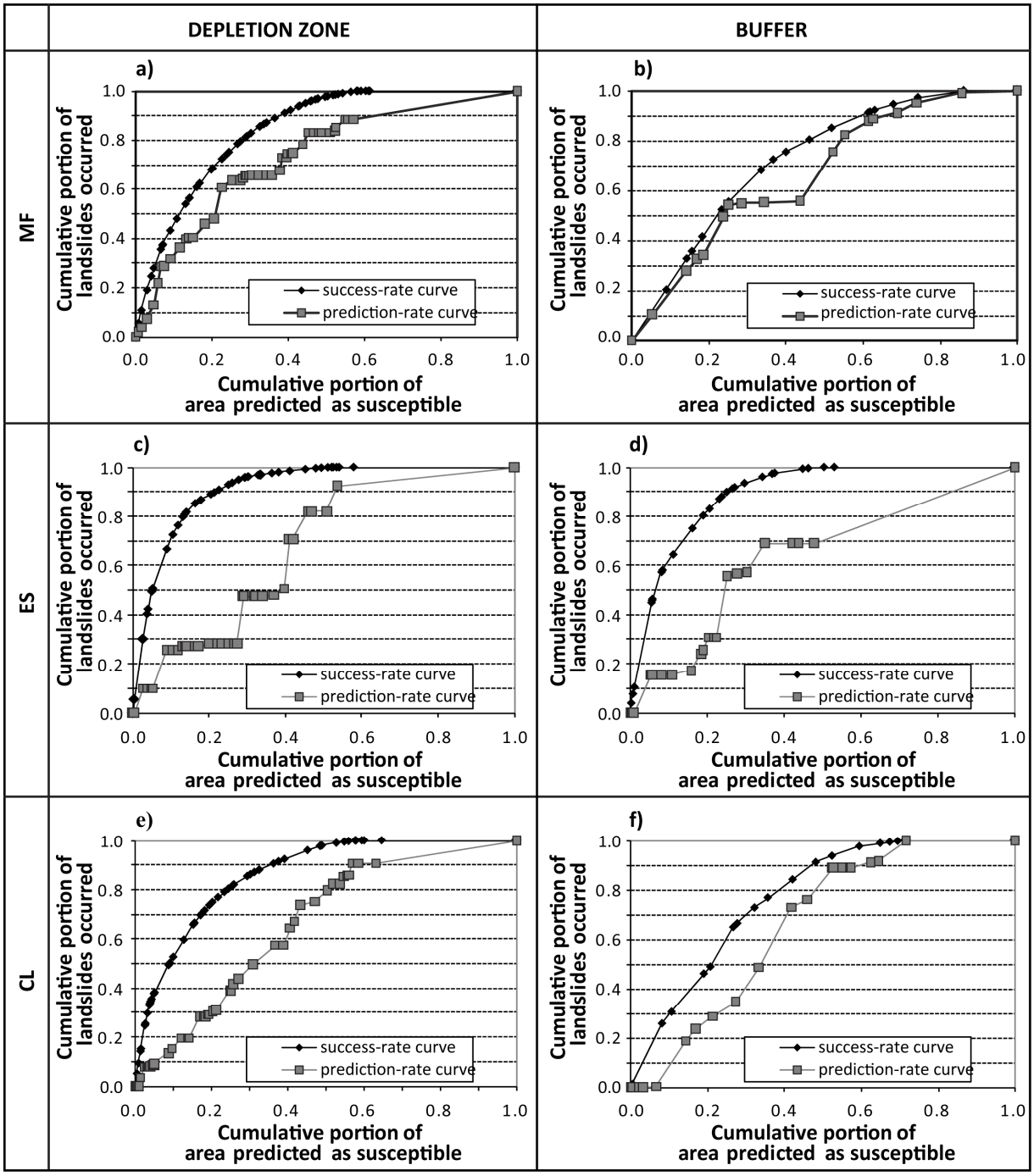

Fig. 7.9 – *Prediction-* and *success-rate curves* for mud flows, earth slumps and complex landslides, generated using the procedure proposed by Chung and Fabbri (2003) adapted for vector datasets.

7.7 Discussion

Our contribution is focused on an unbiased causal factor selection procedure when performing conditional analysis in assessing landslide susceptibility. The obtained results

confirm that the unbiased selection of controlling factors is a crucial phase for landslide susceptibility evaluation. However, in the performance of the landslide susceptibility method here presented, the following tricky problems occurred, some of which may be ascribed to our method, others affecting all statistical approaches.

First of all, both the heuristic and the statistical choice of causal factors require an *a priori* knowledge of the main causes of landsliding, as the potential factors must be not only spatially correlated with the distribution of landslides but also in cause/effect relationships with them. This can lead, sometimes, to the exclusion of variables spatially well-correlated with landslide distribution but representing a landslide effect more than a cause for landslides. For the same reason, factors that may vary in response to environmental changes or economical needs, such as land cover, should be used only if significant modification have not been observed during the time interval considered for the landslide inventory.

Once the potential factors have been correctly identified, a further constraint of a successful landslide susceptibility evaluation lies on their suitability for each study case: in fact, each causal factor can be more or less discriminant in explaining the distribution of the same landslide type events in different areas. Our procedure for factor selection provides a useful tool to filter the right set of causal factors really causing landslides in each study area. To give an example, some factors, such as lithology and slope, are the most frequently considered in the international literature on landslide susceptibility evaluation (Crozier 1984; Guzzetti et al., 1999; Irigaray et al. 1999; Fernandez et al. 2003; Ayalew and Yamagishi 2005). But in our study case, we demonstrated that they are not really effective in explaining the distribution of the occurred mud flows. In fact, clayey outcrop is the predominant lithology in the area (75%). This implies that MF buffer area distribution is not well explained by the *L* factor. On the other hand, *D* was selected (Fig, 7.5d and 7.6), since it indirectly accounts as well for geological (lithology, fracturing, permeability, etc.) and morphological (slope, shape and length of slopes, etc.) conditions characterizing the area (Strahler, 1957), thus it better explains the present MF distribution than *L*. At the same time, *S* was discarded when considering MF buffer areas. This result does not mean that *S* is out of the most important factors generally triggering landslides, but that in the study case MF are uniformly distributed on different classes of *S* (Fig. 7.6) as confirmed by field surveys.

To sum up, the applied susceptibility evaluation procedure is useful in filtering, among the potential factors, the ones really discriminant in inducing future landslides for a given study area, especially when this is poorly known. At the same time, it allows limiting the number of factors to be used in conditional analysis, thus avoiding generating too small and diverse map units. In fact the smaller are the map units, the less the landslide probability will be statistically significant, for the same landslide inventory. Moreover, the factor selection method, if combined with the study of correlation between independent variables, does not bring to the loss of information, since the discarded factors are often indirectly accounted for by other variables, as demonstrated by the exclusion of *L* in ES susceptibility analysis.

Some sources of uncertainty were detected in the model performance, but most of them are common to all the landslide susceptibility statistical models. First of all, the quality of the analysis strongly depends on the quality and resolution of the input data (landslide inventory and causal factor maps) and of their representation in GIS environment. Landslide identification and mapping is an error prone procedure, due to the scale-dependent minimum mappable unit, to the lack of historical data and to the degree of agricultural exploitation of slopes. In the study case, for example, the quality of mud flow inventory affected the landslide susceptibility assessment: in fact the area affected by mud flows in the map units, and consequently the calculated *susceptibility index*, were surely underestimated since in the study area MF are frequently and rapidly levelled for the intense agricultural activity. In cases like this, a possible solution for improving the results could be the introduction of a wider set of potential causal factors when applying our selection procedure, in order to search for factors with higher *G* values. Moreover, future outcomes could entail the use of some statistical procedure to associate an error to prediction results.

Another tricky step for a successful susceptibility evaluation is the choice of the features to be used to represent the occurred landslides in the inventory. The performed validation suggested some interesting remarks about the advisability of using either depletion zones or outer buffer areas from depletion zones as representative of the landslides. More precisely, the results underlined that the choice is delicate since, on one hand, buffer zones are more representative of the conditions that preceded the landslide occurrence, but, on the other hand, some gravitational movements can reactivate some previously occurred ones. From this perspective, the obtained validation curves did not allow

performing a unique choice for the study area. To this end, a possible development could involve the detection (and separate analysis) of the re-activated landslides.

7.8 Conclusion

The landslide susceptibility of the Upper Orcia Valley was evaluated through an unbiased factor selection procedure, followed by conditional analysis. The assessment was performed for the most frequent landslide types and considering separately the landslides depletion zones and the outer buffers from depletion zones. Different causal factors were proved to have influence on each landslide type. Conditional analysis allowed the zonation of conditional probability of future landslide occurrence (S_{index}). A validation procedure was finally applied, in which a temporal subdivision of landslide inventory was performed. The results confirmed the efficiency of the selection procedure, which allowed using few causal factors without losing information on the indirect influence of the discarded ones. Even so, the applied susceptibility assessment methodology is affected by some sources of uncertainty, in particular those generally associated with all the statistical approaches, for which the quality of the result is strongly sensitive to quality of the input data.

In conclusion, the conditional analysis, preceded by a bivariate statistical analysis for causal factor selection, provided satisfactory results for the unbiased prediction of landslide susceptibility for the Upper Orcia Valley. The method is conceptually simple but, at the same time, effective in evaluating the conditional probability of hazardous events given a certain combination of causal factors. Even if the knowledge of the study area in an important precondition for successful susceptibility analysis, the proposed factor selection procedure proved to be a useful tool for the unbiased detection of the factors really discriminant for landslides in the study area, and can be very helpful when analyzing new areas. This procedure allowed us to overcome one of the limits of the conditional analysis, which consists in the lack of statistical significance of too small vUCUs generated by the intersection of a large number of subjectively defined influencing factors. The factor selection procedure here proposed differs from others already suggested in the literature,

which provide for selecting the most significant factors after having computed all of their possible combinations and having tested the results. Our factor selection method makes the susceptibility analysis less cumbersome and simplifies the entire procedure, since it provides for using simple statistical indices. Moreover the use of vector datasets allow to create vector easy-to-read susceptibility maps, in which the fragmentation generally characterizing raster outputs is avoided. These characteristics make this susceptibility method easy to be understood and each resulting map easy to be read, thus suitable for policy makers in planning land management strategies.

8. WATER EROSION HAZARD OF UPPER ORCIA VALLEY

In this section, a water erosion hazard evaluation method is proposed, as a result of the application and the widening of the monitoring and estimation techniques applied in the study areas, described in the previous sections.

In fact, the multivariate statistical approach, based on conditional analysis, has been applied to evaluate water erosion hazard of Upper Orcia Valley: the susceptibility evaluation method described in § 7 (Vergari et al., 2011) was combined with the Tu denudation index method, validated in § 6 by means of direct monitoring data, in order to assess erosion hazard, in terms of both spatial and temporal probability of the occurrence of water erosion effects (in particular, the occurrence of *calanchi* badland erosion).

Similar attempts to identify areas prone to soil erosion were carried out in previous works (Märker et al., 1999; Conoscenti et al., 2008a, Conforti et al., 2011, Agkun and Turk, 2011), but they were aimed at assessing soil erosion susceptibility, since they evaluated the spatial probability of erosion landforms occurring in the future, not considering the related erosion intensity.

8.1 Material and methods

In this work, the susceptibility evaluation method described in § 7 has been applied to the denudation landforms due to runoff, *calanchi* badland areas, in order to evaluate the water erosion spatial proneness of the study area. The so evaluated spatial prediction was associated to a temporal prediction, using the Tu grid analysis described in § 6, which estimates erosion rates well, as verified by erosion direct measurements in the study area, thus, obtaining the hazard assessment. In particular, knowing the drainage density of areas presently affected by *calanchi* badlands (Fig. 8.1), the computed estimated erosion rate was associated to areas identified as prone to the occurrence of badland erosion.

As potential erosion causal factors, 8 parameters have been considered (Fig. 8.2): altimetry, amplitude of relief, aspect, slope curvature, drainage density, lithology, slope gradient and stream power index. A DEM with a resolution of 25 m was used to derive the topographic factors. The output raster layers were then aggregated in to 50m cell-sized grids, in order to avoid the excessive vUCU fragmentation and to reconstruct the average slope conditions, as the terrain conditions preceding the instability events should be considered for a well-structured susceptibility analysis (see § 7.1).

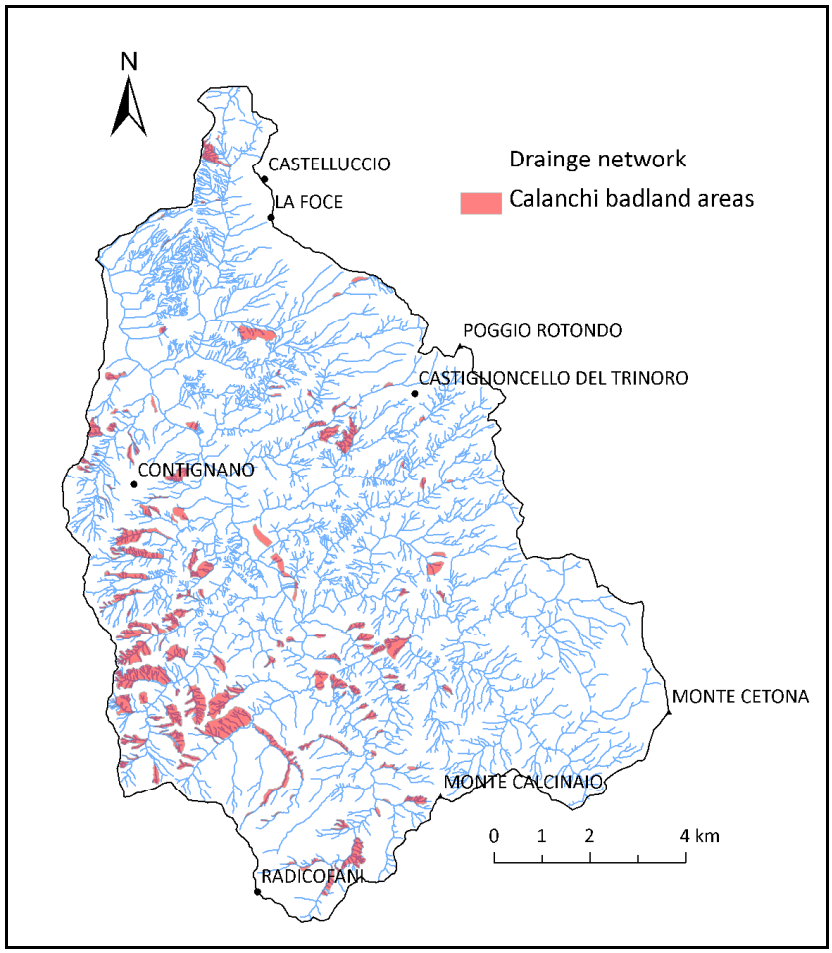

Fig. 8.1 – *Calanchi* badlands areas overlaid to the drainage network map of Upper Orcia Valley.

Amplitude of relief (Fig. 8.2b), slope aspect (Fig. 8.2d), drainage density (Fig. 8.2e), lithology (Fig. 8.2f) and slope (Fig. 8.2g) maps were also used to evaluate Upper Orcia Valley landslide susceptibility (see § 7.6 for details).

Altimetry (Fig. 8.2a) was considered in order to investigate the possible concentration of badland areas in particular elevation intervals.

Slope curvature was investigated with respect to its effect on badland triggering and development (Fig. 8.2c). The term curvature is theoretically defined as the rate of change of slope gradient or aspect, usually in a particular direction (Wilson and Gallant 2000). The curvature of the surface is computed on a cell-by-cell basis, as fitted through that cell and its eight surrounding neighbours. Curvature is the second derivative of the surface or the slope of the slope. Positive values of curvatures define convexity, negative values of curvatures characterize concavity of slope curvature. Values of curvatures around zero indicate that the surface is flat.

The stream power index (SPI) (Fig. 8.2h) is a measure of the erosive power of water overflow based on the assumption that discharge is proportional to the specific catchment area (As) (Moore et al. 1991). The map was carried out by applying the following formula to each cell, using Raster Calculator in ArcGIS:

$$SPI = \ln [AS \times \tan(S)]$$

where As is the specific catchment area in meters and S is the slope gradient in degrees. For cells in which the slope is 0%, NoData was substituted with 0 SPI value in the output raster.

The index SPI is one of the main factors controlling slope erosion processes, since erosive power of running water directly influences slope toe erosion and river incision (Nefeslioglu et al. 2008). It is also indicative of the potential energy available to entrain sediment, so that areas with high stream power indices have a great potential for erosion (Kakembo et al. 2009)

Each factor thematic map were converted in vector layers and then overlaid to the mapped badland areas, in order to investigate the distribution of *calanchi* areas within the different classes of the potential causal factor and identify the factors with no homogeneous distribution. To this end, Lorenz curves and Gini coefficient were computed.

Intersecting the selected causal factors, vUCUs have been identified and delimited, and for vUCU the conditional probability of badland erosion occurrence given the selected factors was computed using formula described in § 7.4.

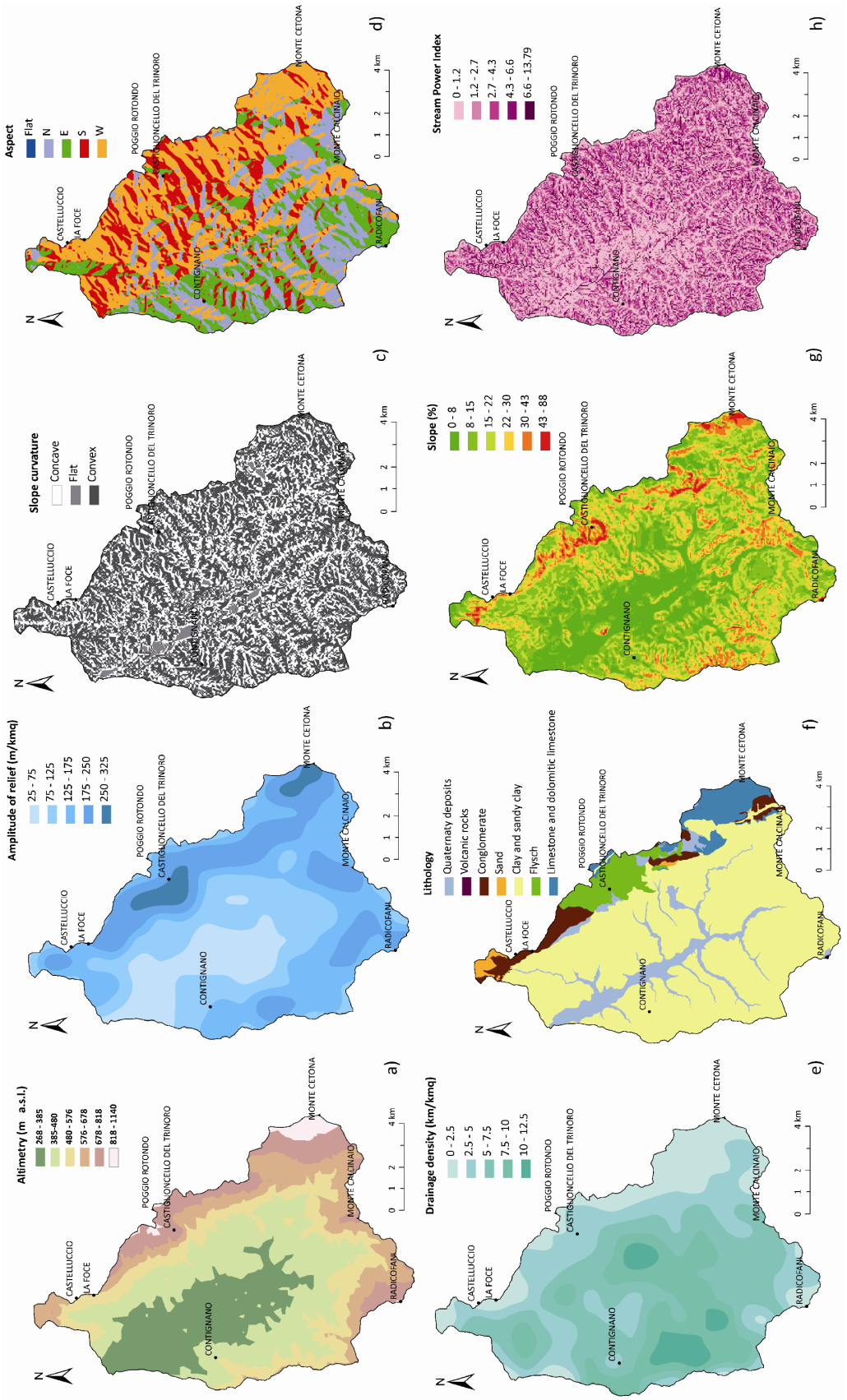

Fig. 8.2 – Potential causal factors considered in the water erosion hazard evaluation of Upper Orcia Valley: a) altimetry, b) amplitude of relief, c) slope curvature, d) aspect, e) drainage density, f) lithology, g) slope, h) stream power index.

8.2 Results

For the study area, the drainage density value for the only *calanchi* badland areas is very high (16,62 km/km^2), and corresponds to an average erosion rate higher than 2 cm/a. This value agree with magnitude order of erosion rates measured at *calanchi* badlands sites of central Italy (§ 2, Della Seta et al., 2009, Vergari et al., submitted a).

The estimated *calanchi* badland denudation intensity represent the present erosion rate of surveyed badland areas in the Upper Orcia Valley (Fig. 8.1). For this reason, in the water erosion susceptibility evaluation the inventory map was not only a spatial representation of badland erosion, but also an estimation of the denudation intensity, thus used to evaluate not the water erosion susceptibility, but the water erosion hazard.

The most influential causal factors in determining water erosion effects were selected applying the factor selection procedure described in § 7.3. Fig. 8.3 shows the Lorenz curves for the considered 8 potential cusal factors, computed after the intersection of the badland inventory map with each of factor maps.

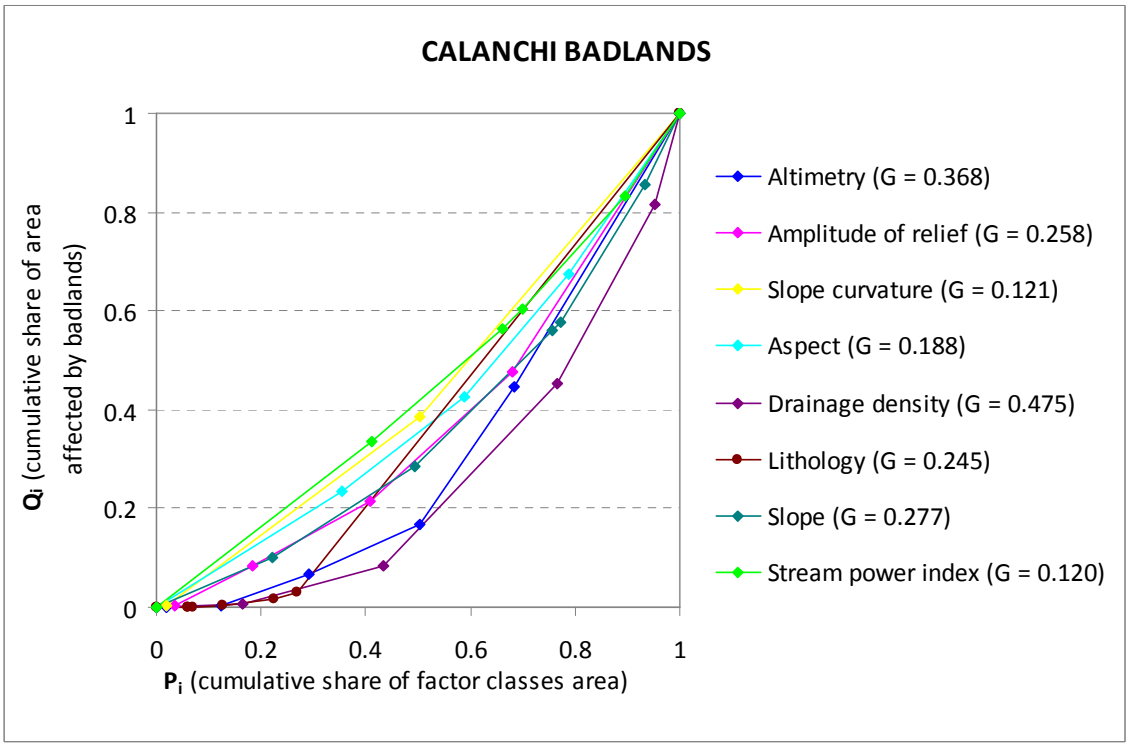

Fig. 8.3 – Lorenz curves for the considered potential causal factors. The Gini coefficient values are shown for each factor.

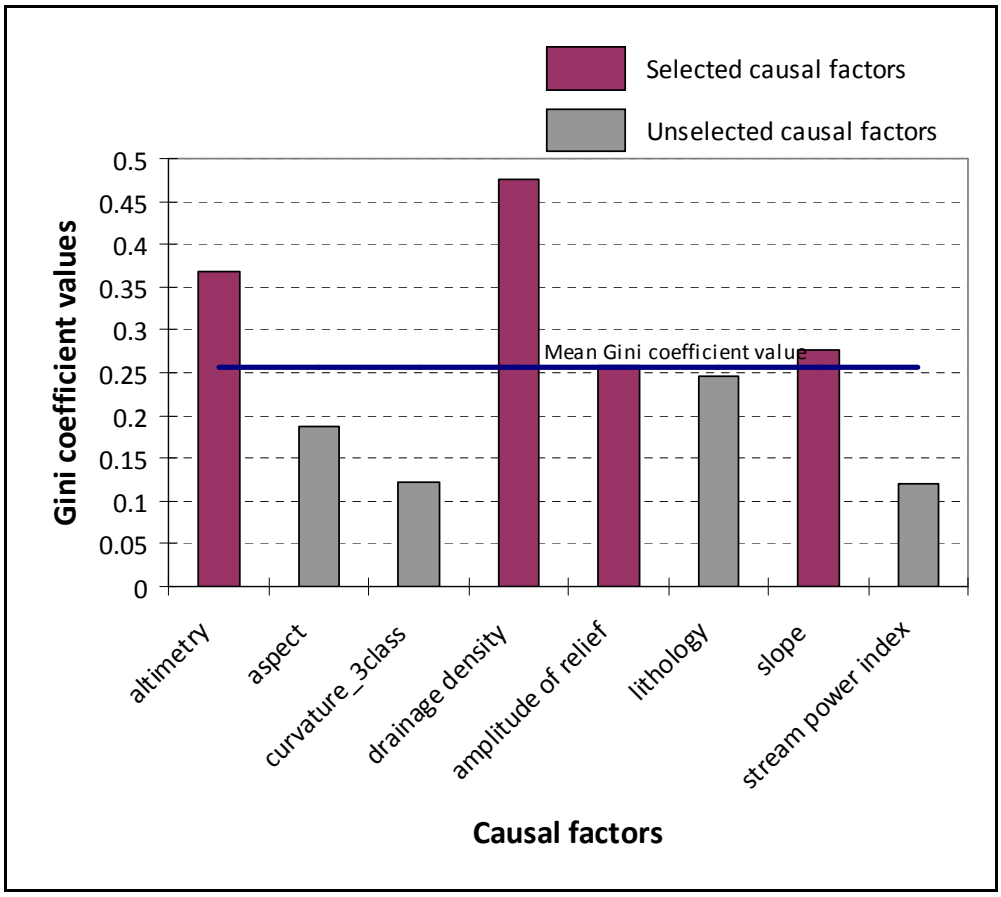

Fig. 8.4 – Histogram of Gini coefficient value distribution of *calanchi* badland areas in each potential causal factor map.

Altimetry, drainage density, amplitude of relief and slope are the selected factors.

The causal factor most important in discriminating areas affected by badland erosion is drainage density, as high values of D identify areas where overland flow is favoured and runoff increase. Altimetry is the second most important factor, since most of *calanchi* areas are widespread up to 700 m a.s.l.. This is also the maximum elevation of clayey outcrops in the study area, while at higher altimetry values other more resistant lithologies are found (Fig. 8.2 a and f). This means that even if lithology was discarded, the information provided by the lithology map is still beheld in the model. As for slope and amplitude of relief, *calanchi* badlands are concentrated in medium slope gradient values (15 – 40%) and in 100 – 200 km/km^2 amplitude of relief interval. Higher amplitude of relief values characterize, in fact, the eastern part of the study area, where calcareous outcrops prevail.

By intersecting the selected causal factors, the water erosion hazard map was carried out (Fig. 8.5). In the map, the hazard values represent the conditional probability of the occurrence of *calanchi* badland erosion with a water erosion rate higher than 2 cm/a. Hazard values were classified in 5 hazard classes of increasing hazard level. Highest hazard values are located in the western sector of the study area, where clayey outcrops are characterized by the very high slope gradient. Many of these areas are totally presently affected by badlands (very high hazard class), but in this sector a wider land is very prone to water erosion, and the development of badland is frequently restrained by the agricultural land remodelling practices. The performed hazard analysis outlines that in more natural conditions, in these areas, badlands could rapidly develop, together with the estimated very high water erosion entity.

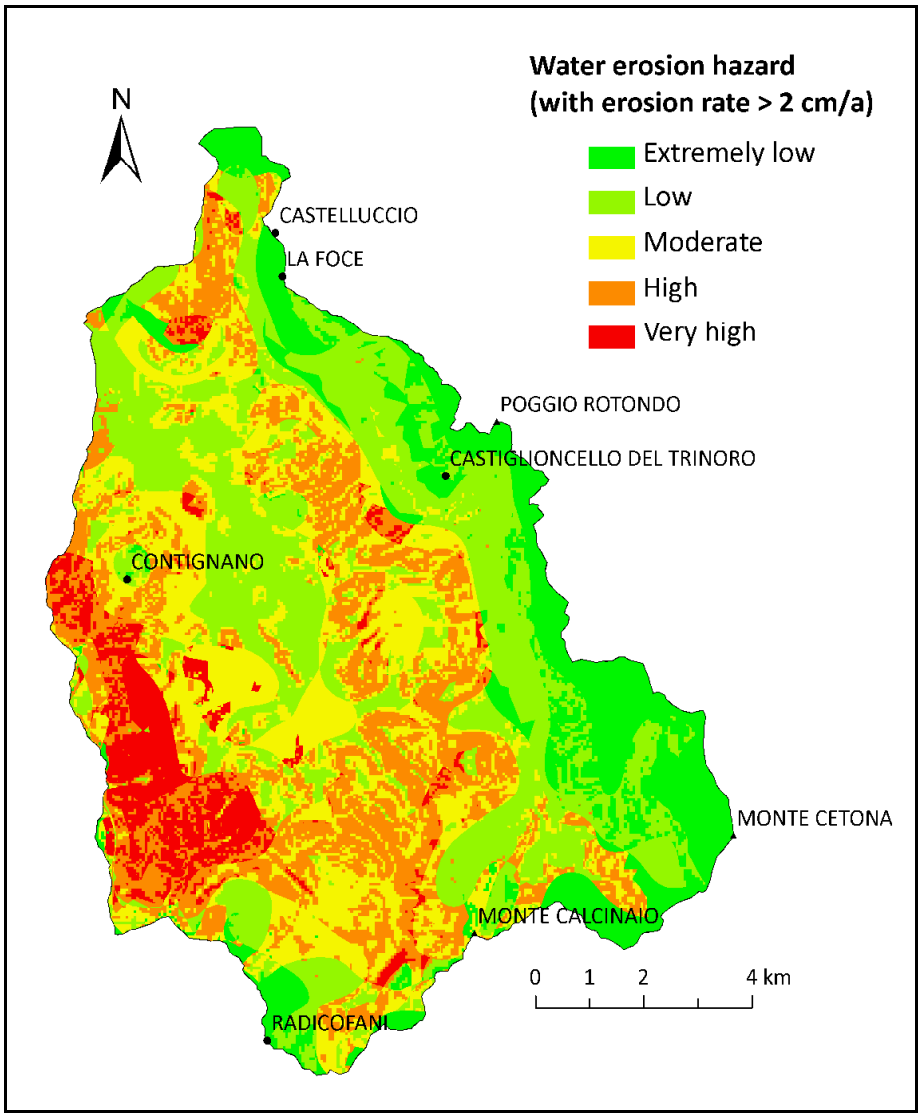

Fig. 8.5 – Water erosion hazard map of Upper Orcia Valley.

DISCUSSION AND CONCLUSIONS

This Ph.D. research project have allowed to define an integrated methodology for denudation intensity estimation and prevision, in areas greatly affected by badlands. The method is based on both quantitative geomorphic analysis and multivariate statistical investigations, in order to better define the relationships between the main denudation effects and the potential causal factors favoring geomorphological instability in badlands areas. A statically based method for water erosion hazard assessment has been proposed (Fig. 9.1), conceived as a spatially distributed prevision of *calanchi* badlands, and associated erosion rate, occurrence. Direct measures of erosion intensity in badlands were used to validate the results of water erosion estimates and previsions.

The proposed geomorphological hazard assessment procedure is appropriate to perform previsions of different types of instability process, such as landsliding, water erosion and flooding. In fact, remaining valid the spatial prevision procedure (susceptibility evaluation method described in §7), when evaluating geomorphological hazard due to processes different from water erosion, the temporal prediction is feasible statically estimating return periods of extreme instability events of a certain intensity, based on a temporal dataset of past events. Temporal datasets are generally more easily available for floods, while landslide hazard zoning may not be practical, since a sufficiently accurate quantitative assessment of landslide frequency is often not possible. In these cases a qualitative system of describing landslide hazard classes may be adopted (Fell et al., 2008).

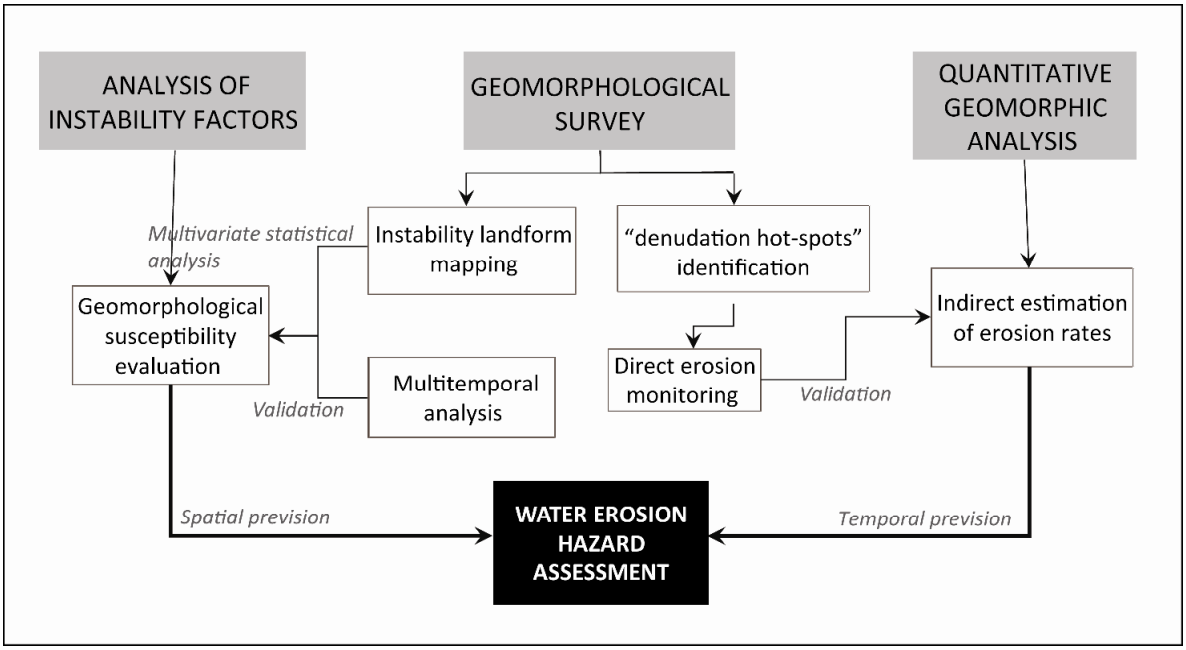

Fig. 9.1 – Concept map of the proposed water erosion hazard evaluation method.

A synthetic description of the main results of this thesis, together with a related discussion, are here reported.

***Tu* denudation index** (Ciccacci et al., 1981,1986) was confirmed to be a good estimator of the suspended sediment yield (SSY) for catchments characterized by the prevalence of sedimentary and weakly coherent outcropping litologies. The improvement of the regression relations contributed to better estimate sedimentary output for catchment widely affected by badland areas. In these basins, in fact, SSY is strongly correlated to the areal ratio affected by badlands to the total catchment area. Thus, using the not-projected drainage density parameter (D_{3d}), instead of the traditional D parameter, even if not improving the SSY estimation for large basins, was considered to better reflect the conditions predisposing erosions than D for smaller catchments, where large *calanchi* badlands and related high slope gradients are present. The dominant role of drainage density in estimating erosion rate for badland areas, parameter that contribute to identify *calanchi* on topographic maps together with contour lines crenulation (Farabegoli and Agostini, 2000), was confirmed by the attempt of zoning the estimated erosion rates using the *Tu* Grid Analysis. This attempt proved to be very efficient in estimating the erosion rate due to runoff within badland areas, as confirmed by the comparison between the estimated and the measured erosion rates. This result seems to increase the prospective of using Tu grid analysis when prolonged

denudation monitoring is not possible. Moreover, even where punctual erosion rates are measured by pin monitoring, the estimated erosion rate map represents a validated continuous representation of water erosion rate for larger areas.

Geomorphological susceptibility, assessed by the use of conditional analysis, and preceded by the proposed new procedure for causal factor selection, provided satisfactory results for the unbiased prediction of landslide and water erosion susceptibility for the Upper Orcia Valley. The method is conceptually simple but, at the same time, effective in evaluating the conditional probability of hazardous events given a certain combination of causal factors. Even if the knowledge of the study area in an important precondition for successful susceptibility analysis, the proposed factor selection procedure has proved to be a useful tool for the unbiased detection of the factors really discriminant for instability landforms in the study area, and can be very helpful when analyzing new areas. This procedure has allowed to overcome one of the limits of the conditional analysis, which consists in the lack of statistical significance of too small vUCUs generated by the intersection of a large number of subjectively defined influencing factors. The factor selection procedure here proposed differs from others already suggested in the literature, which provide for selecting the most significant factors after having computed all of their possible combinations and having tested the results. Our factor selection method makes the susceptibility analysis less cumbersome, since it provides for using simple statistical indices. Moreover the use of vector datasets allow to create vector easy-to-read susceptibility maps, in which the fragmentation generally characterizing raster outputs is avoided. These characteristics make this susceptibility method easy to be understood and each resulting map easy to be read, thus suitable for policy makers in planning land management strategies.

The association of the estimated erosion rate for *calanchi* badland areas to the surveyed landforms allowed to use the susceptibility method to evaluate the **water erosion hazard**, since the temporal information about the erosion processes was related to the spatial data. This procedure is proposed to be applicable when direct erosion rate measures are not available.

Direct measurements of erosion intensiy were primarily used to validate the water erosion estimates and previsions, being these the main scope of this research. Even though, interesting observations have been concluded on the applicability of various methods of erosion monitoring (Tab. 9.1).

The size of the study area, the time available, and the quality of the data required are perhaps the most critical issues to be considered when looking for the most appropriate technique. As well-known, the traditional **erosion pin method** generally allows to carry out very accurate punctual measures, whose error is measurable in few millimeters. So, it can be used to quantify very detailed temporal variations (monthly or after-event ground level changes). On the other hand, **DGPS survey** can be proper when a single hillslope of less than few hectares is being monitored, as the time and effort required would be acceptable. For larger areas or wider time interval, high resolution **photogrammetric analysis** could be more appropriate.

However, all these methods are affected by some limitations (Tab. 9.1). Punctual erosion pin data certainly cannot be representative of large areas. On the other hand, GPS accuracy is affected by many sources of inaccuracy, caused by the satellite position geometry, the multipath effect, the atmospheric effect and clock inaccuracy. Measures perfomed at Bargiano hillslope by means of DGPS survey were affected by a mean elevation error of a less than 3 centimeters. This order of magnitude can be assumed as an acceptable error for the purpose of the DGPS survey of Bargiano site, since metric variations of ground level were recorded for 30-years time-interval. Aerial image resolution and quality, errors caused by the data interpolation in DEM constructing phase instead affect photogrammetric analysis. Moreover, the obtained DEMs should be cleaned by the vegetation cover differences in height between the considered time span, in order to compute a more accurate erosion rate. Thus, rates computed from photogrammetric analysis should be used only in very large time interval analysis (at least some decades).

METHOD	Application scale	Measure error	Limitations
Erosion pins	Punctual measures; monthly variations	mm	Limited representativeness at catchment scale
D-GPS survey	Hillslope scale; annual variations	cm	Time of survey
Digital photogrammetric analysis	Small catchment or hillslope scale; decadal variations	dm	Photogram resolution, accuracy of DEM interpolation phase, vegetation cover

Tab. 9.1 – Applicability and limitations of different methods for erosion rate quantification.

Finally, new data and conclusions allowed to improve the knowledge of the **physical factors causing the initiation and the development of different water erosion landforms** in the studied badland areas.

Comparison of pluviometric data and measured ground level variations for Bargiano site has highlighted that clay removal by water erosion is generally due to intense rainfall event preceded by quite long dry periods, while accumulation (due to gully banks collapsing) is favoured by intense rainfall after a certain number of rainy days (frequent in spring). Moreover, in inter-rill position, where almost the lonely water erosion acts, intense events are significantly more effective than long events.

Considering the distribution of *calanchi* and *biancane* landforms of Upper Orcia Valley among the different classes of the main topographic and physiographic factors, it is a matter of fact that *calanchi* badlands develop on steeper slopes and where higher values of amplitude of relief occur, due to the morphoevolutionary processes. Moreover, observations on present embryonic *biancane* of Lucciolabella site confirm the leading role played by reticular systems of joints in the dissection of original, gently-dipping surfaces. Actually, a resolute difference on dispersivity level of the *biancana* samples of La Piaggia subcatchment was not found with respect to *calanchi* badlands samples of the same subcatchment.

On the other hand, a significant influence of clay properties was observed on the different erosion rates measured during decadal monitoring investigations by means of erosion pins in the study area. *Calanchi* badlands show lower erosion rates due to surface runoff. The major facility of *biancane* clays to be entrained at very low stream powers is reflected in their major dispersivity, while, in badlands, the morphoevolution and sediment removal is predominantly caused by widespread mudsliding from the rill and gully heads, as

also confirmed by the mean positive variations of ground level recorded at some *calanchi* monitoring stations. This observation can be also related to the higher sand content in *calanchi* badlands, which may favour the infiltration processes to the detriment of runoff.

As already observed by several authors, the agricultural exploitation of these lands lead to a decrease of exchangeable cations concentration (and, thus, clay dispersivity), even if the permanent inhibition of chemical dispersion due to increase of soil stability hypothesized by Phillips (1998) cannot be completely agreed. Decadal monitoring and observation in the study area and in other sites of central Italy (Della Seta et al., 2007, 2009) and the investigations conducted in Bargiano site have outlined that badlands initiation is even enhanced by agricultural manipulation: grazing and farming are among the most important triggers for accelerated water erosion, and tillage erosion has been recognized as an increasing factor of water erosion (Torri et al., 2002).

In conclusion, the performed investigations have allowed to conclude some interesting remarks about both the applied and proposed methodologies and the studied areas and related processes. In particular, results from this research have contributed to improve some methods useful to deepen the knowledge of processes and denudation intensity acting in badland areas of Mediterranean drainage basins.

REFERENCES

Acocella, V., Rossetti, F., 2002. The role of extensional tectonics at different crustal levels on granite ascent and emplacement: an example from Tuscany (Italy). Tectonophysics 354, 71–83.

Agnesi, V., Cappadonia, C., Conoscenti, C., 2007. Carta geomorfologica del bacino idrografico del Rio Spinasanta e note illustrative (Sicilia Centro-Settentrionale) Naturalista sicil., S. IV, XXXI (3-4), 127-145.

Agterberg, F. P., 1974. Geomathematics. Mathematical background and geo-science applications. Elsevier Scientific Pub. Co, Amsterdam, New York.

Akgün, A., Türk, N., 2011. Mapping erosion susceptibility by a multivariate statistical method: A case study from the Ayvalık region ,NW Turkey. Computers &Geosciences 37, 1515–1524.

Aleotti, P., Balzelli, P., De Marchi, D., 1996. Le reti neurali nella valutazione della suscettibilità da frana. Geologia Tecnica Ambientale 5(4):37–47.

Alexander, D.E., 1980. I calanchi, accelerated erosion in Italy. Geography 65 (2), 95–100.

Alexander, D.E., 1982. Difference between “calanchi” and “biancane” badlands in Italy. In: Bryan, R., Yair, A. (Eds.), Badlands Geomorphology and Piping. Geobooks, Geoabstracts, Norwick. 408 pp.

Ambrosetti, P., Carboni, M.G., Conti, M.A., Costantini, A., Esu, D., Gandin, A., Girotti, O., Lazzarotto, A., Mazzanti, R., Nicosia, U., Parisi, G., Sandrell, F., 1979. Evoluzione paleografica e tettonica nei bacini tosco-umbrolaziali nel Pliocene e nel Pleistocene inferiore. Mem. Soc. Geol. It., 19, 573-580.

Atkinson, P.M., Massari, R., 1998. Generalized linear modeling of susceptibility to landsliding in the central Apennines, Italy. Computers and Geosciences 24, 373–385.

Aucelli, P.P.C., Baldassarre, M.A., Conforti, M., Della Seta, M., Rosskopf, C.M., Scarciglia, F., Vergari, F., 2010. Assessment of present morphodynamics and related erosion rates by means of direct erosion monitoring and digital photogrammetric analysis: the case study of the Upper Orcia Valley (Tuscany, Italy). Proceedings of the 1st Italian-Russian Workshop on Water Erosion “Slope processes and matter movement”, Moscow, 2010, Faculty of Geography of the MSU, 2010, 96 p.

Avena, G.C., Lupia Palmieri, E., 1969. Analisi geomorfica quantitativa. In: Idrogeologia dell’Alto bacino del Liri (Appennino Centrale). Geologica Romana VIII, 319-378.

Avena, G.C., Giuliano, G., Lupia Palmieri, E., 1967. Sulla valutazione quantitativa della gerarchizzazione ed evoluzione dei reticoli fluviali. Boll. Soc. Geol. Ital. 86, 781–796.

Ayalew, L., Yamagishi, H., 2005. The application of GIS-based logistic regression for landslide susceptibility mapping in the Kakuda-Yahiko Mountains, Central Japan. Geomorphology, 65(1-2), 15-31, doi:10.1016/j.geomorph.2004.06.010.

Baeza, C., Corominas, J., 2001. Assessment of shallow landslide susceptibility by means of multivariate statistical techniques. Earth Surf Proc Land, 26, 1251–1263.

Baldi, P., Bellani, S., Ceccarelli, A., Fiordalisi, A., Squarci, P., Taffi, L., 1994. Correlazioni tra le anomalie termiche ed altri elementi geofisici e strutturali della Toscana meridionale. Stud. Geol. Camerti 1, 139–149.

Barazzuoli, P., Guasparri, G., Salleolini, M., 1993. Il clima, In: La storia naturale della Toscana meridionale, Monte dei Paschi di Siena, Amilcare Pizzi Ed., pp. 141-171.

Barberi, F., Buonasorte, G., Cioni, R., Fiordalisi, A., Foresi, L., Iaccarino, S., Laurenzi, M.A., Sbrana, A., Vernia, L., Villa, I.M., 1994. Plio-Pleistocene geological evolution of the geothermal area of Tuscany and Latium. Mem. Descr. Carta Geol. d'It. 49, 77–134.

Battaglia, S., Leoni, L., Sartori, F., 2002. Mineralogical and grain size composition of clays developing calanchi and biancane erosional landforms. Geomorphology 49, 153–170.

Battaglia, S., Leoni, L., Rapetti, F., Spagnolo, M., 2011. Dynamic evolution of badlands in the Roglio basin (Tuscany, Italy). Catena 86, 14–23.

Beasley, D.B., Huggins, L.F., Monke, E.J., 1980. ANSWERS—a model for watershed planning. Trans Am Soc Agric Eng 23, 938–944.

Bellotti, P., Valeri, P., 1975. Un cilindro di sedimentazione per l'analisi granulometrica delle siltiti e delle argille. Geol. Tecn. 2, 72-76.

Bennett, J.P., 1974. Concepts of mathematical modelling of sediment yield. Water Resources Research 10, 485–492.

Bertini, E.G., Cameli, G. M., Costantini, A., Decandia, F. A., Di Filippo, M., Dini, I., Elter, F. M., Lazzaretto, A., Lotta, D., Pandeli, E., Sandrelli, F., Toro, B., 1991. Struttura geologica fra i monti di Campiglia e Rapolano Terme (Toscana meridionale): stato attuale delle conoscenze e problematiche. St. Geologici Camerti, vol. spec., 1, pp. 155-178.

Betts, H.D, DeRose, R.C., 1999. Digital elevation models as a tool for monitoring and measuring gully erosion. International Journal of Applied Earth Observation and Geoinformation 1, 91–101.

Biasini, A., Salvatore, M.C., 1993. Fotogrammetria digitale e cartografia glaciologica. Atti Ticinensi di Scienze della Terra, Pavia 113–119.

Biasini, A., Salvatore, M.C., 1995. Fotorestituzione digitale della linea di riva: area campione del delta tiberino. Il Quaternario 8 (1), 263–266 (Napoli).

Boardman, J., Parsons, A.J., Holland, R., Holmes, P.J., Washington, R., 2003. Development of badlands and gullies in the Sneeuberg, Great Karoo, South Africa. Catena 50, 165– 184.

Bonham-Carter, G.F., Agterberg, F.P. and Wright, D.F., 1989. Weights of evidence modelling: a new approach to mapping mineral potential. In: Statistical Applications in the Earth Sciences, F.P. Agterberg and G.F. Bonham-Carter, Geological Survey of Canada, 171-183.

Borselli, L., Torri, D., Øygarden, L., De Alba, S., Martı´nez-Casasnovas, J. A., Bazzoffi, P., Jakab, G., 2006. Land Levelling. In: Poesen, J., Boardman, J. (Eds.), Soil and Gully Erosion in Europe. Wiley and sons, Chichester, 643-658.

Bosi, C., Dramis, F, Gentili, B., 1985. Carte geomorfologiche di dettaglio ad indirizzo applicativo e carte di stabilità a base geomorfologica. Geologia Applicata ed Idrogeologia, 20(2), 53-62.

Brabb, E. E., 1984. Innovative approaches to landslide hazard mapping. In: Proceedings of the 4th International Symposium on Landslides, Toronto.

Brath, A., Castellarin, A., Montanari, A., 2002. Assessing the effects of land-use changes on annual average soil losses. Hydrology and Earth Systems Sciences 6(2), 255–265.

Bryan, R. B., Harvey, L. E., 1985. Observations on the Geomorphic Significance of Tunnel Erosion in a Semi-Arid Ephemeral Drainage System. Geografiska Annaler, Series A, Physical Geography, vol. 67 (3/4), 257-272.

Bryan, R.B., Poesen, J., 1989. Laboratory experiments on the influence of slope length on runoff, percolation and rill development. Earth Surface Processes Landforms 14, 211–231.

Bryan, R., Yair, A., 1982. Perspectives on studies of badland geomorphology. In: Bryan, R., Yair, A. (Eds.), Badland geomorphology and piping. Geobooks pp. 1–12.

Buccolini, M., Gentili, B, Materazzi, M., Aringoli, D., Pambianchi, G., Piacentini, G., 2007. Human impact and slope dynamics evolutionary trends in the monoclonal relief of Adriatic area of central Italy. Catena 71, 96–109.

Calvo-Cases, A., Harvey, A.M., 1996. Morphology and development of selected badlands in southeastern Spain: implications on climate changes. Earth Surface Processes and Landforms 21, 725–35.

Calzolari, C., Ungaro, F., 1998. Geomorphic features of a badland (biancane) area (Central Italy): characterization, distribution and quantitative spatial analysis. Catena 31, 237–256.

Calzolari, C., Torri, D., Del Sette, M., Maccherini, S., Bryan, R., 1997. Evoluzione dei suoli e processi di erosione su biancane: il caso delle biancane de La Foce_Val d'Orcia, Siena. Boll. Soc. Ital. Sci. Suolo, Nuova Serie 8, 185–203.

Carmignani, L., Decandia, F.A., Fantozzi, P.L., Lazzarotto, A., Liotta, D., Meccheri, M., 1994. Tertiary extensional tectonics in Tuscany (northern Apennines, Italy). Tectonophysics 238, 295–315.

Carrara, A., 1983. A multivariate model for landslide hazard evaluation. Math Geol, 15, 403–426.

Carrara, A., Cardinali, M., Detti, R., Guzzetti, F., Pasqui, V., Reichenbach, P., 1991. GIS techniques and statistical models in evaluating landslide hazard. Earth Surf Proc Land, 20(5), 427-445.

Carrara, A., Cardinali, M. and Guzzetti, F., 1992. Uncertainty in assessing landslide hazard and risk. ITC Journal, 2, 172-183.

Carrara, A., Cardinali, M., Guzzetti, F. and Reichenbach, P., 1995. GIS technology in mapping landslide hazard. In: Geographical Information Systems in Assessing Natural Hazards, A. Carrara and F. Guzzetti, Kluwer Academic Publisher, Dordrecht, 135-176.

Carrara, A., Crosta, G., Frattini, P., 2003. Geomorphological and historical data in assessing landslide hazard. Earth Surf Proc and Land 28, 1125–1142.

Castelvecchi, A., Vittorini, S., 1970. Osservazioni preliminari per uno studio sull'erosione in Val d'Orcia. In: Soc. Geogr. Ital. (Ed.), Atti XX Congresso Geografico Italiano, Roma, 1967, pp. 151–168.

Chiaverini, I., Colica, A., Del Sette, M., Ostuni D., 1999. Misura dell'erosione: metodi fotogrammetrici applicati in alcune aree argillose dell'Alta Val d'Orcia. Geologia Tecnica e Ambientale, 74(3), 295-303-

Chung, C.J.F., Fabbri, A.G., 1999. Probabilistic prediction models for landslide hazard mapping. Photogramm Eng Rem S, 65(12), 1389-1399.

Chung, C.J.F., Fabbri, A.G., 2003. Validation of Spatial Prediction Models for Landslide Hazard Mapping. Nat Hazards, 30(3), 451-472, DOI: 10.1023/B:NHAZ.0000007172.62651.2b.

Chung, C.J.F., Fabbri, A.G., 2008. Predicting landslides for risk analysis - Spatial models tested by a cross-validation procedure. Geomorphology, 94, 438–452, doi:10.1016/j.geomorph.2006.12.036.

Chung, C.F., Fabbri, A.G., van Westen, C.J., 1995. Multivariate Regression Analysis for Landslide Hazard Zonation. In: Geographical Information Systems in Assessing Natural Hazards, A. Carrara and F. Guzzetti, Kluwer Academic Publisher, Dordrecht, 107-134.

Chung, C.J.F., Kojima, H., Fabbri, A.G., 2002. Stability analysis of prediction models for landslide hazard mapping. In: Applied Geomorphology: Theory and Practice, Allison, R., John Wiley & Sons, Chichester, 3-19, 2002.

Church, M., Slaymaker, H.O., 1989. Disequilibrium of Holocene sediment yield in glaciated British Columbia. Nature 337, 452–54.

Ciccacci, S., Fredi, P., Lupia Palmieri, E., 1977. Rapporti fra trasporto solido e parametri climatici e geomorfici in alcuni bacini idrografici italiani. Atti Conv. Misura del trasporto solido al fondo nei corsi d'acqua, C.N.R., pp. 4.1-4.16.

Ciccacci, S., Fredi, P., Lupia Palmieri, E., Pugliese, F., 1981. Contributo della analisi geomorfica quantitativa alla valutazione dell'entità dell'erosione nei bacini fluviali. Bollettino della Società Geologica Italiana 99, 455–516.

Ciccacci, S., Fredi, P., Lupia Palmieri, E., Pugliese, F., 1986. Indirect evaluation of erosion entity in drainage basins through geomorphic, climatic and hydrological parameters. In: Gardiner, V. (Ed.), International Geomorphology Part II. John Wiley & Sons Ltd, Chichester, pp. 33–48.

Ciccacci, S., D'Alessandro, L., Fredi, P., Lupia Palmieri, E., 1988. Contributo dell'analisi geomorfica quantitativa allo studio dei processi di denudazione nel bacino idrografico del Torrente Paglia (Toscana meridionale–Lazio settentrionale). Geografia Fisica e Dinamica Quaternaria Suppl. I, 171–188.

Ciccacci, S., D'Alessandro, L., Fredi, P., Lupia Palmieri, E., 1992. Relations between morphometric characteristics and denudational processes in some drainage basins of Italy. Z. Geomorphol. N.F. 36, 53–67.

Ciccacci, S., Del Monte, M., Fredi, P., Palmieri, E. L., 1995. Planoaltimetric configuration, denudational processes and morphodynacs of drainage basins, Geologica Romana vol. 31, 1-13.

Ciccacci, S., Del Monte, M., Marini, R., 2003. Denudational processes and recent morphological change in a sample area of the Orcia River Upper Basin (Southern Tuscany). Geogr. Fis. Din. Quat. 26, 97–109.

Ciccacci, S., Del Monte, M., Lupia Palmieri, E., Salvatore, M.C., 2006. Entità dei processi di denudazione e variazioni morfologiche recenti nell'area di Radicofani (Toscana meridionale).. In:

Erosione idrica in ambiente mediterraneo: valutazione diretta e indiretta in aree sperimentali e bacini idrografici, Brigati, Genova, pp. 29-64.

Ciccacci, S., Galiano, M., Roma, M.A., Salvatore, M.C., 2008. Morphological analysis and erosion rate evaluation in badlands of Radicofani area (Southern Tuscany — Italy). Catena 74, 87–97.

Ciccacci, S., Galiano, M., Roma, M.A., Salvatore, M.C., 2009. Morphodynamics and morphological changes of the last 50 years in a badland sample area of Southern Tuscany (Italy). Z. Geomorph. N. F. 53(3), 273-297.

Clerici, A., Perego, S., Tellini, C., Vescovi, P., 2006. A GIS-based automated procedure for landslide susceptibility mapping by the Conditional Analysis method: the Baganza valley case study (Italian Northern Apennines). Environ Geol, 50, 941–961.

Clerici, A., Perego, S., Tellini, C. and Vescovi, P., 2010. Landslide failure and runout susceptibility in the upper T. Ceno valley (Northern Apennines, Italy).Nat Hazards, 52(1), 1-29, DOI: 10.1007/s11069-009-9349-4.

Colica, A., Guasparri, G., 1990. Sistemi di fatturazione nelle argille plioceniche del territorio senese. Implicazioni geomorfologiche. Atti Accad. Fisiocritici, Siena (9), 29-36.

Conforti, M., Aucelli, P.P.C., Robustelli, G., Scarciglia, F., 2011. Geomorphology and GIS analysis for mapping gully erosion susceptibility in the Turbolo stream catchment (Northern Calabria, Italy). Nat Hazards 56, 881–898

Conoscenti, C., Di Maggio, C., Rotigliano, E., 2008(a). Soil erosion susceptibility assessment and validation using a geostatistical multivariate approach: a test in Southern Sicily. Nat Hazards 46,287–305.

Conoscenti, C., Di Maggio, C. and Rotigliano, E., 2008(b). GIS analysis to assess landslide susceptibility in a fluvial basin of NW Sicily (Italy). Geomorphology, 94(3-4), 325-339. doi:10.1016/j.geomorph.2006.10.039.

Cooke, R. U., Doornkamp, J. C., 1974. Geomorphology in environmental management. Oxford, Clarendon Press, p. 413.

Cramer, H., 1999. Mathematical methods of statistics. Princeton University Press, Princeton, N. J., 575 pp.

Cressie, N., 1990. The origins of kriging. Mathematical Geology 22, Number 3, 239-252, DOI: 10.1007/BF00889887

Crozier, M. J., 1984. Field assessment of slope instability. In: Slope Instability. Brunsden D. and Prior D. B., Chichester, Wiley, 103-142.

Cruden, D.M., Varnes, D.J., 1996. Landslide types and processes. Special Report - National Research Council, Transportation Research Board, 247, 36-75, 1996.

D'orazio, M., Laurenzi, M.A., Villa, I.M., 1991. 40Ar/39Ar dating of a shoshonitic lava flow of the Radicofani volcanic center (Southern Tuscany). Acta Vulcanol., 1, pp. 63-67, 1991.

Dai, F.C., Lee, C.F., 2003. A spatiotemporal probabilistic modeling of storm-induced shallow landsliding using aerial photographs and logistic regression. Earth Surf Proc Land, 28, 527-545.

de Araújo, J.C, Knight, D.W., 2005. A review of the measurement of sediment yield in different scales. REM: Revista Escola de Minas, Ouro Preto 58, 257–65.

De Martonne, E. M., 1926. Une nouvelle fonction climatologique: l'indice d'aridité, La Metéorologie, 2, 449-459.

De Roo, A.P.J., Jetten, V.G., 1999. Calibrating and validating the LISEM model for two data sets from the Netherlands and South Africa. Catena 37 (3-4), 477–493.

de Vente, J., Poesen, J., 2005. Predicting soil erosion and sediment yield at the basin scale: scale issues and semi-quantitative models. Earth-Science Reviews 71, 95–125.

de Vente, J., Poesen, J., Verstraeten, G., 2005. The application of semi-quantitative methods and reservoir sedimentation rates for the prediction of basin sediment yield in Spain. Journal of Hydrology 305(1–4), 63–86.

de Vente, J., Poesen, J, Bazzoffi, P., Van Rompaey, A., Verstraeten, G., 2006. Predicting catchment sediment yield in Mediterranean environments: the importance of sediment sources and connectivity in Italian drainage basins. Earth Surface Processes and Landforms 31 8 2006, 1017–1034.

de Vente, J., Poesen, J., Arabkhedri, M., Verstraeten, G., 2007. The sediment delivery problem revisited. Progress in Physical Geography 31(2), 155–178.

Dedkov, A.P., 2004. The relationship between sediment yield and drainage basin area. In Golosov, V., Belyaev, V. and Walling, D.E. (Eds) , Sediment transfer through the fluvial system, Moscow: IAHS publication 288, 197–204.

Del Monte, M., 2003. Caratteristiche morfometriche e morfodinamiche dell'alto bacino del Fiume Orcia (Toscana meridionale). Atti XXVIII Cong. Geogr. It., Roma, Italy, pp. 1933–1975.

Del Monte, M., Fredi, P., Lupia Palmieri, E., Marini, R., 2002. Contribution of quantitative geomorphic analysis to the evaluation of geomorphological hazards. In: Allison, R. (Ed.), Applied Geomorphology: Theory and Practice. J.Wiley & Sons, Chichester, pp. 335–358.

Della Seta, M., Del Monte, M., Fredi, P., Lupia Palmieri, E., 2004. Quantitative morphotectonic analysis as a tool for detecting deformation patterns in soft rock terrains: a case study from the southern Marches, Italy. Géomorphologie, 4, 267-284.

Della Seta, M., Del Monte, M. and Pascoli, A., 2005. Quantitative geomorphic analysis to evaluate flood hazards. Geogr Fis Din Quat, 28(1), 117-124.

Della Seta, M., Del Monte, M., Fredi, P., Lupia Palmieri, E., 2007. Direct and indirect evaluation of denudation rates in Central Italy. Catena 71, 21–30.

Della Seta, M., Del Monte, M., Fredi, P., and Lupia Palmieri, E., 2009. Space-time variability of denudation rates at the catchment and hillslope scales on the Tyrrhenian side of Central Italy.

Delmas, M., Cerdan, O., Mouchel, J.M., Garcin, M., 2009. A method for developing a large-scale sediment yield index for European river basins. J Soils Sediments 9, 613–626.

Dendy, F.E., Bolton, G.C., 1976. Sediment yieldrunoff-drainage area relationships in the United States. Journal of Soil and Water Conservation 31, 264–66.

Desir, G., Marín, C. 2007. Factors controlling the erosion rates in a semi-arid zone (Bardenas Reales, NE Spain). Catena 71, 31–40.

Di Lisio, A., Aucelli, P., Russo, F., 2007. Caratterizzazione morfometrica ed elaborazione di dati geoambientali per la determinazione del dissesto idrogeologico del Vallone Grande (Molise). Rend. Soc. Geol. It. 4, 117-122.

Douglas, I., 1968. Sediment sources and causes in the humid tropics of northeast Queensland, Australia. Brit. Geom. Res. Group, pp. 27-39.

Dramis, F., Gentili, B., 1977. I parametri F (Frequenza di drenaggio) e D (Densità di drenaggio) e le loro variazioni in funzione della scala di rappresentazione cartografica. Boll. Soc. Geol. Ital. 96, 637–651.

EEA, 2007. CLC2006 technical guidelines, EEA Technical report No 17/2007.

Einsele, G., Hinderer, M., 1997. Terrestrial sediment yield and the lifetime of reservoirs, lakes, and larger basins. Geologische Rundschau 86, 288–310.

Evans, R., 1995. Some methods of directly assessing water erosion of cultivated land - a comparison of measurements made on plots and in fields. Progress in Physical Geography 19,115–129.

Fairbridge, R.W. (Ed.), 1968. Encyclopedia of Geomorphology. Reinhold Book, New York.

Falaschi, F., Giacomelli, F., Federici, P. R., Puccinelli, A., D'Amato Avanzi, G., Pochini, A., Ribolini, A., 2009. Logistic regression versus artificial neural networks: landslide susceptibility evaluation in a sample area of the Serchio River valley, Italy. Nat Hazards, 50,551–569, DOI 10.1007/s11069-009-9356-5.

Fang, H., Chen, H., Cai, Q., Li, Q. 2006. Scale effect on sediment yield from sloping surfaces to basins in hilly loess region on the Loess Plateau in China. Environmental Geology, DOI: 10.1007/s00254-006-0513-9.

Farabegoli E., Agostini C., 2000. Identification of Calanco, a badland in the nothern Appennines, Italy. Earth Surf. Proc. Land., 26 (3), 307-318.

Farabollini, P., Gentili, B., Pambianchi, G., 1992. Contributo allo studio dei calanchi: due aree campione nelle Marche. Studi Geologici Camerti 12, 105–115.

Farifteh, J., Soeters, R., 2006. Origin of calanchi and biancane in East Aliano, southern Italy. Geomorphology 77, 142–152.

Faulkner, H., 1990. Vegetation cover density variations and infiltration patterns on piped alkali sodic soils: implications for the modelling of overland flow in semi-arid areas. In: Thornes, J.B. Ed.., Vegetation and Erosion. Wiley, Chichester, pp. 317–346.

Faulkner, H., 2007. Improvements to the dispersion status of piped gully soils following reworking and stabilisation by vegetation. Catena 70, 410-415.

Faulkner, H., Spivey, D., Alexander, R., 2000. The role of some site geochemical processes in the development and stabilisation of three badland sites in Almeria, southern Spain. Geomorphology 35, 87–99.

Faulkner, H., Alexander, R., Wilson, B.R., 2003. Changes to the dispersive characteristics of soils along an evolutionary slope sequence in the Vera badlands, southeast Spain: implications for site stabilization. Catena 50, 243–254.

Faulkner, H., Alexander, R., Teeuw, R., Zukowskyj, P., 2004. Variations in soil dispersivity across a gully head displaying shallow sub-surface pipes, and the role of shallow pipes in rill initiation. Earth Surf. Processes Landf. 29, 1143–1160.

Faulkner, H., Alexander, R., Zukowskyj, P., 2008. Slope–channel coupling between pipes, gullies and tributary channels in the Mocatán catchment badlands, Southeast Spain. Earth Surface Processes and Landforms 33, 1242–1260.

Fell, R., Corominas, J., Bonnard, C., Cascini, L., Leroi, E., Savage, W. Z. on behalf of the JTC-1 Joint Technical Committee on Landslides and Engineered Slopes, 2008. Guidelines for landslide susceptibility, hazard and risk zoning for land-use planning. Engineering Geology 102, 99-111.

Fernandez, T., Irigaray, C., El Hamdouni, R., Chacón, J., 2003. Methodology for landslide susceptibility mapping by means of a GIS application to the Contraviesa Area (Granada, Spain). Nat Hazards, 30(3), 297–308, doi:10.1023/B:NHAZ.0000007092.51910.3f.

Ferro, V., Porto, P., Tusa, G., 1998. Testing a distributed approach for modelling sediment delivery. Hydrological Sciences Journal 43(3), 425–442.

Ferro, V., Di Stefano, C., Minacapilli, M., Santoro, M., 2003. Calibrating the SEDD model for Sicilian ungauged basins. In Erosion prediction in ungauged basins: integrating methods and techniques, De Boer, D., Froehlich, W., Mizuyama, T., Pietroniro, A. (eds). IAHS Publication 279. Sapporo, 151–161.

Foster, G. R., 1982. Modelling the erosion processes. In Hydrologic Modeling of a Small Watershed. American Society of Agricultural Engineers, eds. Hann, C. T., Johnson, H. P. and Brakensick, D. L, pp. 297-380. ASAE, St. Joseph, Michigan, USA.

Foster, G.R., 1986. Understanding ephemeral gully erosion. Committee on Conservation Needs and Opportunities, Soil Conservation. Assessing the National Resources Inventory, Board on Agriculture, National Research Council. National Academy Press, Washington DC, pp. 90–125.

Foster, G.R., Meyer, L.D., 1972. A closed form soil erosion equation for upland erosion. In: Shen, H.W. (Ed.), Sedimentation. Colorado State University, Ft Collins, Colorado, 12.

Fournier, F., 1960. Climat et erosion: la relation entre l'érosion du sol par l'eau et les précipitation atmosphériques. Paris, Press Univ. de France, p. 201.

Gallart, F., Solé, A., Puigdefábregas, J. and Lázaro, R., 2002: Badland systems in the Mediterranean. In Bull, L.J. and Kirkby, M.J., editors, Dryland rivers: hydrology and geomorphology of semi-arid channels, Chichester: Wiley, 299–326.

García-Ruíz, J.M., López-Bermudez, F. 2009: Un caso especial: badlands y sufosión. In Sociedad Española de Geomorfología, editor, Erosión del suelo en España, Zaragoza: SEG, 239–72.

García Ruiz, J.M., Lana Renault, N., Beguería, S., Valero Garcés, B.L., Lasanta, T., Arnáez, J., López Moreno, J.I., Regüés, D., Marti Bono, C., 2004. Temporal and spatial interactions of slope and catchment processes in the central Spanish Pyrenees. In Golosov, V., Belyaev, V. and Walling, D.E. (Eds), Sediment transfer through the fluvial system, Moscow: IAHS publication 288, 21–28.

Gazzolo, T., Bassi, G., 1962. Contributo allo studio del grado di erodibilità dei terreni costituenti i bacini montani dei corsi d'acqua italiani. Giorn. Gen. Civ., pp. 9-19.

Gini, C., 1914. Sulla misura della concentrazione e della variabilità dei caratteri. Atti del Regio Istituto Veneto di Scienze, Lettere e Arti, LXXIII(parte II), 1203-1248.

Gögüs, M., Yener, A.G., 1997. Estimation of sediment yield rates of reservoirs in Turkey, Dix-neuvième Congrès des Grands Barrages. Florence: Commission Internationale De Grands Barrages, 1265–76.

Gorsevski, P.V., Gessler, P., Foltz, R.B., 2000. Spatial prediction of landslide hazard using logistic regression and GIS. In: Proceedings of the 4th Int. Conference on Integrating GIS and Environmental Modeling, Alberta, Canada.

Goudie, A., 1981. The Human Impact: Man's Role in Environmental Change. MIT Press: Cambridge, Massachusetts.

Gregory, K.J., Walling, D.E., 1973. Drainage basin forms and landforms. Edward Arnold, London

Guasparri, G., 1978. Calanchi e biancane nel territorio senese: studio geomorfologico. L'Universo 58, 97–140.

Guasparri, G., 1993. I lineamenti geomorfologici dei terreni argillosi pliocenici. In: Giusti, F. (Ed.), La storia naturale della Toscana meridionale. Amilcare Pizzi, Milano, Italy, pp. 89–106.

Gutteridge Haskins and Davey, 1991. Integrated Quantity/Quality Modelling—Stage 3, Gutteridge Haskins and Davey, for Department of Water Resources, Sydney, pp. 102.

Guzzetti, F., Carrara, A., Cardinali, M. and Reichenbach, P., 1999. Landslide hazard elavuation: a review of current techniques and their application in a multi-scale study, Central Italy. Geomorphology 31, 181-216, doi:10.1016/S0169-555X(99)00078-1.

Guzzetti, F., Reichenbach, P., Ardizzone, F., Cardinali, M., Galli, M., 2006. Estimating the quality of landslide susceptibility models. Geomorphology, 81, 166–184, doi:10.1016/j.geomorph.2006.04.007.

Haan, C.T., Barfield, B.J., Hayes, J.C., 1994. Design Hydrology and Sedimentology for Small Catchments. Academic Press 588 pp.

Hammond, C., Hall, D., Miller, S., Swetik, P., 1992. Level I Stability Analysis (LISA) Documentation for Version 2, General Technical Report INT-285, USDA Forest Service Intermountain Research Station. 121.

Haregeweyn, N., Poesen, J., Nyssen, J., Verstraeten, G., de Vente, J., Govers, G., Deckers, S., Moeyersons, J. 2005: Specific sediment yield in Tigray-Northern Ethiopia: assessment and semi-quantitative modelling. Geomorphology 69, 315–31.

He Y., Beighley, E. R., 2008. GIS-based regional landslide susceptibility mapping: a case study in southern California. Earth Surf Proc Land, 33, 380 –393.

Hollingsworth, R. and Kovacs, G.S., 1981. Soil slumps and debris flows: prediction and protection. Bulletin American Association of Engineering Geologists, 18(1), 17-28.

Imeson, A.C., Kwaad, F.J., Verstraten, J.M., 1982. The relationship of soil physical and chemical properties to the development of badlands in Morocco. In: Bryan, R., Yair, A. (Eds.), Badlands Geomorphology and Piping. Geobooks, Geoabstracts, Norwick. 408 pp.

Irigaray Fernàndez, C., Fernández Del Castillo, T., El Hamdouni, R.,Chacón Montero, J., 1999. Verification of landslide susceptibility mapping: a case study. Earth Surf Proc Land, 24, 537-544.

Iverson, R.M., 2000. Landslide triggering by rain infiltration. Water Resour Res, 36(7), 1897–1910.

Jacobacci, A., Martelli, G., Nappi, G., 1967. Note illustrative della Carta Geologica d'Italia, Foglio 129, S. Fiora. Roma: La litograf, 61 pp.

Jacobacci, A., Martelli, G., Nappi, G., 1969. Note illustrative della Carta Geologica d'Italia, Foglio 121, Montepulciano. Ercolano: Poligrafica & Cartevalori, 73 pp.

Jain, M.K., Kothyari, U.C., 2000. Estimation of soil erosion and sediment yield using GIS. Hydrological Sciences Journal 45, 771–786.

Jenks, G.F., Caspall, F.C., 1971. Error on Choroplethic Maps: Definition, Measurement, Reduction. Ann Assoc Am Geogr, 61(2), 217-244.

Jetten, V., Favis-Mortlock, D., 2006. Modelling soil erosion in Europe. In: Boardman, J., Poesen, J. (Eds.), Soil Erosion in Europe. J. Wiley & Sons, Chichester, pp. 695–716.

Jiongxin, X., Yunxia, Y., 2005. Scale effects on specific sediment yield in the Yellow River basin and geomorphological explanations. Journal of Hydrology 307, 219–32.

Kakembo, V., Xanga, W.W., Rowntree, K., 2009. Topographic thresholds in gully development on the hillslopes of communal areas in Ngqushwa Local Municipality, Eastern Cape, South Africa. Geomorphology 110, 188–195.

Kaplan, E., Hegarty, C., 2006. Understanding GPS: Principles and Application. Second Edition, Artech House, 730 pp.

Kelley, W.P., 1964. Review of investigations on cation exchange and semi-arid soils. Soil Science, 97, 80–88.

Kinnell, P.I.A., 2000. AGNPS-UM: applying the USLE-M within the agricultural non point source pollution model. Environmental Modelling and Software 15(3), 331–341.

Krishnaswamy, J., Richter, D.D., Halpin, P.N., Hofmockel, M.S., 2001. Spatial pattern of suspended sediment yields in a humid tropical watershed in Costa Rica. Hydrological Processes 15, 2237–57.

Laflen, J.M., Lane, L.J., Foster, G.R., 1991. WEPP: A new generation of erosion prediction technology. Journal of Soil and Water Conservation 46, 34–38.

Lane, L. J., Shirley, E. D. and Singh, V. P., 1988. Modelling erosion on hillslopes. In Modelling Geomorphological Systems, ed. M. G. Anderson, pp. 287-308.

Lane, L. J., Nichols, M. H. and Paige, G. B., 1995. Modeling erosion on hillslopes: Concept, theory, and data. In International Congress on Modelling and Simulation Proceedings, eds. P. Binning, H. Bridgman and B. Williams. Vol. 1, pp. 1-7.

Lane, L.J., Hernandez, M., Nichols, M. 1997. Processes controlling sediment yield from watersheds as function of spatial scale. Environmental Modelling and Software 12, 355–69.

Langbein, W. B., Schumm, S. A., 1958. Yield of sediment in relation to mean annual precipitation, Trans. Am. Geoph. Un., pp. 1076-1084.

Lazzarotto, A., 1993. Elementi di geologia. In: Giusti, F. (Ed.), La storia naturale della Toscana meridionale. Amilcare Pizzi, Milano, Italy, pp. 20–87.

Lee, S., Ryu, J., Min, K., Won, J., 2001. Development of Two Artificial Neural Network Methods for Landslide Susceptibility Analysis. Proceedings of the Geoscience and Remote Sensing Symposium, IGARSS '01, IEEE 2001 International, 9-13 July 2001, 5, 2364-2366, DOI: 10.1109/IGARSS.2001.978003.

Lesschen, J. P., Cammeraat, L. H., Nieman, T., 2008. Erosion and terrace failure due to agricultural land abandonment in a semi-arid environment. Earth Surface Processes and Landforms 33, 1574–1584 DOI: 10.1002/esp.1676.

Liotta, D.,1991. The Arbia–ValMarecchia Line, northern Apennines. Eclogae Geol. Helv. 84, 413–430.

Liotta, D., 1996. Analisi del settore centromeridionale del bacino pliocenico di Radicofani (Toscana meridionale). Boll. Soc. Geol. Ital. 115, 115–143.

Lopez-Bermudez, F., Romero-Díaz, M.A., 1989. Piping erosion and badland development in Southeast Spain. In: Yair, A., Berkowicz, B. (Eds.), Arid and Semi-arid Environments—Geomorphological and Pedological Aspects. Catena, Suppl., vol. 14, pp. 59– 73.

Lorenz, M.O., 1905. Methods of Measuring the Concentration of Wealth. Publ Am Stat Assoc, 9(70), 209-219.

Lupia Palmieri, E., 1983. Il problema della valutazione dell'entità dell'erosione nei bacini fluviali. Atti del XXIII Congresso Geografico Italiano, II, 143-176.

Lupia Palmieri, E., Ciccacci, S., Civitelli, G., Corda, L., D'Alessandro, L.,DelMonte, M., Fredi, P., Pugliese, F., 1995. Geomorfologia quantitativa e morfodinamica del territorio abruzzese. I — Il bacino idrografico del Fiume Sinello. Geogr. Fis. Din. Quat. 18, 31–46.

Lupia Palmieri, E., Centamore, E., Ciccacci, S., D'Alessandro, L., Del Monte, M., Fredi, P., Pugliese, F., 2001. Geomorfologia quantitativa e morfodinamica del territorio abruzzese. III - Il bacino idrografico del Fiume Saline. Geogr. Fis. Dinam. Quat., 24 (2), 157-176.

Märker, M., Flügel, W.A., Rodolfi, G., 1999. Das Konzept der ''Erosions Response Units'' (ERU) und seine Anwendung am Beispiel des semi-ariden Mkomazi-Einzugsgebietes in der Provinz Kwazulu/Natal, Südafrika. In: Tübinger Geowissenschaftliche Studien, Reihe D.: Geoökologie und Quartaerforschung. Angewandte Studien zu Massenverlagerungen, Tübingen.

Mancini, M., Girotti, O., Cavinato, G.P., 2003-2004. Il Pliocene e il Quaternario della Media Valle del Tevere. Geologica Romana, XXXVII, 175-236.

Maner, S.B., 1958. Factors affecting sediment delivery rates in the Red Hills physiographic area. Transactions of the American Geophysical Union 39, 669–75.

Mannaerts, C.M., Gabriels, D., 2000. A probabilistic approach for predicting rainfall soil erosion losses in semiarid areas. Catena 40, 403– 420.

Marignani, M., Rocchini, D., Torri, D., Chiarucci, A., Maccherini, S., 2008. Planning restoration in a cultural landscape in Italy using an object-based approach and historical analysis. Landscape and Urban Planning 84, 28–37.

Marini, R., 1995. Contributo della geomorfologia quantitativa alla valutazione della pericolosità geomorfologica. PhD Thesis, Università degli Studi di Roma "La Sapienza", Roma.

Martinez-Casasnovas, J.A,, Anton-Fernández, C., Ramos, M.C., 2003. Sediment production in large gullies of the Mediterranean area (NE Spain) from high-resolution digital elevation models and geographical information systems analysis. Earth Surface Processes and Landforms 28, 443–456.

Martini, I.P., Sagri, M., Colella, A., 2001. Neogene-Quaternary basins of the inner Apennines and Calabrian arc. In: Vai, G.B., Martini, I.P., (Eds.), Anatomy of an Orogen: the Apennines and Adjacent Mediterranean Basins, 375-400, Kluwer Academic Publishers, Dordrecht.

Merritt, W.S., Letcher, R.A., Jakeman, A.J., 2003. A review of erosion and sediment transport models. Environmental Modelling & Software 18, 761–799.

Milliman, J.D., Meade, R.H., 1983. World wide, delivery of river sediment to the oceans. The Journal of Geology 91, 1–21.

Milliman, J.D., Syvitski, J.P.M., 1992. Geomorphic/tectonic control of sediment discharge to the ocean: the importance of small mountainous rivers. The Journal of Geology 100, 525–44.

Millington, A. C., 1986. Reconnaissance scale soil erosion mapping using a simple geographic information system in the humid tropics. In: Land Evaluation for Land-use Planning and Conservation in Sloping Areas: International Workshop, Enschede, The Netherlands, 17-21 December, 1984, ed. Siderius,W., pp. 64-81.

Mitchell, J.K., 1976. Fundamentals of Soil Behavior. Wiley, New York, 422 pp.

Montgomery, D.R., Dietrich, W.E., 1994. A physically based model for the topographic control of shallow landsliding. Water Resour Res, 30(4), 1153-1171, 1994.

Montgomery, D.R., Wright, R.H., Booth T., 1991. Debris flow hazard mitigation for colluvium-filled swales. Bulletin Association of Engineering Geologists, 28(3), 303-323.

Moore, I.D., Grayson, R.B., Ladson, A.R., 1991. Digital terrain modeling: a review of hydrological, geomorphological, and biological applications. Hydrol process 5, 3–30.

Moretti, S., Rodolfi, G., 2000. A typical "calanchi" landscape on the Eastern Apennine margin (Atri, Central Italy): geomorphological features and evolution. Catena 40, 217–228.

Morgan, R.P.C., 2001. A Simple Approach to Soil Loss Prediction: A Revised Morgan-Morgan-Finney Model. Catena 44, 305-322

Morgan, R.P.C., 2005. Soil Erosion and Conservation. 3rd edition, Blackwell Publishing, Oxford, 304 pp. ISBN 1-4051-1781-8.

Morgan, R.P.C., Morgan, D.D.V., Finney, H.J., 1984. A Predictive Model for the Assessment of Soil Erosion Risk. Journal of Agricultural Engineering Research 30,245-253

Morgan, R.P.C., Quinton, J.N., Smith, R.E., Govers, G., Poesen, J.W.A., Auerswald, K., Chisci, G., Torri, D., Styczen, M.E., 1998. The European soil erosion model (EUROSEM): a process-based approach

for predicting sediment transport from fields and small catchments. Earth Surface Processes and Landforms 23, 527–544.

Nadal-Romero, E., Regüés, D., 2010. Geomorphological dynamics of subhumid mountain badland areas – weathering, hydrological and suspended sediment transport processes: A case study in the Aragua´s catchment (Central Pyrenees) and implications for altered hydroclimatic regimes. Progress in Physical Geography 34(2), 123–150.

Nadal-Romero, E., Regüés, D., Martí-Bono, C., Serrano-Muela, P., 2007. Badlands dynamics in the Central Pyrenees: temporal and spatial patterns of weathering processes. Earth Surfaces Processes and Landforms 32, 888–904.

Nadal-Romero, E., Latron, J., Lana-Renault, N., Serrano-Muela, P.,Martí-Bono, C., Regüés, D., 2008(a). Temporal variability in hydrological response within a small catchment with badland areas, Central Pyrenees. Hydrological Science Journal 53, 629–39.

Nadal-Romero, E., Latron, J., Martí-Bono,C., Regüés,D., 2008(b). Temporal distribution of suspended sediment transport in a humid Mediterranean badland area: the Araguás catchment, Central Pyrenees. Geomorphology 97, 601–16.

Nearing, M. A., Foster, G. R., Lane, L. J. and Finkner, S. C. (1989) A process-based soil erosion model for USDA-water erosion prediction project technology. Transactions of the American Society of Agricultural Engineering 32, 1587-1593.

Nearing, M. A., Lane, L. J. and Lopes, V. L., 1994. Modeling soil erosion. In Soil Erosion Research Methods, ed. Rattan Lal, pp. 127-156. Soil and Water Conservation Society and St. Lucie Press.

Neeley, M.K., Rice, R.M., 1990. Estimating risk of debris slides after timber harvest in northwestern California, Bulletin American Association of Engineering Geologists, 27(3), 281-289.

Nefeslioglu, H.A., Duman, T.Y., Durmaz, S., 2008. Landslide susceptibility mapping for a part of tectonic Kelkit Valley (Eastern Black Sea region of Turkey). Geomorphology, 94, 401–418, doi:10.1016/j.geomorph.2006.10.036.

Okimura, T., Kawatani, T., 1987. Mapping of the potential surface-failure sites on granite slopes, in: In: International Geomorphology 1986, Gardiner, V., J.Wiley & Sons, Part I, 121-138.

Ohlmacher, C.G., Davis, C.J., 2003. Using multiple regression and GIS technology to predict landslide hazard in northeast Kansas. USA, Eng Geol, 69, 331–343.

Osterkamp, W.R., Toy, T.J., 1997. Geomorphic considerations for erosion prediction. Environmental Geology 29, 152–57.

Pack, R.T., Tarboton, D.G., Goodwin, C.N., 1999. GIS-based landslide susceptibility mapping with SINMAP. In: Proceedings of the 34th Symposium on Engineering Geology and Geotechnical Engineering, Bay J. A., Logan, Utah.

Panizza, M., 1987. Il ruolo della geomorfologia nella valutazione dell'impatto ambientale. VI Congresso Nazionale dell'Ordine dei Geologi, Venezia Fondazione Cini, 125-135.

Pappalardo, M., Porrotto, C., Spagnolo, M., 2001. Ricostruzione paleomorfologica dell’area vulcanica di Radicofani (Toscana sud-orientale). Atti. Soc. Tosc. Sc. Nat. Mem., Ser. A, 107, 17-26.

Pearson, K., 1896. Mathematical contributions to the Theory of the Evolution-III, Regression, Heredity and Panmixia. Philosophical Transactions of the Royal Society A, 187, 253-318.

Phillips, C.P., 1998. The Crete Senesi, Tuscany. A vanishing landscape? Landscape Urban Plann. 41, 19–26.

Piccarreta, M., Faulkner, H., Bentivenga, M. and Capolongo, D. 2006: The influence of physico-chemical material properties on erosion processes in the badlands of Basilicata, southern Italy. Geomorphology 81, 235–51.

Pinna, S., Vittorini, S., 1989. Su alcune caratteristiche delle argille Plioceniche della Val d'Era (Toscana), in rapporto alla genesi di calanchi e biancane. Geogr. Fis. Din. Quat. 12, 131–137.

Poesen, J., Hooke, J. M., 1997. Erosion, flooding and channel management in Mediterranean Environments of southern Europe. Progress in Physical Geography, 21 (2):157–199.

Poesen, J., Nachtergaele, J., Verstraeten, G., Valentin, C., 2003. Gully erosion and environmental change: importance and research needs. Catena 50, 91–133.

Pradhan, B., Lee, S., 2010. Landslide susceptibility assessment and factor effect analysis: backpropagation artificial neural networks and their comparison with frequency ratio and bivariate logistic regression modelling. Environ Modell Softw, 25, 747–759.

Prosser, I.P., Young, B., Rustomji, P., Hughes, A., Moran, C., 2001. A model of river sediment budgets as an element of river health assessment. In: Proceedings of the International Congress on Modelling and Simulation (MODSIM'2001), December 10–13, pp. 861–866.

PSIAC, 1968. Report of the water management subcommittee on factors affecting sediment yield in the Pacific southwest area and selection and evaluation of measures for reduction of erosion and sediment yield. Pacific Southwest Inter-Agency Committee.

Pugnaire, F.I., Luque, M.T., Armas, C., Gutierrez, L., 2006. Colonization processes in semi-arid Mediterranean old-fields. Journal of Arid Environments 65, 591–603.

Radoane, M., Radoane, N., 2005. Dams, sediment sources and reservoir silting in Romania. Geomorphology 71, 112–25.

Remondo, J. Gonzales, A., Diaz de Teràn, J.R., Cendrero, A., Fabbri, A., Chung, C.J.F., 2003. Validation of Landslide Susceptibility Maps; Examples and Applications from a Case Study in Northern Spain, Nat Hazards, 30(3), 437-449, DOI: 10.1023/B:NHAZ.0000007201.80743.fc.

Renard, K.G., Foster, G.R., Weesies, G.A., Porter, J.P., 1991. RUSLE – Revised Universal Soil Loss Equation. J. Soil Water Conserv. 46(1), 30-33.

Renard, K.G., Foster, G.R., Weesies, G.A., McCool, D.K., Yoder, D.C., 1997. Predicting soil erosion by water: a guide to conservation planning with the revised universal soil loss equation (RUSLE). 703. US Department of Agriculture: Washington D.C. Agriculture Handbook.

Rengasamy, P., Greene, R.S.B., Ford, G.W., Mehanni, A.H., 1984. Identification of dispersive behaviour and the management of red-brown earths. Aust. J. Soil Res. 22, 413–431.

Renwick, W.H., Smith, S.V., Bartley, J.D., Buddemeier, R.W., 2005. The role of impoundments in the sediment budget of the conterminous United States. Geomorphology 71, 99–111.

Restrepo, J.D., Kjerfve, B., Hermelin, M., Restrepo, J.C., 2006. Factors controlling sediment yield in a major South American drainage basin: the Magdalena River, Colombia. Journal of Hydrology 316, 213–32.

Richter, G., Negendank, J.F.W.,1977. Soil erosion processes and their measurement in the German area of Moselle River. Earth Surface Processes and Landforms 2, 261–278.

Robinson, D.A., Phillips, C.P., 2001. Crust development in relation to vegetation and agricultural practice on erosion susceptible, dispersive clay soils from central and southern Italy. Soil Tillage Res. 60, 1–9.

Rolfe, B.N., Miller, R.F., McQueen, I.S., 1960. Dispersion characteristics of montmorillonite, kaolinite and illite clays in waters of varying quality and their control with phosphate dispersants. United States Geological Survey Professional Paper 334-G, 229-271.

Romero-Díaz, A., Marin Sanleandro, P., Sanchez Soriano, A., Belmonte Serrato, F., Faulkner, H., 2007. The causes of piping in a set of abandoned agricultural terraces in southeast Spain. Catena 69, 282–293.

Rose, C.W., 1993. Erosion and sedimentation. In: Bonell, M., Hufschmidt, M.M., Gladwell, J.S. (Eds.), Hydrology and Water Management in the Humid Tropics: Hydrological Research Issues and Strategies for Water Management. Cambridge University Press, pp.301–343.

Rose, C. W., Williams, J. R., Sander, G. C. and Barry, D. A., 1983(a). A mathematical model of soil erosion and deposition processes: I. Theory for a plane land element. Soil Science Society of America Journal, 47, 991-995.

Rose, C. W., Williams, J. R., Sander, G. C. and Barry, D. A., 1983(b). A mathematical model of soil erosion and deposition processes: II. Application to data from an arid-zone catchment. Soil Science Society of America Journal 47, 996-1000.

Rose, C.W., Coughlan, K.J., Ciesiolka, L.A.A., Fentie, B., 1997. Program GUEST (Griffith University Erosion System Template), a new soil conservation methodology and application to cropping systems in tropical steeplands. ACIAR Technical Reports 40, 34–58.

Salvini, R., 2008. Analisi morfometriche delle Crete Senesi mediante Remote Sensing e GIS. Mem. Descr. Carta Geol. D'Italia, LXXVIII, 245-252.

Scheidegger, A.E.,1961. Mathematicalmodels of slope development.Geol. Soc.Am. Bull. 72, 37–50.

Scheidegger, A.E., 1964. Lithologic variations in slope development theory. U.S. Geol. Surv. Circ. 485.

Schiefer, E., Slaymaker, H.O., Klinkenberg, B., 2001. Physiographically controlled allometry of specific sediment yield in the Canadian cordillera: a lake sediment-based approach. Geografiska Annaler 83A, 55–65.

Schumm, S.A., 1962. Erosion on miniature pediments in Badlands National Monument, South Dakota. Geological Society of America Bulletin 73, 719–724.

Shainberg, I., 1992. Chemical and mineralogical components of crusting. In: Sumner, M.E., Stewart Eds.., Soil Crusting: chemical and physical processes. Lewis Publishers, Boca Raton, FL, pp. 33–54.

Sherard, J.L., Decker, R.S. Eds.., 1976. Dispersive clays, related piping, and erosion in geotechnical projects. ASTM Special Technical Publication 623 American Society for Testing and Materials, Philadelphia, 479 pp.

Sherard, J.L., Dunnigan, L.P., Decker, R.S., 1976. Identification and nature of dispersive soils. J. Geotech. Eng. Div. 102, 287– 301.

Slaymaker, O., 2006. Towards the identification of scaling relations in drainage basin sediment budgets. Geomorphology 80, 8–19.

Soeters, R., Van Westen, C.J., 1996. Slope stability: recognition, analysis and zonation. In: Landslides: investigation and mitigation, Turner, A.K. and Shuster, R.L., Trasportation research board-National research council, 129-177.

Solé-Benet, A., Calvo, A., Cerdà, A., Lázaro, R., Pini, R., Barbero, J. 1997: Influences of micro-relief patterns and plant cover on runoff related to processes in badlands from Tabernas (SE Spain). Catena, 31, 28–38.

Strahler, A.N., 1957. Quantitative analysis of watershed geomorphology. American Geophysical Union Transactions 38, 913–920.

Summerfield, M.A., Hulton, N.J., 1994. Natural controls of fluvial denudation rates in major world drainage basins. Journal of Geophysical Research 99(B7), 871–83.

Süzen, M.L., Doyuran, V., 2004. Data driven bivariate landslide susceptibility assessment using geographical information systems: a method and application to Asarsuyu catchment, Turkey. Eng Geol, 71(3-4), 303-321. doi:10.1016/S0013-7952(03)00143-1.

Takken, I., Beuselinck, L., Nachtergaele, J., Govers, G., Poesen, J., Degraer, G., 1999. Spatial evaluation of a physically-based distributed erosion model (LISEM). Catena 37 (3-4), 431–447.

Terlien, M.T.J., van Westen, C.J., van Asch., Th.W.J., 1995. Deterministic modelling in GIS-based landslide hazard assessment. In: Geographical Information Systems in Assessing Natural Hazards, A. Carrara and F. Guzzetti, Kluwer Academic Publisher, Dordrecht, 57-77.

Thornthwaite, C. W., 1948. An Approach toward a Rational Classification of Climate. Geographical Review 38 (1), 55-94.

Torri, D., Bryan, R.B., 1997. Micropiping processes and biancane evolution in Southeast Tuscany, Italy. Geomorphology 20, 219–235.

Torri, D., Colica, A., Rockwell, D., 1994. Preliminary study of the erosion mechanisms in a biancana badland (Tuscany, Italy). Catena 23, 281–294.

Torri, D., Borselli, L., Calzolari, C., Yañez, M.S., Salvador Sanchis, M.P., 2002. Soil erosion, land use, soil qualities and soil functions: effects of erosion. Proceedings of the third International Congress Man and Soil at the Third Millennium, 2002, Rubio, J.L., Morgan, R.P.C., Asins, S., Andreu, V. (Eds), Geoforma Ediciones.

Tokunaga, E., 1984. Ordering of divide segments and law of divide segments numbers. Transactions. Japanese Geomorphological Union 5, 71–77.

Tokunaga, E., 2000. Dimension of a channel network and space-filling properties of its basin. Transactions, Japanese Geomorphological Union 21 (4), 431–499.

Van Rompaey, A.J.J., Verstraeten, G., Van Oost, K., Govers, G., Poesen, J., 2001. Modelling mean annual sediment yield using a distributed approach. Earth Surface Processes and Landforms 26(11), 1221–1236.

Van Rompaey, A., Bazzoffi, P., Jones, R.J.A., Montanarella, L., 2005. Modeling sediment yields in Italian catchments. Geomorphology 65(1–2), 157–169.

van Westen, C.J., Seijmonsbergen, A.C., Manotvani, F., 1999. Comparing Landslide Hazard Maps. Natural Hazards 20, 137–158.

Varnes, D.J., 1984. Landslide hazard zonation: a review of principles and practice. Commission of Landslide of IAEG, UNESCO, Natural Hazads, 3, UNESCO, Paris, 63 pp.

Vergari, F., Della Seta, M., Del Monte, M., Fredi, P., Lupia Palmieri, E., 2011. Landslide susceptibility assessment in the Upper Orcia Valley (Southern Tuscany, Italy) through conditional analysis: a contribution to the unbiased selection of causal factors. Natural Hazards and Earth System Sciences, 11, 1475–1497.

Vergari, F., Della Seta, M., Del Monte, M., Fredi, P., Lupia Palmieri, E., submitted(a). Short-term evolution of some Mediterranean denudation hot spots: the role of rainfall variations and human impact. Geomorphology, Under review.

Vergari, F., Della Seta, M., Del Monte, M., Barbieri, M., submitted(b). Badlands denudation “hot spots”: the role of parent material properties on geomorphic processes in 20-years monitored sites of southern Tuscany (Italy). CATENA, Under review.

Verstraeten, G., Poesen, J., 2001. Factors controlling sediment yield from small intensively cultivated catchments in a temperate humid climate. Geomorphology 40, 123–144.

Verstraeten, G., Poesen, J., 2002. Using sediment deposits in small ponds to quantify sediment yield from small catchments: possibilities and limitations. Earth Surf. Process. Landforms 27, 1425–1439.

Verstraeten, G., Poesen, J., de Vente, J., Koninckx, X., 2003. Sediment yield variability in Spain: a quantitative and semiqualitative analysis using reservoir sedimentation rates. Geomorphology 50(4), 327–348.

Vittorini, S., 1977. Osservazioni sulle origini e sul ruolo di due forme di erosione nelle argille: calanchi e biancane. Boll. Soc. Geogr. Ital. (Serie 10) 6, 25–54.

Walling, D.E., 1983. The sediment delivery problem. Journal of Hydrology 65, 209–37.

Walling, D.E., 1991. Drainage basin studies. InSlaymaker,O. (Ed.), Field experiments and measurement programs in Geomorphology. Rotterdam, Balkema, 17–60.

Wang, H. B., Sassa, K., 2006. Rainfall-induced landslide hazard assessment using artificial neural networks. Earth Surf Proc Land, 31, 235–247, DOI: 10.1002/esp.1236.

Wheater, H. S., Jakeman, A. J. and Beven, K. J., 1993. Progress and direction in rainfall-runoff modelling. Proceedings of International Congress on Modelling and Simulation, December 6-10, 1993, University of Western Autralia, 1, 101-132.

Wilson, J.P., Gallant, J.C. 2000. Terrain analysis: principles and applications. Wiley & Sons, Inc., Canada

Williams, J.R., H.D.Berndt. 1977. Sediment yield prediction based on watershed hydrology. Trans. Of the ASAE. pp 1100-1104.

Wischmeier, W.H., Smith, D.D., 1978. Predicting rainfall erosion losses: a guide to conservation planning. Agriculture Handbook No. 537, US Department of Agriculture: Washington DC.

Young, R.A., Onstad, C.A., Bosch, D.D., Anderson, W.P.. 1989. AGNPS: A nonpoint-source pollution model for evaluating agricultural watersheds. Journal of Soil and Water Conservation 44(2), 168–173.

Yu, B., Rose, C.W., Cielsiolka, C.A.A., Coughlan, K.J., Fentie, B., 1997. Towards a framework for runoff and soil loss prediction using GUEST technology. Australian Journal of Soil Research 35, 1191–1212.

Zachar, D., 1982. Soil Erosion. Elsevier, Amsterdam.

Zêzere, J.L., Trigo, R.M., Trigo, I.F., 2004. Shallow and deep landslides induced by rainfall in the Lisbon region (Portugal): assessment of relationships with the North Atlantic Oscillation Source. Nat Hazards Earth Sys, 5(3), 331–344.

Zhang, L., O'Neill, A.L., Lacey, S., 1996. Modelling approaches to the prediction of soil erosion in catchments. Environmental Software 11, 123-133.

Zukowskyj, P.M. and Teeuw, R.M., 2000. Interpolated Digital Elevation Models, Differential Global Positioning System Surveys and Digital Photogrammetry: A Quantitative Comparison of Accuracy from a Geomorphological Perspective. Proceedings of the 5th International Conference on GeoComputation, University of Greenwich, United Kingdom, 23 - 25 August 2000

http://labtopo.ing.unipg.it/ (January 10th, 2010)

CSIRO TOPOG Home page, http://www.clw.csiro.au/topog/intro/intro.html.

UNIVERSITA' DI ROMA "LA SAPIENZA"
DIPARTIMENTO DI SCIENZE DELLA TERRA
LABORATORIO SEDIMENTOLOGICO
Analisi Granulometrica

ANNEX 3

Analista: Francesca Vergari
Campagna: Toscana - Val d'Orcia
Longitudine: 724795
Sistema: UTM
Quota: 559 (s.l.m)

Data di prelievo: 21/05/2009
Campione: L1
Latitudine: 4768132
Datum: WGS84 32N

Phi	Micron	% Trattenuta	% Cumulata
-1,00	2000,00	0,00	0,00
-0,50	1414,00	0,00	0,00
0,00	1000,00	0,00	0,00
0,50	707,00	0,00	0,00
1,00	500,00	0,00	0,00
1,50	354,00	0,00	0,00
2,00	250,00	0,00	0,00
2,50	177,00	0,00	0,00
3,00	125,00	0,00	0,00
3,50	88,00	0,00	0,00
4,00	62,00	1,25	1,25
4,25	53,00	1,36	2,61
4,50	44,00	1,86	4,47
4,75	37,00	2,28	6,75
5,00	31,00	3,15	9,90
5,25	26,00	3,55	13,45
5,50	22,00	3,51	16,96
5,75	19,00	3,34	20,30
6,00	16,00	4,21	24,51
6,25	13,00	5,52	30,03
6,50	11,00	5,85	35,88
6,75	9,00	4,99	40,87
7,00	8,00	4,63	45,50
7,25	7,00	5,28	50,78
7,50	6,00	5,53	56,31
7,75	5,00	5,24	61,55
8,00	4,00	5,52	67,07
8,25	3,00	5,37	72,44
8,50	2,76	4,14	76,58
8,75	2,00	3,75	80,33
9,00	1,95	4,02	84,35
11,00	0,49	15,65	100,00

Parametri Statistici Folk e Ward, 1957		Popolazioni Wentworth, 1922	
Media	7,21	Popolazione > 2 mm	00,00 %
Classamento	1,63	Sabbia	01,25 %
Asimmetria	-0,04	Limo	65,82 %
Appuntimento	0,84	Argilla	32,93 %

Percentili	Phi	Micron
1	3,97	63,80
5	4,57	42,20
16	5,44	23,10
25	6,02	15,40
50	7,21	6,70
75	8,40	3,00
84	8,98	2,00
95	9,47	1,40

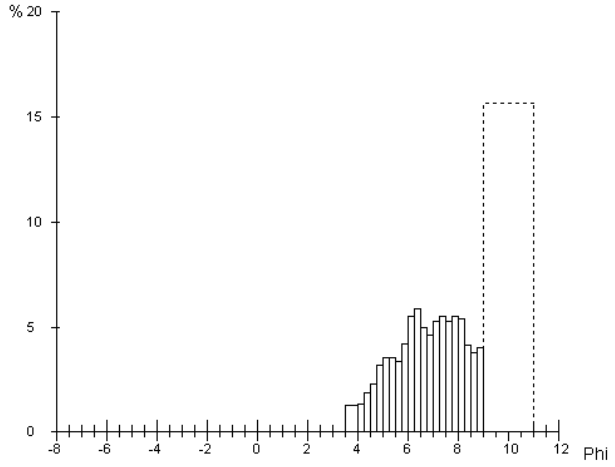

UNIVERSITA' DI ROMA "LA SAPIENZA"
DIPARTIMENTO DI SCIENZE DELLA TERRA
LABORATORIO SEDIMENTOLOGICO
Analisi Granulometrica

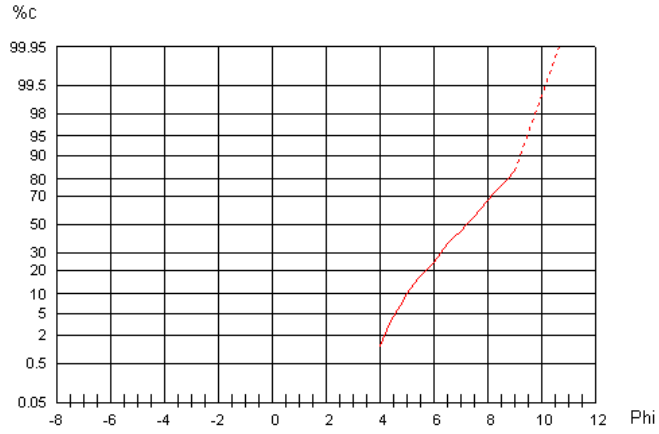

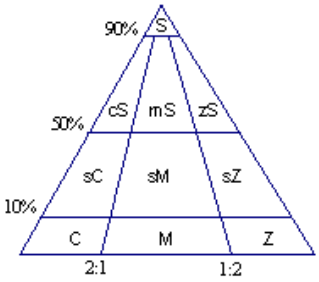

S	Sabbia
cS	Sabbia argillosa
mS	Sabbia fangosa
zS	Sabbia limosa
sC	Argilla sabbiosa
sM	Fango sabbioso
sZ	Limo sabbioso
C	Argilla
M	Fango
Z	Limo

(Folk, 1954)

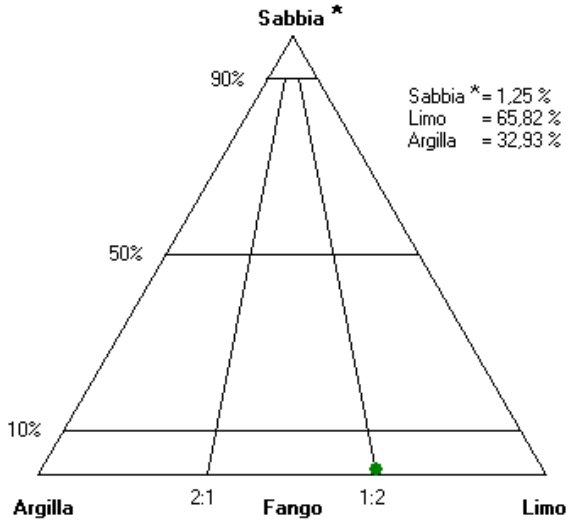

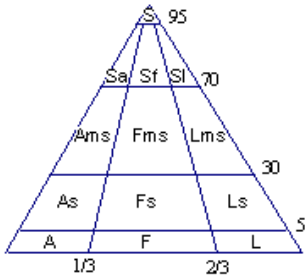

S	Sabbia
Sa	Sabbia argillosa
Sf	Sabbia fangosa
Sl	Sabbia limosa
Ams	Argilla molto sabbiosa
Fms	Fango molto sabbioso
Lms	Limo molto sabbioso
As	Argilla sabbiosa
Fs	Fango sabbioso
Ls	Limo sabbioso
A	Argilla
F	Fango
L	Limo

(Tortora, 1999)

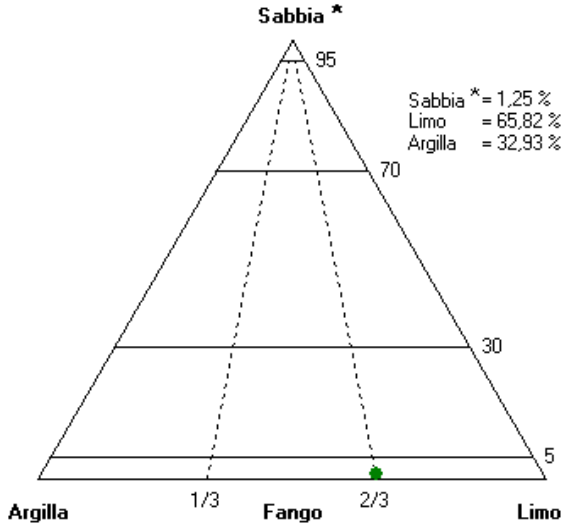

* comprensiva dell'eventuale frazione maggiore di 2 mm.

UNIVERSITA' DI ROMA "LA SAPIENZA"
DIPARTIMENTO DI SCIENZE DELLA TERRA
LABORATORIO SEDIMENTOLOGICO
Analisi Granulometrica

Analista: Francesca Vergari
Campagna: Toscana - Val d'Orcia
Longitudine: 724795
Sistema: UTM
Quota: 559 (s.l.m)

Data di prelievo: 21/05/2009
Campione: L1A
Latitudine: 4768132
Datum: UTM WGS84 32T

Phi	Micron	% Trattenuta	% Cumulata
-1,00	2000,00	0,00	0,00
-0,50	1414,00	0,00	0,00
0,00	1000,00	0,00	0,00
0,50	707,00	0,00	0,00
1,00	500,00	0,00	0,00
1,50	354,00	0,00	0,00
2,00	250,00	0,00	0,00
2,50	177,00	0,00	0,00
3,00	125,00	0,00	0,00
3,50	88,00	0,00	0,00
4,00	62,00	0,28	0,28
4,25	53,00	0,68	0,96
4,50	44,00	1,09	2,05
4,75	37,00	1,49	3,54
5,00	31,00	2,16	5,70
5,25	26,00	2,47	8,17
5,50	22,00	2,56	10,73
5,75	19,00	2,65	13,38
6,00	16,00	3,53	16,91
6,25	13,00	4,65	21,56
6,50	11,00	4,86	26,42
6,75	9,00	4,07	30,49
7,00	8,00	3,82	34,31
7,25	7,00	4,60	38,91
7,50	6,00	5,15	44,06
7,75	5,00	5,27	49,33
8,00	4,00	5,97	55,30
8,25	3,00	6,15	61,45
8,50	2,76	5,04	66,49
8,75	2,00	4,83	71,32
9,00	1,95	5,41	76,73
11,00	0,49	23,27	100,00

Parametri Statistici Folk e Ward, 1957		Popolazioni Wentworth, 1922	
Media	7,63	Popolazione > 2 mm	00,00 %
Classamento	1,52	Sabbia	00,28 %
Asimmetria	-0,18	Limo	55,02 %
Appuntimento	0,77	Argilla	44,70 %

Percentili	Phi	Micron
1	4,26	52,10
5	4,93	32,80
16	5,94	16,30
25	6,43	11,60
50	7,78	4,60
75	8,92	2,10
84	9,18	1,70
95	9,61	1,30

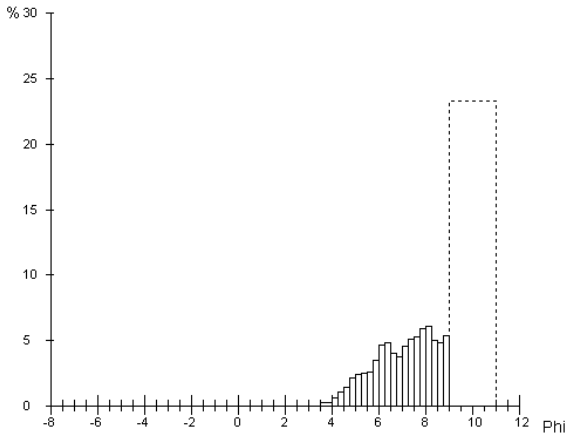

UNIVERSITA' DI ROMA "LA SAPIENZA"
DIPARTIMENTO DI SCIENZE DELLA TERRA
LABORATORIO SEDIMENTOLOGICO
Analisi Granulometrica

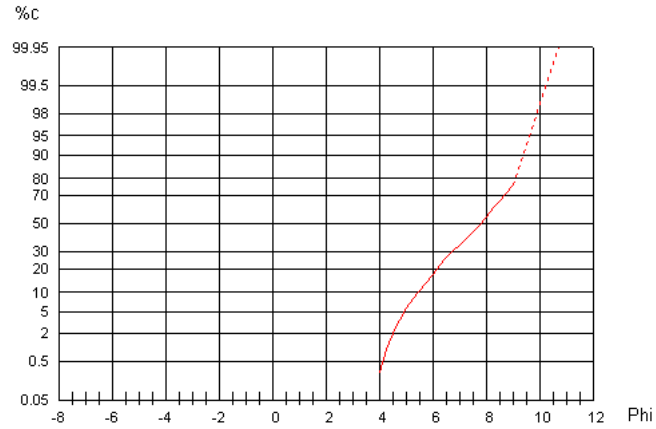

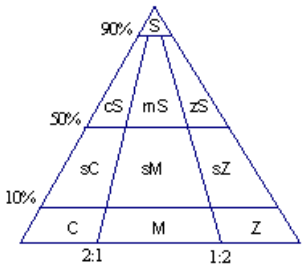

S	Sabbia
cS	Sabbia argillosa
mS	Sabbia fangosa
zS	Sabbia limosa
sC	Argilla sabbiosa
sM	Fango sabbioso
sZ	Limo sabbioso
C	Argilla
M	Fango
Z	Limo

(Folk, 1954)

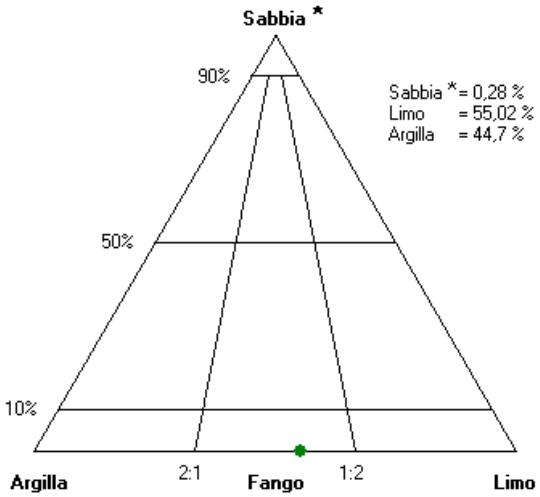

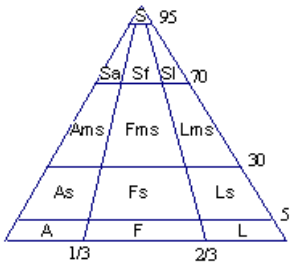

S	Sabbia
Sa	Sabbia argillosa
Sf	Sabbia fangosa
Sl	Sabbia limosa
Ams	Argilla molto sabbiosa
Fms	Fango molto sabbioso
Lms	Limo molto sabbioso
As	Argilla sabbiosa
Fs	Fango sabbioso
Ls	Limo sabbioso
A	Argilla
F	Fango
L	Limo

(Tortora, 1999)

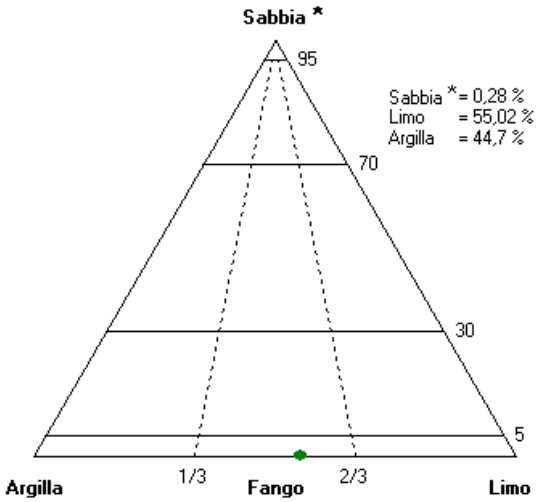

* comprensiva dell'eventuale frazione maggiore di 2 mm.

UNIVERSITA' DI ROMA "LA SAPIENZA"
DIPARTIMENTO DI SCIENZE DELLA TERRA
LABORATORIO SEDIMENTOLOGICO
Analisi Granulometrica

Analista: Francesca Vergari
Campagna: Toscana - Val d'Orcia
Longitudine: 724795
Sistema: UTM
Quota: 559 (s.l.m)

Data di prelievo: 21/05/2009
Campione: L1B
Latitudine: 4768132
Datum: UTM WGS84 32T

Phi	Micron	% Trattenuta	% Cumulata
-1,00	2000,00	0,00	0,00
-0,50	1414,00	0,00	0,00
0,00	1000,00	0,00	0,00
0,50	707,00	0,00	0,00
1,00	500,00	0,00	0,00
1,50	354,00	0,00	0,00
2,00	250,00	0,00	0,00
2,50	177,00	0,00	0,00
3,00	125,00	0,00	0,00
3,50	88,00	0,00	0,00
4,00	62,00	0,37	0,37
4,25	53,00	0,79	1,16
4,50	44,00	1,23	2,39
4,75	37,00	1,65	4,04
5,00	31,00	2,36	6,40
5,25	26,00	2,72	9,12
5,50	22,00	2,80	11,92
5,75	19,00	2,83	14,75
6,00	16,00	3,68	18,43
6,25	13,00	4,76	23,19
6,50	11,00	4,92	28,11
6,75	9,00	4,07	32,18
7,00	8,00	3,77	35,95
7,25	7,00	4,50	40,45
7,50	6,00	5,03	45,48
7,75	5,00	5,13	50,61
8,00	4,00	5,81	56,42
8,25	3,00	5,98	62,40
8,50	2,76	4,91	67,31
8,75	2,00	4,70	72,01
9,00	1,95	5,27	77,28
11,00	0,49	22,72	100,00

Parametri Statistici Folk e Ward, 1957		Popolazioni Wentworth, 1922	
Media	7,58	Popolazione > 2 mm	00,00 %
Classamento	1,55	Sabbia	00,37 %
Asimmetria	-0,17	Limo	56,05 %
Appuntimento	0,76	Argilla	43,58 %

Percentili	Phi	Micron
1	4,22	53,80
5	4,86	34,40
16	5,84	17,50
25	6,34	12,30
50	7,72	4,70
75	8,89	2,10
84	9,17	1,70
95	9,60	1,30

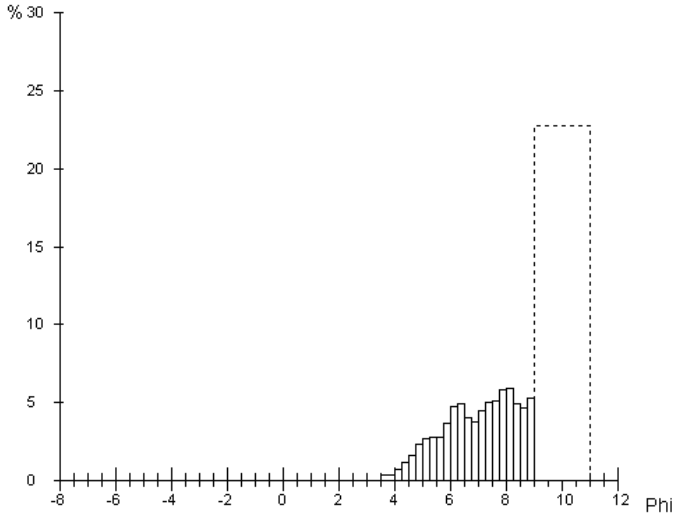

UNIVERSITA' DI ROMA "LA SAPIENZA"
DIPARTIMENTO DI SCIENZE DELLA TERRA
LABORATORIO SEDIMENTOLOGICO
Analisi Granulometrica

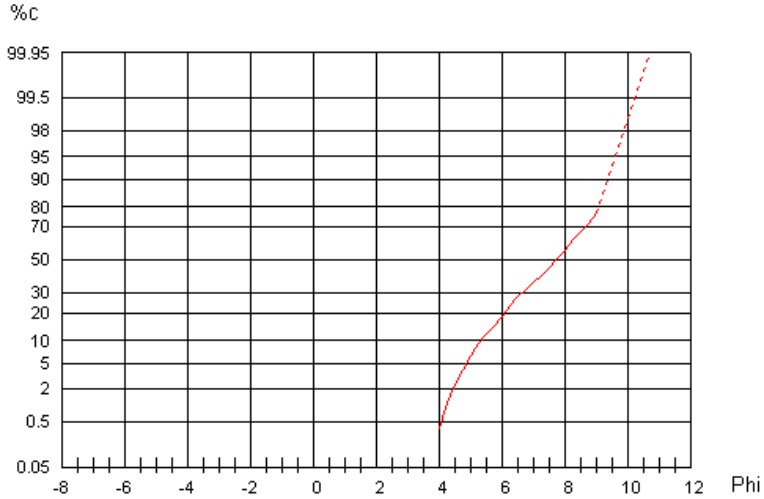

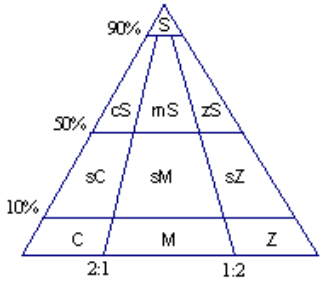

S	Sabbia
cS	Sabbia argillosa
mS	Sabbia fangosa
zS	Sabbia limosa
sC	Argilla sabbiosa
sM	Fango sabbioso
sZ	Limo sabbioso
C	Argilla
M	Fango
Z	Limo

(Folk, 1954)

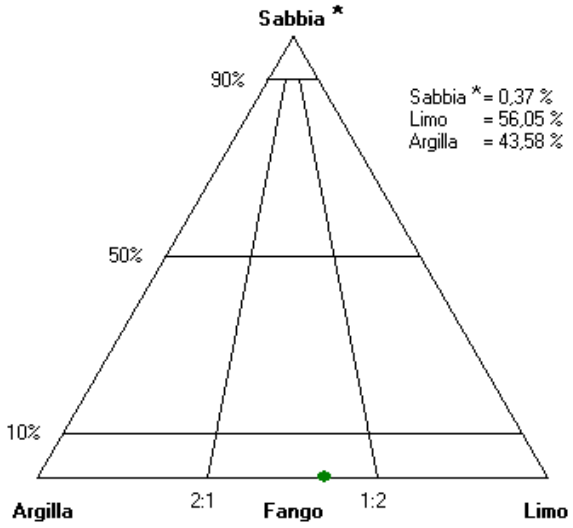

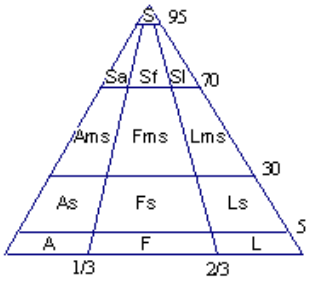

S	Sabbia
Sa	Sabbia argillosa
Sf	Sabbia fangosa
Sl	Sabbia limosa
Ams	Argilla molto sabbiosa
Fms	Fango molto sabbioso
Lms	Limo molto sabbioso
As	Argilla sabbiosa
Fs	Fango sabbioso
Ls	Limo sabbioso
A	Argilla
F	Fango
L	Limo

(Tortora, 1999)

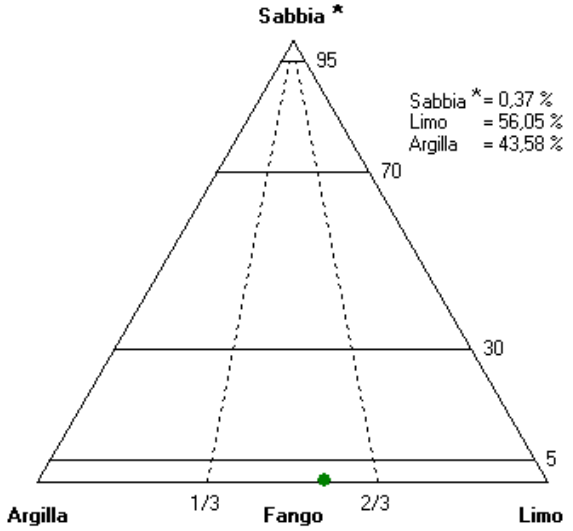

* comprensiva dell'eventuale frazione maggiore di 2 mm.

UNIVERSITA' DI ROMA "LA SAPIENZA"
DIPARTIMENTO DI SCIENZE DELLA TERRA
LABORATORIO SEDIMENTOLOGICO
Analisi Granulometrica

Analista: Francesca Vergari
Campagna: Toscana - Val d'Orcia
Longitudine: 724799
Sistema: UTM
Quota: 556 (s.l.m)

Data di prelievo: 21/05/2009
Campione: L2A
Latitudine: 4768132
Datum: WGS84 32N

Phi	Micron	% Trattenuta	% Cumulata
-1,00	2000,00	0,00	0,00
-0,50	1414,00	0,00	0,00
0,00	1000,00	0,00	0,00
0,50	707,00	0,00	0,00
1,00	500,00	0,00	0,00
1,50	354,00	0,00	0,00
2,00	250,00	0,00	0,00
2,50	177,00	0,00	0,00
3,00	125,00	0,00	0,00
3,50	88,00	0,00	0,00
4,00	62,00	0,02	0,02
4,25	53,00	0,18	0,20
4,50	44,00	0,45	0,65
4,75	37,00	0,78	1,43
5,00	31,00	1,29	2,72
5,25	26,00	1,55	4,27
5,50	22,00	1,65	5,92
5,75	19,00	1,84	7,76
6,00	16,00	2,72	10,48
6,25	13,00	3,82	14,30
6,50	11,00	4,16	18,46
6,75	9,00	3,66	22,12
7,00	8,00	3,66	25,78
7,25	7,00	4,69	30,47
7,50	6,00	5,50	35,97
7,75	5,00	5,79	41,76
8,00	4,00	6,70	48,46
8,25	3,00	6,98	55,44
8,50	2,76	5,77	61,21
8,75	2,00	5,56	66,77
9,00	1,95	6,24	73,01
11,00	0,49	26,99	100,00

Parametri Statistici Folk e Ward, 1957		Popolazioni Wentworth, 1922	
Media	7,89	Popolazione > 2 mm	00,00 %
Classamento	1,37	Sabbia	00,02 %
Asimmetria	-0,21	Limo	48,44 %
Appuntimento	0,84	Argilla	51,54 %

Percentili	Phi	Micron
1	4,63	40,30
5	5,37	24,20
16	6,36	12,20
25	6,95	8,10
50	8,06	3,80
75	9,04	1,90
84	9,25	1,60
95	9,66	1,20

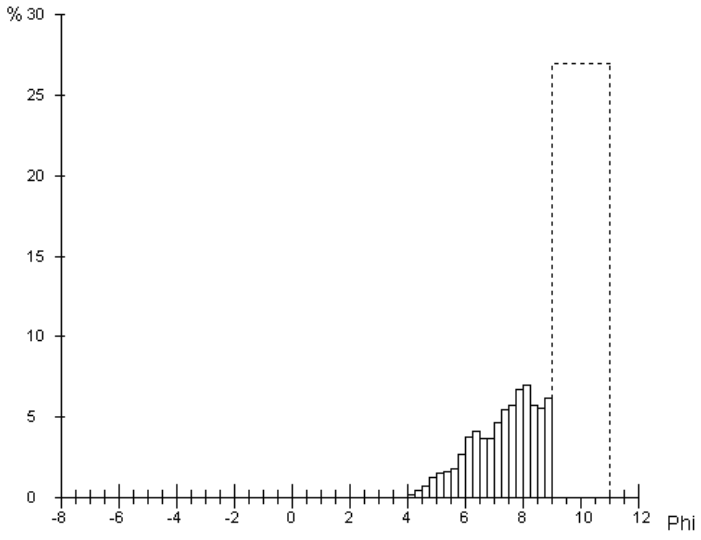

UNIVERSITA' DI ROMA "LA SAPIENZA"
DIPARTIMENTO DI SCIENZE DELLA TERRA
LABORATORIO SEDIMENTOLOGICO
Analisi Granulometrica

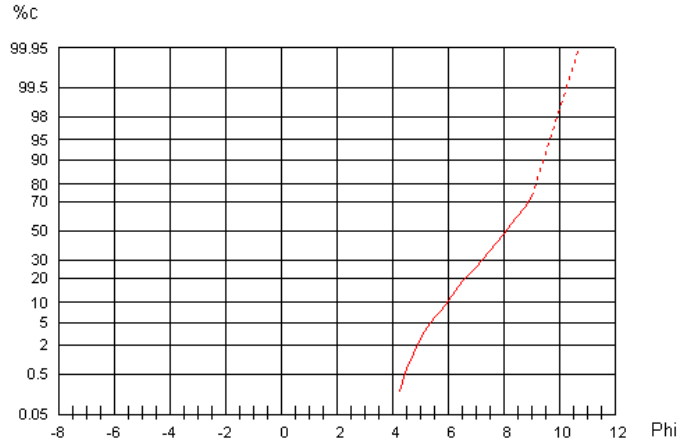

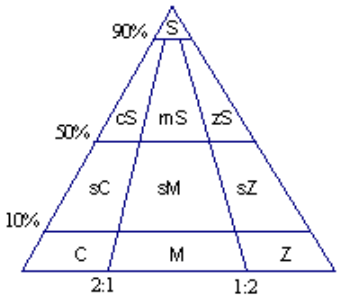

S	Sabbia
cS	Sabbia argillosa
mS	Sabbia fangosa
zS	Sabbia limosa
sC	Argilla sabbiosa
sM	Fango sabbioso
sZ	Limo sabbioso
C	Argilla
M	Fango
Z	Limo

(Folk, 1954)

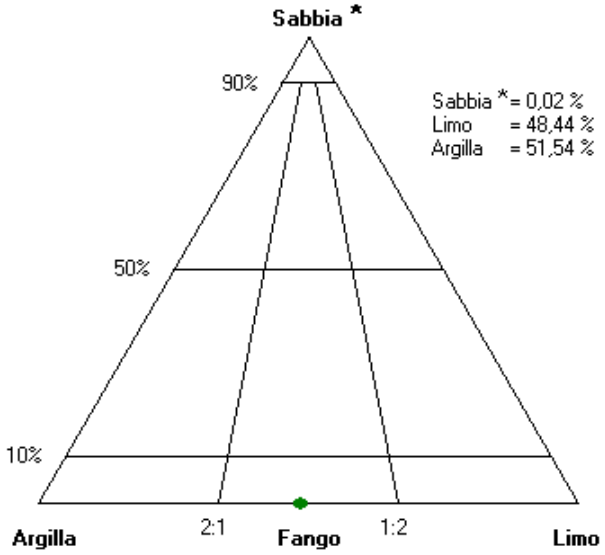

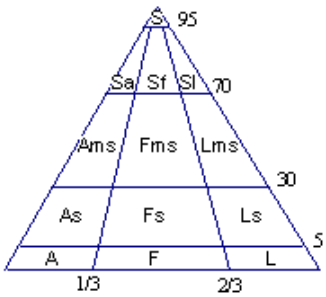

S	Sabbia
Sa	Sabbia argillosa
Sf	Sabbia fangosa
Sl	Sabbia limosa
Ams	Argilla molto sabbiosa
Fms	Fango molto sabbioso
Lms	Limo molto sabbioso
As	Argilla sabbiosa
Fs	Fango sabbioso
Ls	Limo sabbioso
A	Argilla
F	Fango
L	Limo

(Tortora, 1999)

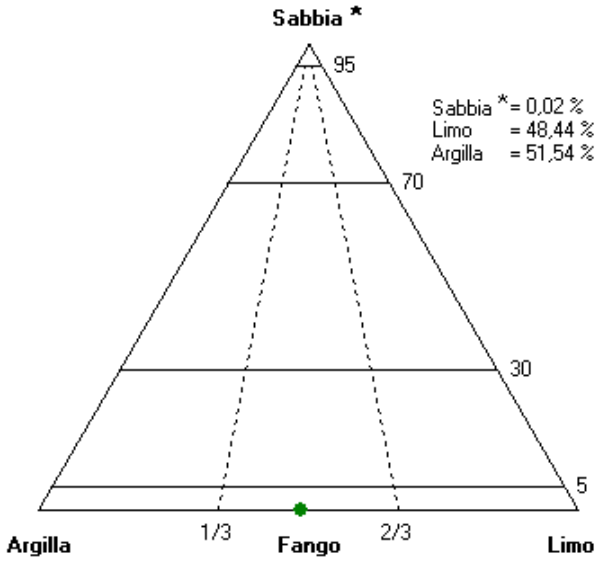

* comprensiva dell'eventuale frazione maggiore di 2 mm.

UNIVERSITA' DI ROMA "LA SAPIENZA"
DIPARTIMENTO DI SCIENZE DELLA TERRA
LABORATORIO SEDIMENTOLOGICO
Analisi Granulometrica

Analista: Francesca Vergari
Campagna: Toscana - Val d'Orcia
Longitudine: 724799
Sistema: UTM
Quota: 556 (s.l.m)

Data di prelievo: 21/05/2009
Campione: L2FA
Latitudine: 4768132
Datum: WGS84 32N

Phi	Micron	% Trattenuta	% Cumulata
-1,00	2000,00	0,00	0,00
-0,50	1414,00	0,00	0,00
0,00	1000,00	0,00	0,00
0,50	707,00	0,00	0,00
1,00	500,00	0,00	0,00
1,50	354,00	0,00	0,00
2,00	250,00	0,00	0,00
2,50	177,00	0,00	0,00
3,00	125,00	0,00	0,00
3,50	88,00	0,00	0,00
4,00	62,00	0,00	0,00
4,25	53,00	0,07	0,07
4,50	44,00	0,37	0,44
4,75	37,00	0,79	1,23
5,00	31,00	1,40	2,63
5,25	26,00	1,76	4,39
5,50	22,00	1,94	6,33
5,75	19,00	2,18	8,51
6,00	16,00	3,18	11,69
6,25	13,00	4,42	16,11
6,50	11,00	4,81	20,92
6,75	9,00	4,20	25,12
7,00	8,00	4,09	29,21
7,25	7,00	5,02	34,23
7,50	6,00	5,69	39,92
7,75	5,00	5,82	45,74
8,00	4,00	6,57	52,31
8,25	3,00	6,73	59,04
8,50	2,76	5,48	64,52
8,75	2,00	5,20	69,72
9,00	1,95	5,77	75,49
11,00	0,49	24,51	100,00

Parametri Statistici Folk e Ward, 1957		Popolazioni Wentworth, 1922	
Media	7,79	Popolazione > 2 mm	00,00 %
Classamento	1,39	Sabbia	00,00 %
Asimmetria	-0,16	Limo	52,31 %
Appuntimento	0,79	Argilla	47,69 %

Percentili	Phi	Micron
1	4,70	38,60
5	5,34	24,70
16	6,24	13,20
25	6,74	9,30
50	7,91	4,20
75	8,98	2,00
84	9,20	1,70
95	9,63	1,30

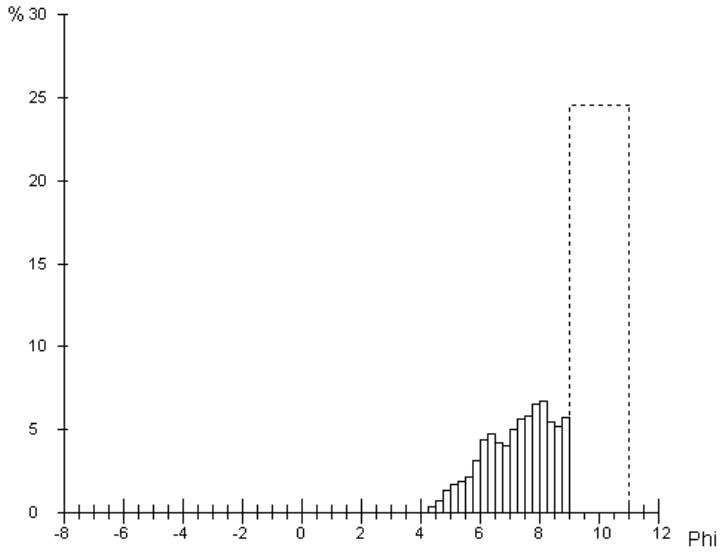

UNIVERSITA' DI ROMA "LA SAPIENZA"
DIPARTIMENTO DI SCIENZE DELLA TERRA
LABORATORIO SEDIMENTOLOGICO
Analisi Granulometrica

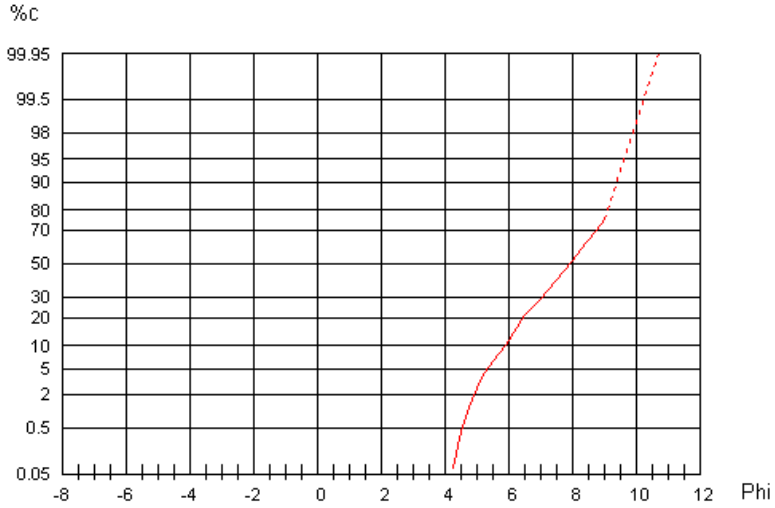

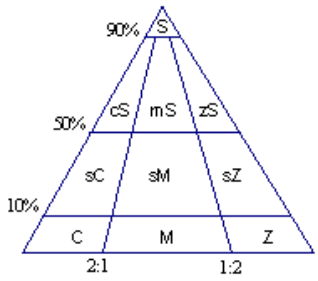

S	Sabbia
cS	Sabbia argillosa
mS	Sabbia fangosa
zS	Sabbia limosa
sC	Argilla sabbiosa
sM	Fango sabbioso
sZ	Limo sabbioso
C	Argilla
M	Fango
Z	Limo

(Folk, 1954)

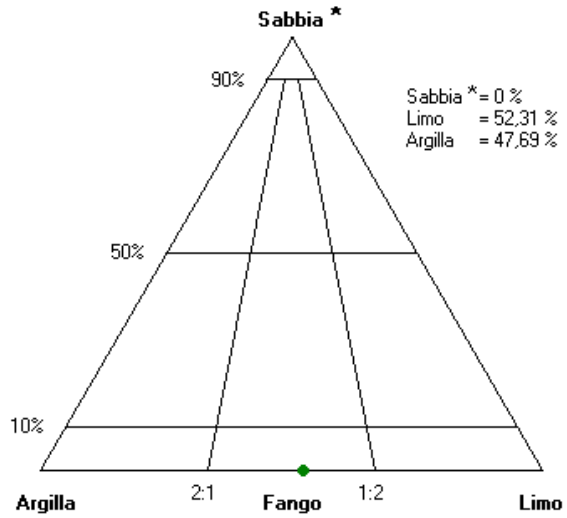

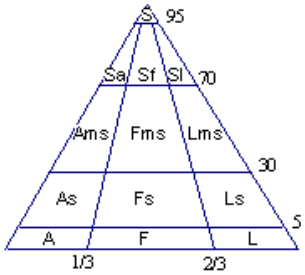

S	Sabbia
Sa	Sabbia argillosa
Sf	Sabbia fangosa
Sl	Sabbia limosa
Ams	Argilla molto sabbiosa
Fms	Fango molto sabbioso
Lms	Limo molto sabbioso
As	Argilla sabbiosa
Fs	Fango sabbioso
Ls	Limo sabbioso
A	Argilla
F	Fango
L	Limo

(Tortora, 1999)

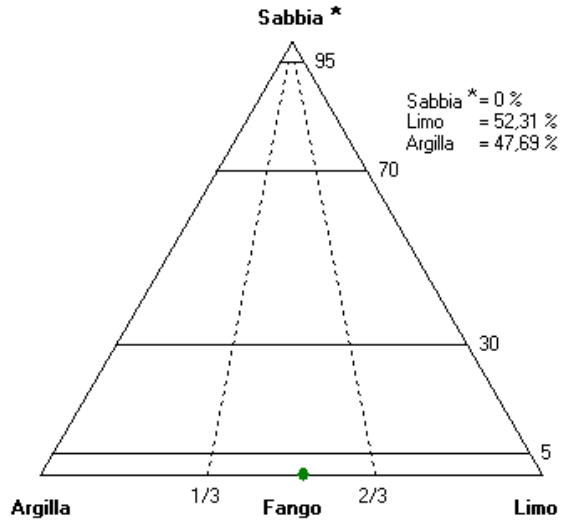

* comprensiva dell'eventuale frazione maggiore di 2 mm.

X

UNIVERSITA' DI ROMA "LA SAPIENZA"
DIPARTIMENTO DI SCIENZE DELLA TERRA
LABORATORIO SEDIMENTOLOGICO
Analisi Granulometrica

Analista: Francesca Vergari
Campagna: Toscana - Val d'Orcia
Longitudine: 724799
Sistema: UTM
Quota: 556 (s.l.m)

Data di prelievo: 21/05/2009
Campione: L2FB
Latitudine: 4768132
Datum: WGS84 32N

Phi	Micron	% Trattenuta	% Cumulata
-1,00	2000,00	0,00	0,00
-0,50	1414,00	0,00	0,00
0,00	1000,00	0,00	0,00
0,50	707,00	0,00	0,00
1,00	500,00	0,00	0,00
1,50	354,00	0,00	0,00
2,00	250,00	0,00	0,00
2,50	177,00	0,00	0,00
3,00	125,00	0,00	0,00
3,50	88,00	0,00	0,00
4,00	62,00	0,43	0,43
4,25	53,00	0,53	0,96
4,50	44,00	0,78	1,74
4,75	37,00	1,21	2,95
5,00	31,00	1,90	4,85
5,25	26,00	2,21	7,06
5,50	22,00	2,24	9,30
5,75	19,00	2,29	11,59
6,00	16,00	3,17	14,76
6,25	13,00	4,38	19,14
6,50	11,00	4,81	23,95
6,75	9,00	4,29	28,24
7,00	8,00	4,24	32,48
7,25	7,00	5,23	37,71
7,50	6,00	5,86	43,57
7,75	5,00	5,89	49,46
8,00	4,00	6,53	55,99
8,25	3,00	6,57	62,56
8,50	2,76	5,26	67,82
8,75	2,00	4,89	72,71
9,00	1,95	5,36	78,07
11,00	0,49	21,93	100,00

Parametri Statistici Folk e Ward, 1957		Popolazioni Wentworth, 1922	
Media	7,67	Popolazione > 2 mm	00,00 %
Classamento	1,46	Sabbia	00,43 %
Asimmetria	-0,15	Limo	55,56 %
Appuntimento	0,82	Argilla	44,01 %

Percentili	Phi	Micron
1	4,27	52,00
5	5,02	30,80
16	6,08	14,80
25	6,56	10,60
50	7,77	4,60
75	8,85	2,20
84	9,15	1,80
95	9,59	1,30

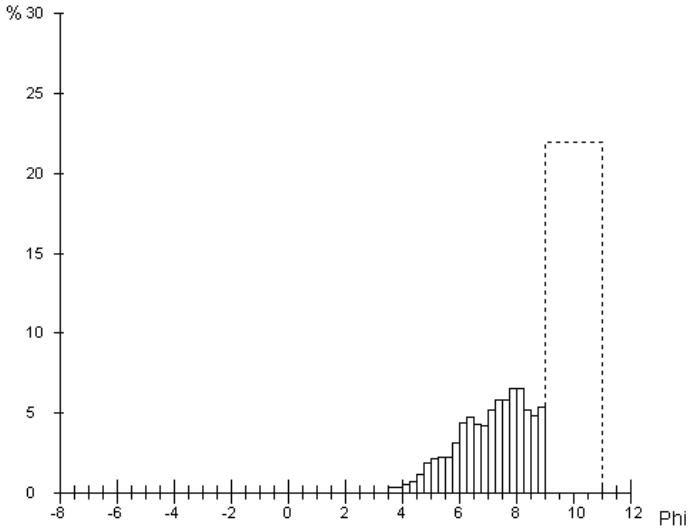

UNIVERSITA' DI ROMA "LA SAPIENZA"
DIPARTIMENTO DI SCIENZE DELLA TERRA
LABORATORIO SEDIMENTOLOGICO
Analisi Granulometrica

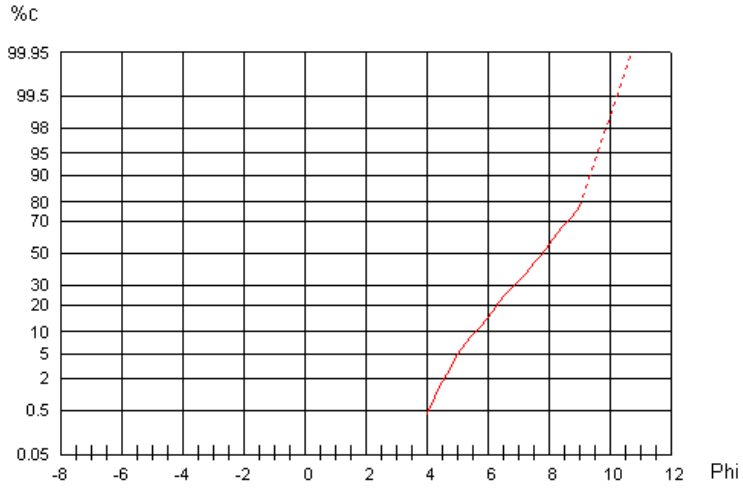

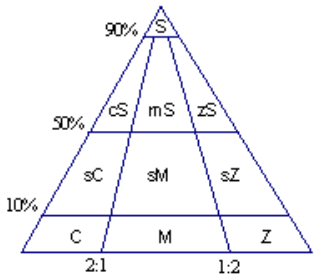

S	Sabbia
cS	Sabbia argillosa
mS	Sabbia fangosa
zS	Sabbia limosa
sC	Argilla sabbiosa
sM	Fango sabbioso
sZ	Limo sabbioso
C	Argilla
M	Fango
Z	Limo

(Folk, 1954)

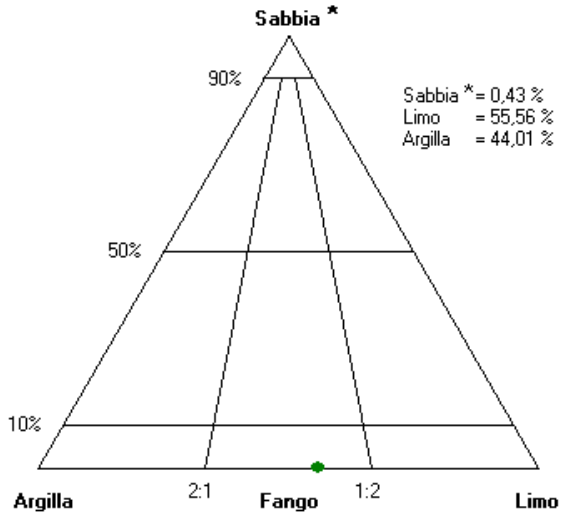

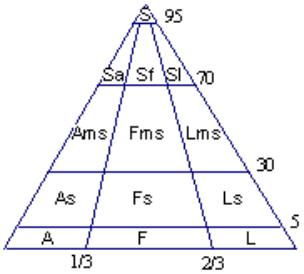

S	Sabbia
Sa	Sabbia argillosa
Sf	Sabbia fangosa
Sl	Sabbia limosa
Ams	Argilla molto sabbiosa
Fms	Fango molto sabbioso
Lms	Limo molto sabbioso
As	Argilla sabbiosa
Fs	Fango sabbioso
Ls	Limo sabbioso
A	Argilla
F	Fango
L	Limo

(Tortora, 1999)

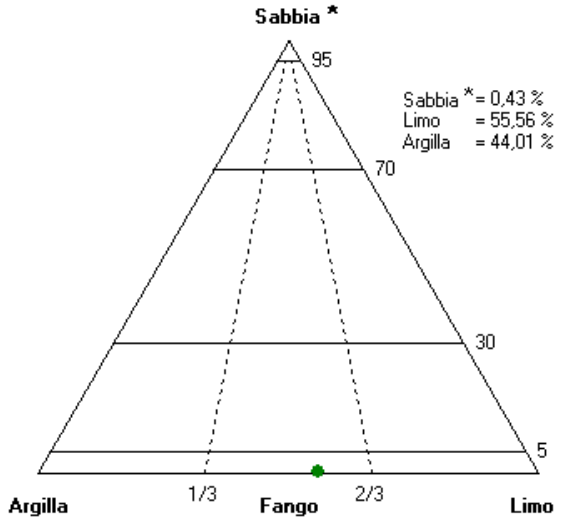

* comprensiva dell'eventuale frazione maggiore di 2 mm.

UNIVERSITA' DI ROMA "LA SAPIENZA"
DIPARTIMENTO DI SCIENZE DELLA TERRA
LABORATORIO SEDIMENTOLOGICO
Analisi Granulometrica

Analista: Francesca Vergari
Campagna: Toscana - Val d'Orcia
Longitudine: 724799
Sistema: UTM
Quota: 556 (s.l.m)

Data di prelievo: 21/05/2009
Campione: L2FC
Latitudine: 4768132
Datum: WGS84 32N

Phi	Micron	% Trattenuta	% Cumulata
-1,00	2000,00	0,00	0,00
-0,50	1414,00	0,00	0,00
0,00	1000,00	0,00	0,00
0,50	707,00	0,00	0,00
1,00	500,00	0,00	0,00
1,50	354,00	0,00	0,00
2,00	250,00	0,00	0,00
2,50	177,00	0,00	0,00
3,00	125,00	0,00	0,00
3,50	88,00	0,00	0,00
4,00	62,00	0,08	0,08
4,25	53,00	0,30	0,38
4,50	44,00	0,63	1,01
4,75	37,00	1,01	2,02
5,00	31,00	1,58	3,60
5,25	26,00	1,89	5,49
5,50	22,00	2,03	7,52
5,75	19,00	2,22	9,74
6,00	16,00	3,14	12,88
6,25	13,00	4,29	17,17
6,50	11,00	4,58	21,75
6,75	9,00	3,92	25,67
7,00	8,00	3,79	29,46
7,25	7,00	4,67	34,13
7,50	6,00	5,34	39,47
7,75	5,00	5,55	45,02
8,00	4,00	6,37	51,39
8,25	3,00	6,60	57,99
8,50	2,76	5,44	63,43
8,75	2,00	5,23	68,66
9,00	1,95	5,88	74,54
11,00	0,49	25,46	100,00

Parametri Statistici Folk e Ward, 1957		Popolazioni Wentworth, 1922	
Media	7,78	Popolazione > 2 mm	00,00 %
Classamento	1,43	Sabbia	00,08 %
Asimmetria	-0,20	Limo	51,31 %
Appuntimento	0,79	Argilla	48,61 %

Percentili	Phi	Micron
1	4,50	44,30
5	5,19	27,30
16	6,19	13,70
25	6,71	9,60
50	7,95	4,10
75	9,01	1,90
84	9,22	1,70
95	9,64	1,30

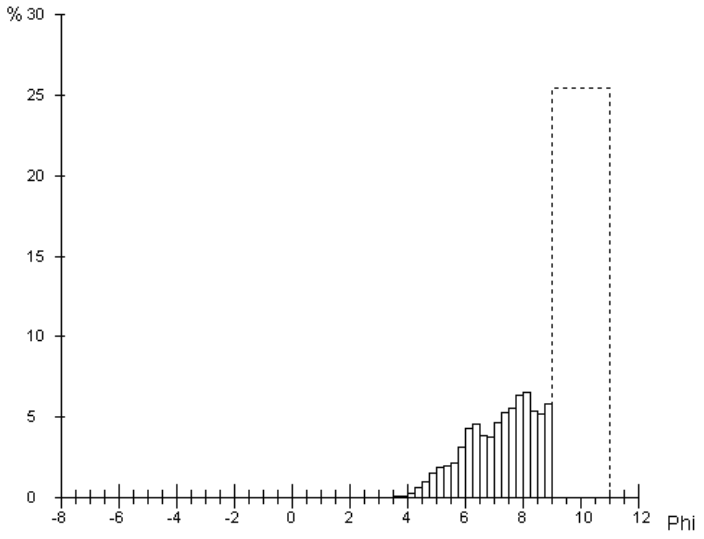

UNIVERSITA' DI ROMA "LA SAPIENZA"
DIPARTIMENTO DI SCIENZE DELLA TERRA
LABORATORIO SEDIMENTOLOGICO
Analisi Granulometrica

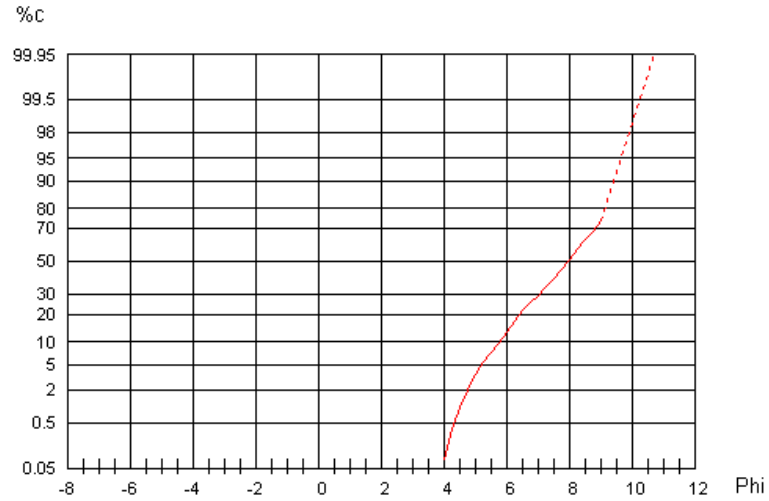

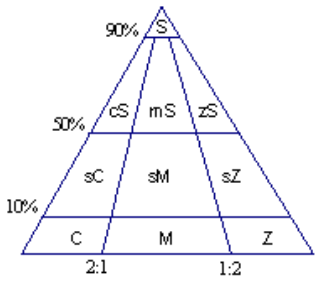

S	Sabbia
cS	Sabbia argillosa
mS	Sabbia fangosa
zS	Sabbia limosa
sC	Argilla sabbiosa
sM	Fango sabbioso
sZ	Limo sabbioso
C	Argilla
M	Fango
Z	Limo

(Folk, 1954)

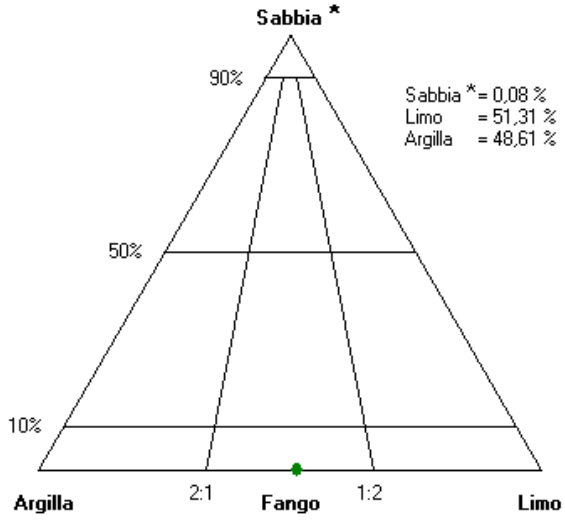

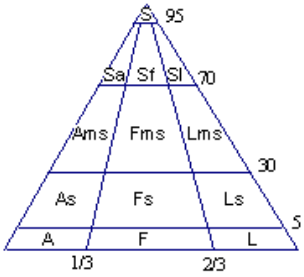

S	Sabbia
Sa	Sabbia argillosa
Sf	Sabbia fangosa
Sl	Sabbia limosa
Ams	Argilla molto sabbiosa
Fms	Fango molto sabbioso
Lms	Limo molto sabbioso
As	Argilla sabbiosa
Fs	Fango sabbioso
Ls	Limo sabbioso
A	Argilla
F	Fango
L	Limo

(Tortora, 1999)

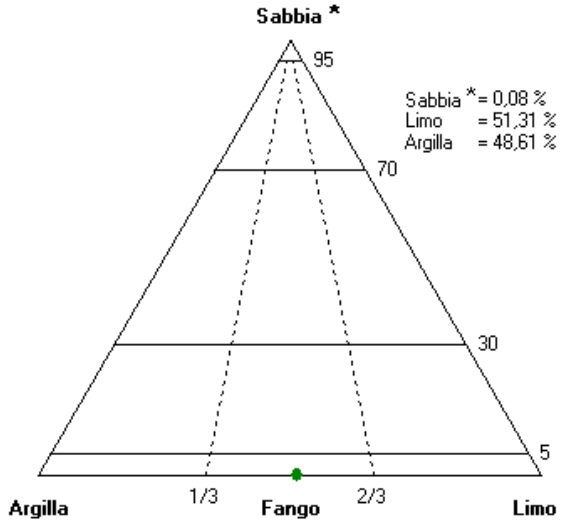

* comprensiva dell'eventuale frazione maggiore di 2 mm.

UNIVERSITA' DI ROMA "LA SAPIENZA"
DIPARTIMENTO DI SCIENZE DELLA TERRA
LABORATORIO SEDIMENTOLOGICO
Analisi Granulometrica

Analista: Francesca Vergari
Campagna: Toscana - Val d'Orcia
Longitudine: 724801
Sistema: UTM
Quota: 554 (s.l.m)

Data di prelievo: 21/05/2009
Campione: L3
Latitudine: 4768126
Datum: WGS84 32N

Phi	Micron	% Trattenuta	% Cumulata
-1,00	2000,00	0,00	0,00
-0,50	1414,00	0,00	0,00
0,00	1000,00	0,00	0,00
0,50	707,00	0,00	0,00
1,00	500,00	0,00	0,00
1,50	354,00	0,00	0,00
2,00	250,00	0,00	0,00
2,50	177,00	0,00	0,00
3,00	125,00	0,00	0,00
3,50	88,00	0,00	0,00
4,00	62,00	0,00	0,00
4,25	53,00	0,18	0,18
4,50	44,00	0,50	0,68
4,75	37,00	0,91	1,59
5,00	31,00	1,53	3,12
5,25	26,00	1,90	5,02
5,50	22,00	2,06	7,08
5,75	19,00	2,24	9,32
6,00	16,00	3,15	12,47
6,25	13,00	4,30	16,77
6,50	11,00	4,60	21,37
6,75	9,00	3,92	25,29
7,00	8,00	3,76	29,05
7,25	7,00	4,62	33,67
7,50	6,00	5,28	38,95
7,75	5,00	5,50	44,45
8,00	4,00	6,33	50,78
8,25	3,00	6,58	57,36
8,50	2,76	5,45	62,81
8,75	2,00	5,27	68,08
9,00	1,95	5,96	74,04
11,00	0,49	25,96	100,00

Parametri Statistici Folk e Ward, 1957		Popolazioni Wentworth, 1922	
Media	7,80	Popolazione > 2 mm	00,00 %
Classamento	1,42	Sabbia	00,00 %
Asimmetria	-0,20	Limo	50,78 %
Appuntimento	0,79	Argilla	49,22 %

Percentili	Phi	Micron
1	4,61	40,90
5	5,25	26,30
16	6,21	13,50
25	6,73	9,40
50	7,97	4,00
75	9,02	1,90
84	9,23	1,70
95	9,65	1,20

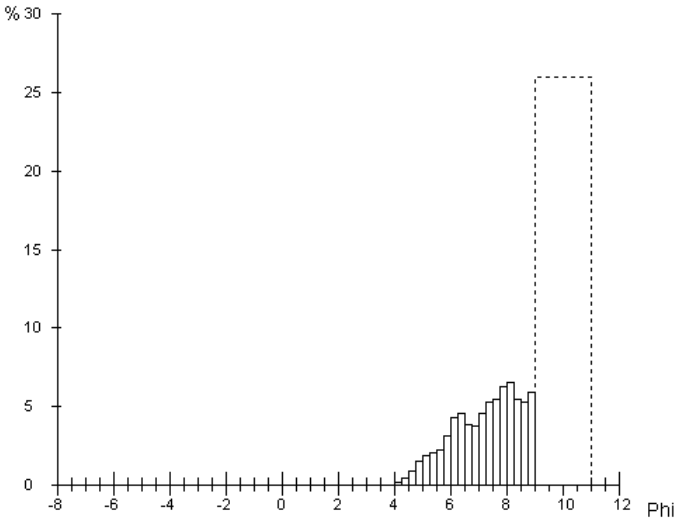

UNIVERSITA' DI ROMA "LA SAPIENZA"
DIPARTIMENTO DI SCIENZE DELLA TERRA
LABORATORIO SEDIMENTOLOGICO
Analisi Granulometrica

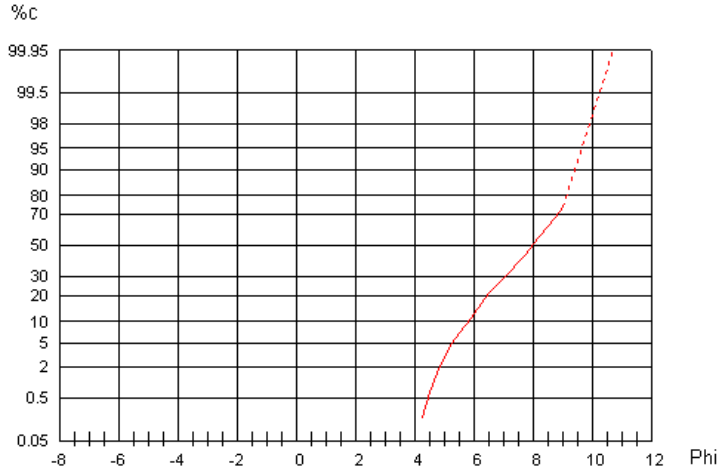

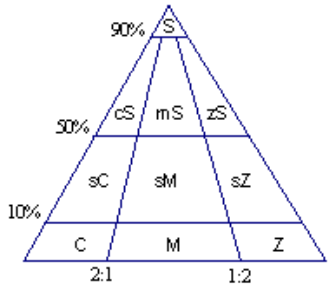

S	Sabbia
cS	Sabbia argillosa
mS	Sabbia fangosa
zS	Sabbia limosa
sC	Argilla sabbiosa
sM	Fango sabbioso
sZ	Limo sabbioso
C	Argilla
M	Fango
Z	Limo

(Folk, 1954)

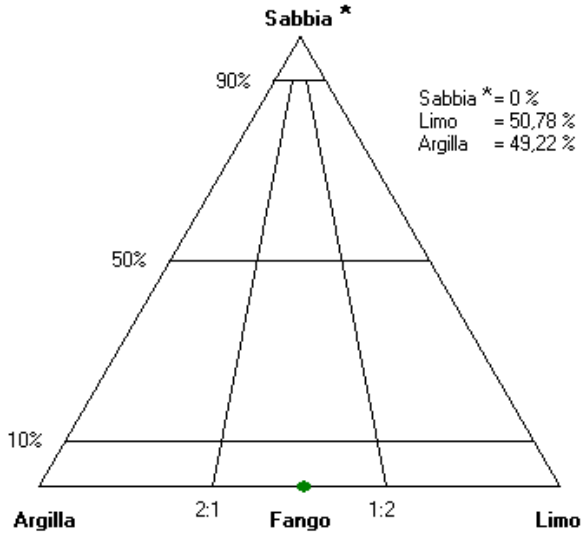

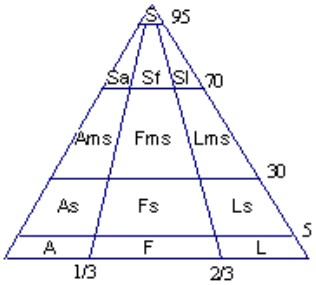

S	Sabbia
Sa	Sabbia argillosa
Sf	Sabbia fangosa
Sl	Sabbia limosa
Ams	Argilla molto sabbiosa
Fms	Fango molto sabbioso
Lms	Limo molto sabbioso
As	Argilla sabbiosa
Fs	Fango sabbioso
Ls	Limo sabbioso
A	Argilla
F	Fango
L	Limo

(Tortora, 1999)

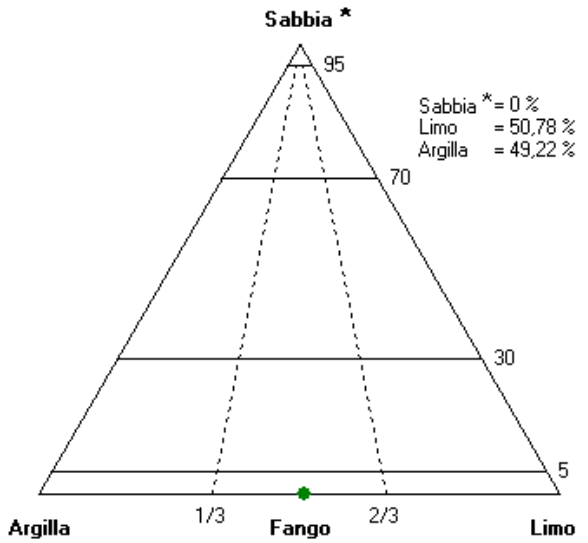

* comprensiva dell'eventuale frazione maggiore di 2 mm.

UNIVERSITA' DI ROMA "LA SAPIENZA"
DIPARTIMENTO DI SCIENZE DELLA TERRA
LABORATORIO SEDIMENTOLOGICO
Analisi Granulometrica

Analista: Francesca Vergari
Campagna: Toscana - Val d'Orcia
Longitudine: 724801
Sistema: UTM
Quota: 554 (s.l.m)

Data di prelievo: 21/05/2009
Campione: L3B
Latitudine: 4768126
Datum: WGS84 32N

Phi	Micron	% Trattenuta	% Cumulata
-1,00	2000,00	0,00	0,00
-0,50	1414,00	0,00	0,00
0,00	1000,00	0,00	0,00
0,50	707,00	0,00	0,00
1,00	500,00	0,00	0,00
1,50	354,00	0,00	0,00
2,00	250,00	0,00	0,00
2,50	177,00	0,00	0,00
3,00	125,00	0,00	0,00
3,50	88,00	0,00	0,00
4,00	62,00	0,12	0,12
4,25	53,00	0,40	0,52
4,50	44,00	0,76	1,28
4,75	37,00	1,15	2,43
5,00	31,00	1,78	4,21
5,25	26,00	2,11	6,32
5,50	22,00	2,22	8,54
5,75	19,00	2,34	10,88
6,00	16,00	3,23	14,11
6,25	13,00	4,35	18,46
6,50	11,00	4,63	23,09
6,75	9,00	3,93	27,02
7,00	8,00	3,74	30,76
7,25	7,00	4,56	35,32
7,50	6,00	5,19	40,51
7,75	5,00	5,38	45,89
8,00	4,00	6,18	52,07
8,25	3,00	6,43	58,50
8,50	2,76	5,32	63,82
8,75	2,00	5,14	68,96
9,00	1,95	5,77	74,73
11,00	0,49	25,27	100,00

Parametri Statistici Folk e Ward, 1957		Popolazioni Wentworth, 1922	
Media	7,75	Popolazione > 2 mm	00,00 %
Classamento	1,46	Sabbia	00,12 %
Asimmetria	-0,20	Limo	51,95 %
Appuntimento	0,78	Argilla	47,93 %

Percentili	Phi	Micron
1	4,43	46,40
5	5,10	29,10
16	6,11	14,40
25	6,62	10,10
50	7,92	4,10
75	9,01	1,90
84	9,22	1,70
95	9,64	1,30

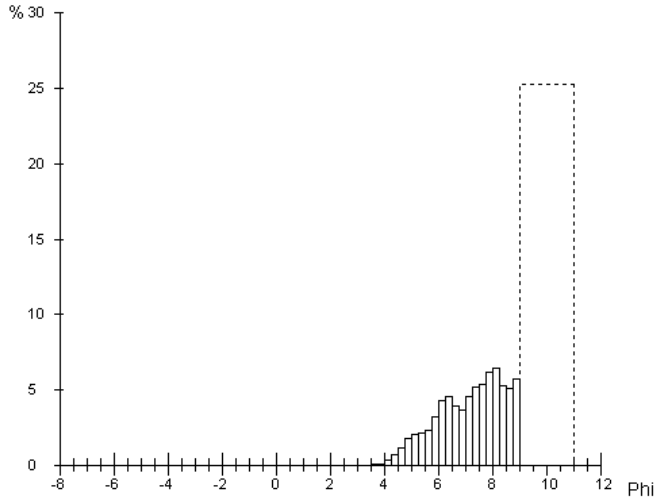

UNIVERSITA' DI ROMA "LA SAPIENZA"
DIPARTIMENTO DI SCIENZE DELLA TERRA
LABORATORIO SEDIMENTOLOGICO
Analisi Granulometrica

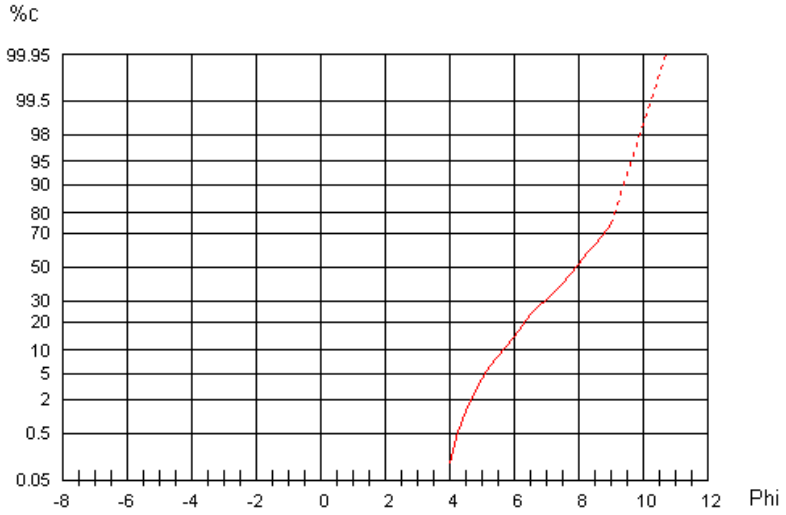

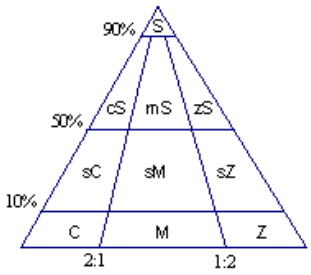

S	Sabbia
cS	Sabbia argillosa
mS	Sabbia fangosa
zS	Sabbia limosa
sC	Argilla sabbiosa
sM	Fango sabbioso
sZ	Limo sabbioso
C	Argilla
M	Fango
Z	Limo

(Folk, 1954)

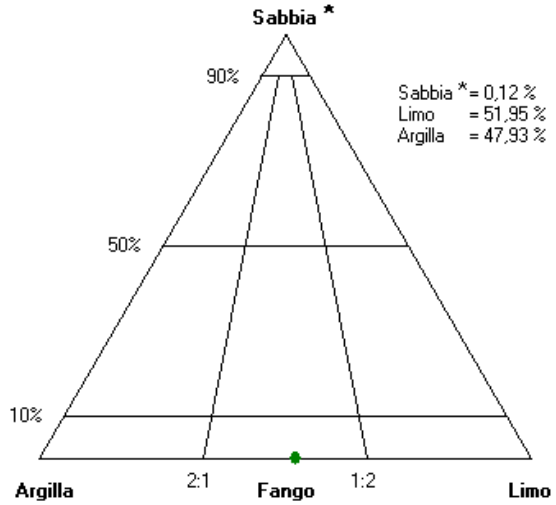

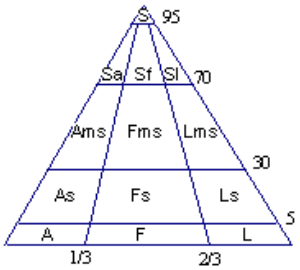

S	Sabbia
Sa	Sabbia argillosa
Sf	Sabbia fangosa
Sl	Sabbia limosa
Ams	Argilla molto sabbiosa
Fms	Fango molto sabbioso
Lms	Limo molto sabbioso
As	Argilla sabbiosa
Fs	Fango sabbioso
Ls	Limo sabbioso
A	Argilla
F	Fango
L	Limo

(Tortora, 1999)

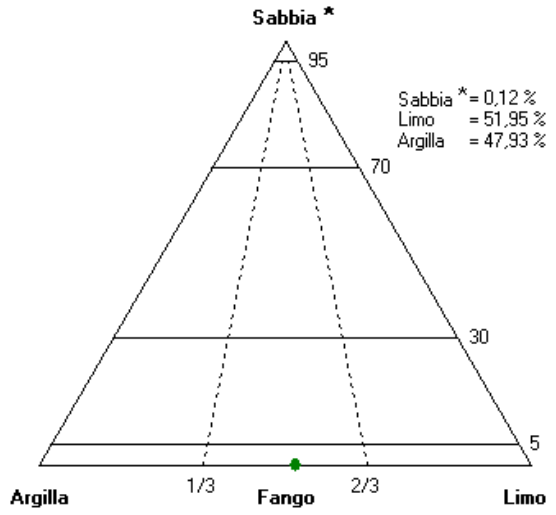

* comprensiva dell'eventuale frazione maggiore di 2 mm.

UNIVERSITA' DI ROMA "LA SAPIENZA"
DIPARTIMENTO DI SCIENZE DELLA TERRA
LABORATORIO SEDIMENTOLOGICO
Analisi Granulometrica

Analista: Francesca Vergari
Campagna: Toscana - Val d'Orcia
Longitudine: 724808
Sistema: UTM
Quota: 556 (s.l.m)

Data di prelievo: 21/05/2009
Campione: L4A
Latitudine: 4768129
Datum: WGS84 32T

Phi	Micron	% Trattenuta	% Cumulata
-1,00	2000,00	0,00	0,00
-0,50	1414,00	0,00	0,00
0,00	1000,00	0,00	0,00
0,50	707,00	0,00	0,00
1,00	500,00	0,00	0,00
1,50	354,00	0,00	0,00
2,00	250,00	0,00	0,00
2,50	177,00	0,00	0,00
3,00	125,00	0,00	0,00
3,50	88,00	0,00	0,00
4,00	62,00	0,29	0,29
4,25	53,00	0,76	1,05
4,50	44,00	1,29	2,34
4,75	37,00	1,81	4,15
5,00	31,00	2,64	6,79
5,25	26,00	3,05	9,84
5,50	22,00	3,15	12,99
5,75	19,00	3,18	16,17
6,00	16,00	4,19	20,36
6,25	13,00	5,57	25,93
6,50	11,00	5,93	31,86
6,75	9,00	5,10	36,96
7,00	8,00	4,77	41,73
7,25	7,00	5,52	47,25
7,50	6,00	5,84	53,09
7,75	5,00	5,58	58,67
8,00	4,00	5,92	64,59
8,25	3,00	5,77	70,36
8,50	2,76	4,46	74,82
8,75	2,00	4,04	78,86
9,00	1,95	4,32	83,18
11,00	0,49	16,82	100,00

Parametri Statistici Folk e Ward, 1957		Popolazioni Wentworth, 1922	
Media	7,38	Popolazione > 2 mm	00,00 %
Classamento	1,53	Sabbia	00,29 %
Asimmetria	-0,04	Limo	64,30 %
Appuntimento	0,83	Argilla	35,41 %

Percentili	Phi	Micron
1	4,24	52,90
5	4,84	34,90
16	5,74	18,70
25	6,21	13,50
50	7,37	6,10
75	8,51	2,70
84	9,02	1,90
95	9,50	1,40

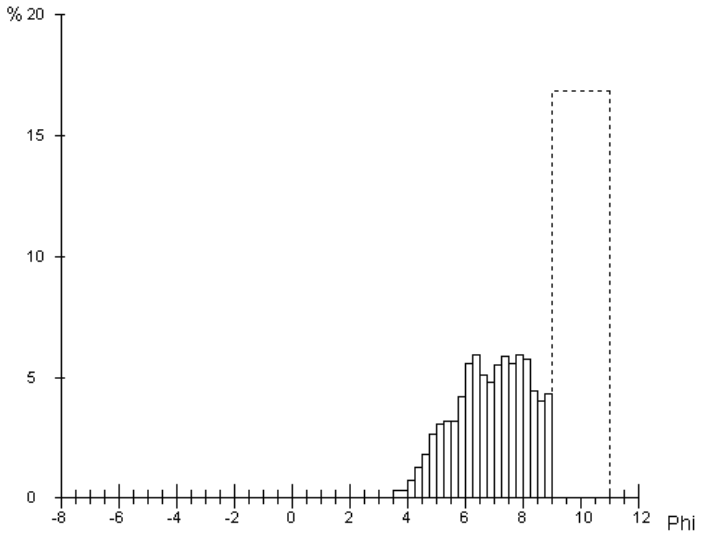

UNIVERSITA' DI ROMA "LA SAPIENZA"
DIPARTIMENTO DI SCIENZE DELLA TERRA
LABORATORIO SEDIMENTOLOGICO
Analisi Granulometrica

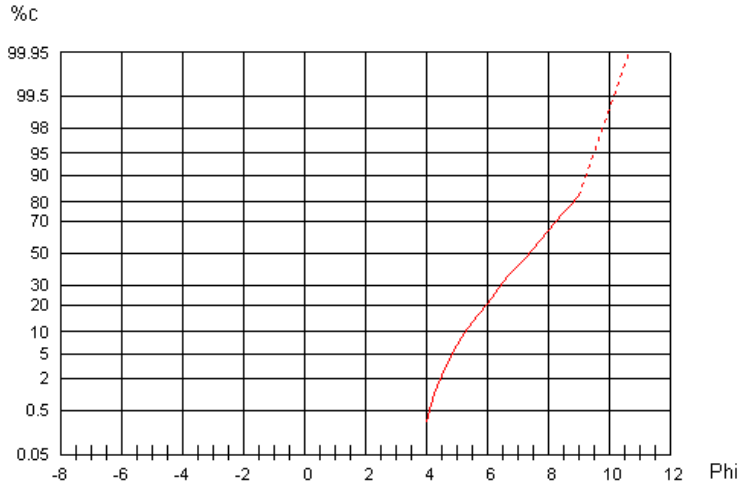

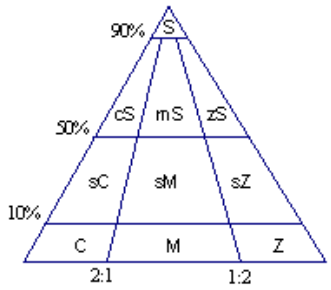

S	Sabbia
cS	Sabbia argillosa
mS	Sabbia fangosa
zS	Sabbia limosa
sC	Argilla sabbiosa
sM	Fango sabbioso
sZ	Limo sabbioso
C	Argilla
M	Fango
Z	Limo

(Folk, 1954)

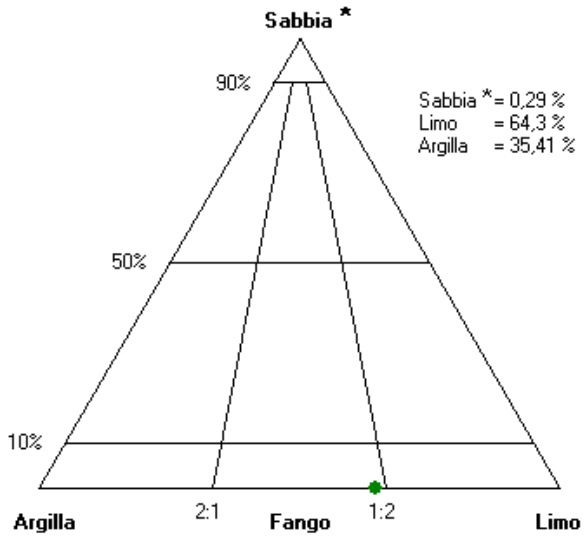

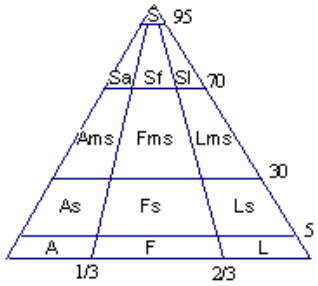

S	Sabbia
Sa	Sabbia argillosa
Sf	Sabbia fangosa
Sl	Sabbia limosa
Ams	Argilla molto sabbiosa
Fms	Fango molto sabbioso
Lms	Limo molto sabbioso
As	Argilla sabbiosa
Fs	Fango sabbioso
Ls	Limo sabbioso
A	Argilla
F	Fango
L	Limo

(Tortora, 1999)

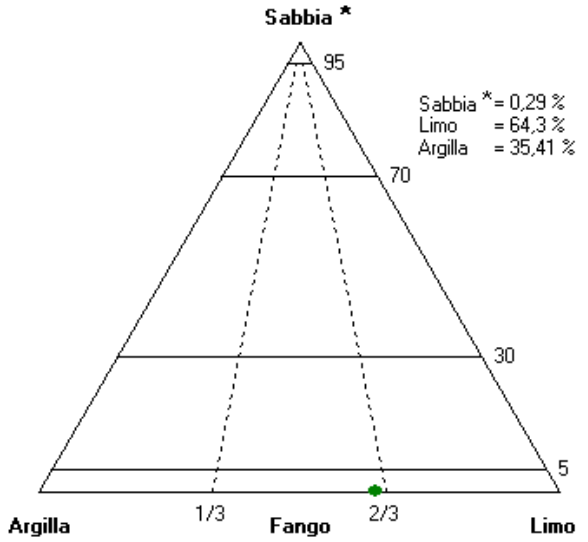

* comprensiva dell'eventuale frazione maggiore di 2 mm.

XX

UNIVERSITA' DI ROMA "LA SAPIENZA"
DIPARTIMENTO DI SCIENZE DELLA TERRA
LABORATORIO SEDIMENTOLOGICO
Analisi Granulometrica

Analista: Francesca Vergari
Campagna: Toscana - Val d'Orcia
Longitudine: 724808
Sistema: UTM
Quota: 556 (s.l.m)

Data di prelievo: 21/05/2009
Campione: L4B
Latitudine: 4768129
Datum: WGS84 32T

Phi	Micron	% Trattenuta	% Cumulata
-1,00	2000,00	0,00	0,00
-0,50	1414,00	0,00	0,00
0,00	1000,00	0,00	0,00
0,50	707,00	0,00	0,00
1,00	500,00	0,00	0,00
1,50	354,00	0,00	0,00
2,00	250,00	0,00	0,00
2,50	177,00	0,00	0,00
3,00	125,00	0,00	0,00
3,50	88,00	0,00	0,00
4,00	62,00	0,11	0,11
4,25	53,00	0,39	0,50
4,50	44,00	0,79	1,29
4,75	37,00	1,25	2,54
5,00	31,00	1,92	4,46
5,25	26,00	2,29	6,75
5,50	22,00	2,45	9,20
5,75	19,00	2,61	11,81
6,00	16,00	3,57	15,38
6,25	13,00	4,78	20,16
6,50	11,00	5,05	25,21
6,75	9,00	4,27	29,48
7,00	8,00	4,04	33,52
7,25	7,00	4,86	38,38
7,50	6,00	5,44	43,82
7,75	5,00	5,50	49,32
8,00	4,00	6,18	55,50
8,25	3,00	6,31	61,81
8,50	2,76	5,12	66,93
8,75	2,00	4,86	71,79
9,00	1,95	5,40	77,19
11,00	0,49	22,81	100,00

Parametri Statistici Folk e Ward, 1957		Popolazioni Wentworth, 1922	
Media	7,66	Popolazione > 2 mm	00,00 %
Classamento	1,47	Sabbia	00,11 %
Asimmetria	-0,15	Limo	55,39 %
Appuntimento	0,77	Argilla	44,50 %

Percentili	Phi	Micron
1	4,43	46,40
5	5,07	29,80
16	6,04	15,30
25	6,49	11,10
50	7,78	4,60
75	8,90	2,10
84	9,17	1,70
95	9,60	1,30

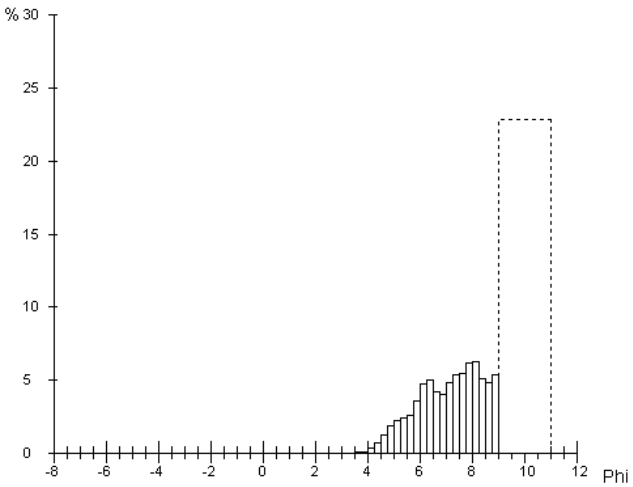

UNIVERSITA' DI ROMA "LA SAPIENZA"
DIPARTIMENTO DI SCIENZE DELLA TERRA
LABORATORIO SEDIMENTOLOGICO
Analisi Granulometrica

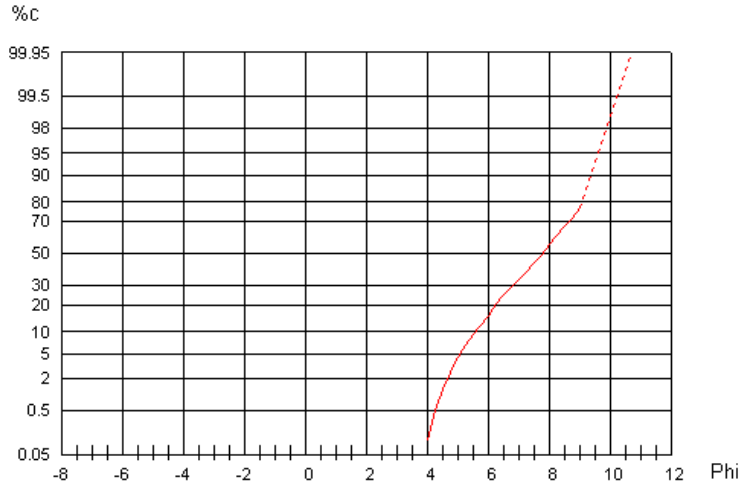

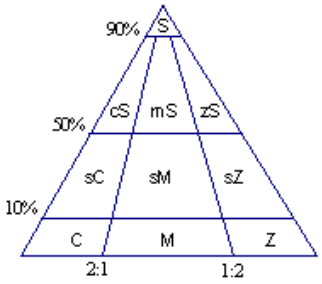

S	Sabbia
cS	Sabbia argillosa
mS	Sabbia fangosa
zS	Sabbia limosa
sC	Argilla sabbiosa
sM	Fango sabbioso
sZ	Limo sabbioso
C	Argilla
M	Fango
Z	Limo

(Folk, 1954)

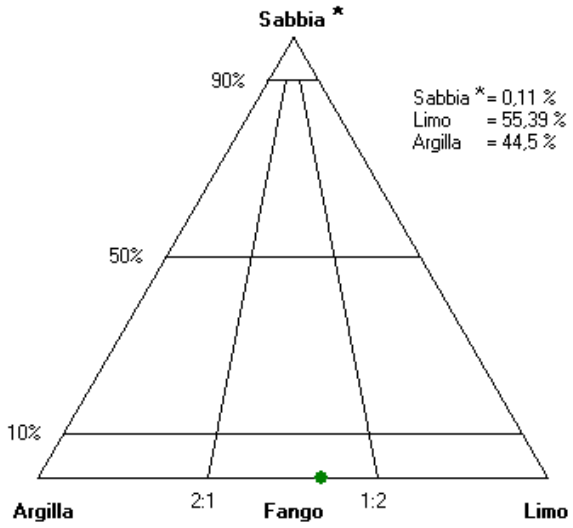

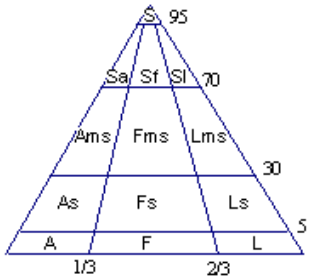

S	Sabbia
Sa	Sabbia argillosa
Sf	Sabbia fangosa
Sl	Sabbia limosa
Ams	Argilla molto sabbiosa
Fms	Fango molto sabbioso
Lms	Limo molto sabbioso
As	Argilla sabbiosa
Fs	Fango sabbioso
Ls	Limo sabbioso
A	Argilla
F	Fango
L	Limo

(Tortora, 1999)

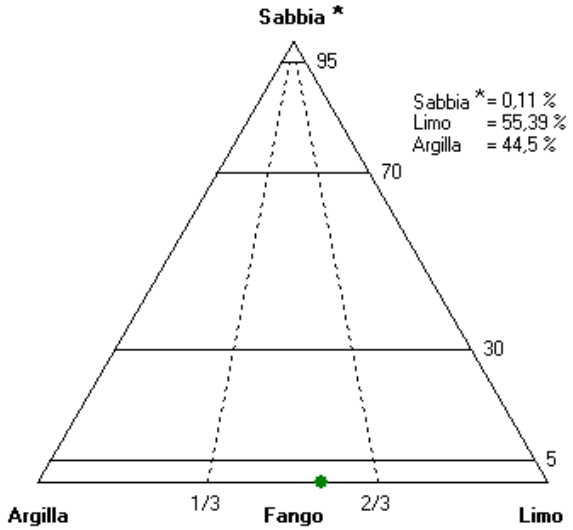

* comprensiva dell'eventuale frazione maggiore di 2 mm.

UNIVERSITA' DI ROMA "LA SAPIENZA"
DIPARTIMENTO DI SCIENZE DELLA TERRA
LABORATORIO SEDIMENTOLOGICO
Analisi Granulometrica

Analista: Francesca Vergari
Campagna: Toscana - Val d'Orcia
Longitudine: 724801
Sistema: UTM
Quota: 555 (s.l.m)

Data di prelievo: 21/05/2009
Campione: L5A
Latitudine: 4768127
Datum: WGS84 32N

Phi	Micron	% Trattenuta	% Cumulata
-1,00	2000,00	0,00	0,00
-0,50	1414,00	0,00	0,00
0,00	1000,00	0,00	0,00
0,50	707,00	0,00	0,00
1,00	500,00	0,00	0,00
1,50	354,00	0,00	0,00
2,00	250,00	0,00	0,00
2,50	177,00	0,00	0,00
3,00	125,00	0,00	0,00
3,50	88,00	0,00	0,00
4,00	62,00	0,06	0,06
4,25	53,00	0,33	0,39
4,50	44,00	0,74	1,13
4,75	37,00	1,19	2,32
5,00	31,00	1,91	4,23
5,25	26,00	2,33	6,56
5,50	22,00	2,50	9,06
5,75	19,00	2,64	11,70
6,00	16,00	3,58	15,28
6,25	13,00	4,78	20,06
6,50	11,00	5,05	25,11
6,75	9,00	4,28	29,39
7,00	8,00	4,04	33,43
7,25	7,00	4,85	38,28
7,50	6,00	5,41	43,69
7,75	5,00	5,48	49,17
8,00	4,00	6,16	55,33
8,25	3,00	6,29	61,62
8,50	2,76	5,11	66,73
8,75	2,00	4,85	71,58
9,00	1,95	5,42	77,00
11,00	0,49	23,00	100,00

Parametri Statistici Folk e Ward, 1957		Popolazioni Wentworth, 1922	
Media	7,67	Popolazione > 2 mm	00,00 %
Classamento	1,47	Sabbia	00,06 %
Asimmetria	-0,15	Limo	55,27 %
Appuntimento	0,77	Argilla	44,67 %

Percentili	Phi	Micron
1	4,47	45,10
5	5,09	29,30
16	6,04	15,20
25	6,49	11,10
50	7,78	4,50
75	8,90	2,10
84	9,17	1,70
95	9,61	1,30

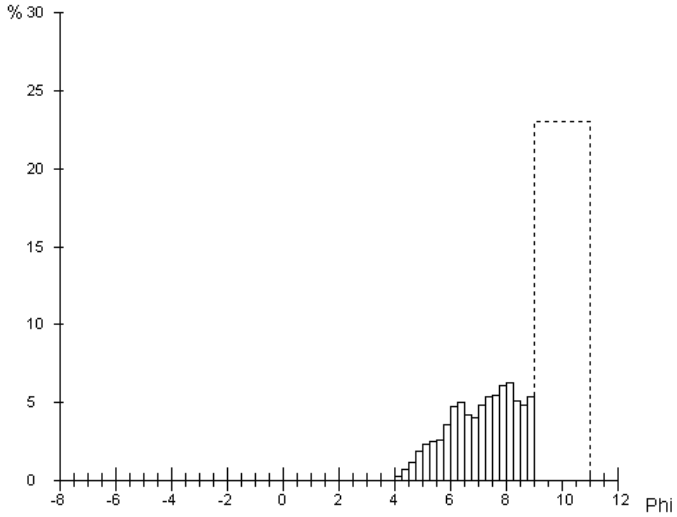

UNIVERSITA' DI ROMA "LA SAPIENZA"
DIPARTIMENTO DI SCIENZE DELLA TERRA
LABORATORIO SEDIMENTOLOGICO
Analisi Granulometrica

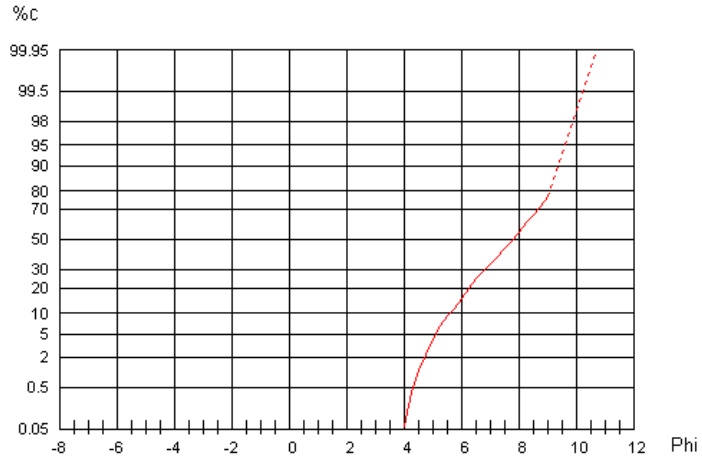

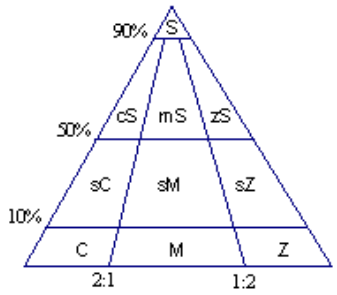

S	Sabbia
cS	Sabbia argillosa
mS	Sabbia fangosa
zS	Sabbia limosa
sC	Argilla sabbiosa
sM	Fango sabbioso
sZ	Limo sabbioso
C	Argilla
M	Fango
Z	Limo

(Folk, 1954)

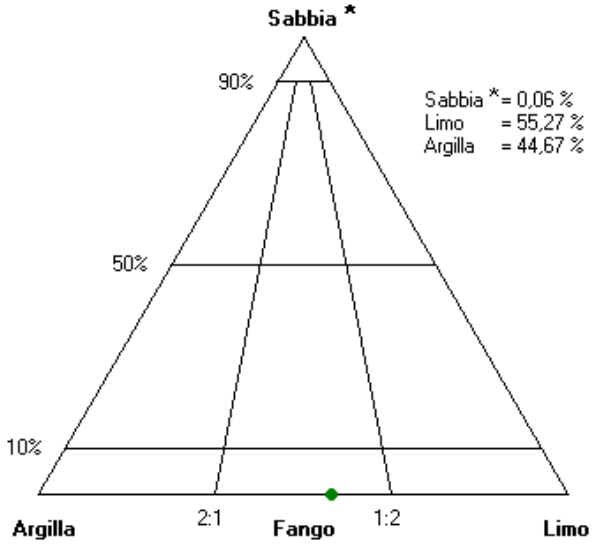

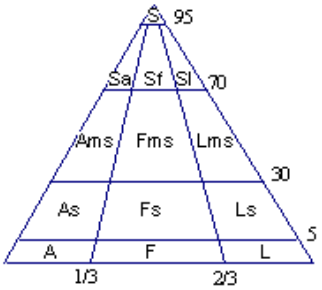

S	Sabbia
Sa	Sabbia argillosa
Sf	Sabbia fangosa
Sl	Sabbia limosa
Ams	Argilla molto sabbiosa
Fms	Fango molto sabbioso
Lms	Limo molto sabbioso
As	Argilla sabbiosa
Fs	Fango sabbioso
Ls	Limo sabbioso
A	Argilla
F	Fango
L	Limo

(Tortora, 1999)

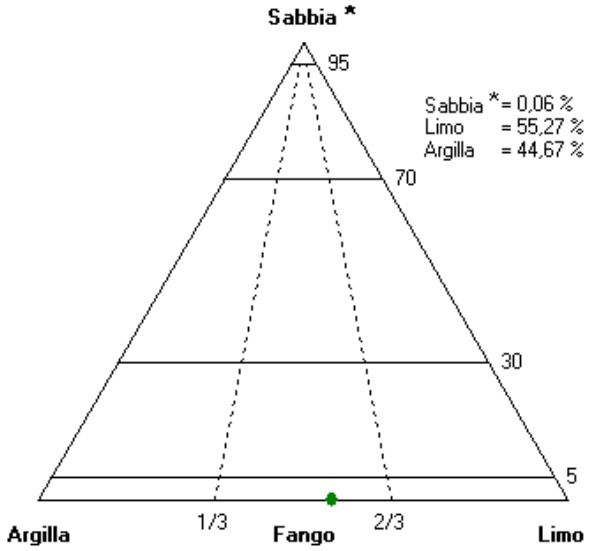

* comprensiva dell'eventuale frazione maggiore di 2 mm.

UNIVERSITA' DI ROMA "LA SAPIENZA"
DIPARTIMENTO DI SCIENZE DELLA TERRA
LABORATORIO SEDIMENTOLOGICO
Analisi Granulometrica

Analista: Fantini-Mari
Campagna: Toscana - Val d'Orcia
Longitudine: 724801
Sistema: UTM
Quota: 555 (s.l.m)

Data di prelievo: 26/04/2010
Campione: L5B
Latitudine: 4768127
Datum: WGS84 32N

Phi	Micron	% Trattenuta	% Cumulata
-1,00	2000,00	0,00	0,00
-0,50	1414,00	0,00	0,00
0,00	1000,00	0,00	0,00
0,50	707,00	0,00	0,00
1,00	500,00	0,00	0,00
1,50	354,00	0,00	0,00
2,00	250,00	0,00	0,00
2,50	177,00	0,00	0,00
3,00	125,00	0,00	0,00
3,50	88,00	0,00	0,00
4,00	62,00	0,00	0,00
4,25	53,00	0,15	0,15
4,50	44,00	0,52	0,67
4,75	37,00	0,96	1,63
5,00	31,00	1,59	3,22
5,25	26,00	1,95	5,17
5,50	22,00	2,09	7,26
5,75	19,00	2,26	9,52
6,00	16,00	3,15	12,67
6,25	13,00	4,24	16,91
6,50	11,00	4,50	21,41
6,75	9,00	3,82	25,23
7,00	8,00	3,68	28,91
7,25	7,00	4,56	33,47
7,50	6,00	5,25	38,72
7,75	5,00	5,49	44,21
8,00	4,00	6,34	50,55
8,25	3,00	6,61	57,16
8,50	2,76	5,48	62,64
8,75	2,00	5,30	67,94
9,00	1,95	5,99	73,93
11,00	0,49	26,07	100,00

Parametri Statistici Folk e Ward, 1957		Popolazioni Wentworth, 1922	
Media	7,80	Popolazione > 2 mm	00,00 %
Classamento	1,43	Sabbia	00,00 %
Asimmetria	-0,21	Limo	50,55 %
Appuntimento	0,79	Argilla	49,45 %

Percentili	Phi	Micron
1	4,61	41,00
5	5,23	26,60
16	6,20	13,60
25	6,74	9,40
50	7,98	4,00
75	9,02	1,90
84	9,23	1,70
95	9,65	1,20

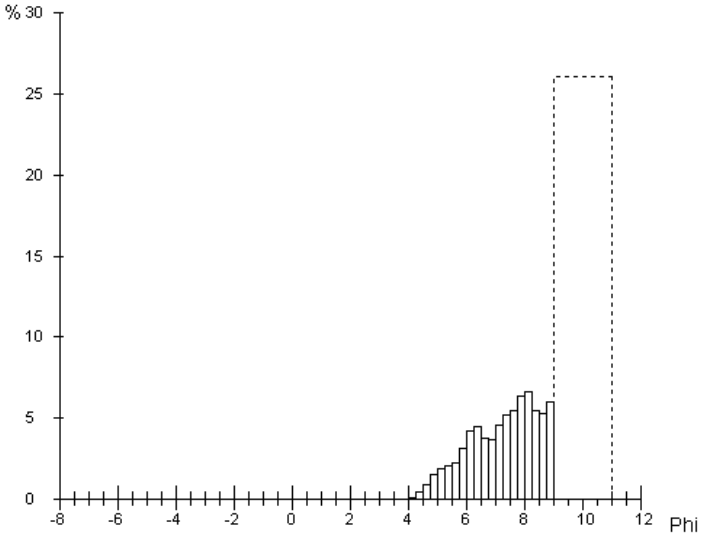

UNIVERSITA' DI ROMA "LA SAPIENZA"
DIPARTIMENTO DI SCIENZE DELLA TERRA
LABORATORIO SEDIMENTOLOGICO
Analisi Granulometrica

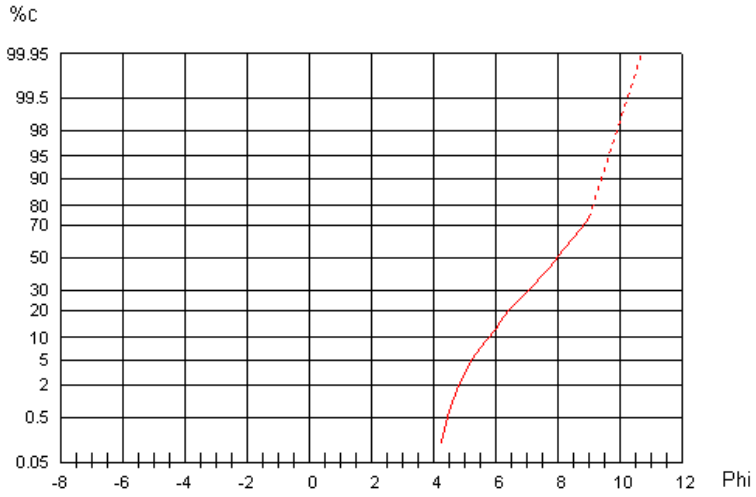

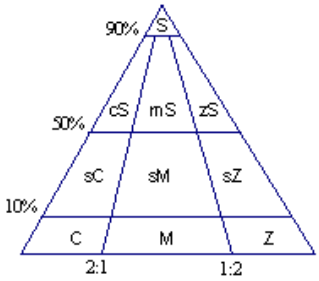

S	Sabbia
cS	Sabbia argillosa
mS	Sabbia fangosa
zS	Sabbia limosa
sC	Argilla sabbiosa
sM	Fango sabbioso
sZ	Limo sabbioso
C	Argilla
M	Fango
Z	Limo

(Folk, 1954)

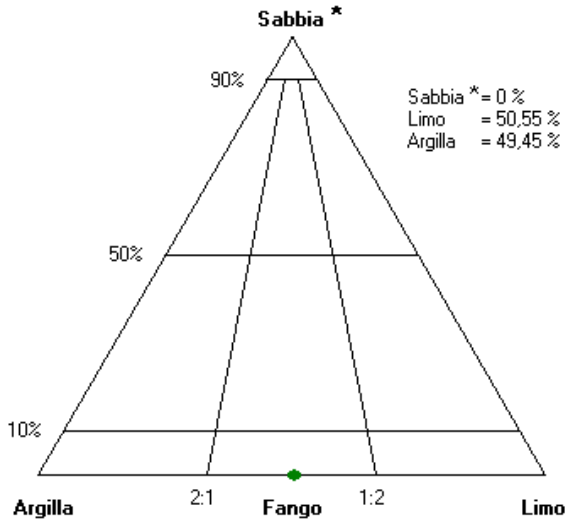

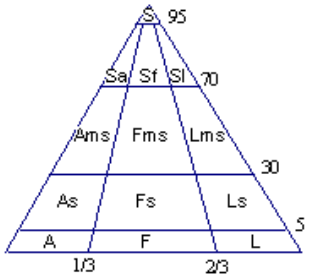

S	Sabbia
Sa	Sabbia argillosa
Sf	Sabbia fangosa
Sl	Sabbia limosa
Ams	Argilla molto sabbiosa
Fms	Fango molto sabbioso
Lms	Limo molto sabbioso
As	Argilla sabbiosa
Fs	Fango sabbioso
Ls	Limo sabbioso
A	Argilla
F	Fango
L	Limo

(Tortora, 1999)

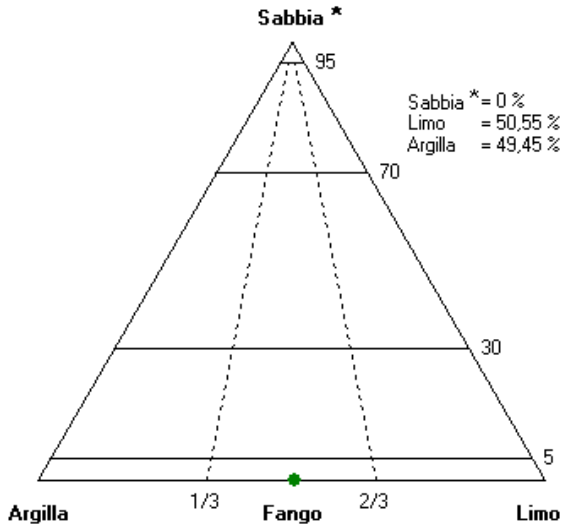

* comprensiva dell'eventuale frazione maggiore di 2 mm.

UNIVERSITA' DI ROMA "LA SAPIENZA"
DIPARTIMENTO DI SCIENZE DELLA TERRA
LABORATORIO SEDIMENTOLOGICO
Analisi Granulometrica

Analista: Francesca Vergari
Campagna: Toscana - Val d'Orcia
Longitudine: 724801
Sistema: UTM
Quota: 555 (s.l.m)

Data di prelievo: 21/05/2009
Campione: L5C
Latitudine: 4768127
Datum: WGS84 32N

Phi	Micron	% Trattenuta	% Cumulata
-1,00	2000,00	0,00	0,00
-0,50	1414,00	0,00	0,00
0,00	1000,00	0,00	0,00
0,50	707,00	0,00	0,00
1,00	500,00	0,00	0,00
1,50	354,00	0,00	0,00
2,00	250,00	0,00	0,00
2,50	177,00	0,00	0,00
3,00	125,00	0,00	0,00
3,50	88,00	0,00	0,00
4,00	62,00	0,04	0,04
4,25	53,00	0,28	0,32
4,50	44,00	0,65	0,97
4,75	37,00	1,09	2,06
5,00	31,00	1,74	3,80
5,25	26,00	2,12	5,92
5,50	22,00	2,26	8,18
5,75	19,00	2,42	10,60
6,00	16,00	3,32	13,92
6,25	13,00	4,45	18,37
6,50	11,00	4,70	23,07
6,75	9,00	3,97	27,04
7,00	8,00	3,77	30,81
7,25	7,00	4,61	35,42
7,50	6,00	5,25	40,67
7,75	5,00	5,43	46,10
8,00	4,00	6,22	52,32
8,25	3,00	6,45	58,77
8,50	2,76	5,33	64,10
8,75	2,00	5,13	69,23
9,00	1,95	5,76	74,99
11,00	0,49	25,01	100,00

Parametri Statistici Folk e Ward, 1957		Popolazioni Wentworth, 1922	
Media	7,75	Popolazione > 2 mm	00,00 %
Classamento	1,45	Sabbia	00,04 %
Asimmetria	-0,19	Limo	52,28 %
Appuntimento	0,77	Argilla	47,68 %

Percentili	Phi	Micron
1	4,51	43,90
5	5,15	28,10
16	6,12	14,40
25	6,62	10,10
50	7,91	4,20
75	9,00	2,00
84	9,21	1,70
95	9,64	1,30

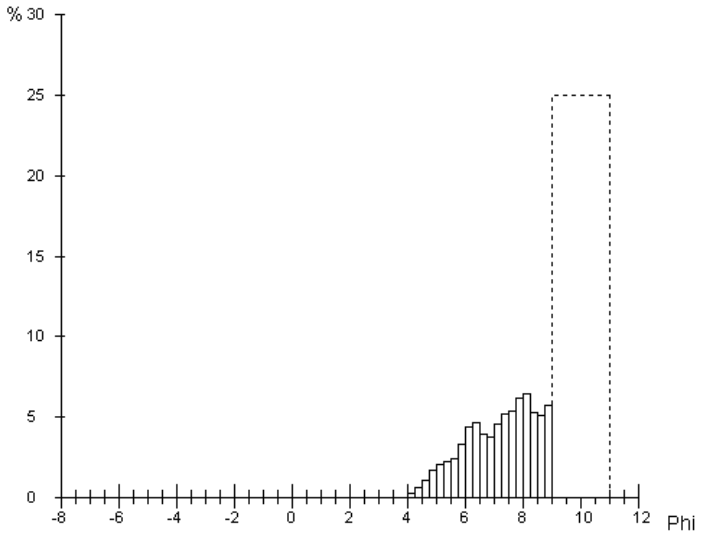

UNIVERSITA' DI ROMA "LA SAPIENZA"
DIPARTIMENTO DI SCIENZE DELLA TERRA
LABORATORIO SEDIMENTOLOGICO
Analisi Granulometrica

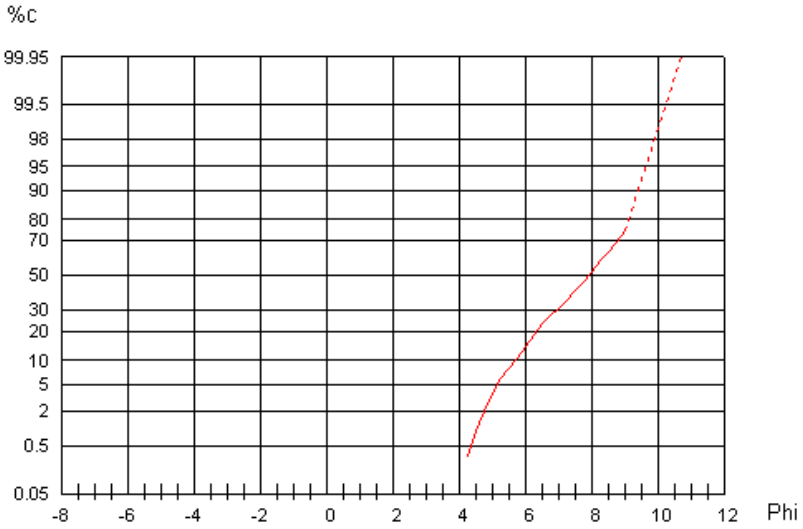

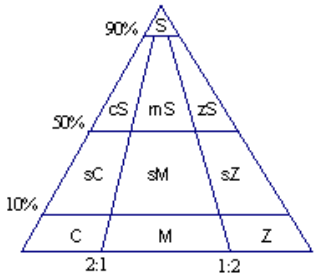

S	Sabbia
cS	Sabbia argillosa
mS	Sabbia fangosa
zS	Sabbia limosa
sC	Argilla sabbiosa
sM	Fango sabbioso
sZ	Limo sabbioso
C	Argilla
M	Fango
Z	Limo

(Folk, 1954)

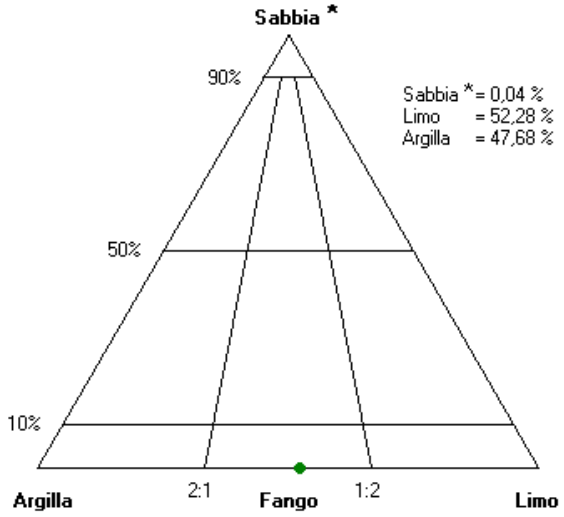

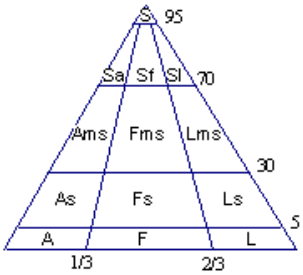

S	Sabbia
Sa	Sabbia argillosa
Sf	Sabbia fangosa
Sl	Sabbia limosa
Ams	Argilla molto sabbiosa
Fms	Fango molto sabbioso
Lms	Limo molto sabbioso
As	Argilla sabbiosa
Fs	Fango sabbioso
Ls	Limo sabbioso
A	Argilla
F	Fango
L	Limo

(Tortora, 1999)

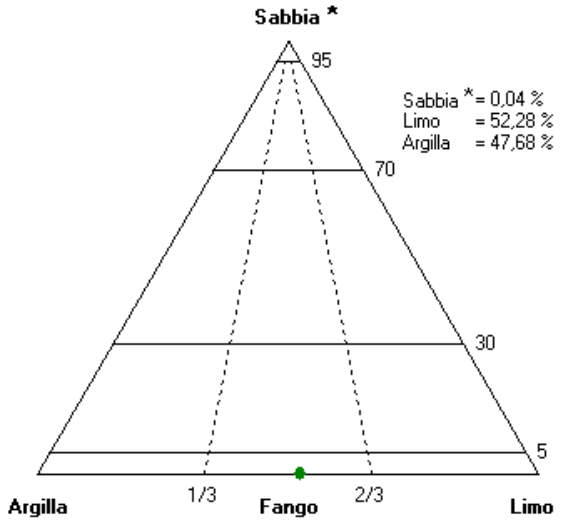

* comprensiva dell'eventuale frazione maggiore di 2 mm.

UNIVERSITA' DI ROMA "LA SAPIENZA"
DIPARTIMENTO DI SCIENZE DELLA TERRA
LABORATORIO SEDIMENTOLOGICO
Analisi Granulometrica

Analista: Francesca Vergari
Campagna: Toscana - Val d'Orcia
Longitudine: 724841
Sistema: UTM
Quota: 549 (s.l.m)

Data di prelievo: 21/05/2009
Campione: L6A
Latitudine: 4768128
Datum: WGS84 32N

Phi	Micron	% Trattenuta	% Cumulata
-1,00	2000,00	0,00	0,00
-0,50	1414,00	0,00	0,00
0,00	1000,00	0,00	0,00
0,50	707,00	0,00	0,00
1,00	500,00	0,00	0,00
1,50	354,00	0,00	0,00
2,00	250,00	0,00	0,00
2,50	177,00	0,00	0,00
3,00	125,00	0,00	0,00
3,50	88,00	0,00	0,00
4,00	62,00	0,31	0,31
4,25	53,00	0,60	0,91
4,50	44,00	0,86	1,77
4,75	37,00	1,15	2,92
5,00	31,00	1,69	4,61
5,25	26,00	1,98	6,59
5,50	22,00	2,09	8,68
5,75	19,00	2,24	10,92
6,00	16,00	3,13	14,05
6,25	13,00	4,27	18,32
6,50	11,00	4,60	22,92
6,75	9,00	3,98	26,90
7,00	8,00	3,86	30,76
7,25	7,00	4,74	35,50
7,50	6,00	5,39	40,89
7,75	5,00	5,55	46,44
8,00	4,00	6,31	52,75
8,25	3,00	6,52	59,27
8,50	2,76	5,35	64,62
8,75	2,00	5,11	69,73
9,00	1,95	5,71	75,44
11,00	0,49	24,56	100,00

Parametri Statistici Folk e Ward, 1957		Popolazioni Wentworth, 1922	
Media	7,74	Popolazione > 2 mm	00,00 %
Classamento	1,46	Sabbia	00,31 %
Asimmetria	-0,19	Limo	52,44 %
Appuntimento	0,80	Argilla	47,25 %

Percentili	Phi	Micron
1	4,28	51,30
5	5,06	30,10
16	6,12	14,40
25	6,63	10,10
50	7,89	4,20
75	8,98	2,00
84	9,20	1,70
95	9,63	1,30

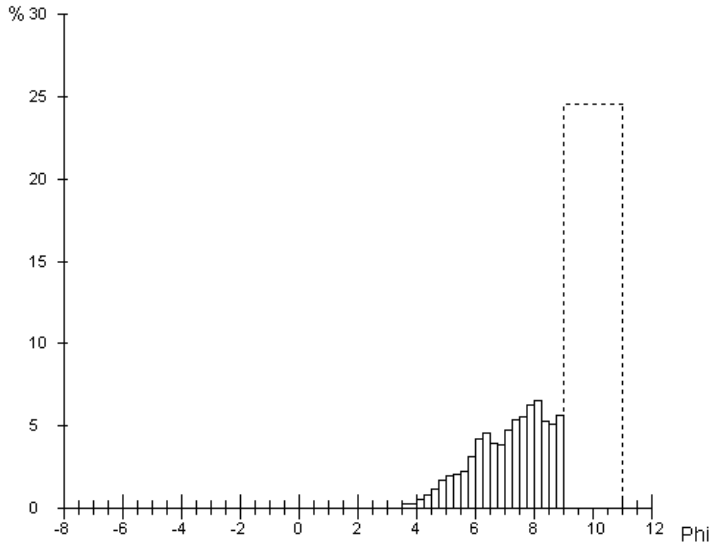

UNIVERSITA' DI ROMA "LA SAPIENZA"
DIPARTIMENTO DI SCIENZE DELLA TERRA
LABORATORIO SEDIMENTOLOGICO
Analisi Granulometrica

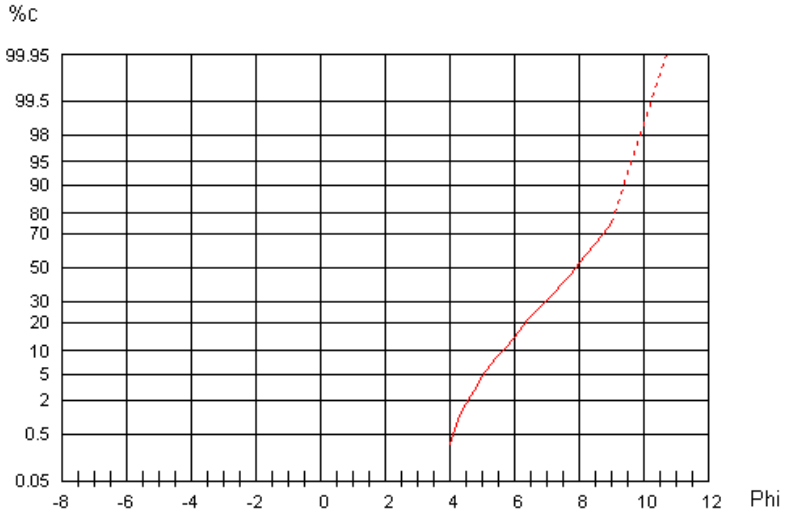

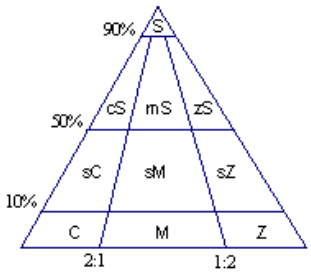

S	Sabbia
cS	Sabbia argillosa
mS	Sabbia fangosa
zS	Sabbia limosa
sC	Argilla sabbiosa
sM	Fango sabbioso
sZ	Limo sabbioso
C	Argilla
M	Fango
Z	Limo

(Folk, 1954)

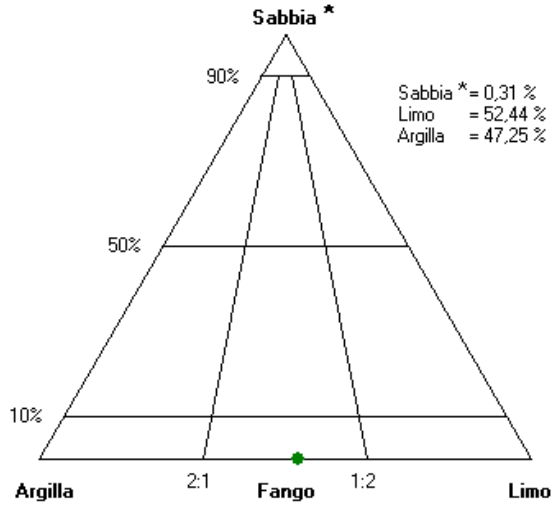

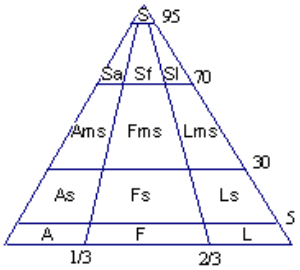

S	Sabbia
Sa	Sabbia argillosa
Sf	Sabbia fangosa
Sl	Sabbia limosa
Ams	Argilla molto sabbiosa
Fms	Fango molto sabbioso
Lms	Limo molto sabbioso
As	Argilla sabbiosa
Fs	Fango sabbioso
Ls	Limo sabbioso
A	Argilla
F	Fango
L	Limo

(Tortora, 1999)

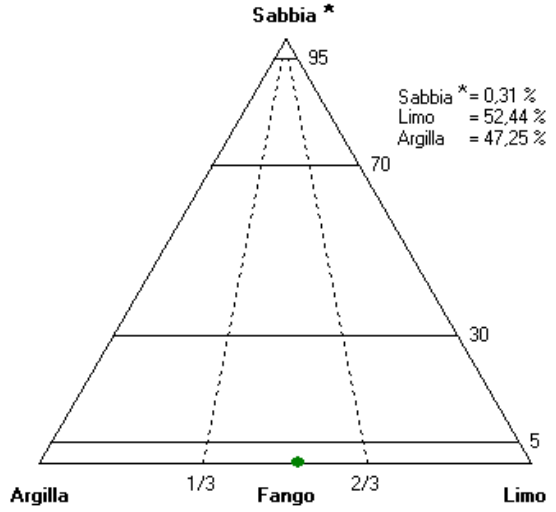

* comprensiva dell'eventuale frazione maggiore di 2 mm.

XXX

UNIVERSITA' DI ROMA "LA SAPIENZA"
DIPARTIMENTO DI SCIENZE DELLA TERRA
LABORATORIO SEDIMENTOLOGICO
Analisi Granulometrica

Analista: Francesca Vergari
Campagna: Toscana - Val d'Orcia
Longitudine: 724841
Sistema: UTM
Quota: 549 m (s.l.m)

Data di prelievo: 21/05/2009
Campione: L6B
Latitudine: 4768128
Datum: WGS84 32N

Phi	Micron	% Trattenuta	% Cumulata
-1,00	2000,00	0,00	0,00
-0,50	1414,00	0,00	0,00
0,00	1000,00	0,00	0,00
0,50	707,00	0,00	0,00
1,00	500,00	0,00	0,00
1,50	354,00	0,00	0,00
2,00	250,00	0,00	0,00
2,50	177,00	0,00	0,00
3,00	125,00	0,00	0,00
3,50	88,00	0,00	0,00
4,00	62,00	0,03	0,03
4,25	53,00	0,21	0,24
4,50	44,00	0,50	0,74
4,75	37,00	0,88	1,62
5,00	31,00	1,46	3,08
5,25	26,00	1,78	4,86
5,50	22,00	1,90	6,76
5,75	19,00	2,07	8,83
6,00	16,00	2,98	11,81
6,25	13,00	4,12	15,93
6,50	11,00	4,46	20,39
6,75	9,00	3,88	24,27
7,00	8,00	3,77	28,04
7,25	7,00	4,70	32,74
7,50	6,00	5,40	38,14
7,75	5,00	5,62	43,76
8,00	4,00	6,46	50,22
8,25	3,00	6,73	56,95
8,50	2,76	5,56	62,51
8,75	2,00	5,36	67,87
9,00	1,95	6,01	73,88
11,00	0,49	26,12	100,00

Parametri Statistici Folk e Ward, 1957		Popolazioni Wentworth, 1922	
Media	7,83	Popolazione > 2 mm	00,00 %
Classamento	1,41	Sabbia	00,03 %
Asimmetria	-0,20	Limo	50,19 %
Appuntimento	0,81	Argilla	49,78 %

Percentili	Phi	Micron
1	4,59	41,40
5	5,27	25,90
16	6,25	13,10
25	6,80	9,00
50	7,99	3,90
75	9,02	1,90
84	9,23	1,70
95	9,65	1,20

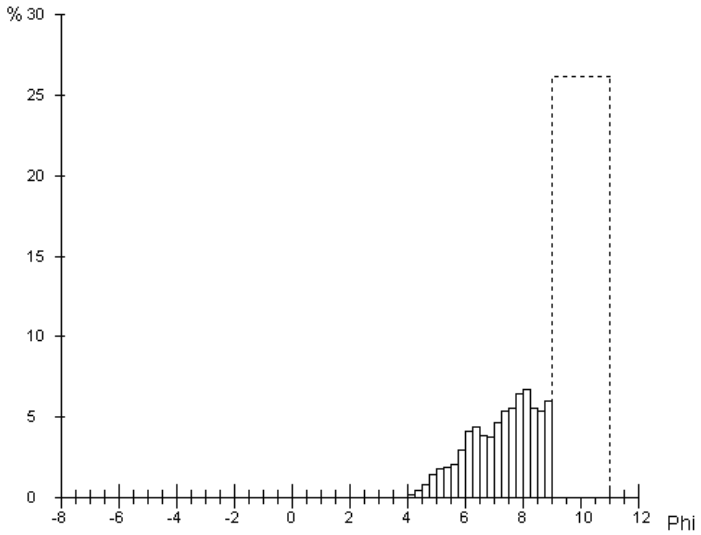

UNIVERSITA' DI ROMA "LA SAPIENZA"
DIPARTIMENTO DI SCIENZE DELLA TERRA
LABORATORIO SEDIMENTOLOGICO
Analisi Granulometrica

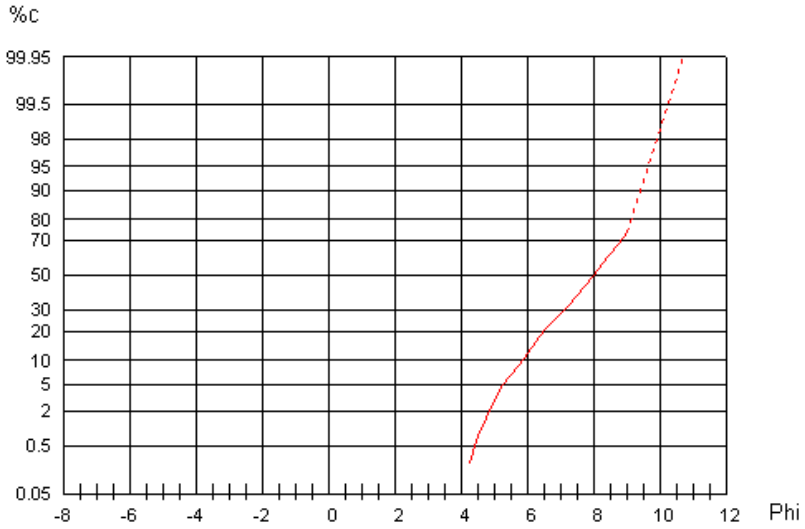

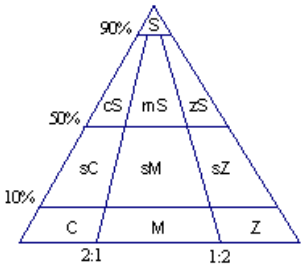

S	Sabbia
cS	Sabbia argillosa
mS	Sabbia fangosa
zS	Sabbia limosa
sC	Argilla sabbiosa
sM	Fango sabbioso
sZ	Limo sabbioso
C	Argilla
M	Fango
Z	Limo

(Folk, 1954)

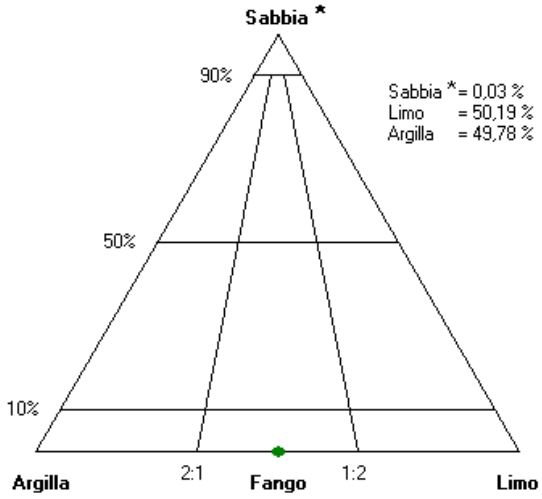

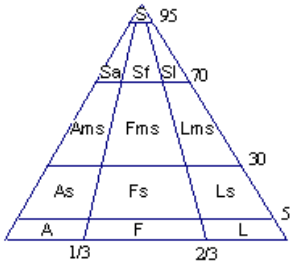

S	Sabbia
Sa	Sabbia argillosa
Sf	Sabbia fangosa
Sl	Sabbia limosa
Ams	Argilla molto sabbiosa
Fms	Fango molto sabbioso
Lms	Limo molto sabbioso
As	Argilla sabbiosa
Fs	Fango sabbioso
Ls	Limo sabbioso
A	Argilla
F	Fango
L	Limo

(Tortora, 1999)

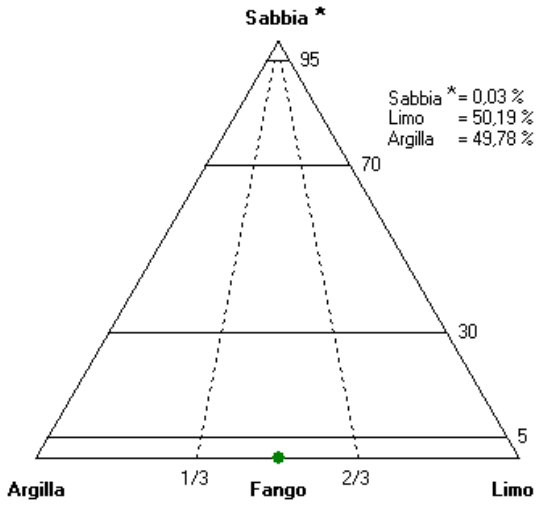

* comprensiva dell'eventuale frazione maggiore di 2 mm.

UNIVERSITA' DI ROMA "LA SAPIENZA"
DIPARTIMENTO DI SCIENZE DELLA TERRA
LABORATORIO SEDIMENTOLOGICO
Analisi Granulometrica

Analista: Francesca Vergari
Campagna: Toscana - Val d'Orcia
Longitudine: 0723934
Sistema: UTM
Quota: 324 m (s.l.m.)

Data di prelievo: 20/05/2009
Campione: M1
Latitudine: 4763996
Datum: WGS84 32N

Phi	Micron	% Trattenuta	% Cumulata
-1,00	2000,00	0,79	0,79
-0,50	1414,00	0,26	1,05
0,00	1000,00	0,29	1,34
0,50	707,00	0,49	1,83
1,00	500,00	0,77	2,60
1,50	354,00	1,04	3,64
2,00	250,00	1,89	5,53
2,50	177,00	2,94	8,47
3,00	125,00	5,65	14,12
3,50	88,00	9,00	23,12
4,00	62,00	9,97	33,09
4,25	53,00	2,57	35,66
4,50	44,00	2,90	38,56
4,75	37,00	2,74	41,30
5,00	31,00	2,99	44,29
5,25	26,00	2,92	47,21
5,50	22,00	2,66	49,87
5,75	19,00	2,40	52,27
6,00	16,00	2,83	55,10
6,25	13,00	3,45	58,55
6,50	11,00	3,46	62,01
6,75	9,00	2,79	64,80
7,00	8,00	2,54	67,34
7,25	7,00	2,91	70,25
7,50	6,00	3,11	73,36
7,75	5,00	2,99	76,35
8,00	4,00	3,22	79,57
8,25	3,00	3,18	82,75
8,50	2,76	2,49	85,24
8,75	2,00	2,29	87,53
9,00	1,95	2,52	90,05
11,00	0,49	9,95	100,00

Parametri Statistici Folk e Ward, 1957		Popolazioni Wentworth, 1922	
Media	5,67	Popolazione > 2 mm	00,79 %
Classamento	2,44	Sabbia	32,30 %
Asimmetria	0,05	Limo	46,48 %
Appuntimento	0,75	Argilla	20,43 %

Percentili	Phi	Micron
1	-0,59	1502,10
5	1,88	272,50
16	3,12	115,20
25	3,60	82,40
50	5,51	21,90
75	7,64	5,00
84	8,37	3,00
95	9,30	1,60

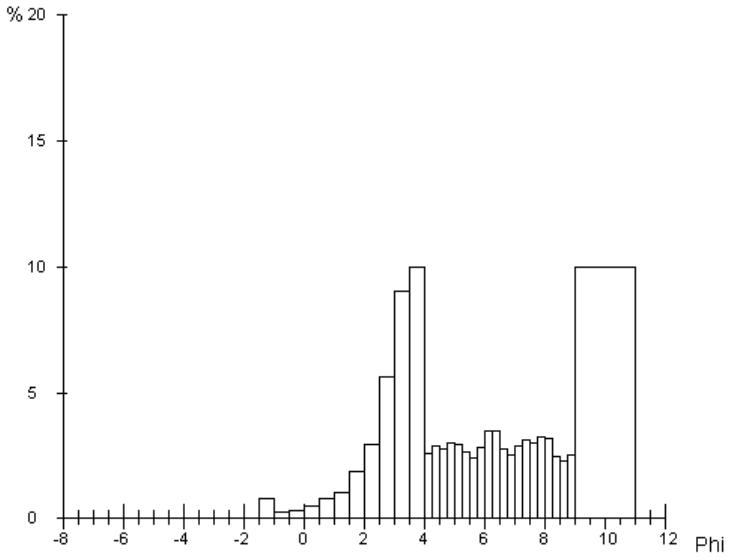

UNIVERSITA' DI ROMA "LA SAPIENZA"
DIPARTIMENTO DI SCIENZE DELLA TERRA
LABORATORIO SEDIMENTOLOGICO
Analisi Granulometrica

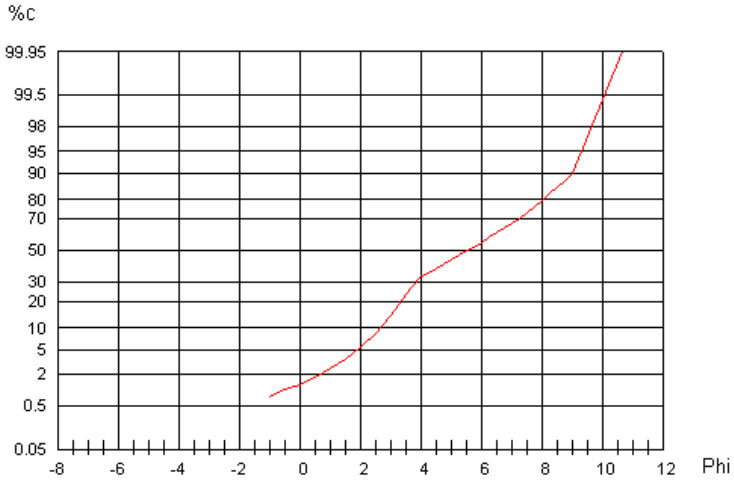

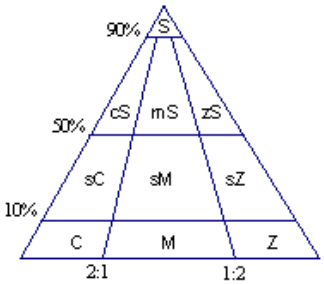

S	Sabbia
cS	Sabbia argillosa
mS	Sabbia fangosa
zS	Sabbia limosa
sC	Argilla sabbiosa
sM	Fango sabbioso
sZ	Limo sabbioso
C	Argilla
M	Fango
Z	Limo

(Folk, 1954)

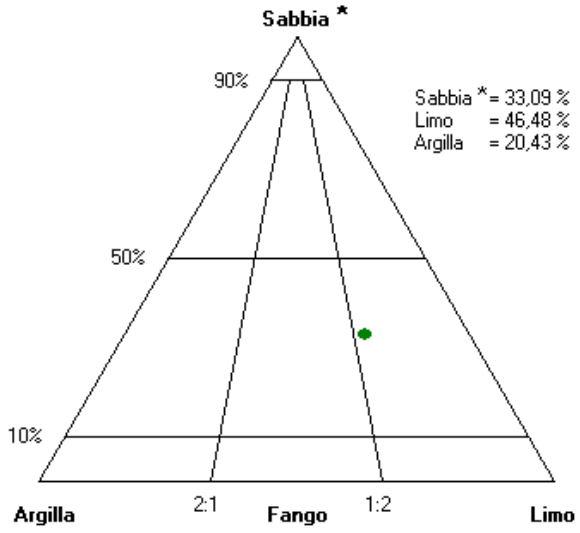

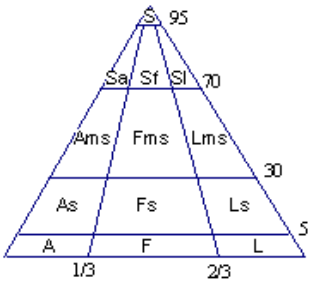

S	Sabbia
Sa	Sabbia argillosa
Sf	Sabbia fangosa
Sl	Sabbia limosa
Ams	Argilla molto sabbiosa
Fms	Fango molto sabbioso
Lms	Limo molto sabbioso
As	Argilla sabbiosa
Fs	Fango sabbioso
Ls	Limo sabbioso
A	Argilla
F	Fango
L	Limo

(Tortora, 1999)

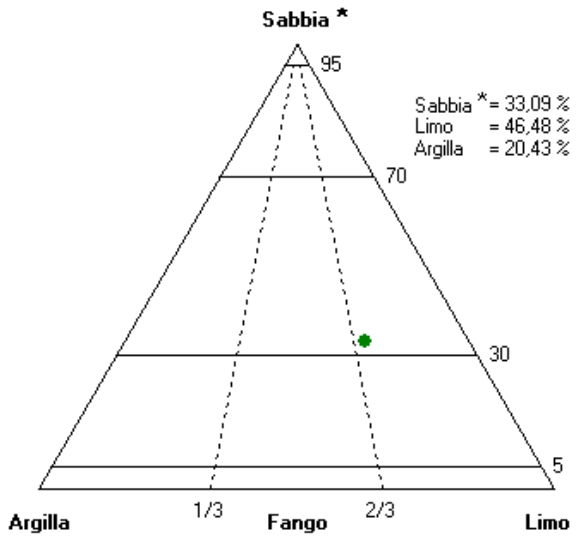

* comprensiva dell'eventuale frazione maggiore di 2 mm.

UNIVERSITA' DI ROMA "LA SAPIENZA"
DIPARTIMENTO DI SCIENZE DELLA TERRA
LABORATORIO SEDIMENTOLOGICO
Analisi Granulometrica

Analista: Francesca Vergari
Campagna: Toscana - Val d'Orcia
Longitudine: 0722552
Sistema: UTM
Quota: 575 m (s.l.m)

Data di prelievo: 20/05/2009
Campione: M7
Latitudine: 4759151
Datum: WGS84 32N

Phi	Micron	% Trattenuta	% Cumulata
-1,00	2000,00	2,35	2,35
-0,50	1414,00	0,33	2,68
0,00	1000,00	0,23	2,91
0,50	707,00	0,28	3,19
1,00	500,00	0,38	3,57
1,50	354,00	0,42	3,99
2,00	250,00	0,53	4,52
2,50	177,00	0,71	5,23
3,00	125,00	1,61	6,84
3,50	88,00	1,56	8,40
4,00	62,00	3,86	12,26
4,25	53,00	1,39	13,65
4,50	44,00	1,68	15,33
4,75	37,00	1,80	17,13
5,00	31,00	2,21	19,34
5,25	26,00	2,38	21,72
5,50	22,00	2,40	24,12
5,75	19,00	2,49	26,61
6,00	16,00	3,38	29,99
6,25	13,00	4,53	34,52
6,50	11,00	4,81	39,33
6,75	9,00	4,10	43,43
7,00	8,00	3,84	47,27
7,25	7,00	4,49	51,76
7,50	6,00	4,85	56,61
7,75	5,00	4,74	61,35
8,00	4,00	5,16	66,51
8,25	3,00	5,12	71,63
8,50	2,76	4,05	75,68
8,75	2,00	3,74	79,42
9,00	1,95	4,10	83,52
11,00	0,49	16,48	100,00

Parametri Statistici Folk e Ward, 1957		Popolazioni Wentworth, 1922	
Media	6,92	Popolazione > 2 mm	02,35 %
Classamento	2,19	Sabbia	09,91 %
Asimmetria	-0,25	Limo	54,25 %
Appuntimento	1,02	Argilla	33,49 %

Percentili	Phi	Micron
1	-1,10	2140,70
5	2,34	196,90
16	4,60	41,40
25	5,59	20,80
50	7,15	7,00
75	8,46	2,80
84	9,01	1,90
95	9,49	1,40

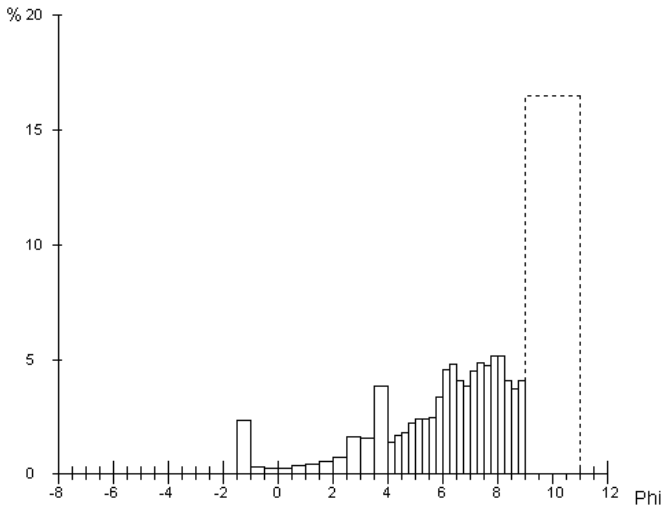

UNIVERSITA' DI ROMA "LA SAPIENZA"
DIPARTIMENTO DI SCIENZE DELLA TERRA
LABORATORIO SEDIMENTOLOGICO
Analisi Granulometrica

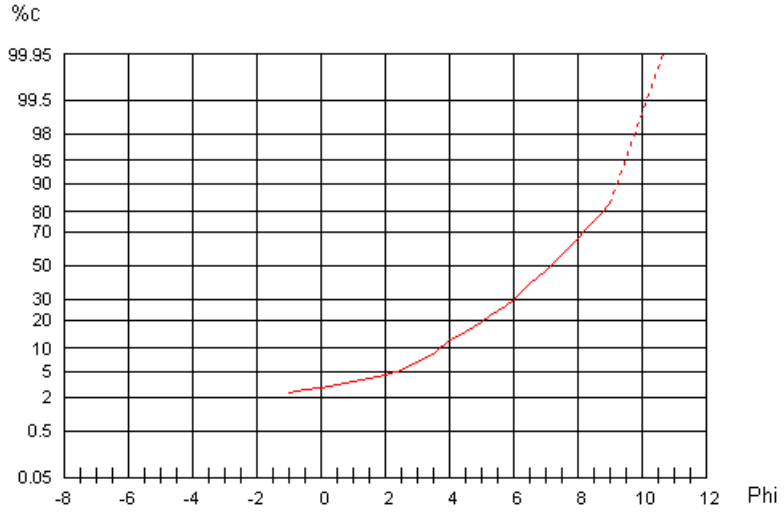

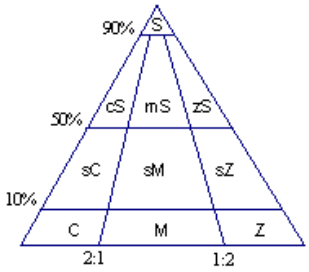

S	Sabbia
cS	Sabbia argillosa
mS	Sabbia fangosa
zS	Sabbia limosa
sC	Argilla sabbiosa
sM	Fango sabbioso
sZ	Limo sabbioso
C	Argilla
M	Fango
Z	Limo

(Folk, 1954)

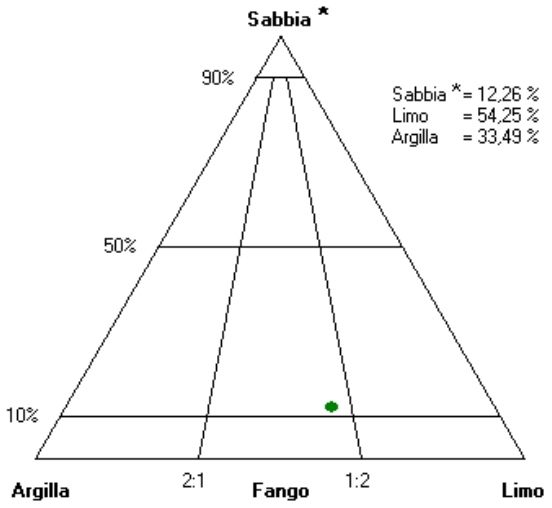

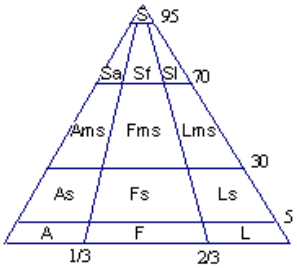

S	Sabbia
Sa	Sabbia argillosa
Sf	Sabbia fangosa
Sl	Sabbia limosa
Ams	Argilla molto sabbiosa
Fms	Fango molto sabbioso
Lms	Limo molto sabbioso
As	Argilla sabbiosa
Fs	Fango sabbioso
Ls	Limo sabbioso
A	Argilla
F	Fango
L	Limo

(Tortora, 1999)

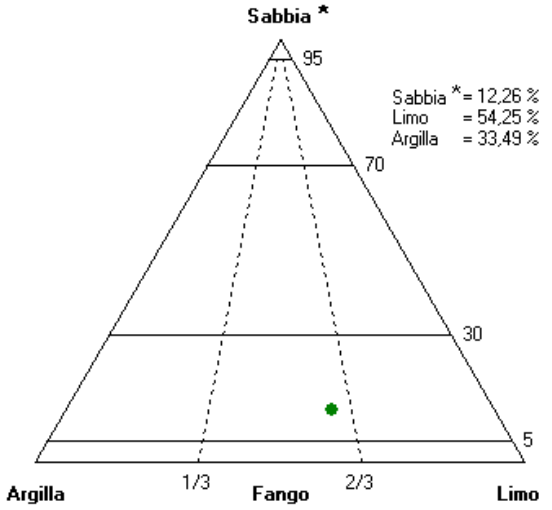

* comprensiva dell'eventuale frazione maggiore di 2 mm.

UNIVERSITA' DI ROMA "LA SAPIENZA"
DIPARTIMENTO DI SCIENZE DELLA TERRA
LABORATORIO SEDIMENTOLOGICO
Analisi Granulometrica

Analista: Francesca Vergari
Campagna: Toscana - Val d'Orcia
Longitudine: 0722534
Sistema: UTM
Quota: 555 (s.l.m)

Data di prelievo: 20/05/2009
Campione: M9
Latitudine: 4759015
Datum: WGS84 32N

Phi	Micron	% Trattenuta	% Cumulata
-3,00	8000,00	1,23	1,23
-2,50	5657,00	0,00	1,23
-2,00	4000,00	0,25	1,48
-1,50	2828,00	0,12	1,60
-1,00	2000,00	0,06	1,66
-0,50	1414,00	0,13	1,79
0,00	1000,00	0,15	1,94
0,50	707,00	0,19	2,13
1,00	500,00	0,30	2,43
1,50	354,00	0,44	2,87
2,00	250,00	0,63	3,50
2,50	177,00	0,91	4,41
3,00	125,00	1,03	5,44
3,50	88,00	1,14	6,58
4,00	62,00	1,20	7,78
4,25	53,00	0,36	8,14
4,50	44,00	0,59	8,73
4,75	37,00	0,83	9,56
5,00	31,00	1,24	10,80
5,25	26,00	1,45	12,25
5,50	22,00	1,60	13,85
5,75	19,00	1,90	15,75
6,00	16,00	2,88	18,63
6,25	13,00	4,14	22,77
6,50	11,00	4,58	27,35
6,75	9,00	4,06	31,41
7,00	8,00	3,98	35,39
7,25	7,00	4,87	40,26
7,50	6,00	5,47	45,73
7,75	5,00	5,51	51,24
8,00	4,00	6,15	57,39
8,25	3,00	6,22	63,61
8,50	2,76	5,01	68,62
8,75	2,00	4,69	73,31
9,00	1,95	5,20	78,51
11,00	0,49	21,49	100,00

Parametri Statistici Folk e Ward, 1957		Popolazioni Wentworth, 1922	
Media	7,54	Popolazione > 2 mm	01,66 %
Classamento	1,87	Sabbia	06,12 %
Asimmetria	-0,29	Limo	49,61 %
Appuntimento	1,13	Argilla	42,61 %

Percentili	Phi	Micron
1	-3,03	8149,60
5	2,80	143,90
16	5,77	18,30
25	6,37	12,10
50	7,69	4,80
75	8,83	2,20
84	9,14	1,80
95	9,58	1,30

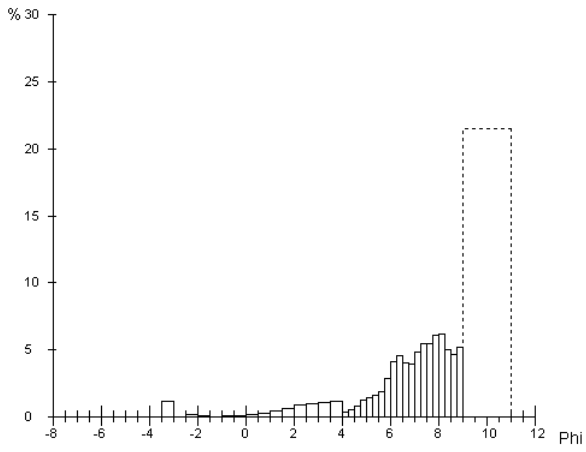

UNIVERSITA' DI ROMA "LA SAPIENZA"
DIPARTIMENTO DI SCIENZE DELLA TERRA
LABORATORIO SEDIMENTOLOGICO
Analisi Granulometrica

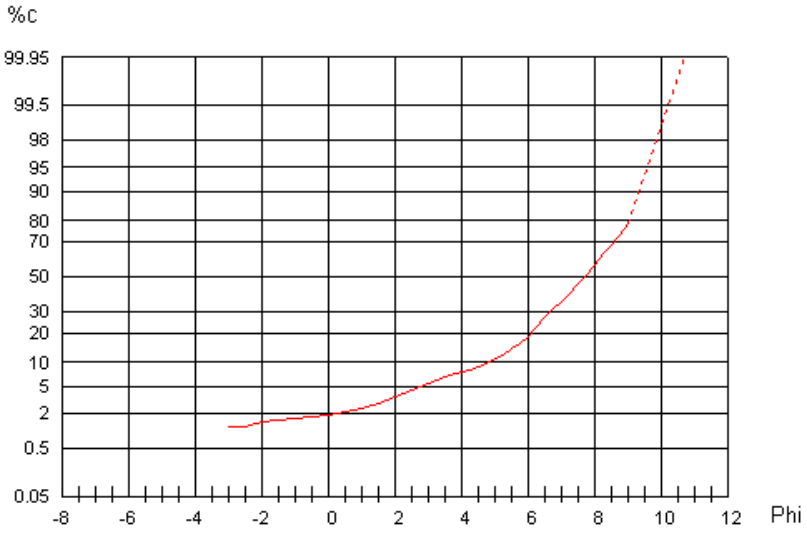

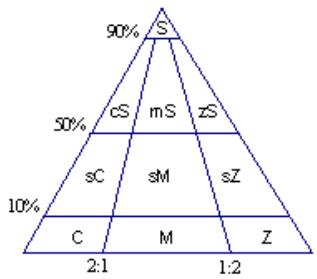

S	Sabbia
cS	Sabbia argillosa
mS	Sabbia fangosa
zS	Sabbia limosa
sC	Argilla sabbiosa
sM	Fango sabbioso
sZ	Limo sabbioso
C	Argilla
M	Fango
Z	Limo

(Folk, 1954)

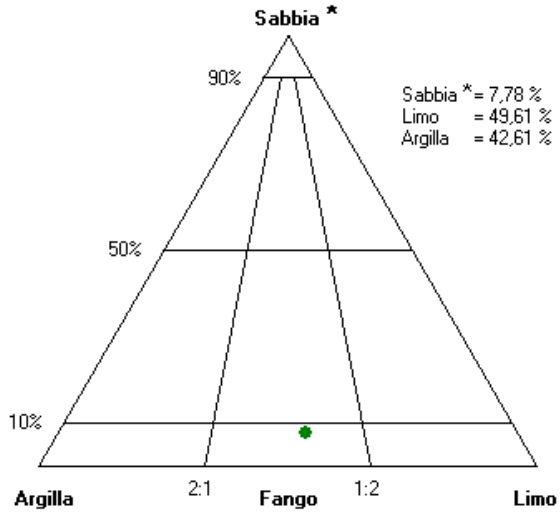

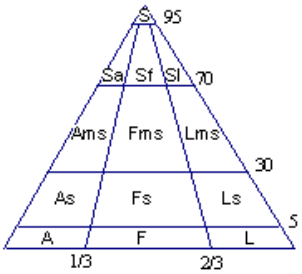

S	Sabbia
Sa	Sabbia argillosa
Sf	Sabbia fangosa
Sl	Sabbia limosa
Ams	Argilla molto sabbiosa
Fms	Fango molto sabbioso
Lms	Limo molto sabbioso
As	Argilla sabbiosa
Fs	Fango sabbioso
Ls	Limo sabbioso
A	Argilla
F	Fango
L	Limo

(Tortora, 1999)

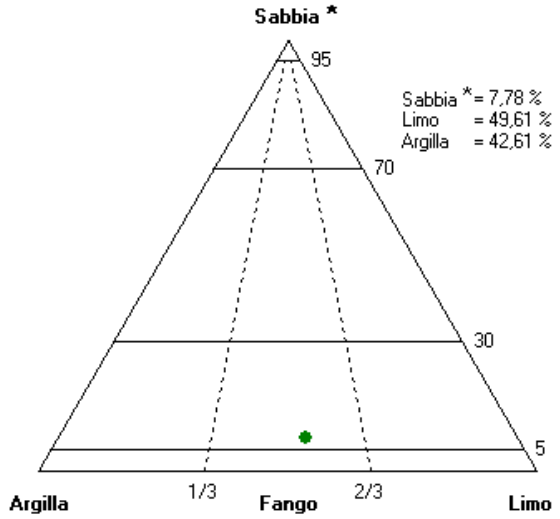

* comprensiva dell'eventuale frazione maggiore di 2 mm.